UNIVERSITÀ
DEGLI STUDI
FIRENZE

DOTTORATO DI RICERCA IN
AREA DEL FARMACO E TRATTAMENTI INNOVATIVI

CICLO XXIX

COORDINATORE Prof. Teodori Elisabetta

Design, synthesis and pharmacological evaluation of new adenosine receptor ligands

Settore Scientifico Disciplinare CHIM/08

Dottorando
Dott. Betti Marco

Tutore Scientifico
Prof. Catarzi Daniela

Tutore Teorico
Prof. Colotta Vittoria

Coordinatore
Prof. Teodori Elisabetta

Anni 2013/2016

TABLE OF CONTENTS

1. Introduction

Adenosine signaling has long been a target for drug development, with adenosine itself or its derivatives being used clinically since the 1940s. In the 1970s it became clear that there are receptors for adenosine, and there was evidence that methylxanthines such as caffeine, the most commonly consumed drug in the world, produces many of its actions by acting as antagonists at adenosine receptors. Towards the end of the twentieth century it became clear that there are subtypes of adenosine receptors, now recognized as a family of four, that are present in most vertebrates. In fact, extracellular adenosine exerts its actions via specific G protein-coupled receptors (GPCRs) divided into four adenosine receptor (AR) subtypes termed A_1, A_{2A}, A_{2B} and A_3. Since the heterogeneity of ARs and their widespread expression throughout the body, the development of drugs that selectively affect specific AR subtypes and/or specific components of adenosine signaling will hopefully provide new therapeutic opportunities for a large variety of human diseases. The knowledge of the complexity of regulatory mechanism controlling the receptor biological response under physiological and pathological conditions (1) (2) represent a crucial starting point in the development of adenosine-based drugs. In fact, these receptors are widely expressed and it was demonstrated that they are implicated in several biological functions, both physiological and pathological. These include cardiac rhythm and circulation (3) (4), lipolysis, renal blood flow (5) (6), immune function (7), sleep regulation (8) (9), angiogenesis (10), inflammatory diseases (11) (12), ischemia-reperfusion (13) and neurodegenerative disorders (14). Adenosine itself is used clinically (15) for the treatment of supraventricular tachycardia (16) (15), and many clinically used drugs (including dipyridamole and methotrexate) may exert their effects by altering extracellular adenosine concentrations and signaling. In fact, several pharmacological compounds specifically targeting individual ARs have now entered the clinic or clinical studies are ongoing. However, only one AR specific agent, the A_{2A} AR agonist regadenoson (Lexiscan; Astellas Pharma), has so far gained approval from the US Food and Drug Administration (FDA). Many research programs focused on the adenosine signaling in order to identify bioactive compounds that could be useful for the therapy of many AR-mediated diseases (17). The complexity of adenosine signaling was primarily responsible for the failure of one of the largest clinical trials for an A_1 receptor antagonist so far (18) (19). Moreover, since its discovery in the 1983, A_{2B} AR lack a selective and potent full agonist that could be helpful in order to deepen the physiopathological properties of this receptor (20). In fact, until now NECA, a non-selective AR agonist, has been used as elected ligand for the activation of the A_{2B} AR for the understanding of the signaling pathway mediated by this receptor, but, obviously with scarce results (21).

1.1 G-Protein Coupled Receptors

The superfamily of seven transmembrane domain (7TM) G-protein coupled receptors (GPCRs) represent the largest family of membrane proteins in the human genome and nowadays the richest source of targets and then drugs for the pharmaceutical industry. There has been remarkable progress in the field of GPCR biology during the past three decades. Notable milestones include the cloning of the first GPCR genes, and the sequencing of the human genome revealing the size of the GPCR family and the number of orphan GPCRs. In fact, a recent and detailed analysis of the human genome reveals over 800 unique GPCRs, of which approximately 460 are predicted to be olfactory receptors (22). Based on sequence similarity within the 7TM segments, these receptors could be described by belonging to five families (23):

- the rhodopsin family (701 members)
- the adhesion family (24 members)
- the frizzled/taste family (24 members)
- the glutamate family (15 members)
- the secretin family (15 members).

The physiologic function of a huge part of these 800 GPCRs is nowadays unknown: these receptors are referred to as orphan GPCRs. However, deorphanization of non-olfactory GPCRs is tough process (24), as they are a promising group of targets for the pharmaceutical industry. Actually, the number of still orphan GPRS is significantly decreasing, highlighting the efforts of scientific community on this task.

1.1.1 Structure and ligands

GPCRs bear a common structural signature made of seven hydrophobic transmembrane (TM) segments, with an extracellular amino terminus and an intracellular carboxyl terminus (Figure 1). The most variable structures among the family of GPCRs are the COOH terminus, the intracellular loop between TM5 and TM6, and the NH_2 terminus, where the greatest diversity is observed. This sequence is relatively short (10–50 amino acids) for monoamine and peptide receptors, and much larger (350–600 amino acids) for glycoprotein hormone receptors, and the glutamate family receptors. The largest amino terminal domains are observed in the adhesion family receptors. Interestingly, this structural and functional similarity of GPCRs stands in contrast to the structural diversity of the natural GPCR ligands (25).

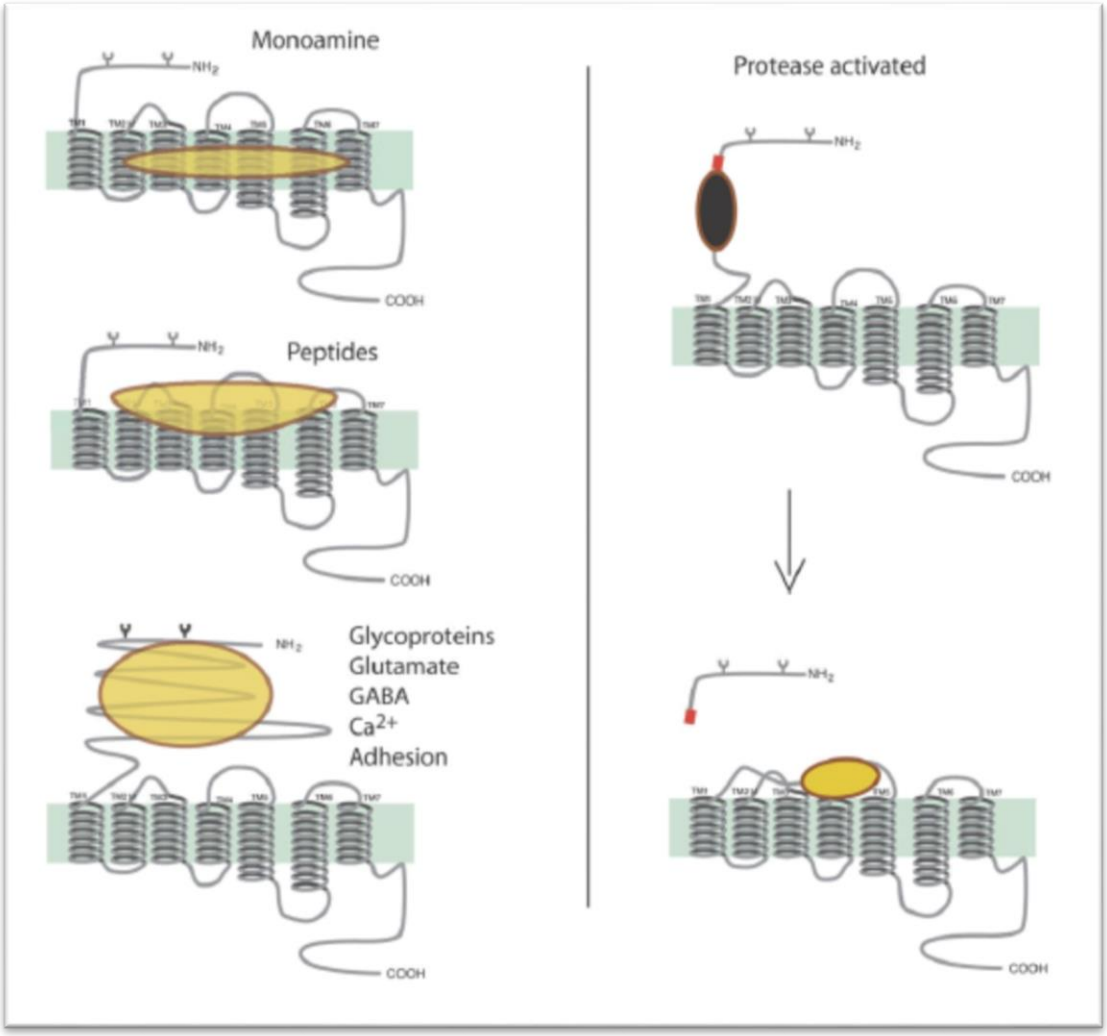

Figure 1: GPCRs diversity in NH2 and COOH termini and ligand binding position.

In fact, ligands can range from subatomic particles (a photon), to ions (H^+ and Ca^{2+}), to small organic molecules, to peptides and proteins. While many small organic agonists bind within the TM segments, peptide hormones and proteins often bind to the amino terminus and extracellular sequences joining the TM domains. However, size of the ligand alone cannot be used to predict the location of the binding site: for instance, glycoprotein hormones, glutamate, and Ca^{2+} all activate their respective receptors by binding to relatively large amino terminal domains (25) (26). Furthermore, it has been possible to identify small allosteric modulators that bind at the TM domains for many GPCRs that bind their native agonists on the extracellular loops or the NH_2 terminus (27) (28) (29). Our understanding of GPCR structure is based largely on the high-resolution structures of the inactive state of rhodopsin (Figure 2). Rhodopsin is commonly used for structural studies than most other GPCRs because it is possible to obtain large quantities of highly enriched protein from bovine retina and it is also a remarkably stable GPCR, retaining function under conditions that denature many other GPCRs.

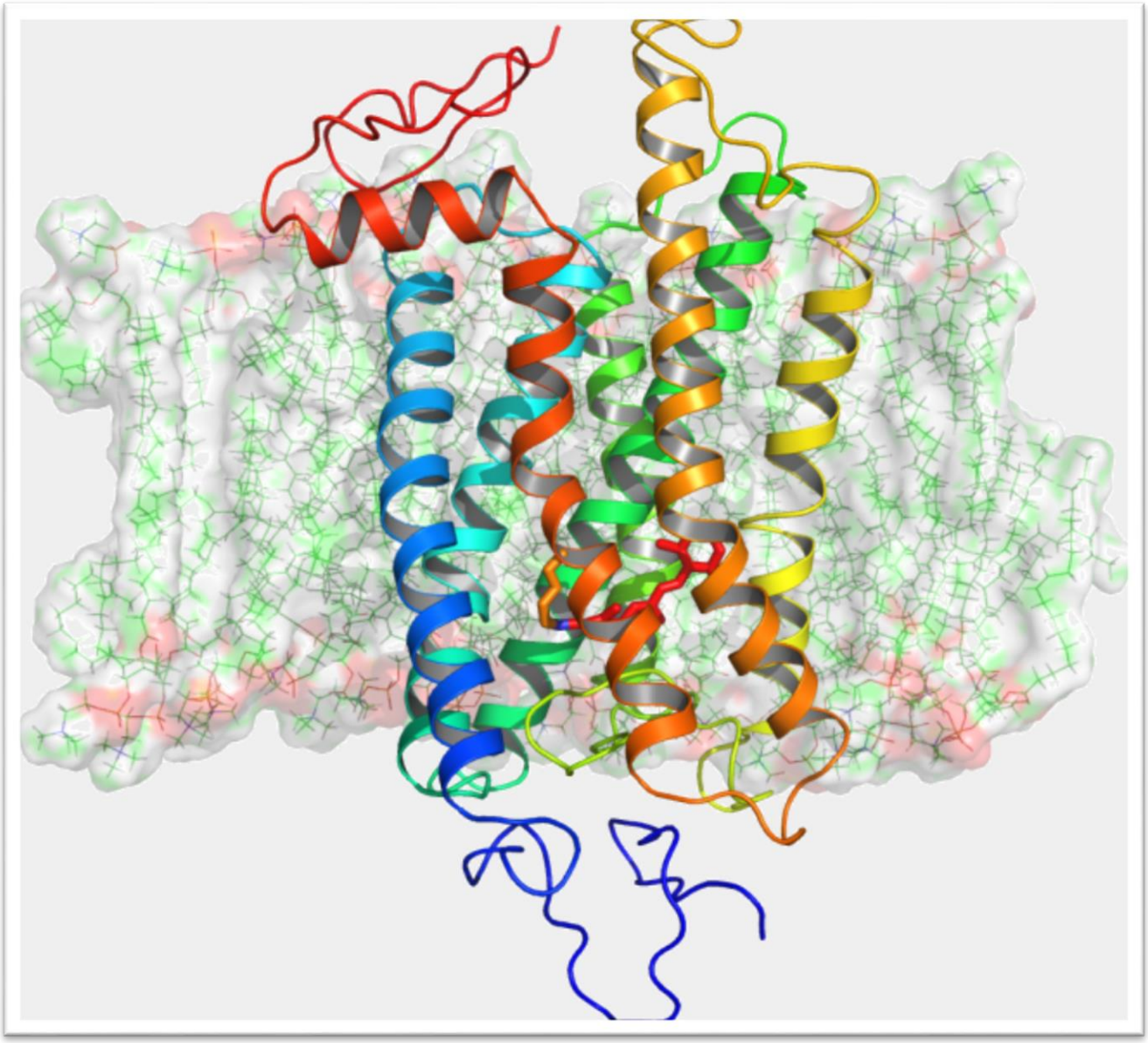

Figure 2: Crystallographic structure of rhodopsin co-crystallized with 11-cis-retinal

Moreover, there are many evidences that let to affirm that GPCRs exist as dimers (or oligomers) and that these dimers may be important for G protein activation. Dimerization is an important mechanism of receptor activation for the glutamate family of GPCRs (26) (30), where ligand-induced changes in the dimer interface of the amino terminal ligand binding domain has been demonstrated by crystallography (31) (32). However, the role of dimerization in the activation of rhodopsin family members is less clear and it remains to be seen if a receptor dimer is required for G protein activation in some cases. The effect of agonist binding on the formation or disruption of dimers is not consistent among the rhodopsin family members that have been examined (33). Moreover, ligands interact with individual receptor monomers, and there is currently no evidence that ligands could stand in between receptor dimers or span the dimer. If changes in dimerization

occur, it is likely a frequently occurring secondary consequence of ligand-induced changes in the arrangement of the TM segments. Evidence in support of this comes from biophysical studies on leukotriene B4 homodimers demonstrating that ligand binding to one protomer leads to conformational changes in its partner (34). While dimers may be important for G protein activation, it is essential to understand the agonist-induced structural changes that occur in the context of individual GPCR monomers.

1.2 Purinergic Signaling

Adenosine receptors or P1 receptors belong to the large family of purinergic receptors, described and divided in two subtypes, P1 and P2, by Geoffrey Burnstock in 1972 (35). Burnstock introduced the concept of purinergic signaling after it was shown that ATP was a transmitter in non-adrenergic, non-cholinergic inhibitory nerves in the guinea-pig taenia coli (36) and the term purinergic receptor was introduced only to describe specific membrane protein that mediate relaxation of gut smooth cells activated by adenosine triphosphate (ATP) (P2) or adenosine (P1). P2 receptors have further been divided into two families, P2Y and P2X. P2X receptors are ligand-gated ion channels, whereas the P1 or adenosine receptors (ARs) A_1, A_{2A}, A_{2B} and A_3 and P2Y receptors ($P2Y_1$, $P2Y_2$, $P2Y_4$, $P2Y_6$, $P2Y_{11}$, $P2Y_{12}$, $P2Y_{13}$ and $P2Y_{14}$) are GPCRs. P2X receptors are nonselective cation channels responsible for mediating excitatory postsynaptic responses, similar to nicotinic and ionotropic glutamate receptors. P2X receptors are distinct from the rest of the widely known ligand-gated ion channels, as the genetic encoding of these particular channels, indicates the presence of only two transmembrane domains within the channels. These purinergic receptors have been shown to be widely distributed throughout the CNS, being present early in evolution in neurons and glia; therefore, are arguably the most abundant receptors in living organisms (37). ATP acts as neurotransmitter while interacting with P2 receptors mainly as a fast excitatory response mediator or as a potent mediator in long-term processes like cell proliferation, growth and development, diseases and cytotoxicity. Nowadays, it is not fully clarified whether various physiological nucleotide-receptor agonists (e.g. ATP, ADP, UTP, UDP, UDP sugars and NAD^+) are released by common mechanisms or not. The main ways through which ATP is released extracellularly at this moment known are:

- Exocytotic neuronal vesicular release, (38)
- Vesicular release of ATP from astrocytes, (39) which perhaps involves lysosomes, (40)
- ATP binding cassette transporters, (41)
- Connexin or pannexin hemichannels, (42)
- Plasmalemmal voltage-dependent anion channels, (43)
- P2X7 receptors, (44)

- Vesicular nucleotide transporter (VNUT), secretory and synaptic vesicles in which ATP can be accumulated and released by a Cl^- dependent vesicular nucleotide transporter. (45)

ATP and other nucleotides undergo rapid enzymatic degradation by ectonucleotidases after release. Ectonucleotidases are divided in several families and each everyone of these families are expressed in the brain:

- Ectonucleoside triphosphate diphosphohydrolases E-NTPDases, hydrolyze ATP and ADP to AMP,
- Ectonucleotide pyrophosphatase and/or phosphodiesterases E-NPPs hydrolyze ATP and ADP to AMP and Dinucleoside polyphosphates, NAD^+ and UDP sugars,
- Ecto-5'-nucleotidase also called CD73 (Cluster of Differentiation 73) hydrolyze AMP to adenosine,
- Alkaline phosphatases equally hydrolyze nucleoside tri, di and monophosphates. (37)

1.2.1 Purinergic Transimission

Nucleotides and nucleosides signaling that define the purinergic transmission can be seen as a temporal sequence. (46) Nucleotides released physiologically or pathologically from intracellular sources provide either an immediate or a delayed response to a local challenge to tissues or cells. (47) The released nucleotides can act on the same or on neighboring cells, either to open fast cation channels or for signaling on a slower time scale at metabotropic GPCRs. On a more prolonged time scale, the adenine nucleotides are converted by the sequential action of ectonucleotidases to the nucleoside adenosine for activation of the ARs (Figure 3). Thus ectonucleotidases control the lifetime of nucleotide transmitters and additionally, by degrading or interconverting the originally released ligands, they also produce mediators for additional P2 receptors and nucleosides. Besides the catabolic pathways, nucleotide interconverting enzymes exert their action by nucleotide re-phosphorylation and extracellular synthesis of ATP (e.g. ectonucleoside diphosphate kinase and adenylate kinase). Furthermore, adenosine can also be sourced intracellularly, through subpopulations of neurons and/or astrocytes that release adenosine directly (48). These transformations and sequential receptor effects are related to overall biological functions irregularly occurring, such as cytoprotection, vascular adaptations, and immune effects, which may be effects in contrast at different points in the time sequence (e.g. the rapid effects of nucleotides on P2 receptors tend to boost the immune response, while the slower AR effects generally attenuate the immune response). (46)

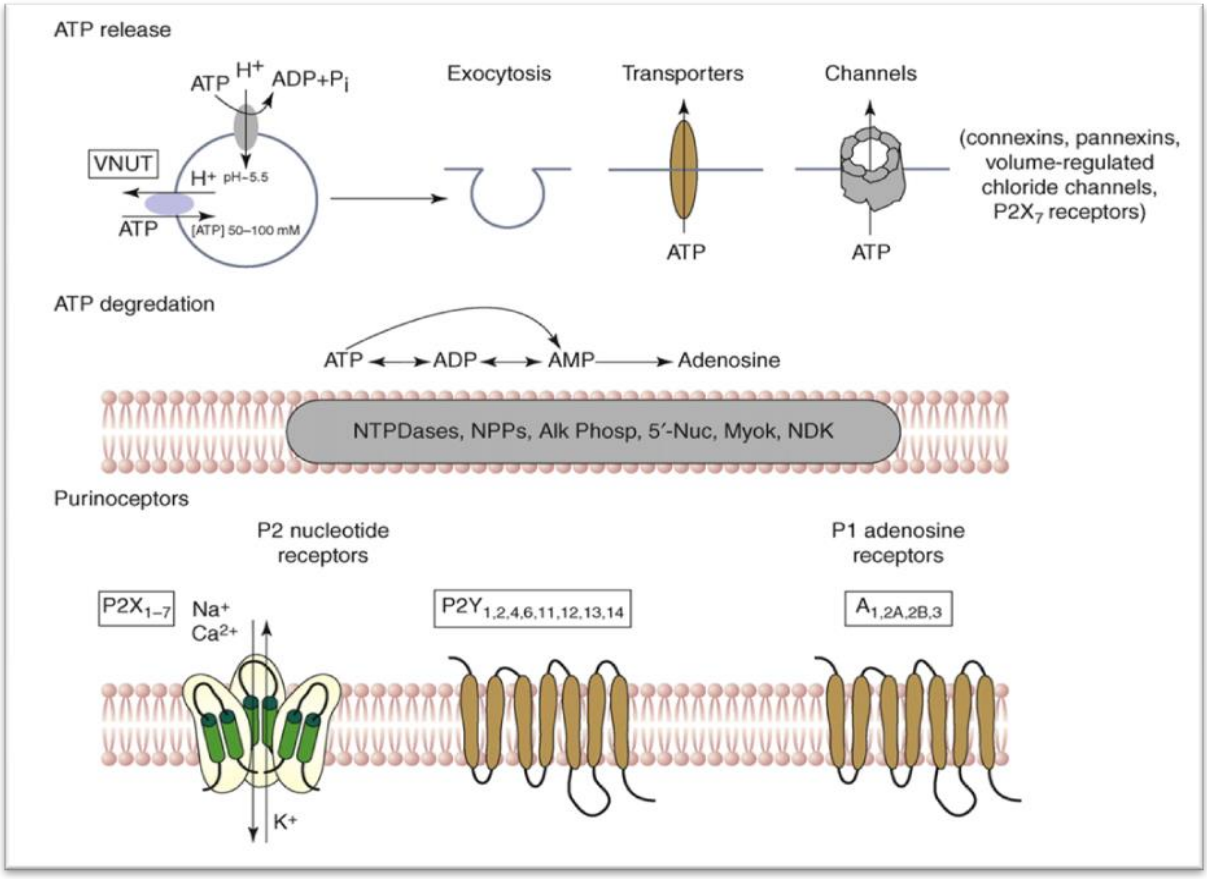

Figure 3: Mechanisms of ATP release, degradation and reception. Abbreviations: Alk-Phos, alkaline phosphatase; Myok, myokinase (adenylate kinase); NDK, nucleoside diphosphate kinase; NPPs, nucleotide pyrophosphatase and/or phosphodiesterases; 50-Nuc, 50-nucleotidase; VNUT, vesicular nucleotide transporter. (37)

1.3 Adenosine Receptors

As previously said the adenosine receptors subtypes (A_1, A_{2A}, A_{2B} and A_3) are members of the superfamily of GPCRs belonging to the subfamily of rhodopsin-like receptors and thus, show the typical heptahelical structure. Within the rhodopsin-like family A GPCRs, the TM domain is more highly conserved than the extracellular loops (ELs). TM helices, consisting of 25-30 amino acid residues each, are connected by six loops, three intracellular (IL) loops and three ELs. A disulfide link is formed between two cysteine residues present in TM3 and EL2, which are conserved in most GPCRs in order to promote packing and stabilization of a restricted number of conformations of these 7 TMs. Extracellular regions contain sites exerting post-translational modifications, such as glycosilation. The A_1 and A_3 contain also sites for palmitoylation in the C-terminus domain. The A_{2A} AR has a long C-terminal segment of more than 120 amino acid residues, which is not required for coupling to Gs, probably useful as a binding site for “accessory” proteins. The sequence

identity between the human (h) A_1 and A_3 ARs is 49%, and the hA_{2A} and hA_{2B} ARs are 59% identical. Some of these particular conserved residues point to specific functions. In deep, there are two peculiar His residues in TMs 6 and 7 of A_1, A_{2A}, and A_{2B} ARs: in the A_3 AR, this His residue is lacking but another His residue can be found in TM3. All this His residues have been indicated by mutagenesis studies to be important in recognition and/or activation of the receptor (1) (49). In the beginning, adenosine receptors were divided in subtypes A_1 and A_2 following their ability to increase or decrease the activity of adenylate cyclase (AC), respectively (50) (51). Then, A_2 receptors were further classified, by Daly and coworkers (52), relying on their affinity for the endogenous ligand adenosine: A_{2A} with high affinity (0.1-1 µM) and A_{2B} with low affinity (>10 µM). Moreover, A_3 AR was identified in 1991 through a polymerase chain reaction (PCR) performed on rat cDNA encoding a GPCR that showed high affinity (58%) with A_1 and A_{2A} AR (53). This "new" receptor revealed an unconventional low homology between its homologous in other species (e.g. 72% versus rat A_3 AR) considering the other ARs (85-95 % of homology versus rat).

1.3.1 Crystallographic structure

Despite 25 years were passed since the discover of all AR subtypes, nowadays only the crystal structure of A_{2A} AR has been determined. Nevertheless, ARs characterization began long before the determination of the crystal structure of A_{2A} AR: prior to the report of the crystallographic structure of the A_{2A} AR (54), the only method to represent the 3D structure of the ARs passed through molecular modeling studies. This approach relied on information from convergent sources: homology modeling of the protein and ligand docking, receptor mutagenesis (1995) (55), and both qualitative and quantitative structure activity relationship (SAR) of ligands. The structure of the A_{2A} AR was determined in multiple forms with different ligands. Both antagonist-bound and agonist-bound states of the receptor were solved initially by the Stevens's group using the stabilizing fusion protein T4 lysozyme. Jaakola and coworkers (54), obtained the 2.6 Å crystal structure of A_{2A} AR engineered the receptor to improve on thermostability by the insertion of the very stable lysozyme from T4 bacteriophage (T4L) for most of the third intracellular loop (Leu209-Ala221), and by deletion of the larger part of the very flexible C terminus (Ala317-Ser412) (Figure 4). This construct (A_{2A}-T4L-C) was further stabilized during purification with high concentrations of sodium chloride and cholesterol and a receptor-saturating concentration of the antagonist theophylline, which was replaced by the high affinity agonist 4-(2-(7-amino-2-(2-furyl)-1,2,4-triazolo[2,3-*a*]-1,3,5-triazin-5-yl)amino)ethyl)phenol (ZM241385, Figure 14) in the final purification step. A_{2A} AR complexes crystallized by Heptares Therapeutics using thermostabilized receptors by systematic scanning mutagenesis (StaRs) include several other agonists and antagonists (56).

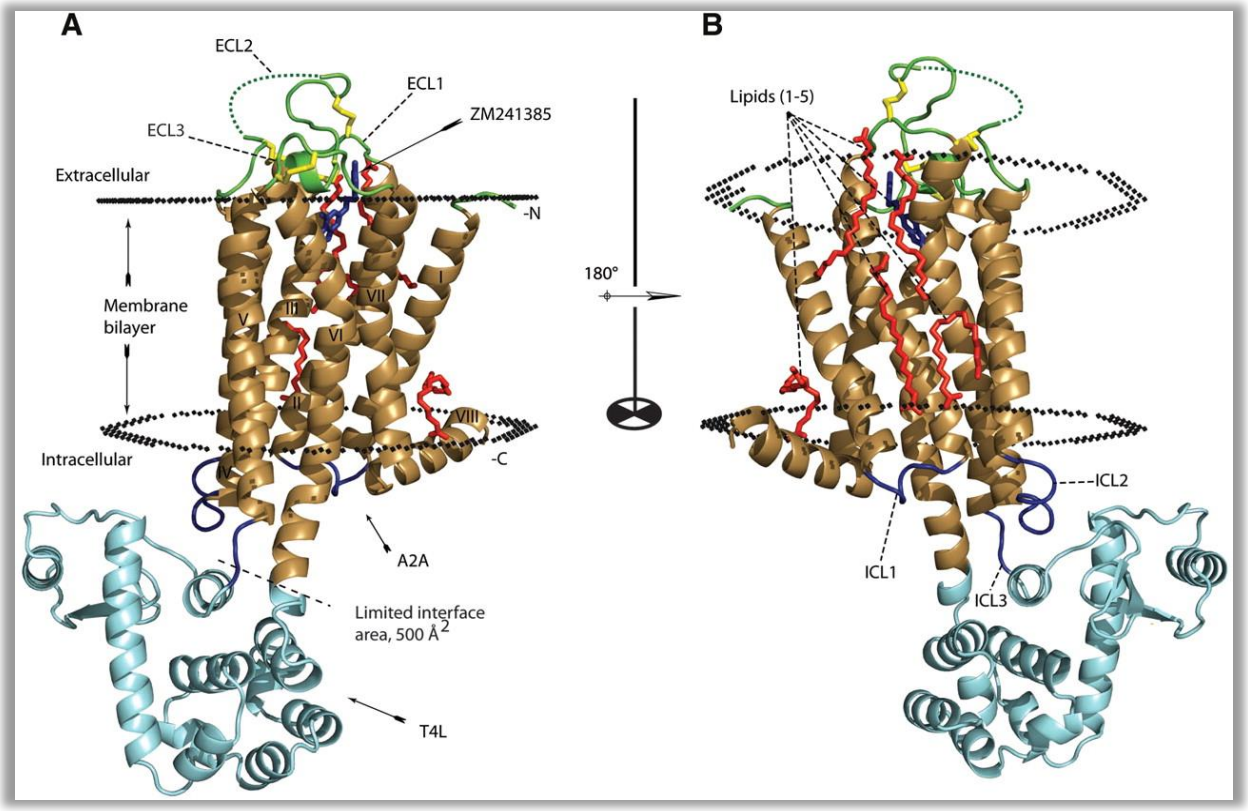

Figure 4: Crystal structure of A2A-T4L-ΔC. (A) Overall topology of A2A-T4L-ΔC. The transmembrane part of A2A-ΔC structure is colored brown (helices I to VIII), and the T4L is in cyan. The structure is viewed perpendicular to the plasma membrane. ZM241385 is colored blue, and the five lipid molecules bound to the receptor are colored red. The four disulfide bonds are yellow. The sulfate ions are omitted. The extracellular loops (ECL1 to 3) are colored green, and the intracellular loops are colored blue (54).

The differences in the particular architecture of agonist- and antagonist-bound conformations have been analyzed in detail for the A_{2A} AR and by analogy to other ARs (57). The conformation of the A_{2A} AR complex with UK-432097 (Figure 5) (57), although lacking a G-protein or equivalent, displays features of an active-like conformation, e.g., ionic lock spreading. TMs 5, 6, and 7 engage in most of the conformation movement that leads to receptor activation, while the only pronounced movement within TMs 1-4 is a piston-like upward movement of TM3 to accommodate an agonist.

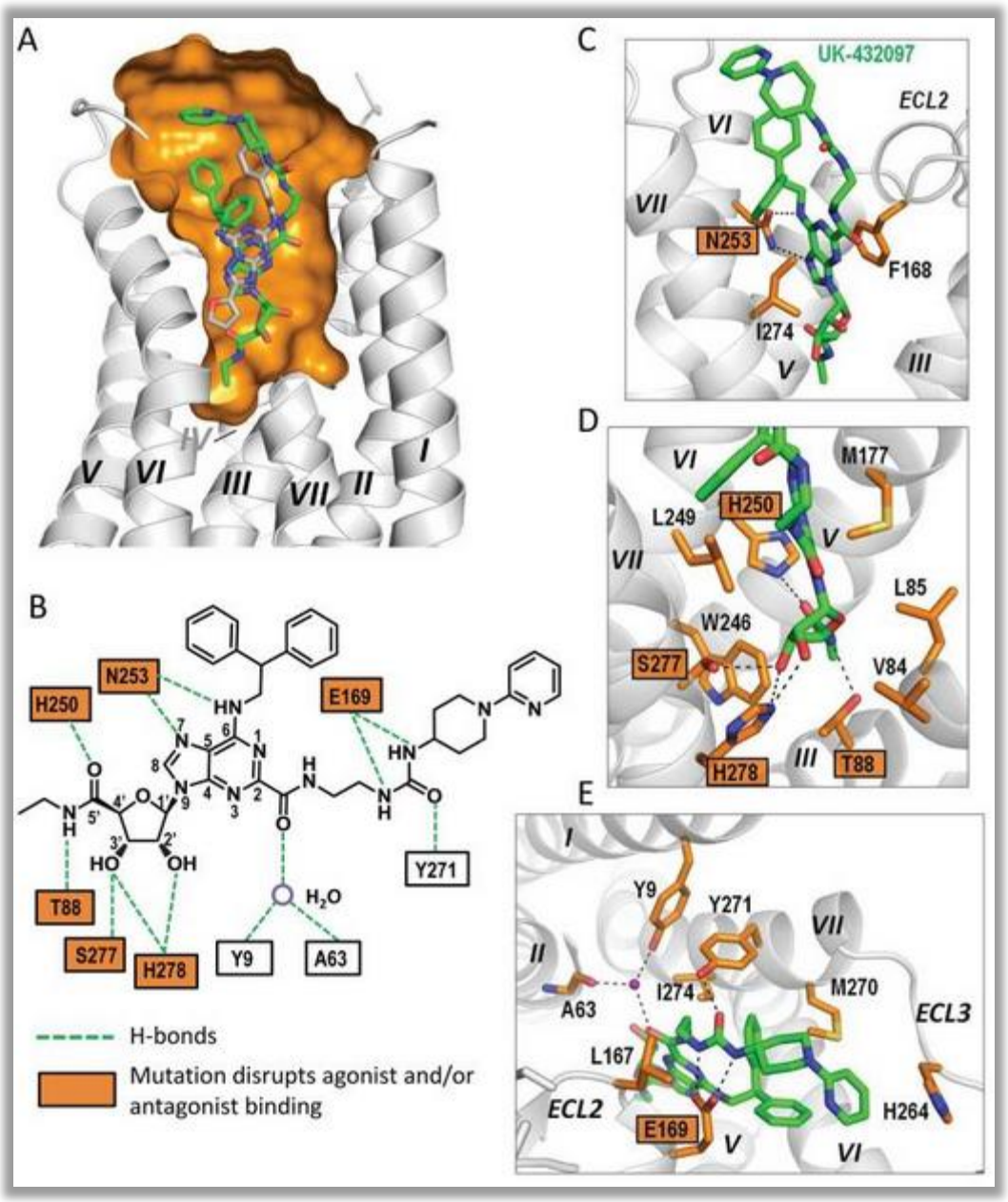

Figure 5: Ligand UK-432097 and its binding cavity. (A) Overall view of the ligand-binding cavity. The transmembrane part of $A_{2A}AR$ is shown as ribbon and colored gray (helices I to VII). Ligand UK-432097 is shown as bright green stick. For comparison, ligand ZM241385 (gray stick) is also shown at the position when the two complex structures were superimposed. The binding cavity is represented by orange. (B) Schematic representation of the hydrogen-bonding interactions (green dashed lines) between $A_{2A}AR$ and UK-432097. (C) Molecular interactions within the ligand-binding cavity for UK-432097 around the adenine moiety. Interacting residues are shown as sticks with side chains colored orange. Hydrogen bonds between $A_{2A}AR$ and ligand are shown as black dotted lines. (D) Molecular interactions around the ribose moiety. (E) Molecular interactions around the ligand substitution sites. A water molecule is shown as purple sphere. In (B)-(E), residue mutations reported to disrupt agonist and/or antagonist binding are indicated with orange squares (57).

The agonist-bound structure of $A_{2A}AR$ features a contracted ribose binding region in which hydrophilic residues (His) of the pocket are drawn toward H bonding groups of the ribose (Figure 6).[201]

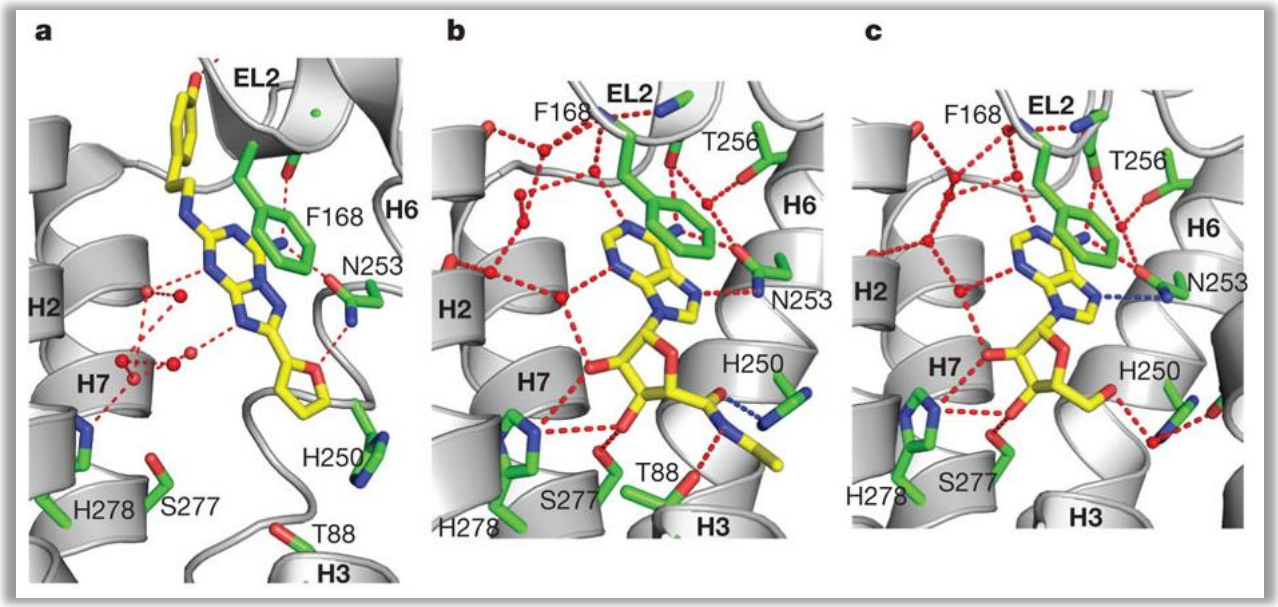

Figure 6: Structures of the $hA_{2A}R$ in cartoon representation are shown bound to the following ligands: (a) ZM241385; (b) NECA; and (c) adenosine.[20a]

1.3.2 Homomers and Heteromers

Adenosine receptors, like other class A GPCRs, have been thought to exclusively occur in a monomeric state for a long time. Monomeric receptors are enough to induce signaling. At least some studies suggest signaling via dimers occurs only at higher receptor densities. More recently, however, evidence is accumulating that adenosine receptors can form dimeric or, more generally speaking, multimeric or oligomeric structures. Through self-association, homo-oligomers ("homomers") can be formed. Hetero-oligomerization leading to "heteromers" may be the consequence of the association between adenosine receptors and preferred partners, mostly other GPCRs, including other adenosine receptor subtypes. This phenomenon has been demonstrated through a variety of experimental techniques, mostly in artificial cell lines. The use of overexpressed recombinant receptors may result in the creation of many more oligomers than naturally exist. In some cases, bioluminescence resonance energy transfer (BRET) may detect interactions between receptors that are in close proximity in a compact structure such as a coated pit, rather than forming true molecular dimers. Furthermore, GPCRs contain hydrophobic regions that can oligomerize, even after solubilization in sodium dodecyl sulfate (SDS). Hence, receptor dimerization or oligomerization may occur after solubilization in detergent and not be representative of receptor structure and organization in the membrane (1).

In theory, four homomeric pairs can be predicted for adenosine receptors, but only reports with experimental evidence for the occurrence of A_1-A_1 and A_{2A}-A_{2A} homomers have been published.

A_1-A_1. Both Ciruela (58) and Yoshioka (59) used antibodies against the wild-type adenosine A_1 receptor to show how immunoprecipitation experiments analyzed with Western blotting revealed higher order bands in some instances. In another recent study by Briddon (60), A_1-A_1 homomers, predominantly located at the cell surface, were identified with Bimolecular Fluorescence Complementation (BiFC) techniques in CHO cells expressing *yellow fluorescent protein* (YFP) tagged receptors.

A_{2A}-A_{2A}. The first evidence for A_{2A} receptor homodimerization was provided by Canals et al. (2004)[60]. The authors used both FRET and BRET techniques as well as immunoblotting to show that in transfected HEK293 cells, overexpressed recombinant A_{2A} AR exist as both homodimers and monomers. They demonstrated, by means of cell surface biotinylation experiments, that after detergent solubilization, approximately 90% of the cell surface recombinant A_{2A} AR species exists as a homodimer. The same pattern of dimer formation was observed for an engineered A_{2A} AR lacking the C terminus, whereas this receptor mutant was no longer able to dimerize with the dopamine D_2 receptor. A_{2A} AR homodimerization was also demonstrated with BiFC techniques by Vidi (61), who also used a combination of fluorescence resonance energy transfer (FRET) and BiFC techniques to demonstrate that recombinant A_{2A} AR exist as higher order oligomers, consisting of at least three monomers, at the plasma membrane of differentiated neuronal cells.

Available evidence points to the interaction of both A_1 and A_{2A} ARs with other GPCRs, however no direct data have been reported for adenosine A_{2B} and A_3 ARs.

A_1-A_{2A}. The two receptors are co-localized in striatal glutamatergic nerve terminals, both pre- and post-synaptically. This was demonstrated in immunogold blotting and, after detergent solubilization, co-immunoprecipitation experiments (62). In HEK293 cells transfected with tagged A_1 as well as A_{2A} ARs, evidence in BRET and FRET experiments was found for a direct interaction between the two recombinant receptors. Radioligand binding studies in membranes of these Human Embryonic Kidney 293 cells (HEK293) demonstrated that agonist binding to the A_{2A} AR influenced the affinity of (*R*)-N^6-phenylisopropyladenosine (R-PIA, Figure 11) for the A_1 AR, but not vice versa. These findings constitute a mechanism for fine-tuning the release of glutamate by adenosine.

Nevertheless, heteromerizations such as A_1-$P2Y_1$ (59), A_1-$P2Y_2$, A_1-D_1, A_{2A}-CB_1 (61) and A_{2A}-D_2-CB_1, A_{2A}-D_3, , and A_1-Thromboxane A_2 (1) have been demonstrated in many studies in literature.

A_{2A}-D_2 The heteromeric pair of A_{2A} AR and D_2 receptors is probably the most studied combination. In fact, double immunofluorescence experiments with confocal laser microscopy showing substantial co-localization of recombinant A_{2A} AR and dopamine D_2 receptors in cell membranes of SH-SY5Y human neuroblastoma cells stably transfected with human D_2 receptor, as well as in cultured striatal cells have been performed (63) (64)

There are evidences that heteromerization may also occur between adenosine receptors and proteins belonging to other superfamilies, in particular adenosine deaminase and calmodulin, like A_1-D_1 with adenosine deaminase and A_{2A}-D_2 with calmodulin. There is thus very good evidence that recombinant adenosine receptors can form homo- and heteromultimers. It is less clear, however, whether this has important pharmacological consequences in physiological tissues. In a dimeric complex, both receptors may not be simultaneously active and signaling. This implies that the signaling pathway and consequentially the derived response can be very complex. It is unclear which rules determine how partnerships are formed. Thus, the fact that adenosine receptors can form multimeric complexes with different members will necessitate much more work on signaling in intact cells in vivo (65).

1.3.3 Desensitization

Continued or repeated exposures to an agonist usually result in a flat receptor-mediated response followed by decreasing of this response despite the continual presence of agonist. Kinetically, this process is called desensitization (66). GPCRs undergo desensitization through a complex phenomenon involving multiple and temporally distinct components. The mechanisms underlying a rapid desensitization frequently involve receptor phosphorylation by a family of G protein-coupled receptor kinases (GRKs) resulting in their preferential binding to arrestins, that promote desensitization by uncoupling the receptor from its G-protein, leading to impaired receptor function (67). Following desensitization, many GPCRs internalize by an arrestin-dependent process via clathrin-coated pits which leads to the subsequent intracellular dephosphorylation of the receptor, and its re-insertion into the cell membrane leading to a resensitized state (68). More prolonged agonist activation generally leads to a subsequent down-regulation by lysosomes (69). These processes that form the physiological life of a receptor are deeply involved in the receptor-related response. It has been already shown that activation of all four AR subtypes eventually leads to their desensitization by different mechanisms. Actually, most of these observations are made following administration of non-hydrolysable agonists to cell cultures and animals and it is yet unclear how significant a role receptor desensitization plays in regulation of ARs by adenosine *in vivo* under physiological conditions. Studies have shown that upon addition of agonists, the A_1 AR is phosphorylated and internalized slowly, with a half-life of several hours. In contrast, A_{2A} and A_{2B} ARs demonstrate a more rapid rate of down-regulation, usually lasting about an hour. Finally, the down-regulation and desensitization of the A_3 AR occurs within minutes (70). Thus, it is important to understand their regulation in order to design drugs that can exploit or avoid the receptor-mediated signaling to treat diseases.

A_1 AR: Several studies have been carried out to understand the molecular mechanisms underlying A_1 AR desensitization. In an early study, Parson and Stiles (71) showed that the A_1 AR in rat adipocytes desensitized upon chronic administration of A_1 AR agonist R-PIA (Figure 11), over a period of six days by Alzet minipumps (Alza Corporation, Vacaville, CA, USA). A decrease in A_1 AR levels and reduced inhibition of isoproterenol-stimulated adenylyl cyclase activity was detected following R-PIA treatment. These changes were associated with decreased levels of pertussis-sensitive G proteins, but an increase in Gs proteins in the plasma membranes. Furthermore, adipocyte membranes obtained from R-PIA-treated rats showed enhance isoproterenol and forskolin-stimulated adenylyl cyclase. These studies suggest that adipocytes increase the stimulatory response (*i.e.*, increase in adenylyl cyclase activity) because of a chronic activation of the A_1 AR. A subsequent study performed in cultured adipocytes confirmed the *in vivo* findings and further demonstrated that desensitization of the A_1 AR was associated with desensitization of insulin-dependent glucose transport (72). This suggests a common link between desensitization of the A_1 AR and insulin receptor. A later study by Longabaugh and coworkers (73) confirmed the previous findings that desensitization of the A_1 AR to R-PIA was linked to reductions in A_1 AR and Gi proteins and an increase in Gs_α proteins, but showed that the changes in Gi_α proteins were not dependent by alternations in their mRNA levels. Jajoo *et al.* (74) deepened the role of β-arrestin 1/extracellular signal-regulated kinase (ERK1/2) MAPK pathway in the regulation of A_1 AR desensitization and recovery in ductus deferens smooth muscle (DDT1-MF2) cells. They reported that applying the A_1 AR agonist R-PIA for 24 h resulted in a decrease of A_1 AR on the membrane which was associated with an unexpected 11-fold increase in A_1 AR mRNA. This effect was dependent on β-arrestin 1, knocked-down by siRNA blocked R-PIA-mediated down-regulation of the A_1 AR. In addition, β-arrestin 1 knockdown by siRNA suppressed R-PIA-dependent ERK1/2 and activator protein-1 (AP-1) activities and reduced the induction of A_1 AR mRNA. Interestingly, withdrawal of the agonist after a 24 h exposure resulted in rapid recovery of plasma membrane A_1 AR, which was dependent on the *de novo* protein synthesis and on the activity of ERK1/2 but independent of β-arrestin1 and NF-κB. These findings suggest that the β-arrestin 1/ERK1/2 pathway, which contributes to the desensitization and down-regulation of A_1 AR, is also able to prime the transcriptional machinery for rapid synthesis of the A_1 AR after withdrawal of the agonist. Chick embryo retina cultures of eight days treated for 48 h with CGS 21680 and *N*6-(2(3,5-dimethoxyphenyl)-2-(2-methylphenyl)ethyl)-adenosine (DPMA), selective A_{2A} AR agonists, showed an increased expression of A_1AR. This effect was blocked by the selective A_{2A} AR antagonist, ZM 241385 (Figure 14), and PKA inhibitor N-[2-[[3-(4-bromophenyl)-2-propenyl]amino]ethyl]-5-isoquinolinesulfonamide (H89) (75). These *in vitro* findings were confirmed in an *in vivo* study where chick embryo retinas were treated for 48 h with A_1 AR agonist CGS 21680 (Figure 13). In this study, CGS 21680 was able to increase the expression of A_1 AR which was blocked by selective A_{2A}AR antagonists, SCH 58261 and ZM 241385. Interestingly, under normal conditions, endogenous adenosine produced and released into the environment of the retina appears to control A_{2A} AR-mediated

expression of A_1 AR, since the treatment with ZM 241385 and SCH 58261 aa alone was capable of reducing the expression of A_1 AR (76). These findings indicate that up-regulation of A_1 AR by long-term activation of A_{2A} AR depends on classical AR signaling pathway.

A_{2A} AR: Short-term agonist exposure induced a rapid desensitization of A_{2A} AR-stimulated AC activity which was associated with a diminished receptor-Gs coupling, and agonist-stimulated phosphorylation of the A_{2A} AR. Longer agonist treatment, on the other side, resulted in down-regulation in total receptor number and up-regulation of α-subunits of G_i (77). The structural requirements necessary for the agonist-induced desensitization of A_{2A} AR resides in its COOH-terminus. Palmer and Stiles (78) introduced various mutations in the 95 amino acid sequence of the COOH-terminus of A_{2A} AR which contains ten different phosphorylation sites and identified Thr298 to be essential in agonist-induced receptor phosphorylation and short-term desensitization, being, at the same time, not involved in long-term desensitization of A_{2A} AR function. These findings confirm that short-term and long-term desensitization of A_{2A} AR could be mediated by structurally distinct regions of the receptor protein and may involve different mechanisms.

A_{2B} AR: A serine residue (Ser329), close to the COOH-terminus, was revealed as critical for the rapid agonist-induced desensitization and internalization of the receptor (79) through point mutation or deletion studies of rat A_{2B} AR stably expressed in CHO cells. Due to a GRK-2 and arrestin-dependent mechanism, A_{2B} AR undergoes rapid agonist-induced desensitization and internalization. Expression of a dominant negative mutant of GRK-2 in NG108-15 cells (80) or antisense-induced inhibition of non-visual arrestins (arrestin-2 and -3) in human embryonic kidney (HEK-293) cells (81) efficiently reduced the rate of agonist-induced desensitization and internalization of endogenous A_{2B} AR. In another study, A_{2B} AR was shown to internalize in an arrestin- and dynamin-sensitive manner (82). On the other hand, second messenger-dependent kinases, such as PKA and PKC, did not seem to be involved in agonist-mediated phosphorylation and subsequent desensitization of A_{2B} AR (83). Human astrocytoma cells which endogenously expressed A_{2B}AR showed that tumor necrosis factor α (TNFα), a pro-inflammatory cytokine, markedly reduced agonist-dependent receptor phosphorylation on threonine residues and attenuated agonist-mediated A_{2B} AR desensitization (84). TNFα-induced inhibition of A_{2B} AR desensitization could result in prolonged A_{2B} AR responsiveness and may contribute unregulated activation of astrocytes that eventually occurs in neurodegenerative diseases. In a recent study, it was proposed that A_{2A} AR is involved in the expression of A_{2B} AR in human embryonic kidney cell line, AD-293, transfected simultaneously with mouse A_{2A} AR and A_{2B} AR. It was found that newly synthesized A_{2B} AR is retained in the endoplasmic reticulum (ER) and is eventually targeted for degradation by the proteasomes that, when inhibited, was not sufficient to enhance maturation and surface expression of the receptor. These findings support the notion that A_{2A} AR and A_{2B} AR form heterodimer complexes for trafficking and function (85).

A_3 AR: A_3 AR undergoes rapid desensitization of receptor function after prolonged application of an agonist, as a result of phosphorylation of the receptor protein by members of the family of GRKs (86) (87). It was demonstrated (88) that a triple mutant, Thr307/Ala307, Thr318/Ala318 and Thr319/Ala319 within the COOH-terminus, showed marked reduction in agonist-stimulated phosphorylation and desensitization of rat A_3 AR. Individual mutations of each residue showed that Thr318 and Thr319 are the two major sites for phosphorylation where Thr318 appeared to be necessary to observe phosphorylation at Thr319, but not *vice versa*. Moreover, mutation of two palmitoylation sites of rat A_3 AR within the COOH-terminus, Cys302 and Cys305, which controls the GRK phosphorylation sites, revealed basal phosphorylation even in the absence of an agonist. This suggests an important regulatory role of these palmitoylation sites in receptor desensitization. Receptor kinetics of A_3 AR was studied (89) in human astrocytoma cells. Short-term exposure to the agonist 2-chloro-*N*6-(3-iodobenzyl)-*N*-methyl-5'-carbamoyladenosine (Cl-IBMECA, Figure 17) caused rapid receptor desensitization followed by internalization within 15 and 30 min, respectively. Agonist removal resulted in recycling of the A_3 ARs to the cell surface within 120 min. Long-term exposure (1–24 h) resulted in a higher receptor down-regulation and the restoration of receptor levels was also slow (24 h). MAPK was shown to regulate agonist-induced phosphorylation of A_3 AR where its stimulation mediated activation of ERK1/2 within 5 min of agonist exposure in CHO cells stably expressing A_3 AR. Treatment with PD98059, a well-characterized MAPK kinase inhibitor, showed impaired receptor phosphorylation, desensitization and internalization by inhibiting GRK-2 translocation from cytosol to the plasma membrane. These data suggest that A_3 AR activation is regulated by ERK1/2 in a feedback mechanism which controls GRK-2 activity and prevents receptor phosphorylation (90). These findings could explain the dual and opposite role of A_3 AR in neuroprotection and neurodegenerative diseases.

1.3.4 Physiopathological role of ARs

Receptor name	Human gene	G proteins	Localization	Potency of adenosine*
A_1 AR	*ADORA1*	$G_{i,o}$	Broad distribution: high in nerves, heart, kidney and adipose tissue	10^{-8} to 10^{-7}
A_{2A} AR	*ADORA2A*	$G_{s/olf}$	Broad distribution: very high in basal ganglia; high in nerves, blood vessels and immune cells	10^{-8} to 10^{-7}
A_{2B} AR	*ADORA2B*	G_s ($G_{q/11}$; $G_{12/13}$)	Broad distribution, but generally low abundance	3×10^{-7} to 10^{-5}
A_3 AR	*ADORA3*	$G_{i,o}$	Restricted distribution, varying in different species: high in mast cells	10^{-8} to 10^{-7}

Table 1: Adenosine receptors distribution and signaling. *The potency (in mol/l) is determined by the effect of the agonist in cells expressing approximately 2 × 105 receptors per cell.

Adenosine is fully considered a homeostatic regulator due to the wide range of effects mediated the binding at adenosine receptors. ARs play an important role in several key physiological processes, ranging from neuromodulation to immune regulation, and from vascular function to metabolic control. One approach that has proved to be particularly effective in uncovering the normal physiological roles of adenosine receptors is genetic knockout mouse models (91) for all four adenosine receptors (*Adora1*, *Adora2a*, *Adora2b* and *Adora3* are the genes encoding A_1, A_{2A}, A_{2B} and A_3 ARs, respectively, see Table 1 above) generated by the targeted deletion of either of the two critical exons of the adenosine receptors (92). Although detection of the pathophysiological roles of adenosine signaling requires models of disease in the genetically modified organism, the available genetic knockout mouse models have actually provided important evidences. Two lines of *Adora1*-knockout mice have been generated (93) and *Adora1*-knockout mice exhibit decreased fertility, a significant decrease in lifespan and an increased risk of seizures (6). In the kidney, studies conducted on knockout mice have confirmed that the stimulation at A_1 AR on the glomerular afferent arteriole reduces renal blood flow and the glomerular filtration rate, and stimulation of the A_1 receptor on the proximal tubules increases sodium and water reabsorption. These studies led to the rational approach for developing A_1 receptor antagonists to control renal dysfunction in patients with acute heart failure. A_{2A} AR are expressed at high levels in the dorsal striatum, a critical basal ganglia structure involved in motor control, where they are co-localized with dopamine D_2 receptors: they inhibit D_2 receptor binding in the striatum and immediate-early gene expression. The behavioral effect given by the application of A_{2A} AR antagonists partly overlap with those of D_2 receptor agonists, useful for the treatment of Parkinson's disease (PD), in which D_2 receptors are fully involved, and also influencing working memory (94), reversal learning (95) and goal-oriented behavior (96), although leaving spatial reference memory, motor function and anxiety-like behaviors intact. Regarding A_{2A} AR, three strains of *Adora2a*-knockout mice have been generated exhibiting reduced exploratory behavior and an higher score in anxiety tests, with male mice being much more aggressive towards intruders (97). Due to the reduced activity they gain weight, especially as fat. Their response to acute pain stimuli is slower and their blood pressure and heart rate are elevated (98). Genetic *Adora2a*-knockout models have uncovered complex roles of the A_{2A} AR in tissue protection: in fact, A_{2A} AR activation confers tissue protection in peripheral organs (99), while its inactivation confers neuroprotection against brain injury (100). Genetic knockout models have shown that both A_1 and A_{2A} AR are involved in mediating the sleep-promoting properties of adenosine in the brain (101) and the arousal effects of caffeine seen in wild-type animals are dampened in *Adora2a*-knockout mice (9) lead to consider that AR ligands could be used as normal cognitive enhancers or sleep promoters. Moving on A_{2B} AR, several strains of *Adora2b*-knockout mice have also been generated (102) (103). Assumed A_{2B} AR as a low-affinity receptor that is mostly expressed at low levels, it could be quiet unexpected that *Adora2b*-knockout mice have very strong phenotypes, especially in relation to the vasculature (103). *Adora2b*-knockout mice show reduced inflammation of the vascular tissue at the baseline and suffer from increased vascular leakiness in several

organs (104). A major reason for this evident effect of A_{2B} AR could be that local adenine nucleotide signaling is fully involved in this compartment and thus adenosine levels can transitorily be considerably high (104). However, an increased susceptibility to ischemic and inflammatory wounds is observed in the intestine, liver, kidney, lung and heart of *Adora2b*-knockout mice (105) (106), with disorders characterized by higher extracellular adenosine levels. Under such conditions, studies in *Adora2b*-knockout mice have shown that A_{2B} receptor signaling is implicated in attenuating hypoxia-driven inflammation and in the adaptation of tissues to conditions of limited oxygen availability. Moreover, activation of the A_{2B} AR has been shown to promote bone cell differentiation, control glucose homeostasis and regulate hyperlipidemia and atherosclerosis (107) (108). On the other hand, some harmful effects of A_{2B} AR activation have also been reported, including promotion of tumor growth in the bladder and breast, renal fibrogenesis and inflammatory damage in an experimental autoimmune encephalomyelitis (EAE) model of multiple sclerosis (109) (110).

Knockout of the A_3 AR in mice was similarly surprising, resulting in marked phenotypes even at locations where the receptors have a low density (for example, the brain) and where ligands have little effect. (111) Interestingly A_3 AR knockout mice shown an increased protection from the ischemic damage both in Langendorff heart and *in viv*o coronary occlusion model versus wild type mice (112). These evidences lead to hypothesize that the proinflammatory role of A_3 AR may be strictly connected with this deletion related effect. Moreover, unknown compensatory changes due to the *adora3* knockout may contribute to the paradox finding of an ischemia-tolerant phenotype (113). A_3 KO animals benefit of hemodynamic changes due to the increase of A_{2A} and A_{2B} ARs signaling and the conjugated increasing in cAMP release. Nevertheless, they suffer of a more pronounced drop of blood pressure than wild-type mice (114). A_3 AR KO mice shown actually protection from renal failure caused by ischemia-reperfusion injury or by myoglobinuria (115): this effect was confirmed by application of A_3 AR antagonist, that could be candidate for the renal failure treatment. Targeted deletion of A_3 AR confirmed the hypothesis that this receptor is involved in glaucoma opening to the treatment of this condition, one of the leading cause of blindness (116).

Adenosine signaling is not largely noticeable in physiological condition, but aberrant adenosine signaling is implicated as a common disease mechanism underlying inflammatory and ischemic tissue damage (117). This includes excessive inflammatory tissue damage such as in acute liver injury, ischemic kidney injury, acute lung injury, traumatic brain injury, ischemic brain injury, epilepsy and some neurodegenerative disorders such as Parkinson's disease and Huntington's disease (91) (118) (100). As such, enhanced adenosine signaling is crucial in these pathological conditions associated with tissue inflammation and remodeling.

Together with dramatic increases in extracellular adenosine levels, conditions of tissue hypoxia are associated with enhanced expression of adenosine receptors, particularly the A_{2A} AR (119) and A_{2B} AR, and a marked induction of ENTPD1 (120) (121) and NT5E, as these pathways are tightly controlled on a

transcriptional level. During ischemia, activation of A_{2B} AR has been shown to promote ischemia tolerance, improve oxygen-efficient metabolism and protect against ischemia-reperfusion injury of the heart, kidneys or intestine (122). Triggering A_{2B} AR can reduce the activation and transmigration of inflammatory cells into post-ischemic tissues and protect against sepsis-induced mortality by dampening an excessive inflammation response to the damage (123). Moreover, activation of A_{2A} receptors on inflammatory cells invading the tissue can be an efficient treatment for reperfusion injury (124) (125): for example, activation of A_{2A} AR expressed on T cells or dendritic cells (126) has been associated with the attenuation of organ injury during hepatic or renal ischemia, respectively. Moreover, A_1 AR are downregulated by hypoxia in C6 glioma cells (127).

Adenosine receptor expression may be different as physiological levels in cancer cells, but the significance of this is yet unclear. Hypoxia in solid tumors is associated with increased levels of ENTPD1-and NT5E-dependent adenosine, causing A_{2A} AR-mediated attenuation of the immune response against cancer. On the other hand, A_{2A} AR inactivation in the brain has been consistently associated with protection against brain damage after ischemia, excitotoxicity, traumatic brain injury (128) (129) and neurodegeneration in Parkinson's disease (130) and Alzheimer's disease (131). In some cases, both sides of the A_{2A} AR modulation have a protective effect, including in animal models of Huntington's disease (132) (133) and spinal cord injury.

Several transcriptional mechanisms contribute to the induction of A_{2A} AR, A_{2B} AR and ecto-nucleotidase expression in response to stress, hypoxia and inflammation and other pathological insults as well as a local increase in adenosine levels. Hypoxia is associated with a transcriptional program that results in the induction of ENTPD1 and NT5E thereby elevating the production of extracellular adenosine production. Moreover, ENTPD1 and NT5E have been implicated in the conversion of ATP and ADP to adenosine on regulatory T cells, thereby providing an autocrine feedback loop to enhance the anti-inflammatory functions of this subset of T cells (134).

1.3.5 Adenosine receptors as therapeutic targets

In the last decades many efforts have been made in order to fully understand AR signaling pathways and many AR ligands have been developed as potential therapeutics useful for a wide range of diseases. Many of the synthetized compounds nowadays are very potent (in the low nanomolar range or even subnanomolar) and selective (100 to 300 times more potent versus the others AR subtypes). However, the biggest issue regards druggability, in particular what may concern tissue distribution and bioselectivity. In fact, ARs have a broad distribution in the human body and some tissues have a larger "receptor reserve" than other tissues (e.g. adipocytes). Decades of expertise and clinical studies gave the chance to better understand how ARs

ligands could be useful in therapy and give a clearer view of a very complex scenario, concerning the openly wide physiopathological range of effects in which ARs are involved in. In theory, ARs ligands application in therapy are partially summarized in Figure 7 and in Table 2 but few of these disease or therapeutic indications are targeted by clinical studies and even less are AR ligands in therapy.

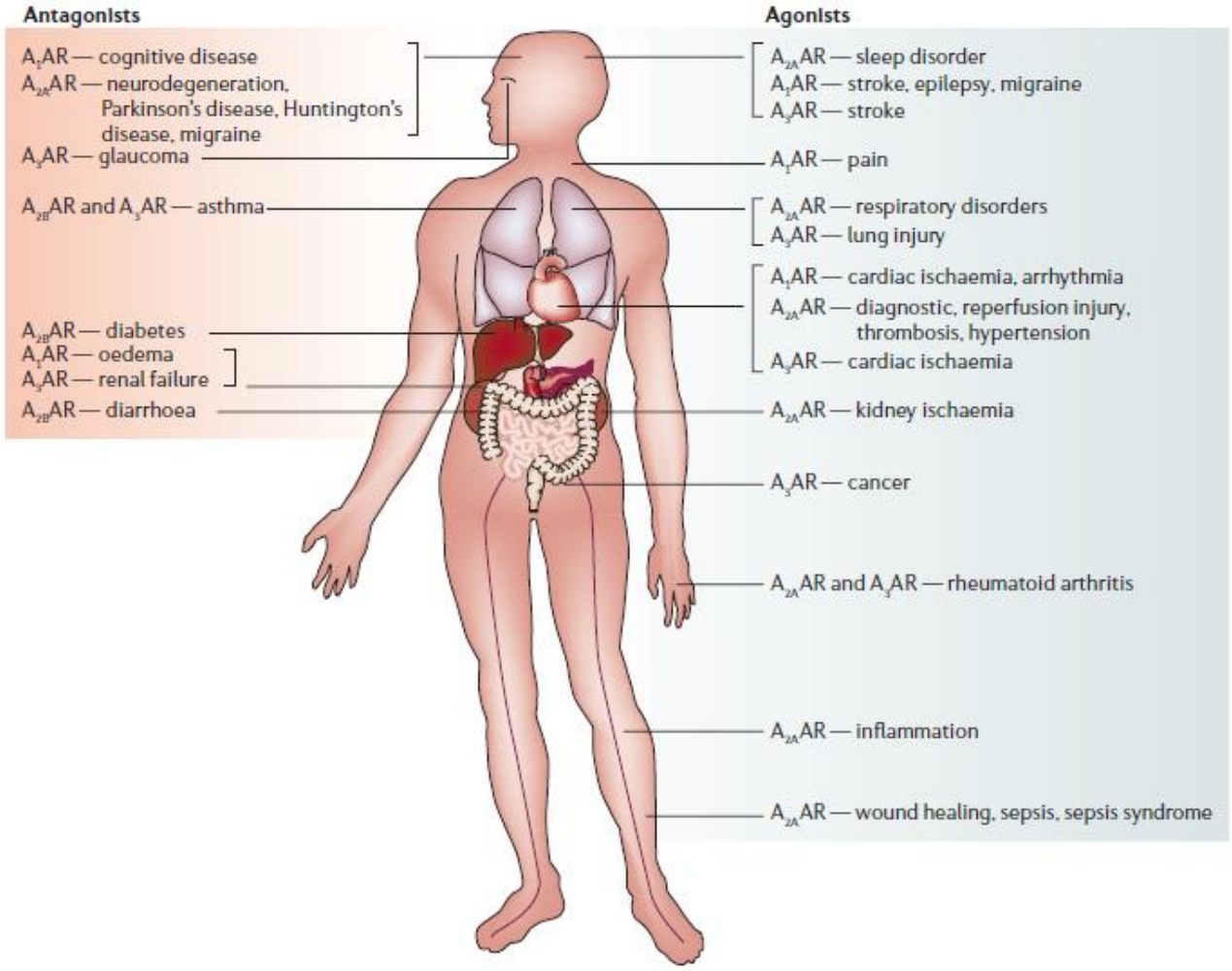

Figure 7: disease targets for selective adenosine receptor ligands (16).

Summarizing, ARs are potential therapeutic targets for Parkinson's disease, chronic heart failure, Inflammatory diseases, autoimmune disorders, chronic neuropathological pain, sickle cell disease and cancer.

Effects	Physiology and pathophysiology
Adenosine A_1 receptors	
Decreased renal blood flow, tubuloglomerular feedback and inhibition of renin release	Physiology
Inhibition of lipolysis	Physiology
Vasoconstriction	Pathophysiology?
Bronchoconstriction	Pathophysiology?
Inhibition of neurotransmitter release	Extreme physiology*
Inhibition of insulin and glucagon release	Physiology
Reduced heart rate	Physiology
Osteoclast activation and bone resorption	Physiology?
Reduced respiration	Extreme physiology*
Sleep	Physiology
Analgesia	Extreme physiology*
Cardiac preconditioning	Pathophysiology
Adenosine A_{2A} receptors	
Wakefulness and locomotion	Physiology
Neurodegeneration (including Parkinson's disease, stroke, traumatic brain injury and Alzheimer's disease)	Pathophysiology
Immunosuppression	Extreme physiology* or pathophysiology
Vasodilation and hypotension	Physiology or extreme physiology*
Blood–brain barrier integrity	Pharmacology
Coronary vasodilation	Physiology or extreme physiology*
Inhibition of platelet aggregation	Extreme physiology*
Angiogenesis	Extreme physiology*
Sickle cell disease	Pathophysiology
Fibrosis	Pathophysiology
Adenosine A_{2B} receptors	
Vascular integrity	Physiology or extreme physiology*
Cardiac preconditioning	Extreme physiology*
Sickle cell disease	Pathophysiology
Pro-inflammation (acute injury) and antiinflammation (some chronic disease states)	Physiology and pathophysiology
Fibrosis	Pathophysiology
Adenosine A_3 receptors	
Increased mast cell activation	Extreme physiology* or pathophysiology
Airway contraction	Pathophysiology
Inflammatory pain	Extreme physiology* or pathophysiology
White cell chemotaxis	Extreme physiology* or pathophysiology
Chronic neuropathic pain relief	Pathophysiology
Anticancer (melanoma)	Pathophysiology

Table 2: Physiological and pathological effects of adenosine receptors (135). *Refers to such conditions such as heavy exercise, being at high altitude and unusually high activity in the pathways of the nervous system.

A_1 AR:

- Chronic heart failure

In patients with acute heart failure is definitely common an impaired renal function directly contributing to deterioration of the heart and associated with an adverse outcome, including increased mortality. Measurement of local adenosine production showed that is often increased in the kidneys of patients with heart failure as a result of hypoxia caused by reduced renal perfusion and by stimulation with diuretics (136). Based on the demonstrated control of renal function and the implication of A_1 AR in the mechanisms associated with renal dysfunction, A_1 AR antagonists were developed. These antagonists reduced the risk of persistent worsening renal failure by more than 50% in a Phase IIb study involving 301 patients with acute heart failure, and improved renal plasma flow in 63 ambulatory patients with chronic heart failure (137). Thus, a placebo-controlled, randomized Phase III trial involving 2,033 patients with acute heart failure (the PROTECT study) was carried out with the A_1 AR antagonist rolofylline (Figure 129; this was the largest study to date involving the use of A_1 AR antagonists targeting renal function. Unfortunately, the results were disappointing and rolofylline did not prevent persistent worsening renal function (18) (138). The reason for this absence of the kidney protective effects is possibly to be due to an enhanced diuretic effect (as evident by more pronounced weight loss), which may have counterweighted the positive effects of rolofylline on the preservation of renal function (19). Moreover, pharmacological and genetic studies have extensively demonstrated that A_1 AR exerts protective effects against ischemic kidney injury and brain injury, which is consistent with the increased frequency of stroke and seizure activity in clinical trials of A_1 AR antagonists (19), thus leading to assert that A_1 AR antagonist develop as chronic heart failure therapeutics should proceed with caution. It is under this framework where a partial A_1 AR agonist could be useful for a potentially hemodynamically neutral therapy that could simultaneously improve cardiomyocyte energetics, cardiac structure and function, and prevent further tissue injury while being well tolerated when added to background medical therapy. Although drug development of a partial A_1 AR agonist remains at an early stage, compelling biologic rationale and encouraging preclinical evidence support continued attention be given to ongoing and future trials with these agents in heart failure (139).

- Cardiovascular system

A_1 AR activation has many effects in the cardiovascular system, including a reduction in heart rate and atrial contractility, and the attenuation of the stimulatory actions of catecholamines on the heart (140) (141). Activation of the A_1 AR by intravenous infusion of adenosine is used to restore normal heart rhythm in patients with paroxysmal supraventricular tachycardia (PSVT). However, for more long-term indications, selective A_1 AR modulators are needed to avoid side effects related to other AR subtypes such as hypotension.

(2S,3S,4R,5R)-5-[6-(cyclopentylamino)purin-9-yl]-N-ethyl-3,4-dihydroxyoxolane-2-carboxamide (Selodenoson, DTI0009, GR 56072, RG 14202; Aderis Pharmaceuticals) is a potent and selective A_1 AR agonist able to control heart rate without lowering blood pressure (142), although it has been reported to have renal toxicity during Phase II clinical trials for its capacity to slow heart rate in atrial fibrillation. A_1 AR selective non-nucleoside derivative capadenoson (BAY68-4986, Figure 11) is in trials for treatment of persistent atrial fibrillation and is now available as a research tool (143).

- Pain

Adenosine exerts multiple influences on pain transmission at peripheral and spinal sites. At peripheral nerve terminals in rodents, A_1 AR activation produces antinociception by decreasing cAMP levels in the sensory nerve terminal (144), thus A_1 AR could be useful for neuropathic pain treatment. The functionally important regulation of membrane in channels seems to be the domain of A_1 AR. Activation of A_1 AR enhances K^+ and Cl^- conductance in neurons, leading to membrane hyperpolarization and postsynaptic reduction of neuronal $Ca2^+$ influx through voltage- and N-methyl D-aspartate receptor-dependent channels. This counteracts, through synaptic and extrasynaptic receptors, nerve cell depolarization (145). A study of 2005 (146) reported that capsaicin-induced glutamate release from rat spinal synaptosomes was inhibited by adenosine and adenosine A_1 AR agonists. These studies suggest that the hyperpolarizing effect of adenosine can inhibit excitation of sensory nerves and ameliorate neuropathic pain at the spinal cord level. Moreover, a 2010 study by Horiuchi et al. (147) showed how hyperalgesia induced by spinal cord injury (SCI) was significantly inhibited by the intrathecal application of 10 nmol Cl-adenosine, a nonselective adenosine receptor agonist. Cl-adenosine significantly inhibited SCI-induced hyperalgesia at concentrations between 10 and 30 nmol in a dose-dependent way. The effect of Cl-adenosine on hyperalgesia after SCI was blocked by the simultaneous application of 8-cyclopentyl- 1,3-dipropylxanthine (DPCPX, Figure 12), an A_1 AR antagonist. This result suggests that the anti-hyperalgesic action of Cl-adenosine is mediated by the stimulation of A_1 AR. Intrathecal application of R-PIA (10 nmol), an A_1 AR agonist (Figure 11), inhibited SCI-induced hyperalgesia. On the other hand, intrathecal application of CGS21680, a selective adenosine A_{2A} AR agonist, did not inhibit SCI-induced hyperalgesia. These results suggest that adenosine inhibited SCI-induced hyperalgesia through the stimulation of A_1 AR. A 2015 study by Imlach et al. (148) investigated the changes in adenosine tone and A_1 AR signaling, together with the actions of a novel A_1 AR positive allosteric modulator (PAM), VCP171 [(2-amino-4-(3-(trifluoromethyl)phenyl)thiophen-3-yl)(phenyl)methanone], on excitatory and inhibitory neurotransmission at spinal cord superficial dorsal horn synapses in a rat partial nerve-injury model of neuropathic pain. In the absence of A_1 AR agonists, superfusion of the A_1 AR antagonist, DPCPX, produced a significantly greater increase in electrically evoked α-amino-3-hydroxy-5-methyl-4-isoxazolepropionic acid receptor–mediated synaptic current (eEPSC) amplitude in both laminae I and II neurons from nerve-injured animals than in controls, suggesting that endogenous adenosine tone is increased in the dorsal horn.

Inhibitory GABAergic and glycinergic synaptic currents were also significantly increased by DPCPX in controls but there was no difference after nerve injury. The A_1 AR agonist, N^6-cyclopentyladenosine, produced greater inhibition of eEPSC amplitude in lamina II but not lamina I of the spinal cord dorsal horn in nerve-injured versus control animals, suggesting a functional increase in A_1 AR sensitivity in lamina II neurons after nerve injury. The A_1 AR PAM, VCP171, indeed produced a greater inhibition of eEPSC amplitude of nerve-injury versus control animals in both lamina I and lamina II neurons. Enhanced adenosine tone and A_1 AR sensitivity at excitatory synapses in the dorsal horn after nerve injury suggest that new generation PAMs of the A1R can be effective treatments for neuropathic pain.

- Parkinson's disease

For what may concern Parkinson's disease (PD), A_1 AR is also expressed in the striatum; based on anatomical and in vivo microdialysis studies, A_1 ARs appear to be localized presynaptically of dopamine axon terminals where they inhibit dopamine release. A_1 AR antagonists facilitate dopamine release in the striatum, and like A_{2A} ARs potentiate dopamine mediated responses (149). Antagonism of both the A_{2A} and A_1 AR would be synergistic (see Figure 8): inhibition of the A_1 receptor will facilitate dopamine release, while inhibition of the A_{2A} AR will enhance postsynaptic responses to dopamine. Interestingly, the A_1 receptor is also concentrated in neocortical and limbic system structures that are important for cognitive function. Pharmacological inhibition of A_1 receptors enhances neurotransmitter release in the hippocampus and enhances performance in animal models of learning and memory (150).

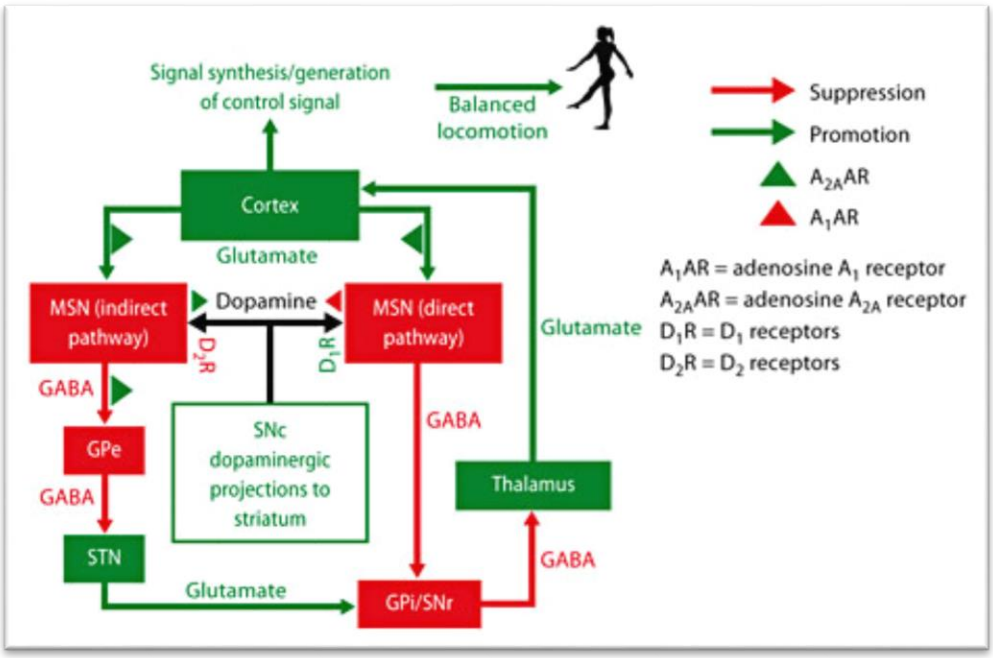

Figure 8: Adenosine receptor implication in the direct and indirect pathways in the motor circuit (151).

A_{2A} AR:

- Parkinson's disease

A_{2A} AR antagonists have emerged as leading non-dopaminergic drugs for the treatment of Parkinson's disease, due to many evidences accumulating in the last decades like the concentrated striatal expression of A_{2A} AR, the antagonistic A_{2A}-D2 receptor interaction and many preclinical studies demonstrating motor benefit in rodent and non-human primate models of Parkinson's disease (94) (152) (153) (154). Six double-blind, placebo controlled clinical Phase IIb and Phase III trials of istradefylline (KW-6002, Figure 14), involving a total of >2,000 patients with advanced Parkinson's disease, and one Phase IIb trial with preladenant (SCH420814, Figure 14), involving 253 patients with advanced Parkinson's disease, have been reported (155). These clinical Phase IIb and Phase III trials have shown a little but significant reduction in the average 'off-time' by about 1.7 hours compared to the optimal l-DOPA (l-3,4-dihydroxyphenylalanine) dose regimen (154). However, another similar Phase III clinical trial with istradefylline in patients with Parkinson's disease did not demonstrate a significant reduction in the 'off-time' compared to placebo (156). These relatively modest motor effects differed from the unambiguously motor benefit of the preclinical studies in which MPTP (1-methyl-4-phenyl-1,2,3,6-tetrahydropyridine) was used in order to cause permanent symptoms of Parkinson's disease by destroying dopaminergic neurons in the substantia nigra of the primates' brain. Clearly, further clinical investigation of A_{2A} AR antagonism is necessary to fully understand its potential as a treatment for Parkinson's disease, strengthened by encouraging and consistent finding in the clinical trials of A_{2A} AR antagonists for Parkinson's disease showing that both istradefylline and preladenant had an excellent safety profile (154) (155). In April 2007, Kyowa Hakko Kirin Pharma filed a new drug application (NDA) for istradefylline for the treatment of advanced Parkinson's disease; however, the FDA issued a non-approval letter in 2008, citing the need for additional efficacy data. Nowadays is ongoing a Phase III long term clinical study in subjects with moderate to severe Parkinson's disease. Currently, several Phase IIb and Phase III trials for A_{2A} AR antagonists (other than istradefylline) are still underway and these agents remain one of the leading non-dopaminergic treatment candidates for Parkinson's disease (157).

- Fibrosis

Both A_{2A} and A_{2B} AR signal for regulation of matrix production via classic GS-mediated activation of cAMP and its downstream signaling molecules. The regulatory actions of the receptors likely involve multiple interconnected pathways (Figure 9), and one of the more interesting aspects of this regulation is the opposing effect of the different levels of cAMP generated (158). Whether this relates to incorporation of alternative signaling pathways at higher levels of cAMP or the activation of discrete signaling pathways at different sites in the cell remains a subject for further investigation. Additionally, adenosine signaling also contributes to fibrosis in organ-specific ways and may have opposite effects in different organs. The deposition of collagen

by fibroblasts is an essential part of wound healing but also contributes to pathologic remodeling of organs, which can lead to substantial morbidity and mortality. Many small molecules contribute to the pathogenesis of fibrosis including the purine adenosine which signals primarily through A_{2A} and A_{2B} AR. These receptors are helpful in order to reduce inflammation and promote wound healing. On the other side, excessive activation leads to architectural disruption and loss of organ integrity in a variety of fibrosing disorders. The development of drugs that selectively target these receptors will disrupt the pathogenesis of fibrosis and slow or arrest the progression of these important diseases.

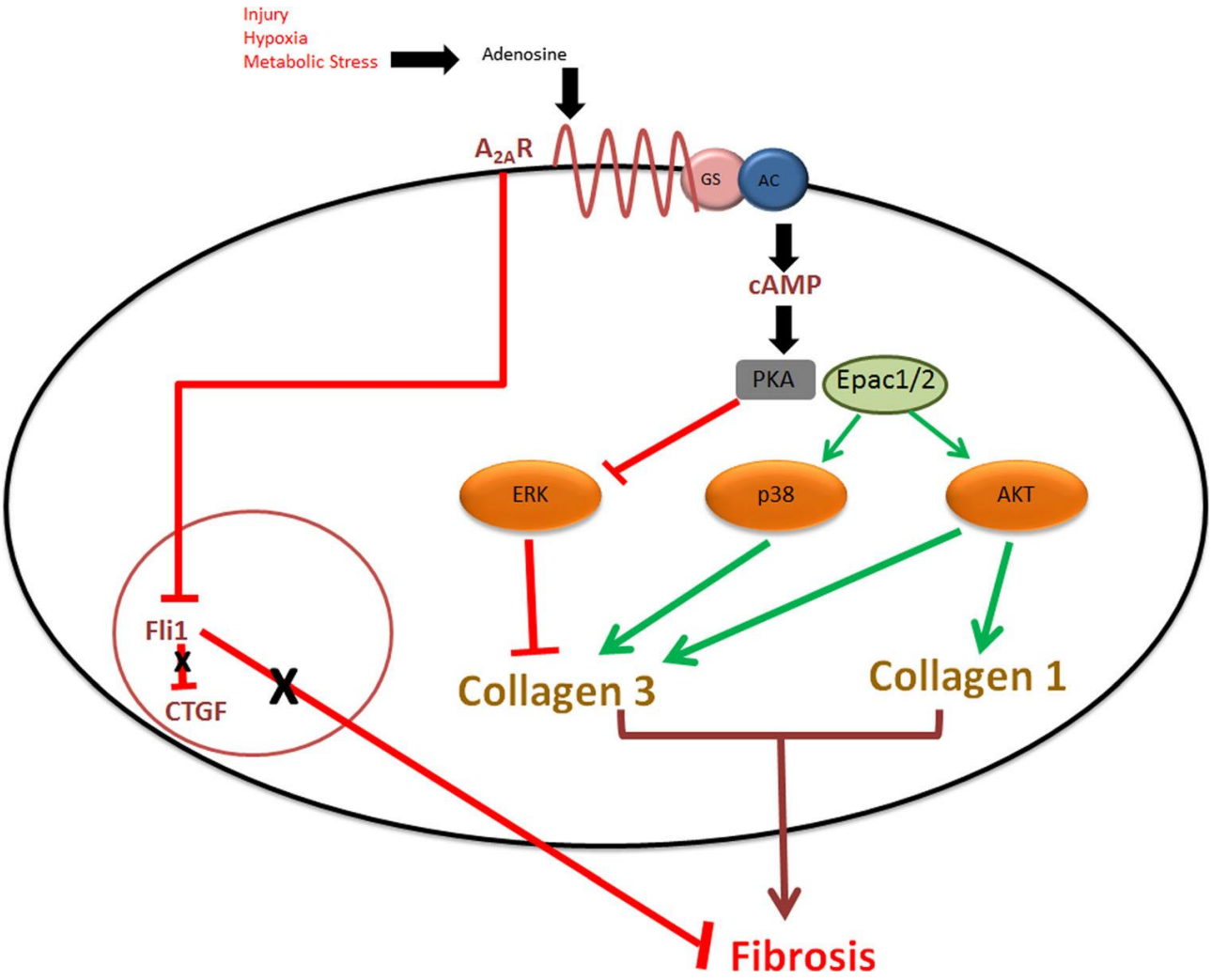

Figure 9: Cross-talk of adenosine receptor signaling pathways leading to collagen deposition and fibrosis. Collagen III is separately regulated by p38, inhibition of ERK via PKA, and Akt pathways. Collagen I is shown being positively regulated by Epac2. Additionally, A_{2A}R inhibits Fli1, which promotes CTGF transcription and fibrosis (158).

- Sickle cell disease

Treatment with an A_{2A} AR agonist has been indicated to attenuate sterile inflammation and T cell activation in this disorder (159). A clinical trial in patients with sickle cell disease is currently being conducted using the

FDA-approved A_{2A} AR agonist 1-[6-amino-9-[(2*R*,3*R*,4*S*,5*R*)-3,4-dihydroxy-5-(hydroxymethyl)oxolan-2-yl]purin-2-yl]- *N*-methylpyrazole-4-carboxamide (Regadenoson, CVT-3146).

- Pain

Assumed that A_{2A} AR is known to exert an hyperalgesic modulation in spinal cord (see A_1 AR above), another study of 2007 by Hussey et al. (160) deepen the role of A_{2A} AR concerning peripheral nociception, monitoring the response of NMDA and NK1 receptor in *adora2* knockout mice. The results showed that there was a significant reduction in nociceptive behaviour as measured by both bites/licks and flinches in response to formalin injection. This pattern was similar when using the selective A_{2A} AR antagonist 5-amino-7-(2-phenylethyl)-2-(2-furyl)-pyrazolo(4,3-e)-1,2,4-triazolo(1,5-c)pyrimidine (SCH58261). Although the response to SCH58261 observed in this study was not dose-dependent, 3 mg/kg and 10 mg/kg were chosen on the basis of their selectivity for the A_{2A} AR. In our study this is also suggested by the lack of significant difference between results obtained using the A_{2A} AR knockout mice and SCH58261. There was a significant reduction in time spent biting/licking the formalin-injected paw during the first phase only, with a reduced number of flinches observed during both the first and second phases of the test. Although the mechanisms underlying the formalin test are complex it was chosen as it consists of two distinct phases, with the first phase being generally accepted to be mediated primarily by direct stimulation of peripheral sensory nerves whilst the second phase is due to an inflammatory component and involves more complex pain circuitry. The reduced response observed during the first phase in A_{2A} AR knockout mice further suggests that peripheral adenosine A_{2A} AR are involved in stimulation of nociceptive afferent fibres projecting to the spinal cord. This contrasts with Borghi et al. (161) who showed that administration of the selective A_{2A} AR agonist CGS21680 (Figure 13) caused a reduction in nociceptive behavior during the first phase which might suggest that the receptor has an antinociceptive role. The reduced response as measured by flinches observed during the second phase of the formalin test in both A_{2A} AR knockout mice and mice treated with SCH58261 further implicates the A_{2A} AR in nociceptive circuits and could be linked to altered NMDA glutamate receptor signalling. The NMDA glutamate receptor is a key proponent of central sensitization which is a feature of the formalin test and occurs as a result of repetitive stimulation of afferent fibres projecting to the spinal cord. This repetitive stimulus induces activation of the NMDA glutamate receptor and leads to calcium entry through the receptor and the consequent changes in the post-synaptic membrane. Thus, the loss or blockade of A_{2A} AR causing a reduction in nociceptive behaviour in the first phase will be associated with reduced direct activation of primary afferent fibres and therefore decreased activation of NMDA glutamate receptors located centrally and this is likely to result in a reduction of the central sensitization which characterizes the second phase. In conclusion, the decrease in NMDA glutamate receptor binding in A_{2A} AR knockout mice and the reduced response to the formalin test in A_{2A} AR knockout mice and mice treated with the selective A_{2A} AR antagonist SCH58261 were most probably caused by changes occurring in peripheral nociceptive transmission as a

consequence of the genetic knockout or blockade of A_{2A} AR at sensory terminals. These results support a key role for the A_{2A} AR in peripheral nociceptive pathways.

A_{2B} AR:

- Inflammation

Much research has focused on the regulation of the inflammatory response by the A_{2B} AR. In a study of 2006, was generated an A_{2B} AR knockout (KO) mouse model (103) showing that the A_{2B} AR is highly expressed on macrophages and that A_{2B} AR KO mice have a mild increase in plasma levels of the pro-inflammatory cytokines, tumor necrosis factor-alpha (TNF-α), and interleukin-6 (IL-6), and decreased plasma levels of the anti-inflammatory cytokine, IL-10, following lipopolysaccharide (LPS) stimulation as compared to wild type (WT) mice. These results suggest that the A_{2B} AR dampens the inflammatory response. Further studies have shown an anti-inflammatory role for the A_{2B} AR. For example, activation of the A_{2B} AR with BAY60-6583, a specific A_{2B} AR agonist, inhibits superoxide generation by neutrophils (162). Importantly, in vivo studies have elucidated mechanisms in addition to alteration of cytokine levels that explain how the A_{2B} AR affects the pathogenesis of inflammation. A_{2B} AR KO mice have increased expression of adhesion molecules intracellular adhesion molecule (ICAM-1) and E-selectin, which increases leukocyte rolling and adhesion (103). Furthermore, A_{2B} AR KO mice exhibit enhanced neutrophil infiltration into tissues under hypoxic conditions (104). These studies suggest that the A_{2B} AR prevents inflammatory cell transmigration into the tissue of interest, one of the first steps in the inflammatory response. In addition, the A_{2B} AR affects alternative macrophage activation. Adenosine and NECA enhance the expression of markers of alternative macrophages (arginase 1, tissue inhibitor of matrix metalloproteinase-1, and macrophage galactose-type C-type lectin-1). Pharmacologic inhibition of the A_{2B} AR or genetic lack of the A_{2B} AR prevents NECA-induced expression of these alternative macrophage markers (163), suggesting that A_{2B} AR promotes alternative macrophage development. Furthermore, Ryzhov et al. generated an A_{2B} AR KO mouse using a different targeting construct and determined the ability of the A_{2B} AR to mediate two actions of NECA: (1) stimulation of IL-6 release and (2) inhibition of LPS-induced TNF-a release (164). In this study, NECA increases plasma IL-6 levels in WT but not A_{2B} AR KO mice, suggesting that the A_{2B} AR promotes inflammation by increasing IL-6 levels. They also found that NECA decreases LPS-induced TNF-a levels in both WT and A_{2B} AR KO mice, suggesting that the A_{2B} AR does not dampen inflammation in response to LPS. Despite these results that suggest that A_{2B} AR activation by NECA promotes inflammation, this study also found that macrophages derived from A2bAR KO mice secrete more TNF-a than WT mice. These studies underlie important considerations in studying the A_{2B} AR as well as other receptors. First, genetic lack of a receptor does not always predict the results of pharmaceutical modulation of the receptor. Knockout mouse models are helpful in determining the role of

a receptor in pathologic processes; however, developmental effects of genetic alteration can impact the interpretation of the results. Lack of the A_{2B} AR throughout development may upregulate other proteins to compensate for lack of the A_{2B} AR. Pharmacologic modulation of a receptor, unlike knockout mouse models, determines how alteration of cellular signaling affects a particular point in time, but may not mimic lifelong lack of a receptor. Second, use of pharmacologic modulators requires thorough understanding of the action of the agents on potentially other targets. The presence and activity of other receptors may influence the effect of A_{2B} AR on particular process. In fact, NECA is a non-specific adenosine receptor agonist that can activate all four of the adenosine receptors, which makes it more difficult to conclude which receptor is responsible for certain actions of the compound. Different cell types, each expressing the A_{2B} AR may have opposing downstream outcomes in response to modulation of the receptor. The initial in vivo studies that supported an anti-inflammatory role for the A_{2B} AR showed that TNF-α levels following LPS injection are greater in A_{2B} AR KO mice, than control counterparts (103). In a different disease model, that of cecal ligation and puncture-induced sepsis, A_{2B} AR signaling on non-hematopoietic cells was the main contributor to reducing cytokine and chemokine production (123). Furthermore, the A_{2B} AR is protective in acute inflammation as evidenced by the findings that A2bAR KO mice have increased pulmonary inflammation following acute injury from hypoxia (104) or ventilator-induced lung injury (107). Overall, when interpreting studies on the role of the A_{2B} AR in inflammation-induced processes, it is important to consider timing of A_{2B} AR activation or inhibition (pharmacologic or genetic), specificity of pharmacologic agents, model systems, and cell types as well as acute versus chronic responses studied. In addition, when studying inflammation in vivo, the influence of housing facilities with potentially somewhat different pathogen screens, could impact experimental outcomes.

- Cancer

Growing evidence indicates that A_{2B} AR potentially plays a pathophysiological role in human cancer (Figure 10) and might serve as a target for novel therapies or co-therapies for cancer. First, A_{2B} AR is highly expressed in various types of tumor cell sort issues and promotes tumor-cell proliferation. For instance, A_{2B} AR was found to be overexpressed in colorectal carcinoma cells and tissues, and inhibition of A_{2B} AR blocked the proliferation of colon cancer cells (165). In prostate cancer, A_{2B} AR increased cancer-cell proliferation in both ligand- dependent, and ligand-independent manners (166) (167). In human oral cancer, A_{2B} AR was shown to be upregulated in oral squamous carcinoma cells, and A_{2B} AR knockdown reduced the proliferation of oral cancer cells through HIF-1a activation (168). Moreover, A_{2B} AR was reported to foster bladder and breast tumor growth in syngeneic mice (110). Second, A_{2B} AR modulates tumor-cell metastasis. A_{2B} AR was implicated in promoting breast cancer cell migration *in vitro* and lung metastasis *in vivo* (169) (170), although the underlying molecular mechanism was not fully elucidated. However, the results of a subsequent study suggested a possible explanation: A_{2B} AR activation suppressed the prenylation of the small GTPase Rap1B

and diminished Rap1B-mediated cell adhesion, which promoted cell migration (171). Third, A_{2B} AR might regulate the tumor microenvironment, including the surrounding blood vessels, immune cells, fibroblasts, and the extracellular matrix. Ryzhov and colleagues provided the first genetic evidence indicating that A_{2B} AR regulates vascular endothelial growth factor (VEGF) production from tumor-infiltrating host immune cells and thereby promotes tumor growth (172). Concomitantly, other groups suggested that A_{2B} AR alters angiogenesis by regulating the production of a wide array of pro- or anti-angiogenic factors such as basic fibroblast growth factor (bFGF), angiopoietin 2, and a subset of cytokines (173) (174) (175). In addition to affecting angiogenesis, A_{2B} AR regulates dendritic-cell differentiation and function (176) (177) and alternative macrophage activation (163) and thus contributes to cancer progression. Thus, A_{2B} AR exerts various effects on tumor progression and metastasis. Notably, most of the aforementioned evidence was collected using *in vitro* systems, and it is critical to further confirm the role of A_{2B} AR in cancer by using *in vivo* models before A_{2B} AR is used as a potential cancer therapeutic target.

- Cardiovascular system

Cardiovascular disease (CVD) comprehends coronary artery disease (myocardial infarction, angina pectoris, heart failure), cerebrovascular disease (stroke, transient ischemic attack), peripheral artery disease, and aortic atherosclerosis and aneurysm. CVD is the leading cause of death in the world (178). Atherosclerosis is an underlying etiologic factor in many types of cardiovascular disease. The pathogenesis of atherosclerosis involves endothelial dysfunction, subendothelial accumulation of low density lipoprotein (LDL) and subsequent oxidation (179). Oxidized LDL promotes endothelial cell expression of adhesion molecules (like ICAM-1 and E-selectin) and secretion of chemokines (like TNF-a), leading to the intimal accumulation of lipid-laden macrophages, called foam cells. Further accumulation of cholesterol, inflammatory cells, and apoptotic cells forms the necrotic core of the atheroma, which is encapsulated by collagen and proliferating smooth muscle cells (179). Intervention at one or several of these steps in the development of atherosclerosis may prevent subsequent thrombotic events. The function of the A_{2B} AR in the pathogenesis of atherosclerosis has been studied. In one approach it was investigated the effect of adenosine on foam cell formation (180) in hypoxic conditions (1% O2) using an in vitro model of foam cell formation, which involved differentiating the human myelomonocytic cell line U937 or human peripheral blood mononuclear cells into macrophages and then incubating the cells with oxidized LDL to form foam cells. The authors found that hypoxia selectively induces A_{2B} AR expression in U937 cells, differentiated macrophages, and foam cells. Moreover, adenosine promotes hypoxia-inducible factor-1a (HIF-1a) protein and HIF-1a induces expression of vascular endothelial growth factor (VEGF) and promotes foam cell formation via the A_{2B} AR and A_3 AR specifically (180). These results suggest that antagonists to the A_{2B} AR and A_3 AR may be beneficial in preventing atherosclerotic plaque formation. In contrast, a later study using an in vivo mouse model of atherosclerosis found that the A_{2B} AR is protective against plaque formation (109). To promote atherosclerosis development, A2bAR KO

mice were bred onto an ApoE background (A_{2B} AR, ApoE double KO) and the mice were fed Western diet. A_{2B} AR, ApoE double KO mice have increased plasma and liver cholesterol and triglycerides and larger atherosclerotic plaque lesions as compared to ApoE mice. Importantly, injection of the A_{2B} AR specific agonist, BAY60-6583 (Figure 15), into ApoE mice reduces atherosclerotic plaque formation and plasma lipid levels. As a mechanism to explain the effect of the A_{2B} AR on lipid metabolism, hepatocytes isolated from A_{2B} AR, ApoE double KO mice express higher levels of sterol regulatory element binding protein-1 (SREBP-1), a key transcription factor in lipogenesis and cholesterol synthesis, while BAY60-6583, reduces hepatocyte expression of SREBP-1. As such, this study identified the A_{2B} AR as atheroprotective secondary to modulation of lipid metabolism and plaque formation.

In addition, adenosine signaling has been implicated in mediating cardioprotective cellular responses to myocardial ischemia (181). Ischemic preconditioning, which involves repeated short episodes of ischemia and reperfusion prior to myocardial infarction (MI), has been shown to reduce infarct size after MI (182). Interestingly, A_{2B} AR gene expression is elevated in the hearts of individuals with ischemic heart disease as compared to healthy controls (102) and A_{2B} AR expression increases after ischemic preconditioning (183). Using a model of murine in situ preconditioning, Eckle et al. (184) showed that A_{2B} AR signaling is necessary for the cardioprotective effect of ischemic preconditioning. Ischemic preconditioning reduces infarct size in WT, A_1 AR KO, A_{2A} AR KO, and A_3 AR KO mice, but not in A_{2B} AR KO mice after 2 hours of reperfusion. Furthermore, activation of the A_{2B} AR with BAY60-6583 reduces infarct size after ischemia. Further studies by the same group showed that A_{2B} AR signaling stabilizes the circadian rhythm protein, period 2 (Per2) within 2 hours to promote a protective metabolic switch in carbohydrate utilization (102). The group also showed that A2bAR signaling in bone marrow-derived cells is primarily responsible for the cardioprotective effect in ischemia-reperfusion injury, suggesting an additional role for A_{2B} AR regulation of inflammation in mediating cardioprotective effect (185). In contrast, amore recent study did not find a role for the A_{2B} AR in acute ischemic preconditioning (186). The authors report no difference in infarct size following ischemic preconditioning in A_{2B} AR KO mice as compared to WT mice. However, consistent with the original report, they find that treatment with BAY60-6583 reduces infarct size and conclude that the A_{2B} AR may play a role in a later phase of ischemic preconditioning.

Moreover, the current management of symptomatic coronary artery disease includes coronary reperfusion with percutaneous coronary intervention (PCI), which involves balloon angioplasty and stent placement at the site of the previous arterial blockage. The pathogenesis of restenosis is believed to involve arterial injury and neointimal proliferation with macrophage accumulation (187). Research into medical therapy that can reduce the rate of restenosis after PCI has gathered interest. One such agent that is being investigated is cilostazol, a phosphodiesterase inhibitor that results in an increase in intracellular cyclic AMP (cAMP). The A_{2B} AR, which when activated also increases cAMP levels, has been studied as a therapeutic target in

restenosis. The A_{2B} AR has been shown to be protective against restenosis following vascular injury. In a 2008 study, a guidewire-induced femoral artery injury model in mice was used to mimic angioplasty (188) A_{2B} AR KO mice have increased neointimal formation following femoral artery injury as compared to WT mice. In addition, the chemokine receptor CXCR4, which promotes cell migration and neointimal hyperplasia, is upregulated in platelets, macrophages, and leukocytes derived from A_{2B} AR KO mice. Furthermore, the A_{2B} AR plays a role in vascular smooth muscle cell (VSMC) proliferation, one of the pathologic steps of restenosis, as VSMCs from A_{2B} AR KO mice proliferate faster than those derived from WT mice. These studies suggest that A_{2B} AR activation may be beneficial in preventing restenosis following PCI, a conclusion that was recently tested. In accordance, a study of 2012 by Bot et al. (189) showed that activation of the A_{2B} AR with BAY60-6583, the A_{2B} AR specific agonist, for 18 days following wire-induced vascular injury of the left common carotid artery in Apolipoprotein E (ApoE) deficient mice reduces lumen stenosis and media size. As a mechanism to explain this result, the authors noted that in vivo and in vitro treatment with BAY60-6585 decreases VSMC proliferation. Moreover, the authors also demonstrated that BAY60-6583 increases collagen content, which suggests that A_{2B} AR activation may also promote plaque stability. Overall, these studies show promising effects of A_{2B} AR agonism on reducing restenosis.

Vascular smooth muscle cells (VSMCs) are important in the regulation of vascular tension and have high expression of the A_{2B} AR (103). VSMCs contract or dilate in response to changes in calcium (Ca^{2+}) levels that result from ligand stimulation of surface receptors (190). It is known that activation of the A_{2B} AR by coupling to Gs and Gq results in downstream increases in cAMP and IP3, respectively. IP3 results in elevated cytosolic Ca^{2+} and contraction of VSMCs whereas increases in cAMP results in decreased Ca^{2+} and relaxation of VSMCs. These changes in Ca^{2+} levels cause perturbation of the cytoskeleton leading to VSMC contraction or relaxation. Ca^{2+} bound to calmodulin in VSMCs activates myosin light chain kinase (MLCK), which phosphorylates the regulatory light chains of myosin by adding a phosphate group to Ser-19. The phosphorylation of myosin light chains causes cycling of myosin heads on actin, which culminates in VSMC contraction. Thus, the specific nature of downstream signaling of the A_{2B} AR (via IP3 or cAMP) in VSMCs alters the final impact of A_{2B} AR stimulation on modulation of VSMC contractility and vascular tension. Several in vitro studies have examined the role of the A_{2B} AR in relaxation of VSMCs, using A_2-type AR agonist-treated, precontracted isolated aortas using a force transducer to measure tension. One study showed that NECA, the nonspecific adenosine receptor agonist as well as CGS21680, the A_{2A} AR specific agonist, elicit vasodilation in Prostaglandin F2α (PGF2α)-precontracted porcine arterial rings (191). When potassium chloride (KCl) is used to precontract the arterial rings, neither NECA nor CGS21680 (Figure 13) treatment causes vasodilation. This study suggests that the A_{2A} AR (and perhaps the A_{2B} AR) are important for vasodilation of porcine arterial rings. In vivo studies have also been undertaken to interrogate the role of the A_{2B} AR in controlling vascular tension and blood pressure. In one study, blood pressure was measured by tail cuff and by arterial catheterization in young (8–12 weeks old) WT and A_{2B} AR KO mice at baseline as well as

following adenosine infusion and showed no difference between genotypes, suggesting that the A_{2B} AR plays no role in blood pressure regulation in young mice (103). In a mouse model of bleomycin-induced pulmonary hypertension secondary to pulmonary fibrosis, A_{2B} AR signaling was found to play a role in vascular remodeling and proliferation. Another study found A_{2B} AR KO mice showed decreased systolic and mean arterial blood pressure with angiotensin II infusion as compared to WT mice (192). Furthermore, angiotensin II-induced ET-1 production in the kidneys of WT mice but not in A_{2B} AR KO mice or mice treated with an A_{2B} AR antagonist. Furthermore, the authors found increased levels of A_{2B} AR mRNA in kidney biopsies of hypertensive chronic kidney disease patients. Together, these in vivo models show that the A_{2B} AR may promote vascular remodeling via factors such as ET-1. As noted, there are seemingly conflicting reports on the role of the A_{2B} AR in regulating vascular dilation and resistance, possibly due to differences in downstream signaling (Gs and/or Gq), cell type, and model system tested. In addition, results are likely influenced by the examined species, as well as the methods employed to measure vascular tension and resistance.

- Renal diseases

Several studies have indicated a critical role of A_{2B} AR in mediating the progression of diabetic nephropathy. Patel et al. and Valladares et al. observed that inhibition of A_{2B} AR activation suppressed VEGF production in glomeruli and further attenuated renal dysfunction in diabetic nephropathy; these data suggested a protective role of A_{2B} AR antagonists in VEGF-induced diabetic nephropathy (193) (194). However, this view was challenged by Tak et al., who reported elevated VEGF levels in diabetic A_{2B} AR-knockout mice (195); concordantly, diabetic nephropathy was highly severe in mice with global or vascular endothelial tissue-specific A_{2B} AR deletion, but not in mice with tubular-epithelial A_{2B} AR deletion. Therefore, Tak et al. suggested that vascular A_{2B} AR signaling is the key mediator of kidney protection during diabetic nephropathy (195). The methods used and the specific tissues studied by the aforementioned groups were distinct, which might explain their conflicting observations on the role of A_{2B} AR during diabetic nephropathy. Moreover, the different time window in which A_{2B} AR inhibition was induced pharmacologically and genetically might also contribute to the discrepancy in the results (196). In addition to playing a role in diabetic nephropathy, A_{2B} AR has been suggested, based on studies on several mouse models, to protect against renal fibrosis. In ADA-deficient mice, a high level of adenosine in kidney tissues resulted in proteinuria and renal fibrosis, and treatment with A_{2B} AR antagonists attenuated renal dysfunction and fibrosis (197). Moreover, genetic deletion of A_{2B} AR protected against renal fibrosis in both mice infused with angiotensin II and mice subjected to unilateral ureteral obstruction (197). Furthermore, renal biopsy samples from patients with chronic kidney disease (CKD) showed higher levels of A_{2B} AR expression than did samples from patients without CKD (192). All of these data suggest that A_{2B} AR could serve as a potential therapeutic target in the treatment of CKD (Figure 10). Acute kidney injury, a devastating kidney disease, is often caused by renal ischemia. Rigorous studies from different laboratories have suggested a pivotal role of A_{2B} AR in acute kidney injury. For example,

Grenz et al. used genetic and pharmacological approaches to reveal a role of A_{2B} AR in protecting against renal injury resulting from ischemia, although the underlying molecular mechanism was not fully clarified (198). Subsequently, the same group proposed two possible explanations for how A_{2B} AR might provide renal protection: one, A_{2B} AR reduces neutrophil-dependent TNF-α production and suppresses inflammation (199); and two, A_{2B} AR promotes optimal post ischemic blood flow within the kidney and thereby ensures the maximal return of blood flow, tissue oxygenation, and removal of waste products from the ischemic kidney through the A_{2B} AR -ENT1 (equilibrative nucleoside transporter) pathway (200).

- Diabetes

Recently, A_{2B} AR in particular has been suggested to function as a critical regulator in diabetes mellitus (DM) (201) (202) (203) (196) (204) (205). In a type I DM model, the non-selective receptor agonist NECA blocked diabetes development, and this appeared to be mediated by A_{2B} AR-dependent suppression of proinflammatory cytokine production (206). These data suggest that A_{2B} AR represents a potential target for the treatment of type I diabetes (Figure 10). Conversely, some of the evidence obtained using a type II DM model indicated that A_{2B} AR plays a pro-diabetic role. Figler et al. suggested that A_{2B} AR activation increases insulin resistance by elevating the production of proinflammatory mediators such as IL-6 and C-reactive protein (207). Deletion of the A2BAR gene and selective blockade of A_{2B} AR in mice reduced hepatic glucose production and enhanced glucose disposal into skeletal muscle and brown adipose tissue (207). By contrast, other studies suggested an anti-diabetic role of A_{2B} AR. Johnston-Cox and colleagues showed that A_{2B} AR plays an essential role in high fat diet (HFD)-induced insulin resistance in mice, and mice lacking A_{2B} AR displayed diminished glucose clearance and elevated insulin resistance and inflammatory cytokine production (202). The underlying cellular mechanism here is mediated by A_{2B} AR expressed in macrophages: reinstatement of macrophage A_{2B} AR expression in A_{2B} AR -null mice restored HFD-induced insulin tolerance and tissue insulin signaling to the level in control mice. The molecular mechanism involves A_{2B} AR altering cAMP signaling and the levels of macrophage cytokine expression and secretion, and this regulates the levels of insulin receptor-2 and downstream insulin signaling (203). Similar results were obtained by Csoka et al., who suggested that A_{2B} AR plays a crucial role in sustaining glucose homeostasis and preventing insulin resistance under normal dietary conditions by regulating alternative macrophage activation. Insulin- and glucose-induced glucose clearance was impaired in A_{2B} AR -knockout mice that were fed chow diet, and these knockout mice also exhibited a low level of physical activity, which might contribute to decreased insulin sensitivity in skeletal muscles. Csoka et al. also highlighted the complex role of A_{2B} AR in regulating liver metabolism (208).

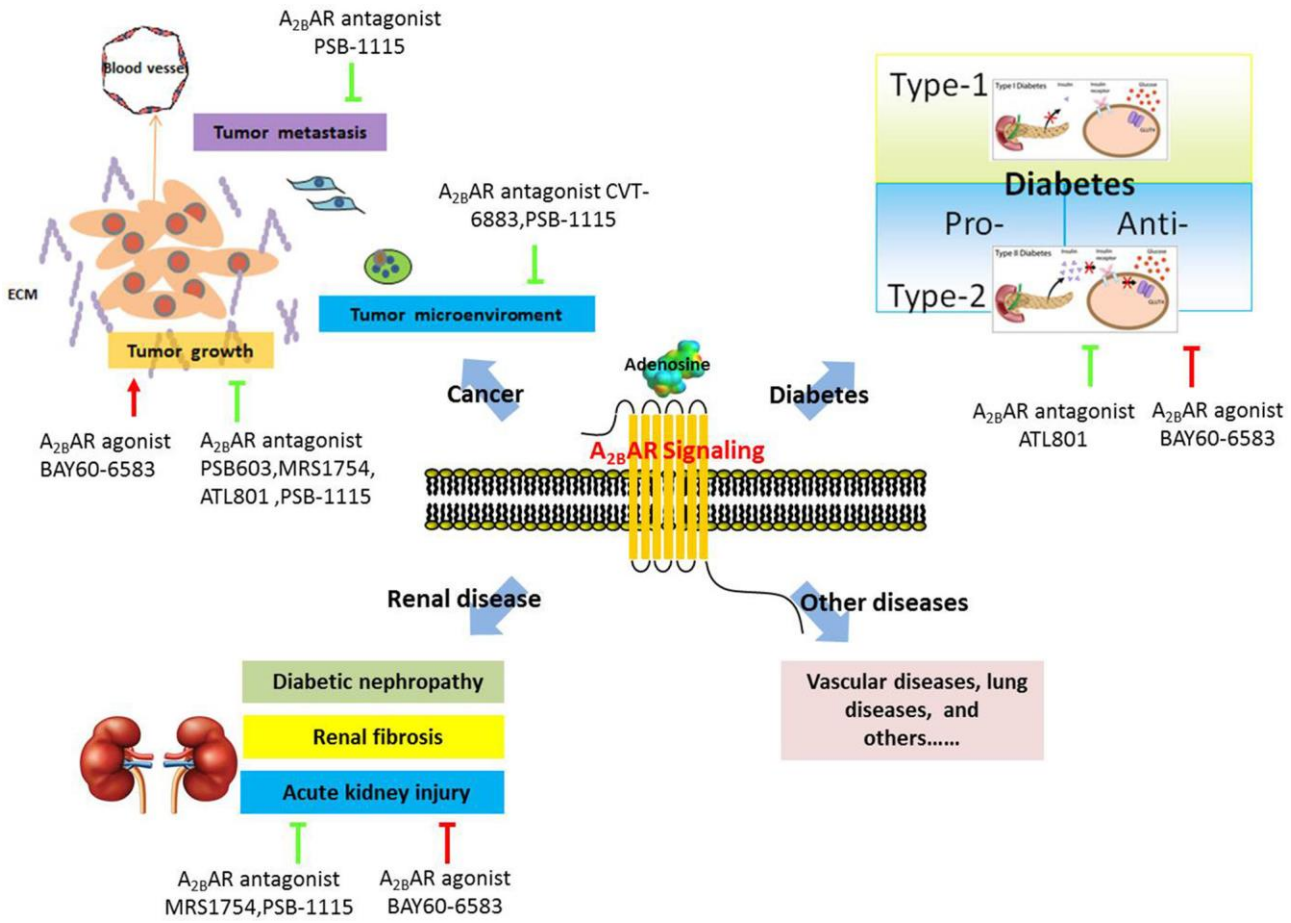

Figure 10: Schematic presentation of the role of A2B AR in various human diseases (21).

- Pain

In a 2016 study, Hu et al. (209) report that sustained elevated circulating adenosine signaling via A_{2B} AR is required for chronic pain behavior and neuronal hypersensitivity in three independent animal models, including adenosine deaminase (ADA) -/-, sickle cell disease (SCD), and complete Freund's adjuvant-injected (CFA) mice. Surprisingly, adenosine-dependent pain behavior did not involve direct and acute actions of A_{2B} AR on primary nociceptors. Instead, elevated adenosine required A_{2B} AR signaling in myeloid cells to stimulate sensory hyperexcitability and hypersensitivity through IL-6 and sIL-6R, and consequent trans-activation of gp130, which stimulates a STAT3-dependent enhancement of TRPV1 gene expression in DRG neurons. These findings reveal an unexpectedly important role for prolonged adenosine-A_{2B} AR signaling in several models of chronic pain and show that these adenosine effects depend upon IL-6 signaling from myeloid cells to transactivate sensory neurons. A particularly important finding was that pain-related behavior induced by prolonged elevation of adenosine levels was not exerted by direct action of adenosine on sensory neurons. Instead, adenosine-induced pain behavior was produced by activating A_{2B} AR in myeloid cells, possibly including microglial cells. Although microglia are well recognized to promote local inflammation and chronic pain (210) (211), emerging evidence indicates that increased peripheral inflammatory responses contribute

to chronic pain (212) (211). Several studies show the specific infiltration of monocyte-derived macrophages under pathological conditions (213), including multiple sclerosis, experimental autoimmune encephalomyelitis, or irradiation prior to BMT. It is possible that A_{2B} AR positive SCD mouse bone marrow derived cells of the myeloid lineage may infiltrate the CNS after irradiation, differentiate into A_{2B} AR positive glia, and contribute to the pain behavior observed in the A_{2B} AR -/- recipient mice. Moreover, Hu et al. (209) have provided considerable genetic and pharmacological evidence that elevated circulating adenosine signaling via myeloid cell A_{2B} AR (including microglial cells) contributes to chronic inflammatory pain and their study lead to a working model for the induction of persistent pain in which activation of A_{2B} AR on myeloid cells by prolonged exposure to adenosine in the blood causes the release of IL-6 from these cells, transactivation of gp130 on nociceptive sensory neurons by a sIL-6R/IL-6 complex, and a consequent pSTAT3-mediated increase in the nociceptive function of sensory neurons that involves enhanced TRPV1 gene expression. These mechanistic findings suggest therapeutic approaches for treating chronic pain including polyethylene glycol-ADA (an FDA approved drug) and application of A_{2B} AR specific antagonists.

A_3 AR:

- Pulmonary system diseases

Adenosine regulates respiratory system through well-known processes. Elevated levels of the nucleoside have been found in bronco-alveolar lavage, blood, and exhaled breath condensate of patients with asthma and chronic obstructive pulmonary disease (COPD). A_3 ARs it is known to be involved in both pro or anti-inflammatory responses depending on the cell type involved (214). In particular, the functional role of A_3 AR in mast cell activation is highlighted by genetic A_3 AR and mast cell KO mice where degranulation appears dependent on A_3 AR activation, thus suggesting that adenosine exposure can result in A_3 AR-dependent airway inflammation (215). Likewise, adenosine fails to induce histamine release from lung mast cells obtained from A_3 AR-KO mice and mediated airway hyper responsiveness by both A_3 AR-dependent and -independent mechanisms in rodents (216). In A_3 AR-KO mice the reconstitution of wild-type mast cells restores the airway hyper responsiveness (217). In contrast, in a bleomycin model of pulmonary inflammation and fibrosis, A_3 ARs have provided anti-inflammatory functions, regulating production of the mediators involved in fibrosis (218) (219). Although A_3 AR protein has not been found in human lung mast cells, but it is highly present in human eosinophils with anti-inflammatory functions (220) (11). As A_3 ARs inhibit degranulation of eosinophils, it has been speculated that specific A_3 AR agonists might be useful in eosinophil-dependent allergic disorders, such as asthma and rhinitis (221). However, adenosine deaminase KO mice treated with selective A_3 AR antagonists have shown a marked attenuation of pulmonary inflammation, decreased eosinophil infiltration, and reduced airway mucus production (222). Interestingly,

COPD patients have shown reduced A_{2B} AR density and an increase in A_{2A} and A_3 ARs in peripheral lung compared with normal lung function in smokers (223). An increase in A_3 ARs found in bronco-alveolar lavage macrophages from COPD patients appears to be closely associated with the presence of high levels of proinflammatory cytokines. In contrast, A_3 AR agonists have been suggested as a potential effective therapy for ischemia-reperfusion-induced lung injury (224). Indeed, inosine has been seen to have anti-inflammatory effects in allergic lung inflammation by recruiting A_3 ARs (225). Accordingly, A_3 AR activation was recently found to attenuate lung ischemia-reperfusion injury through a neutrophil-dependent mechanism, suggesting the use of A_3 AR agonists as a novel therapeutic strategy to prevent lung ischemia-reperfusion injury and primary graft dysfunction after transplantation (226) (227). The role of A_3 AR in the human lung has still to be clarified, although data in recent literature would appear to lean toward a protective effect.

- Rheumatoid arthritis and osteoarthritis

Knowledge of the effects of adenosine has revealed that ARs could be a useful target for rheumatoid arthritis (RA) therapy. Adenosine production has emerged as an important cell mechanism to regulate inflammation due to an increase in receptor density and/or functionality. A_3 AR are upregulated in RA, psoriasis, and Crohn's disease (228). Interestingly they are also overexpressed in untreated RA patients and in methotrexate treated RA patients, and administration of anti–TNF-α drugs normalizes their number and functionality (229). Furthermore, A_3 AR density inversely correlates with Disease Activity Score in 28 or 44 joints, suggesting a direct role of the endogenous activation of these receptors in the control of RA inflammation (230). The overexpression of A_3 AR in RA has been directly linked to the increase in NF-kB, a key player in the pathogenesis of arthritic diseases (231) (228). In RA patients, adenosine suppresses the elevated levels of proinflammatory cytokines such as TNF-α and IL-1b, and clinical evidence has shown that A_3 AR agonists modulate an improvement in signs and symptoms of the disease (232) (233). Furthermore, A_3 AR agonists prevent cartilage damage, osteoclast/osteophyte formation, bone destruction, and markedly reduce pannus and lymphocyte formation in rat models (234) (235). The anti-inflammatory effect of A_3 ARs has also been observed in fibroblast like synoviocytes derived from the synovial fluid of RA patients and is closely associated with a decrease in NF-kB and TNF-α release (236). Oral treatment with CF101 (IB-MECA, Figure 17) has led to amelioration and a marked decrease in clinical manifestations of the disease. In a phase I study in healthy subjects, CF101 proved safe and well tolerated, offering linear pharmacokinetic activity (237). This was confirmed in a now successfully concluded phase II study in RA patients in which CF101 mediated improvement in signs and symptoms, thus suggesting an opportunity for its development as an antirheumatic agent (233). The most common form of arthritis is osteoarthritis (OA), which is the most important cause of disability in older adults. The current recommended treatment of OA involves weight loss, physical therapy, and the use of pain relievers. However, these drugs do not reverse the degenerative process in OA and show some adverse effects on cartilage metabolism (238). It is well known that p38 MAPKs are involved in

controlling such cellular responses as adenosine-mediated proinflammatory cytokine release (239). Accordingly, a pathway involving the reduction in p38 MAPKs, NF-kB, TNF-a, and IL-8 by A_3 AR activation was observed in human synoviocytes (240). It was also reported that the NF-kB signaling pathway is deregulated by the presence of IB-MECA and is involved in OA pathogenesis. In addition, CF101 induces inflammatory cell apoptosis and acts as a cartilage protective agent, suggesting that it may be a suitable candidate for the treatment of OA (235). The safety and efficacy of CF101 has also been evaluated in a phase II clinical study with patients suffering from OA of the knee (241). Interestingly, a link has been found between ARs and their modulation by such physical agents as pulsed electromagnetic fields (PEMFs). In vitro studies on joint cells have suggested that exposure to PEMFs mediates a significant protection against the catabolic effect of proinflammatory cytokines and an anabolic action increasing matrix synthesis and cell proliferation (242).

- Eye diseases

A_3 ARs have been widely implicated in many ocular diseases including dry eyes, glaucoma, and uveitis. In the past, A_3 AR KO mice showed lower intracellular pressure, thus suggesting that A_3 AR antagonists could play a role in the treatment of glaucoma (243). In addition, the use of A_3 AR antagonists appears to be a specific, alternate approach for treating ocular hypertension in patients affected by the pseudoexfoliation syndrome in open angle glaucoma, which is typically associated with anterior chamber hypoxia and elevated intraocular pressure (IOP) (243). Accordingly, a series of nucleoside-derived antagonists have been found to lower IOP across species (244). Recently, it was reported that adenosine may trigger oligodendrocyte death via activation of A_3 AR, suggesting that this mechanism contributes to optic nerve and white matter ischemic damage (245). CF101, a prototypical A_3 AR agonists, entered a clinical phase of drug development. Studies from a phase II clinical trial revealed that it was well tolerated and induced a statistically significant improvement in patients with moderate to severe dry eye syndrome. Interestingly, in the same clinical trial, CF101 decreased IOP, thus demonstrating its efficacy as an IOP-lowering agent. These data, and the anti-inflammatory characteristics of CF101, support pursuing study of this drug as a potential treatment of the signs and symptoms of dry eye syndrome and glaucoma (246) (247). Nowadays, CF101 undergoes a phase II, randomized, double-masked, placebo-controlled, parallel group study of the safety and efficacy of daily IB-MECA administered orally in subjects with elevated intraocular pressure. CF101 has also been effective in an experimental model of autoimmune uveitis, supporting further exploration of this molecule for the treatment of uveitis (248). Oral treatment with CF101, initiated upon disease onset, improves clinical uveitis fundoscopy score and ameliorates the pathologic manifestations of the disease. In fact, in parallel with IOP phase II, CF101 undergoes also a phase II, randomized, double-masked, placebo-controlled study of the safety and efficacy of daily CF101 administered orally in subjects with active, sight-threatening, noninfectious intermediate or posterior uveitis.

- Pain

The contribution of A_3 AR in pain states has been evaluated in different studies. A nociceptive and proinflammatory response resulting in edema formation was first demonstrated after activation of A_3 AR; this effect was mediated by both serotonin and histamine release, most likely from mast cells and subsequent actions on the sensory nerve terminal (249). However, recently, the treatment of chronic neuropathic pain was proposed as a novel potential application of A_3 AR agonists (250). A_3 AR agonists blocked the development of mechanically and chemotherapy-induced neuropathic pain in a dose-dependent fashion and significantly augmented the analgesic effects of currently used analgesics (251). Accordingly, in an animal model of surgery-induced metastasis Cl-IB-MECA significantly reduced bone cancer pain, providing the pharmacologic rationale for using selective A_3 AR agonists as a new approach in chronic neuropathic pain (252). Interestingly, very recently, the first mechanistic insight into beneficial effects of A_3 AR agonists against neuropathic pain has been explored (253) (254). In particular, it has been found that these effects were due to the inhibition of an astrocyte-associated neuroinflammatory.

1.3.6 Adenosine receptors ligands

Medicinal chemistry approaches have been applied to all four of the adenosine receptor subtypes (A_1, A_{2A}, A_{2B}, and A_3) to create selective agonists and antagonists for each. The most recent class of selective AR ligands to be reported is the class of A_{2B} AR agonists. Selective ligands have facilitated research on therapeutic applications on diseases in which ARs are involved and in some cases among the large number of AR ligands have been possible to find good clinical candidates. Prodrug approaches have been developed which improve the bioavailability of the drugs, reduce side-effects, and/or may lead to site-selective effects. The A_{2A} AR agonist regadenoson (Lexiscan®), a diagnostic drug for myocardial perfusion imaging, is the first selective AR agonist to be approved. Other selective agonists and antagonists are or were undergoing clinical trials for a broad range of indications, including capadenoson and tecadenoson (A_1 AR agonists) for atrial fibrillation, or paroxysmal supraventricular tachycardia, respectively, BVT.115959 (A_{2A} AR agonists) for pain, preladenant and istradefylline (A_{2A} AR antagonist) for the treatment of Parkinson's disease, BAY 60-6583 (A_{2B} AR agonist) for angina pectoris, IB-MECA (CF101) and Cl-IB-MECA (CF102) (A_3 AR agonists) for inflammatory diseases and cancer, respectively.

A_1 AR agonists

A scheme of important A_1 AR agonists is shown in Figure 11. A_1 AR agonists tend to be substituted at the N6 position with arylalkyl (R-PIA), cycloalkyl (CPA, CCPA, INO-8875, GR79236X and Capadenoson), bicycloalkyl (5'-Cl-5'-deoxy-(±)-ENBA), or aryl (SPA and GW493838) substituents (255). The C2 and 5' positions also may be substituted with Cl, CCPA and 5'-Cl-5'-deoxy-(±)-ENBA, respectively, or the 5' position with cyclic moieties (GW493838). R-PIA was one of the first AR agonists to be widely used. It was previously defined as a moderately A_1 AR selective agonist, but its use in that capacity is discouraged in favor of more selective nucleosides. A_1 AR agonists CPA and CCPA are widely used pharmacological probes with CCPA being more selective for the A_1 AR. A cautionary note is that many of the selective A_1 AR agonists used routinely such as CPA and CCPA have considerable activity at the A_3 AR. CCPA and agents that increased endogenous adenosine mimicked the acute antinociceptive effect of acupuncture, consistent with the hypothesis that the A_1 AR mediates this effect (256). The agonist INO-8875 7 (also known as Trabodenoson), which is an A_1 agonist in Phase III clinical trials for glaucoma, is also intended for optic neuropathy. A_1-selective nucleoside derivative 8 failed to show efficacy in a clinical trial for dental pain and was tested in a Phase II trial for postherpetic neuralgia or peripheral nerve injury before being discontinued (257). A_1-selective non-nucleoside derivative capadenoson (BAY68-4986) is in trials for treatment of persistent atrial fibrillation and is now available as a research tool (143). Compound 10 is highly selective for the A_1 AR and displayed analgesic activity in the formalin test in mice (258) (259). SPA is a peripherally-selective agonist, due to its permanently charged sulfonate group, that is moderately A_1 AR selective (70-fold). GW493838 was tested in a clinical trial for peripheral neuropathic pain but discontinued (260). UNC32a displayed antinociceptive effects in mice and was suggested to cross the blood brain barrier and act directly through the A_1 AR despite the 5'-phosphate group (261). Partial agonists of the A_1 AR (such as the 2'-deoxy analog of 6) are effective in chronic neuropathic but not acute pain models and lack some of the cardiovascular side effects of full A_1 AR agonists (262). Compound 14 is a moderately selective full A_1 AR agonist that protects in some seizure models (263). It is well tolerated in rodents and does not produce the toxicity upon dose escalation that is typical of more widely used A_1 AR agonists, likely from cardiovascular effects. MRS5474 was shown to induce antidepressant effects through an increase of homer1a in the brain (264).

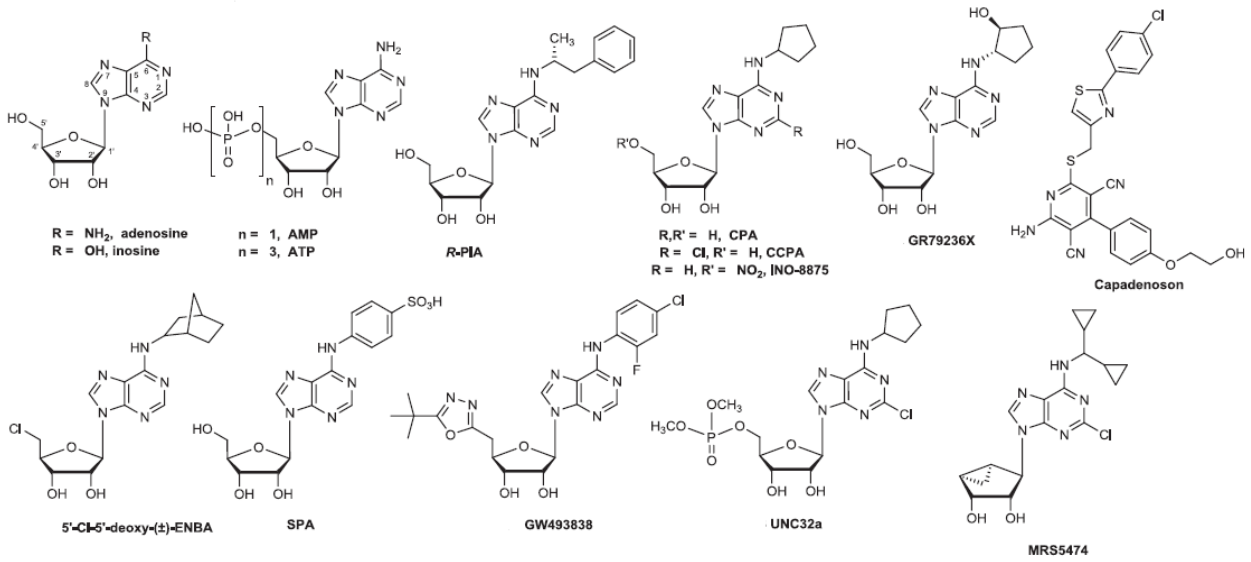

Figure 11: Some important A_1 AR agonists in literature (20)

A_1 AR antagonists

The widely ingested alkylxanthines theophylline (1,3-dimethylxanthine) and caffeine (1,3,7-trimethylxanthine) at physiological concentrations are weak (affinity ≈ 10 mM) nonselective antagonists at ARs. The main caffeine metabolite paraxanthine (1,7-dimethylxanthine) also acts as a central nervous stimulant and with even higher potency than caffeine at ARs and might be useful for treating hypersomnia associated with neurodegenerative diseases (265). 8-p-sulfophenyl derivatives SPT and DPSPX are moderately potent nonselective antagonists of ARs with the added benefits of water solubility and restricted entry to the brain. A_1 AR selective antagonists are derived from non-xanthines cores, e.g. adenine derivative WRC-0571 and pyrrolopyrimidine SLV320. An 8- cycloalkylxanthine derivative DPCPX is the most widely used A_1 AR selective antagonist with nM affinity, but its A_1 AR selectivity is greater in rodents than in human. Several 8-bicycloalkylxanthine derivatives KW3902 (rolofylline) and PSB36 are even more selective for the A_1 AR. As aforementioned, rolofylline was involved in the PROTECT project, a Phase III clinical study targeting renal failure in chronic heart disease (18) (138).

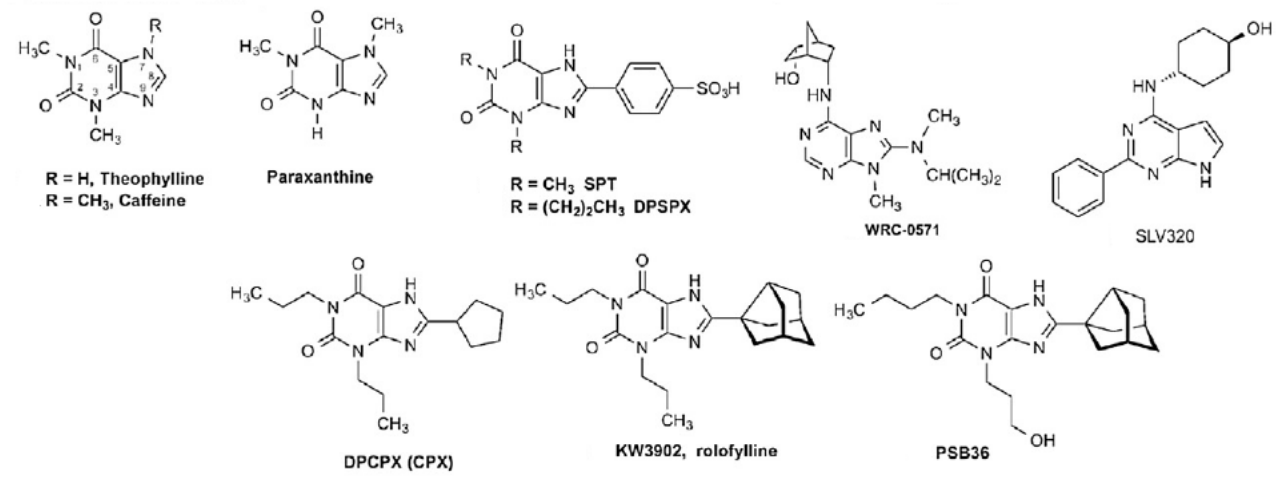

Figure 12: : Some important A1 AR antagonists in literature (20)

A_{2A} AR agonists

A_{2A} AR agonists are often substituted at the C2 position with arylalkyl (CGS21680) or ethynyl (ATL-313) substituents. CGS21680 is a widely used pharmacological probe for activation of the A_{2A} AR, but its high AR subtype selectivity seen in rat and mouse is reduced at human (h) ARs, and its degree of entry into the brain is low. A single intrathecal injection of CGS21680 or ATL-313 was reported to have a long duration of protection against mechanical allodynia and thermal hyperalgesia in a model of chronic constriction injury (CCI) in mice (266). An X-ray structure of the hA_{2A} AR complex with agonist CGS21680 was recently reported (267). Another A_{2A} AR agonist BVT.115959 (structure not disclosed) advanced to clinical trials for pain (260). UK-432097 is a selective A_{2A} AR agonist that was in clinical trials for COPD, which were discontinued due to lack of efficacy. With its large molecular weight and many H-bonding groups, it is not orally bioavailable. However, these molecular features increase the stability of the A_{2A} AR complex, such that it was possible to obtain an X-ray crystallographic structure without extensive stabilizing point mutations (57). This was the first X-ray structure of an AR complex with an agonist to be reported. Although not detected in the X-ray structures, the A_{2A} AR can form in situ various functional homo- and hetero- (e.g. with the A_1 AR or the D2 dopamine receptor) di- or multimers (268) (269) (270). The A_{2A} AR can also heterodimerize with the $P2Y_{1R}$.

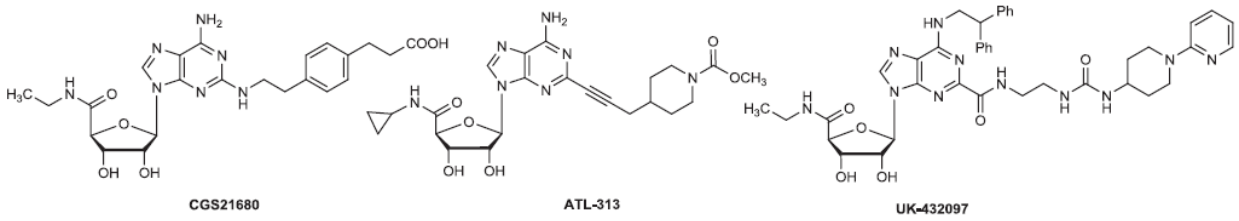

Figure 13: Some important A_{2A} AR agonists in literature (20)

A_{2A} AR antagonist

An 8-styrylxanthine derivative, Istradefylline (KW-6002, Kyowa Hakko), is approved for Parkinson's disease treatment in Japan. The related compound CSC is selective for the A_{2A} AR, but also inhibits monoamino oxidase-2 (MAO-2), two activities that would be beneficial in neurodegenerative diseases. Two A_{2A} AR-selective antagonists, ZM-241385 and SCH-442416, are commonly used as A_{2A} AR -selective pharmacological probes of nM affinity. The X-ray structure of A_{2A} AR complex with ZM-241385 was the first antagonist-bound AR structure to be reported (54), and now a higher resolution structure of 1.8 Å resolution is available (271). To the same family as SCH-442416 belongs Preladenant (SCH-420814, Merck), which was in clinical trials for treatment of Parkinson's disease. A_{2A} AR-selective antagonists Tozadenant (SYN-115, Biotie) and Vipadenant (BII014, V2006, Biogen) were also in clinical trials for the same condition. The A_{2A} AR affinity of SCH-442416 was initially reported in the subnanomolar range, but the Ki value was redetermined to be 4 nM (255). The A_{2A} AR-selective adenine derivative ANR94, with a relatively low molecular weight, is effective in Parkinson's disease models. A_{2A} AR-selective antagonists are also of interest in the context of checkpoint blockade for cancer immunotherapy, possibly by coadministration with other anticancer agents (272).

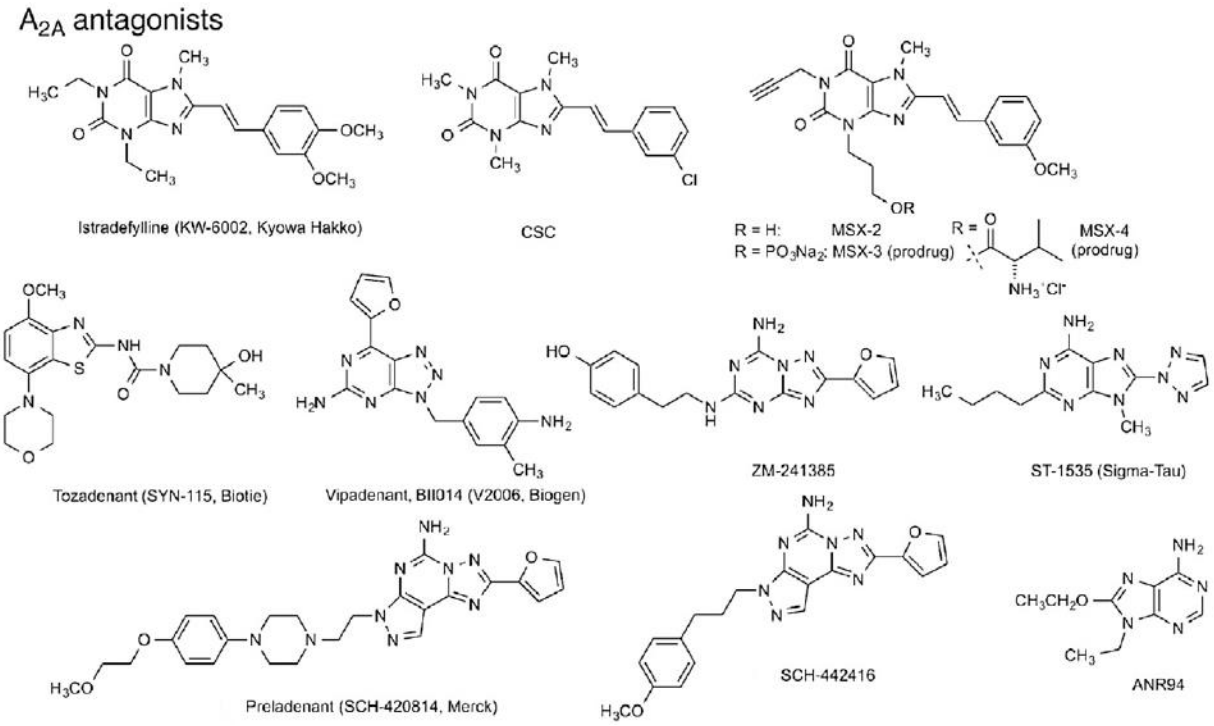

Figure 14: Some important A_{2A} AR antagonists in literature (20)

A_{2B} AR agonists

Because of the widespread distribution of A_{2B} AR and the involvement of this receptor subtype in important (patho)-physiological processes both in peripheral tissues and in the central nervous system, many efforts have been carried out in order to identify potent and selective A_{2B} AR ligands yielded with noteworthy therapeutic potential. However, the lack of highly selective agents has hampered efforts to better characterize the A_{2B} AR subtype and consequently to fully define its therapeutic potential. 5'-(N-ethylcarboxamido)adenosine (NECA), a nonselective agonist, is currently considered to be one of the most potent agonists at the A_{2B} AR, with an EC_{50} of nM (273) expressed in CHO cells and is the most frequently used ligand to activate this subtype. In order to identify selective and high affinity agonists for the A_{2B} AR many efforts have been devoted to modify the purine ring and ribose moiety of the adenosine. Nucleoside-based agonists are the result of modifying the endogenous ligand, adenosine, by substitution at the N6-, and C2-positions of the purine heterocycle and/or at the 5'-position of the ribose moiety. The various substitutions at these positions are designed to increase metabolic stability in biological systems, binding specificity and/or affinity at different adenosine receptor subtypes. In consequence, equally and more selective NECA derivatives, for the A_{2B} AR were obtained. These compounds have EC_{50} values ranging from 82 to 450 nM for the A_{2B} AR and showed selectivity towards the other adenosine receptor subtypes (274). Recently, a new A_{2B} AR agonist 2-[6-amino-3,5-dicyano-4-(4-hydroxyphenyl)pyridin-2-ylsulfanyl]acetamide BAY-606583, was patented by Bayer HealthCare and was used to study the cardioprotective function of A2B receptors (275). This compound is very selective for the A_{2B} AR with an EC50 value of 3–10 nM for the human A_{2B} AR and EC50 values > 10 µM for the A_1, A_{2A} and A_3 AR subtypes, characterized by CHO cells in a gene-reporter assay expressing recombinant human receptors in high density (184). In order to identify selective and high affinity BAY-606583 has been used as a non-nucleoside agonist for selective activation of the A_{2B} AR, but its potency, selectivity and efficacy are less than originally reported (276) (277). Thus, it should be used cautiously and in combination with appropriate antagonists. BAY-606583 is of the same chemical series (3,5-dicyanopyridines) as A_1 AR agonist Capadenoson.

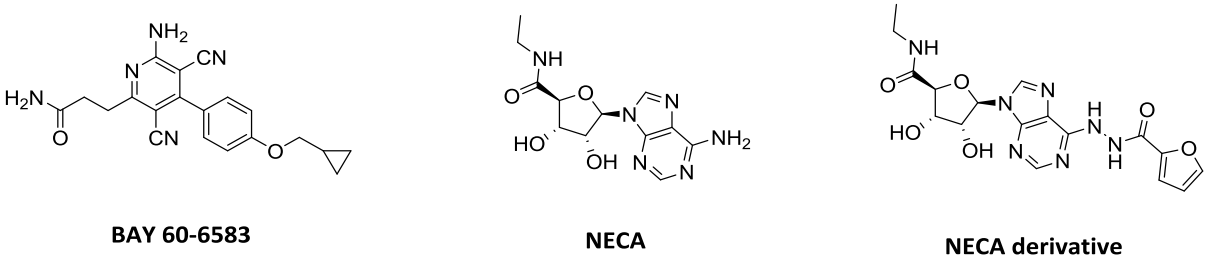

Figure 15: Some important A2B AR agonists in literature

A_{2B} AR antagonists

A_{2B} AR antagonists have recently been reviewed (278). Certain modifications of the xanthine core structure at the 8-position with aryl groups have been found to result in selectivity for the A_{2B} AR. The first antagonist to be reported was MRS1754. Later, groups at Univ. of Bonn, Germany (PSB-1115, PSB-603), University of Ferrara, Italy (MRE-2029-F20), at Gilead Sciences (CVT-6883, GS6201) and at Clinical Data Inc. (ATL802) improved on the degree of selectivity and/or the water solubility of the xanthines as A_{2B} AR. antagonists. For example, GS-6201 (CVT-6883) has a selectivity of 88-fold vs. hA_1 AR, 149-fold vs. hA_{2A} AR, and 49-fold vs. hA_3 AR. PSB-603 shows a particularly high affinity and selectivity, not only in humans, but also in rodents. PSB-1115 exhibits high water-solubility and is therefore useful for in vivo studies, however its A_{2B} AR affinity and selectivity is lower than that for other A_{2B} AR antagonists. Besides xanthines, 2-aminopyrimidine derivatives, such as LAS38096, 2-aminothiazolopyrimidines, benzothiazoles (279), pyridine derivatives (280), have been developed as A_{2B} AR antagonists MRS1754 were introduced by the pharmaceutical industry for possible application to asthma, but neither remains on a clinical path.

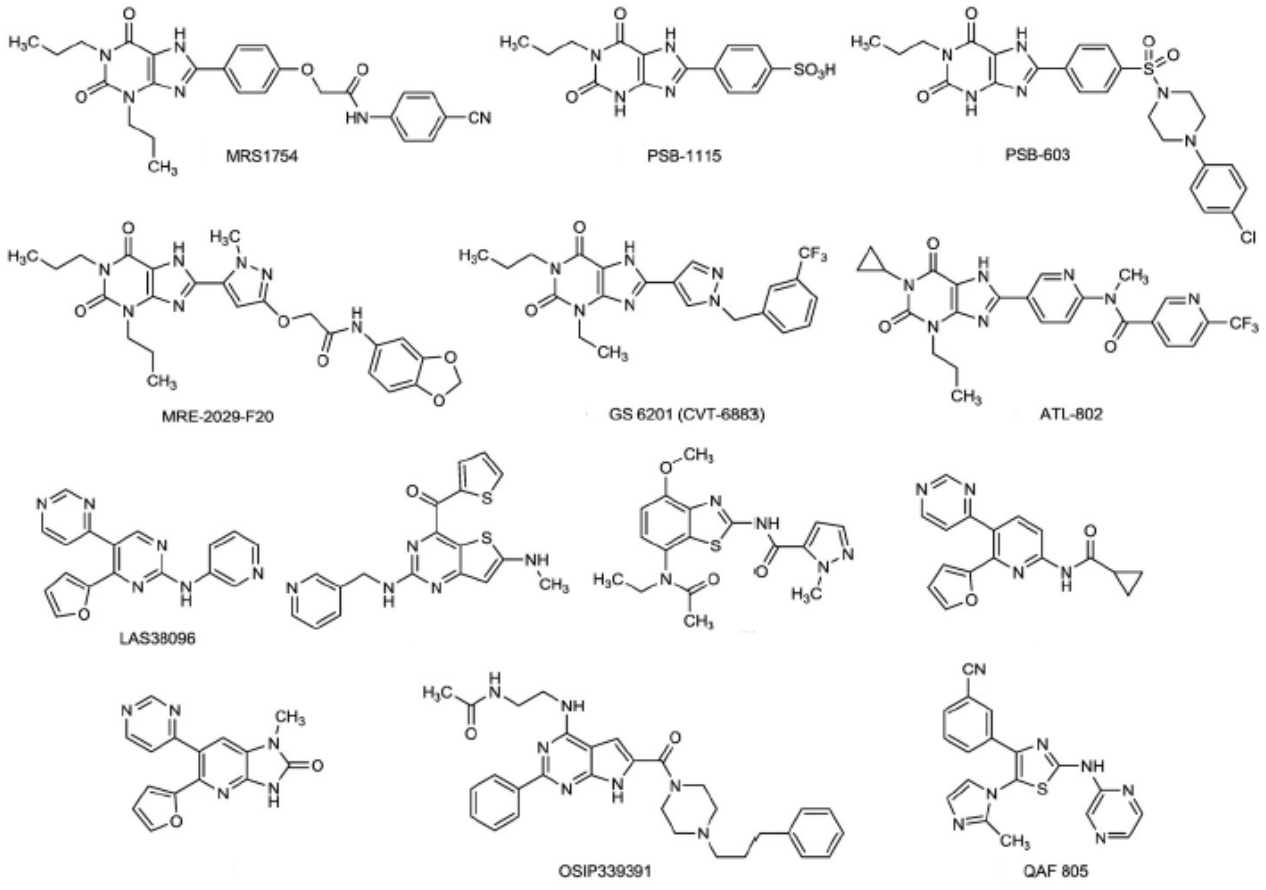

Figure 16: A_{2B} AR selective antagonists in literature (255)

A_3 AR agonists

A_3 AR agonists in Figure 17 are generally adenosine derivatives substituted at the C2, N6 and 5' positions with various substituents. Those groups most favorable for A_3 AR selectivity include: N6 - benzyl or small alkyl; C2 e H, Cl, alkynyl or arylethynyl. IB-MECA (also known as Piclidenoson) and Cl-IB-MECA are widely used pharmacological probes with Cl-IB-MECA being more selective for the A_3 AR, and they are in clinical trials for inflammation (rheumatoid arthritis and psoriasis) and primary liver cancer, respectively (241). HEMADO has been used as a highly selective A_3 AR radioligand of high affinity (281). The actions of A_3 AR agonists IB-MECA and MRS5698 in chronic neuropathic pain and cerebroprotection have been described (282). They completely reverse or prevent allodynia and hyperalgesia in the chronic constriction injury (CCI) model but have no effect on acute pain.

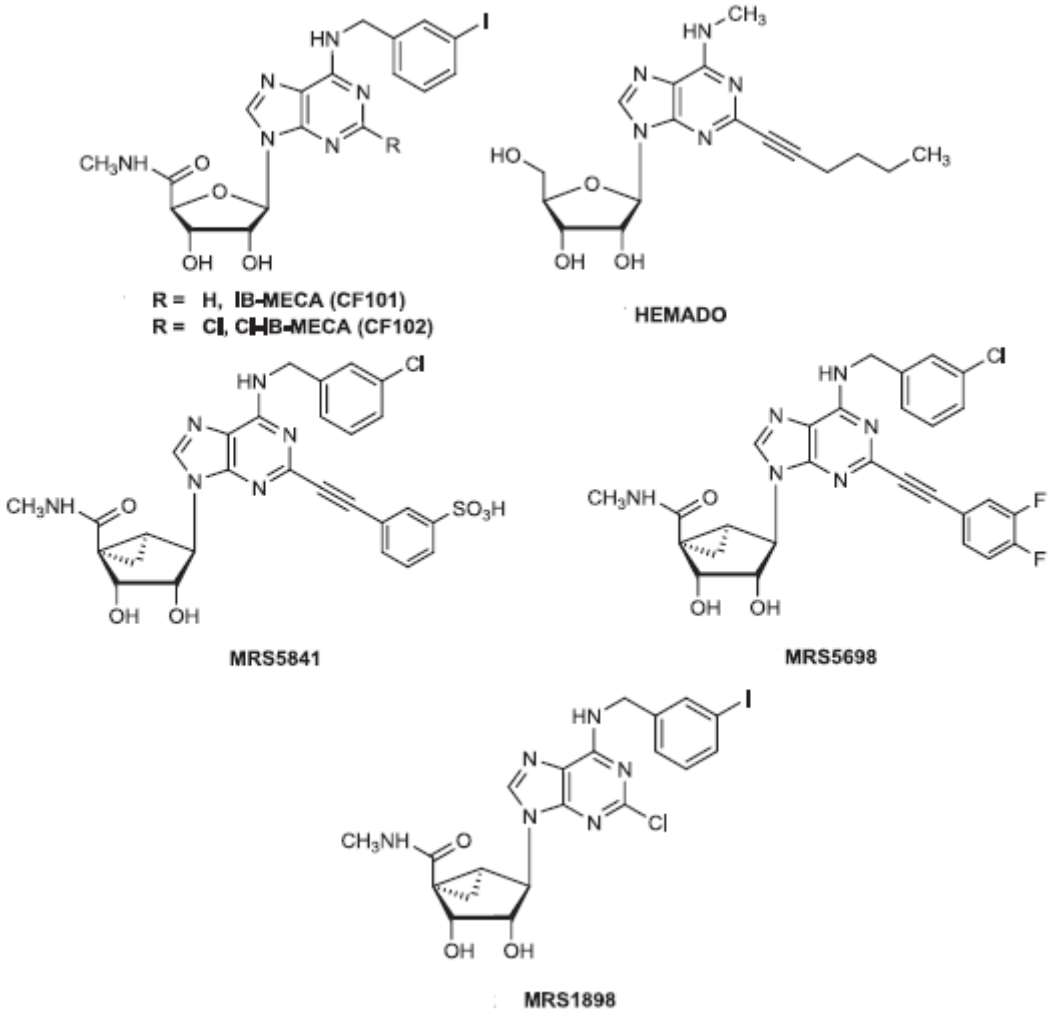

Figure 17: Some A_3 AR selective agonists in literature.

MRS5841, MRS5698 and MRS1898 contain a conformationally constrained bicyclic ring in place of ribose with a North conformation (N)-methanocarba ring system, which adds to the A_3 AR selectivity (283) (284) (285). MRS5698 is a peripherally-selective agonist that is highly A_3 AR selective (250). The pharmacokinetics of MRS5698, administered intraperitoneally in rat, indicates a t1/2 of 1.09 h (285), consistent with its duration of action in vivo in the CCI pain model. MRS5698 is also orally active in the CCI model.

A_3 AR antagonists

In an initial broad screen, several classes of non-xanthine antagonists were identified for the A_3 AR: 1,4-dihydropyridines, pyridines, and flavones. The pyridine derivative MRS1523 (Figure 18) has become a useful tool since it shows relatively high affinity not only for the human but also for the rat A_3 AR. Later it was noted that the potent non-selective AR antagonist CGS15943 could be modified to produce A_3 AR selectivity, and from selective modifications was obtained MRE3008-F20, one of the most potent and selective compounds at hA_3 AR.

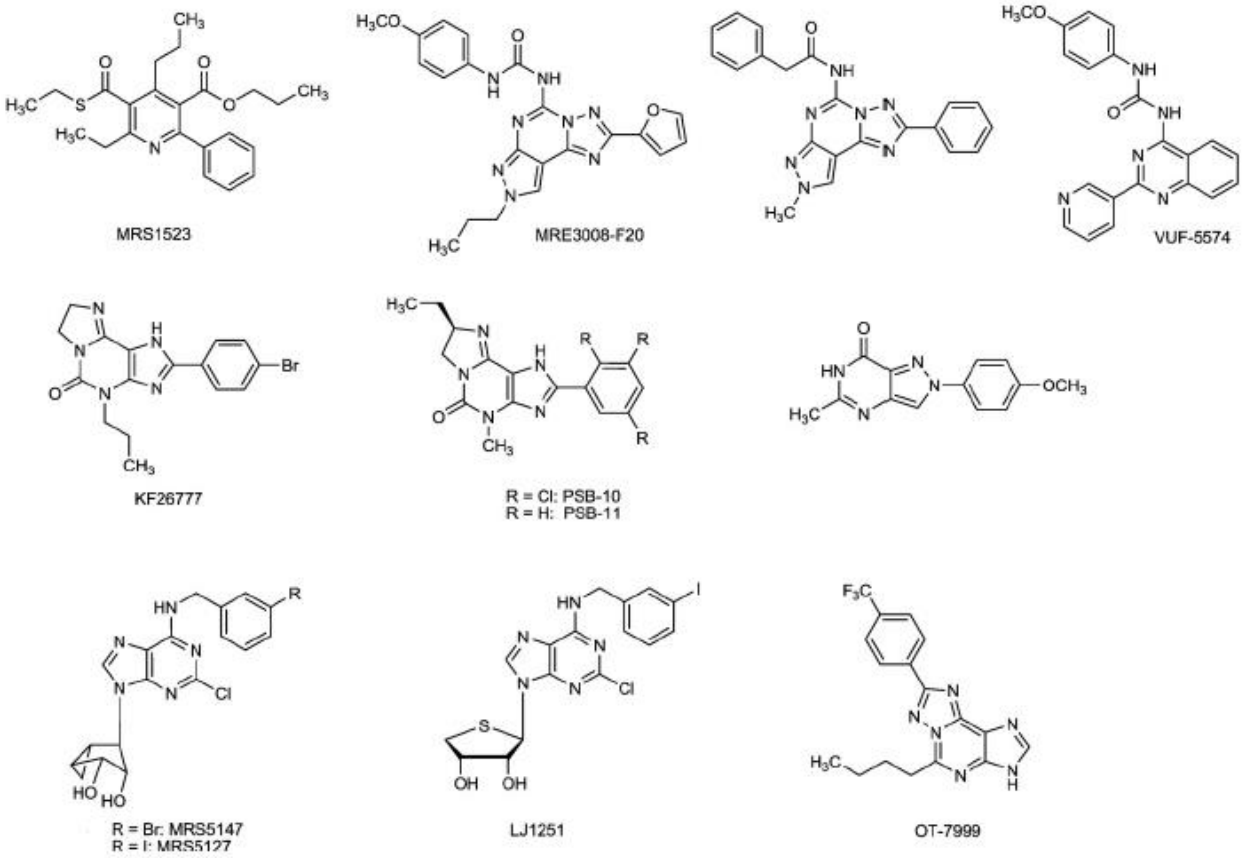

Figure 18: Some A_3 AR antagonists in literature (255)

The urea-substituted quinazoline derivative VUF5574 also possesses high A_{2B} AR affinity and selectivity. Some tricyclic xanthines (KF2677, PSB-10 and PSB-11) have been found to be very potent and selective antagonists at hA_3 AR showing increased water-solubility due to a basic nitrogen atom in the additional imidazole ring. Recently described A_3 AR-selective antagonists include pyrazolopyrimidinones. Many A_3 AR antagonists are much more potent at human as compared to rat A_3 AR. The principles for converting selective A_3 AR agonists into selective A_3 AR antagonists are based on either a conformationally constrained ribose-like ring or one that is truncated at the 4'-position (i.e., missing the ribose CH2OH group entirely). Thus, the nucleoside derivatives MRS5147 and its 3-iodo analogue MRS5127 are highly selective A_3 AR ligands generally across species. MRS5127 was recently reported as a radioligand selective for the A_3 AR (286). The truncated 4'-thioadenosine derivative LJ-1251, which acts as a A_3 AR antagonist across species, was shown to lower intraocular pressure when applied topically (287) (244).

2. Aim of the work

The work characterizing this Ph.D. thesis is part of a wider project that the research group I have joined during my Ph.D. course has undertaken in recent years and is actually developing. In fact, many compounds belonging to different heterocyclic classes were synthesized and evaluated as AR ligands (288) (289) (290) (291). In particular, the studies were focused on the development of selective antagonists for hA_3 and hA_{2A} ARs, and also to obtain combined hA_1/A_{2A} AR ligands with antagonistic activity (292).

As a general trend, AR ligands have been often projected through rational approaches, including molecular modeling studies based on the AR subtype structure they are targeting. In the past, the first approach that was used, usually started from the modification of the endogenous ligand, adenosine. These studies led to many different classes of ligands and several recurring structural features have been identified for defining affinity or efficacy of the compounds at the specific AR subtype (20). Antagonists are characterized by a large structural variability. They are generally nitrogen-containing heterocycles with a mono-, bi- or tricyclic core skeleton. In contrast, there is no such flexibility for the agonists. In fact, the agonist profile of AR ligands has been associated, for a long time, to an adenosine-like structure with the ribose moiety only slightly modified.

However, in the last 15 years, a major breakthrough with respect to both affinity and selectivity was achieved with the discovery of a new class of non-adenosine like compounds, the aminopyridine-3,5-dicarbonitrile series. These ligands first appeared in patent literature and the preliminary data suggested the involvement of the A_{2B} AR as a target (293) (294) (295) but their intriguing characteristics emerged later. Successively, some research (296) reported that non-nucleoside AR agonists show less species differences than the adenosine-like ones and thus more versatility for pharmacological studies (255).

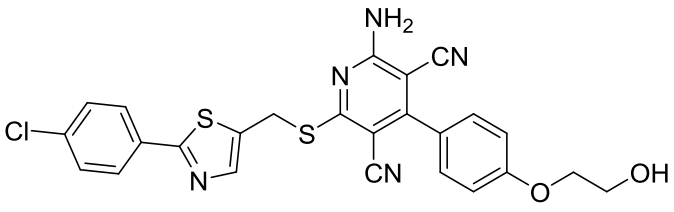

Capadenoson

hA_1AR K_i = 1.4 ± 0.15 nM

hA_{2A} AR K_i = 1%

hA_{2B} AR K_i = 2.5%

hA_3 AR K_i = 1.2%

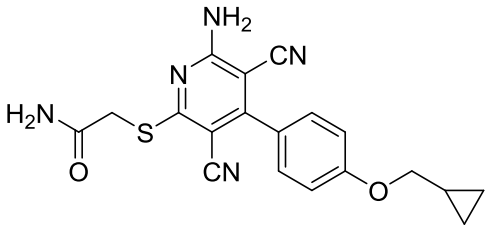

BAY60-6583

hA_1 AR K_i = >10000

hA_{2A} AR K_i = >10000

hA_{2B} AR EC_{50} = 3-10 nM

hA_3 AR K_i = >10000

Figure 19: Non-nucleoside A_1 and A_{2B} AR agonist Capadenoson (BAY68-4986) and BAY60-6583, respectively

Based on the aminopyridine-3,5-dicarbonitrile scaffold, Bayer Healthcare synthesized two interesting compounds belonging to this series: **Capadenoson** (BAY68-4986), a potent and selective A_1 AR agonist, and **BAY60-6583** (Figure 19) which showed high affinity and selectivity for A_{2B} AR. In particular, **BAY60-6583** was a real breakthrough: it was the first potent and selective AR agonist reported in literature with non-adenosine like structure. It has rapidly overcome the use of other nucleoside-like agonist in most of the pharmacological assays regarding A_{2B} AR. In particular it substituted the 5'-(N-ethylcarboxamido)adenosine (**NECA**, see Figure 15) that, since its discover in 1983, has been used as A_{2B} AR elected agonist, despite its scarce selectivity *versus* the other AR subtypes.Although **BAY60-6583** has been largely studied, its real pharmacological profile is nowadays a matter of debate: in the patent describing **BAY60-6583,** Bayer Healthcare assessed its full agonist profile at A_{2B} AR. However, a 2014 study of Hinz et al. (277) reported that **BAY60-6583** behaves as a partial agonist, with a maximum effect of 56% compared with the 100% of **NECA** as reference in cAMP accumulation assays, performed on CHO cells stably transfected with the hemagglutinin (HA)-tagged human A_{2B} AR (CHO-HA-hA_{2B} cells). In contrast, in our pharmacological assay (see Result Section below) **BAY60-6583** acts as full agonist and shows to be less potent at A_{2B} AR than reported by Bayer Healthcare.

Contemporarily, Bayer Healthcare carried on studies on the A_1 AR agonist **Capadenoson** (Figure 19) which was one of the most interesting compound emerged as potentially useful for the treatment of angina being devoid of the side effect (e.g. bradycardia) proper of full agonist compounds. Since A_1 AR are the most extensively investigated among the ARs, the effects of **Capadenoson** emerged as so interesting that now it is in clinical trial for the treatment of persistent atrial fibrillation and also available as research tool (143). More recently, the focus of attention has moved to the antinociceptive effect exerted by A_1 AR agonist at the spinal cord level (144) (145) (146) (147) (148).

Starting from these results, in 2004 Beukers et al. (297) reported a small series of four aminopyridine-3,5-dicarbonitriles and among them **LUF-5845** (Figure 20) resulted highly active at A_{2B} subtype though endowed with a scarce selectivity toward the other ARs.

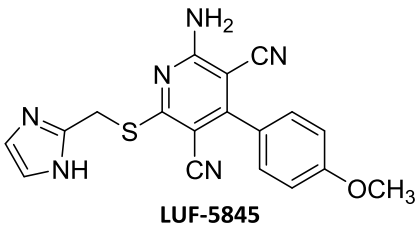

LUF-5845

hA_1 AR K_i = 7 ± 0.8 nM
hA_{2A} AR K_i = 214 ± 37 nM
hA_{2B} AR EC_{50} = 9 ± 3 nM
hA_3 AR K_i = 24 ± 7.6 nM

Figure 20

On this basis, our research group focused attention on the aminopyridine-3,5-dicarbonitrile series in order to obtain new AR ligands and to enlarge the scarcely known structure-activity relationships on this chemical class. In fact, few data are reported in the open literature, the majority of the known being included in patents (255). This kind of scaffold could allow to obtain ligands not only with a wide range of affinities but interestingly with different degrees of efficacy at the different ARs.

In fact, in a master degree thesis developed in our research group (298) four interesting compounds belonging to this chemical class were synthesized and pharmacologically evaluated at the ARs (Figure 21):

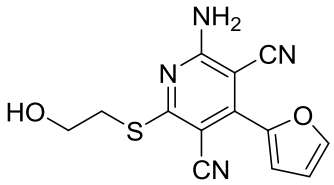

A

hA_1 AR K_i = 57 ± 4 nM
hA_{2A}AR K_i = 27%
hA_{2B} AR EC_{50} = >1000 (7%)
hA_3 AR K_i = 29%

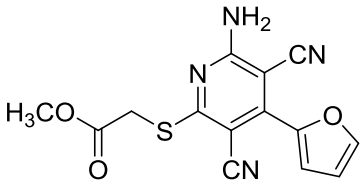

B

hA_1 AR K_i = 108 ± 9 nM
hA_{2A} AR K_i = 17%
hA_{2B} AR EC_{50} = >1000 (4%)
hA_3 AR K_i = 25%

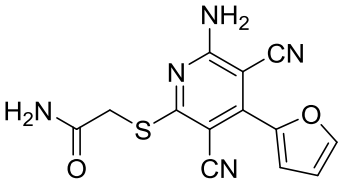

C

hA_1 AR K_i = 175 ± 12 nM
hA_{2A} AR K_i = 21%
hA_{2B} AR EC_{50} = >1000 (17%)
hA_3 AR K_i = 177 ± 15

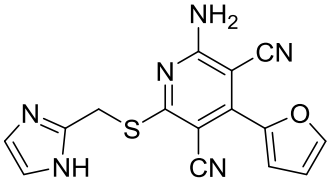

D

hA_1 AR K_i = 12 ± 2 nM
hA_{2A} AR K_i = 26 ± 2 nM
hA_{2B} AR EC_{50} = 1.7 ± 0.2 nM
hA_3 AR K_i = 65 ± 5 nM

Figure 21: Lead compounds for aminopyridine-3,5-dicarbonitrile scaffold modifications

Pharmacological evaluation of these compounds highlighted the good affinity of compounds **A**-**D** at A_1 AR, being **A** and **B** A_1 selective. In contrast, while derivative **C** binds also the A_3 subtype, **D** emerges as totally unselective ligand. Together with the dicyanopyridine derivatives reported in literature (Figure 19 and 20), in this Ph.D. thesis we elect compounds **A**-**C** as leads, in order to evaluate how modifications at the dicyanopyridine core could modulate the affinity and selectivity, but also the pharmacological profile of the members of this chemical class at the AR subtypes. Thus, based on preliminary molecular modelling studies (299) (300), different substituents were introduced in diverse positions on the selected scaffold (Figure 22).

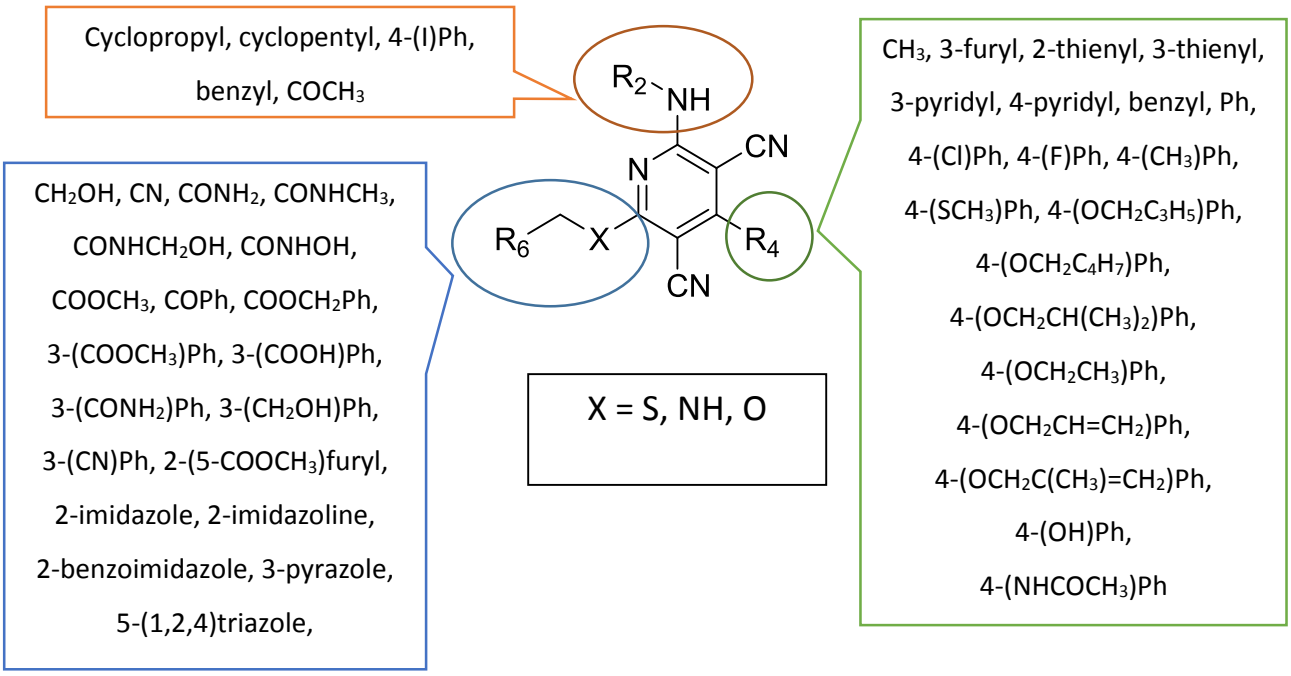

Figure 22: Modifications performed on the aminopyridine-3,5-dicarbonitrile scaffold

Modifications were performed at both R_4 and R_6 positions (see Figure 22) on the dicyanopyridine core. In particular, while various aryl and heteroaryl substituents were introduced at R_4, position R_6 generally contains groups or atoms able to engage hydrogen-bonding interactions with the receptor site, being this latter a condition that seems to be mandatory for the AR receptor interaction. Moreover, it has been investigated substitution (R_2) on the amine function with cycloalkyl, aryl and acyl moieties in order to evaluate how they could have modulated the pharmacological profile of the target compounds on the diverse AR subtypes. Further modifications regard the sulfanyl linker of the leads which has been substituted with an oxygen atom or a secondary amino group.

Two major sets of amino-3,5-dicyanopyridines were synthesized: **DCP1** series that contains compounds preferentially binding the A_1 AR (Table 3) and the **DCP2B** series including compounds designed in order to target the A_{2B} subtype (Table 4). For DCP1 series, SAR investigations were performed at the R_2, R_4 and R_6 positions and also at level of the side chain linker.On the basis of compounds **A**-**C** pharmacological data (Figure 21), major modifications were performed at R_6 position of the dicyanopyridine core while maintaining the 2-furanyl moiety at R_4 or inserting other heteroaryl groups.

DCP1 series

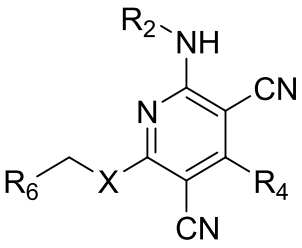

n°	X	R_2	R_4	R_6	n°	X	R_2	R_4	R_6
1	S	H	2-furyl	3-($COOCH_3$)C_6H_4	**14**	S	H	2-furyl	2-pyridyl
2	S	H	2-furyl	3-($CONH_2$)C_6H_4	**15**	S	H	2-furyl	2-phenylthiazol-4-yl
3	S	H	2-furyl	3-(COOH)C_6H_4	**16**	S	H	2-furyl	2-aminothiazol-4-yl
4	S	H	2-furyl	3-(CH_2OH)C_6H_4	**17**	NH	H	2-furyl	CH_2CH_2OH
5	S	H	2-furyl	3-(CN)C_6H_4	**18**	NH	H	2-thienyl	CH_2CH_2OH
6	S	H	2-furyl	methyl 5-furan-2-carboxylate	**19**	NH	H	C_6H_5	CH_2CH_2OH
7	S	H	3-furyl	3-($COOCH_3$)C_6H_4	**20**	O	H	2-furyl	CH_2CH_2OH
8	S	H	2-thienyl	3-($COOCH_3$)C_6H_4	**21**	S	cyclopropyl	2-furyl	CH_2CH_2OH
9	S	H	3-pyridyl	3-($COOCH_3$)C_6H_4	**22**	S	cyclopentyl	2-furyl	CH_2CH_2OH
10	S	H	2-furyl	CN	**23**	S	4-I-C_6H_4	2-furyl	CH_2CH_2OH
11	S	H	2-furyl	$COOCH_2C_6H_5$	**24**	S	$CH_2C_6H_5$	2-furyl	CH_2CH_2OH
12	S	H	2-furyl	COC_6H_5	**25**	S	$COCH_3$	2-furyl	CH_2CH_2OH
13	S	H	2-furyl	3-pyridyl					

Table 3: Synthesized compounds belonging to the DCP1 series

Thus, substituents bearing H-bond acceptor and donor groups were introduced at R_6 (compounds **1**-**16**). Firstly, aryl homologation of the R_6 of the leads **A**-**C** were performed (compounds **1**-**9**) togheter with other variegated modifications (**10**-**14**). Also nitrogen-containing heterocycles were inserted at R_6 (derivatives **13**-**16**) in order to imitate the lead **Capadenoson** (Figure 19). Then, the influence of the nature of the linker X (compounds **17**-**20**) or of the presence of R_2 substituents on the amine function (**21**-**25**) was evaluated. R_2 groups were selected on the basis of the SAR of adenosine-like agonists which preferentially bind the A_1 subtype. Such modifications were performed on the lead **A** or on strictly correlated analogues. As for the **DCP2B** series is concerned, major modifications were performed at R_4 and R_6 positions in order to target the A_{2B} subtype.

DCP2B series

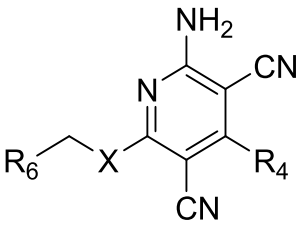

n°	X	R_4	R_6	n°	X	R_4	R_6
26	S	3-furyl	imidazol-2-yl	**47**	S	4-($OCH_2C_3H_5$)-C_6H_4	$CONHCH_3$
27	S	3-thienyl	imidazol-2-yl	**48**	S	4-($OCH_2C_3H_5$)-C_6H_4	$CONHCH_2OH$
28	S	3-pyridyl	imidazol-2-yl	**49**	S	4-($OCH_2C_3H_5$)-C_6H_4	CONHOH
29	S	4-pyridyl	imidazol-2-yl	**50**	S	4-($OCH_2C_3H_5$)-C_6H_4	$COOCH_3$
30	S	$CH_2C_6H_5$	imidazol-2-yl	**51**	S	4-($OCH_2C_3H_5$)-C_6H_4	3-($COOCH_3$)C_6H_4
31	S	4-Cl-C_6H_5	imidazol-2-yl	**52**	S	4-($OCH_2C_3H_5$)-C_6H_4	3-($CONH_2$)C_6H_4
32	S	4-F-C_6H_5	imidazol-2-yl	**53**	S	4-($OCH_2C_4H_7$)-C_6H_4	imidazol-2-yl
33	S	4-CH_3-C_6H_5	imidazol-2-yl	**54**	S	4-($OCH_2C_4H_7$)-C_6H_4	$CONH_2$
34	S	4-SCH_3-C_6H_5	imidazol-2-yl	**55**	S	4-($OCH_2CH(CH_3)_2$)-C_6H_4	imidazol-2-yl
35	S	CH_3	imidazol-2-yl	**56**	S	4-($OCH_2CH(CH_3)_2$)-C_6H_4	$CONH_2$
36	NH	C_6H_5	imidazol-2-yl	**57**	S	4-(OCH_2CH_3)-C_6H_4	imidazol-2-yl
37	S	4-($OCH_2C_3H_5$)-C_6H_4	imidazol-2-yl	**58**	S	4-(OCH_2CH_3)-C_6H_4	$CONH_2$
38	S	4-($OCH_2C_3H_5$)-C_6H_4	imidazol-5-yl	**59**	S	4-(OCH_2CH_3)-C_6H_4	$CONHCH_3$
39	S	4-($OCH_2C_3H_5$)-C_6H_4	4,5-dihydro-1H-imidazol-2-yl	**60**	S	4-(OCH_2CH_3)-C_6H_4	pyrazol-3-yl
40	S	4-($OCH_2C_3H_5$)-C_6H_4	benzoimidazol-2-yl	**61**	S	4-($OCH_2CH=CH_2$)-C_6H_4	imidazol-2-yl
41	S	4-($OCH_2C_3H_5$)-C_6H_4	pyrazol-3-yl	**62**	S	4-($OCH_2CH=CH_2$)-C_6H_4	$CONH_2$
42	S	4-($OCH_2C_3H_5$)-C_6H_4	1,2,4-triazol-1-yl	**63**	S	4-($OCH_2CH=CH_2$)-C_6H_4	pyrazol-3-yl
43	S	4-($OCH_2C_3H_5$)-C_6H_4	1,2,4-triazol-5-yl	**64**	S	4-($OCH_2C(CH_3)=CH_2$)-C_6H_4	imidazol-2-yl
44	S	4-($OCH_2C_3H_5$)-C_6H_4	tetrazol-5-yl	**65**	S	4-($OCH_2C(CH_3)=CH_2$)-C_6H_4	$CONH_2$
45	S	4-($OCH_2C_3H_5$)-C_6H_4	2-aminothiazol-4-yl	**66**	S	4-($NHCOCH_3$)-C_6H_4	imidazol-2-yl
46	S	4-($OCH_2C_3H_5$)-C_6H_4	3-pyridyl	**67**	S	4-($NHCOCH_3$)-C_6H_4	$CONH_2$

Table 4: Synthesized compounds belonging to the DCP2B series

While keeping the imidazol-2yl moiety at R_6 as it in compound **D** (Figure 21), different substituents were introduced at R_4 position (**26**-**37**, Table 4). Firstly, various heteroaryls, poorly investigated in literature, were evaluated together with diverse *para*-substituted phenyl moieties and also benzyl and methyl groups.

In parallel, position R_6 was modified while maintaining the *para*-(cyclopropyloxymethyl)phenyl substituent at R_4 that is typical of **BAY60-6583** (Figure 19). Following the imidazole moiety idea (see the lead compound **D**, Figure 21), preferentially five-membered nitrogen-containing heterocycles bearing H-bond donor and acceptor groups were introduced at R_6 (compounds **38**-**46**, Table 4). Also different carboxyamide bioisosters (**47**-**50**) and their aryl homologues (**51**-**52**) were evaluated by maintaining the possibility of hydrogen bonding interaction at this level. Moreover, by in progress selecting the best substituents at R_6 in term of hA_{2B} AR affinity and selectivity, different *para*-oxysubstituted phenyl groups were introduced at R_4 (compounds **53**-**65**). The O-(cyclo)alkyl and alkenyl substituents were chosen in order to maintain similar electronic and steric hindrance of the O-cyclopropyl moiety of **BAY60-6583**. In addition, the *para*-acetamido substituent (compounds **66**-**67**, Table 4) as containing both H-bond donor and acceptor groups was evaluated.

Moreover, the 3,6-diamino-5-cyano-4-phenyl-thieno[2,3-b]pyridine-2-carboxamide scaffold will be evaluate and obtained by an intramolecular cyclization of the 6-amino-3,5-dicyanopyridines (proved to be AR ligands) bearing a sulfanyl-acetamido substituent at position-2 of the pyridine core. Preliminary investigation was performed on **BAY60-6583** (Figure 23) in order to evaluate how molecular stiffening could influence the affinity and /or the pharmacological profile of these compounds at the ARs.

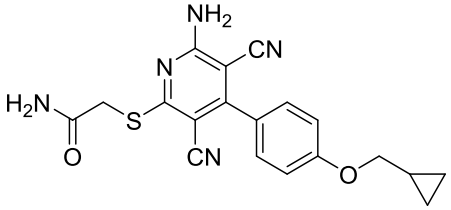

BAY60-6583

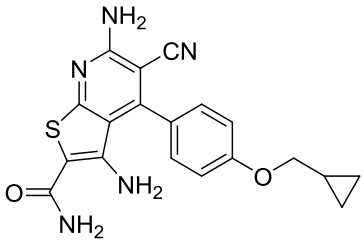

68

Figure 23: Bicyclic compound derived from cyclization of BAY60-6583

In addition to probe a new set of compounds as AR ligands, the information obtained could be useful for SAR studies and molecular modeling rationalization.

Finally, another objective of this work was the synthesis of a small set of compounds, the 7-amino-2-phenylpyrazolo[1,5-c]pyrimidine-4-carbonitriles **70-73** (Figure 24) through a procedure that can be considered brand new for the most part. These compounds can be considered as ensued from a molecular complication of the amino-3,5-dicyanopyridine scaffold by condensation with a pyrazole core. The modification was planned in order to maintain the most important hydrophobic and hydrogen-bonding interactions potentially engaged by the original pattern.

Most of the effort was directed to finalize the procedure to obtain 2-arylpyrazolo[1,5-c]pyrimidines suitably substituted at position 5 in analogy to the lead **DCP1** and **DCP2B** amino-3,5-dicyanopyridines. However, in the preliminary exploration of different synthetic approches yielding the target compounds, a set of 7-amino-substituted derivatives **70-73** were synthesized and evaluated for their affinity at ARs. The latter**,** due to their structure and to the 5-amino-functionalization can be considered as potential A_{2A} AR antagonists if compared for example to the well known **ZM-241385** (Figure 24) even if they are lacking the essential 2-furyl moiety.

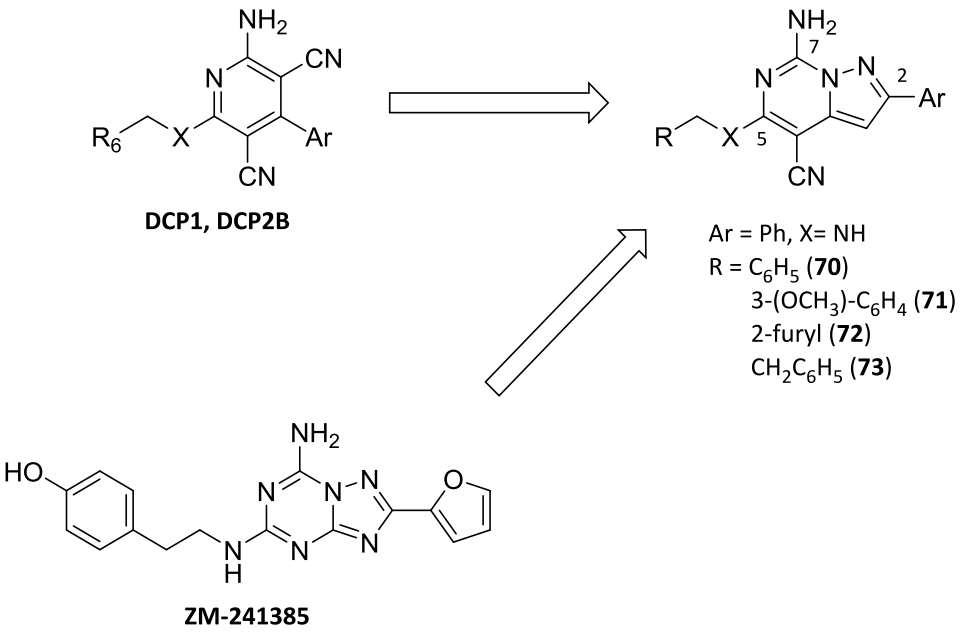

Figure 24: Newly synthesized 7-Amino-2-phenylpyrazolo[1,5-c]pyrimidine-4-carbonitriles and lead compounds

In addition to identify a new scaffold for the development of new AR ligands, this molecular complication approach was undertaken to evaluate the effect of this modification on the pharmacological profile of the new bicyclic derivatives, in particular at A_{2B} AR subtype.

To summarize, the main aim of this Ph.D. research was the investigation of the aminopyridine-3,5-dicarbonitrile chemical class in order to obtain potent and selective AR ligands. The study was an exploration of the potentiality of this scaffold to produce AR ligands with different affinities and pharmacological profiles with an eye to the A_{2B} and A_1 subtypes. Preliminary studies were carried out on 7-amino-2-phenylpyrazolo[1,5-c]pyrimidine-4-carbonitriles (**70-73**) to establish whether this heterocyclic scaffold suitably decorated could lead to the discover of new AR ligands.

3. Chemistry

3.1 Aminopyridine-3,5-dicarbonitriles

In order to achieve the desired aminopyridine-3,5-dicarbonitrile derivatives a short synthetic pathway was developed, following literature and patent advices (293) (294) (295). Most of the aminopyridine-3,5-dicarbonitrile compounds were synthesized applying the same procedures with only some exceptions. In fact, some compounds were synthesized with small deviation from the usual synthetic pathway for a matter of scarce yield or reactivity.

3.1.1 Chemistry of DCP1

For what may concern the aminopyridine-3,5-dicarbonitrile derivatives targeting A_1 AR, the synthesis of compounds **1-16, B** starts from the one-pot cyclization of the suitable commercial aldehyde to give sulfanylphenyl compounds **74-77** (scheme 1)**.** In order to achieve these latter, the condensation reaction was performed by using tetrabutylammonium fluoride (TBAF), producing higher yields with respect to other methods reported in literature (293) (297). Intermediates **74-77** were converted into the sulfanyl derivatives **78-81** with sodium sulfide, which were used in order to obtain compounds **1-16, A** by reacting with the suitable halides in mild alkaline conditions using sodium hydrogencarbonate as base. This reaction afforded final compounds in good yields.

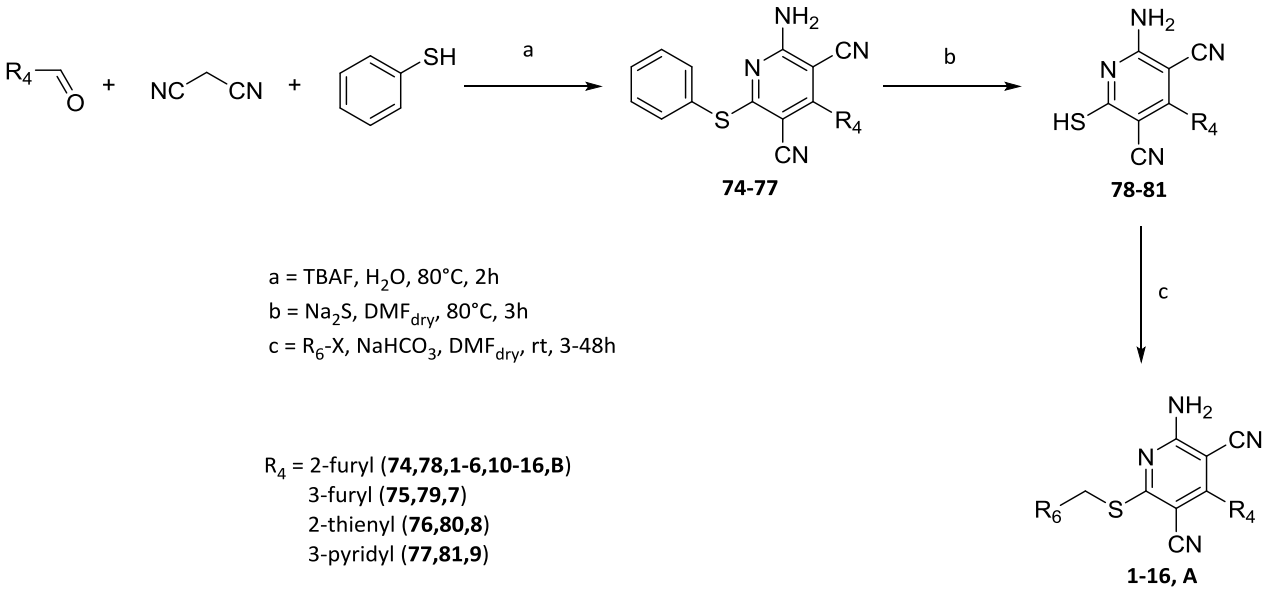

Compound	R_4	R_6
A	2-furyl	CH_2OH
1	2-furyl	3-$(COOCH_3)C_6H_4$
2	2-furyl	3-$(CONH_2)C_6H_4$
3	2-furyl	3-$(COOH)C_6H_4$
4	2-furyl	3-$(CH_2OH)C_6H_4$
5	2-furyl	3-$(CN)C_6H_4$
6	2-furyl	methyl 5-furan-2-carboxylate
7	3-furyl	3-$(COOCH_3)C_6H_4$
8	2-thienyl	3-$(COOCH_3)C_6H_4$
9	3-pyridyl	3-$(COOCH_3)C_6H_4$
10	2-furyl	CN
11	2-furyl	$COOCH_2C_6H_5$
12	2-furyl	COC_6H_5
13	2-furyl	3-pyridyl
14	2-furyl	2-pyridyl
15	2-furyl	2-phenylthiazol-4-yl
16	2-furyl	2-aminothiazol-4-yl

Scheme 1

In order to modify the sulfanyl bridge with an amine linker, compounds **17** and **18** were synthesized starting from intermediates **74** and **76**, respectively, taking advantage of the good property of sulfanylphenyl group

as leaving group in a nucleophile substitution. The reaction was easily performed at 100°C in N,N-dimethylformamide (DMF) using 2-aminoethanol as nucleophile (scheme 2).

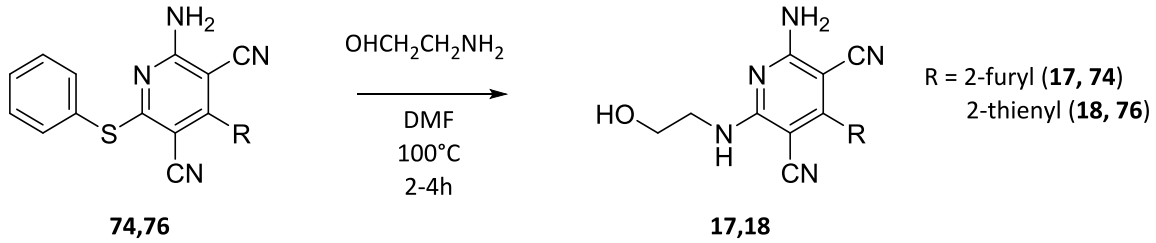

74,76 **17,18**

Scheme 2

Compound **19**, bearing a phenyl group at position R_4, was obtained through the synthesis of the chlorine intermediate **82** (scheme 3), prepared in a one-pot reaction (301) involving triethylorthobenzoate, malononitrile and hydrochloric acid and then used as starting material for coupling with commercial 2-aminoethanol to afford compound **19.**

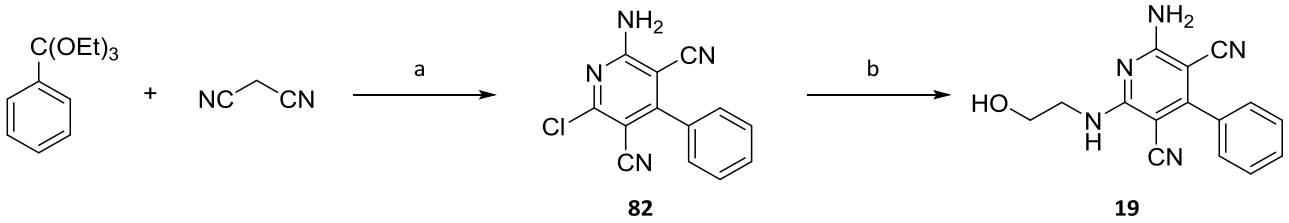

82 **19**

a = HCl 12N, 100°C, 8h
b = 2-aminoethanol, NEt_3, THF/EtOH, reflux, 1.5h

Scheme 3

Pursuing the modifications at the sulfanyl linker, compound **20**, bearing a 6-oxyethanol chain was synthesized. One-pot cyclization of commercial 2-furaldehyde and malononitrile in the presence of $NaOCH_3$, afforded in low yields intermediate **83** (scheme 4) which was converted into the corresponding hydroxy analogue **84** by treatment with concentrated hydrochloric acid and glacial acetic acid at 100°C (302). Then, **84** was used as starting material for the coupling reaction with 2-bromoethanol, performed in microwave reactor, affording final compound **20**.

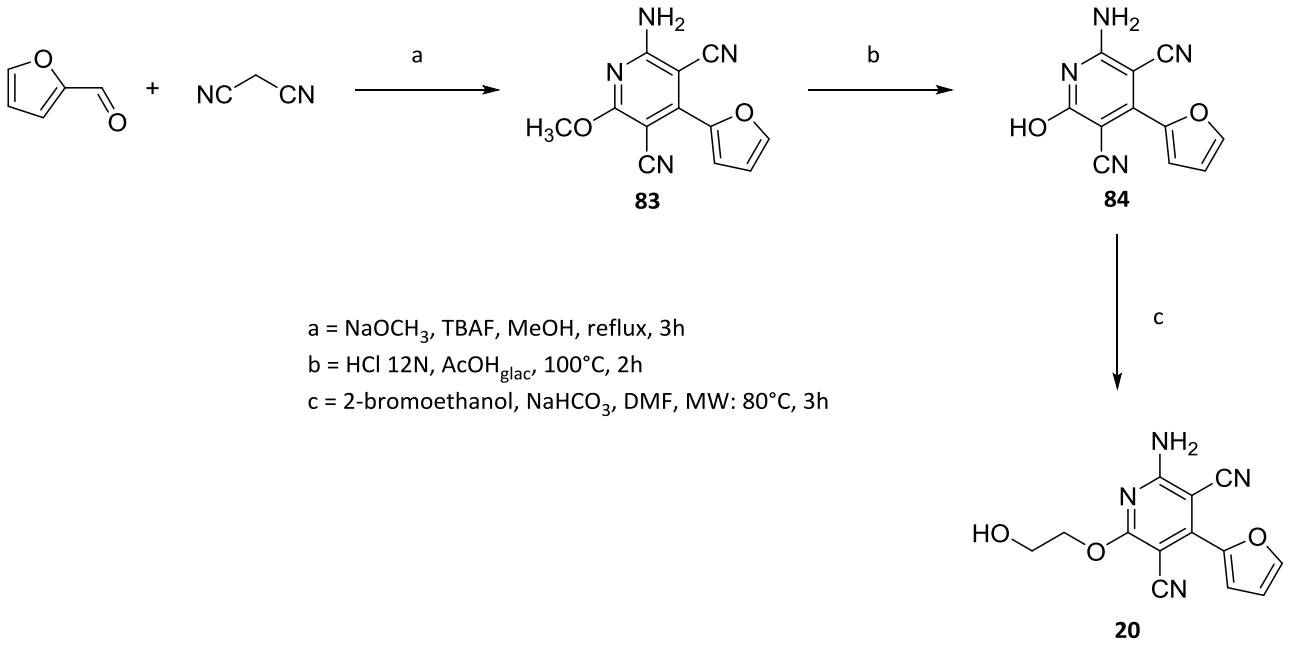

Scheme 4

Replacement of the primary amine function of the lead compound **B** with suitable substituted amino groups (**21-24**) was performed starting from **B** which undergoes Sandmeyer reaction using isoamylnitrite as nitrosonium-donor molecule and $CuCl_2$ (scheme 5) (303). This reaction afforded compound **85** in good yields. Thus, the 2-chlorine atom of **85** was replaced with the suitable substituted amine yielding final compounds **21-24** in high yields.

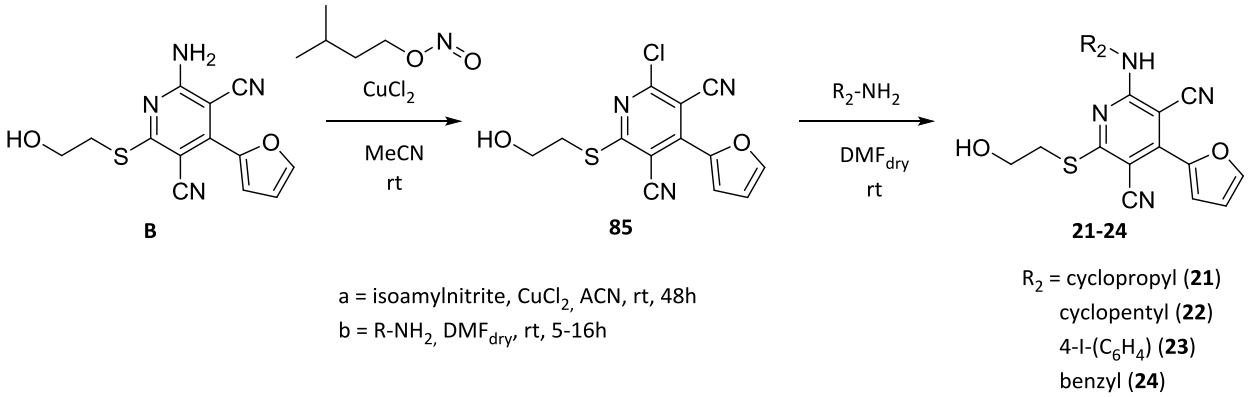

Scheme 5

Finally, derivative **25**, bearing an acetyl moiety at the amino group, was synthesized starting from the reaction of the derivative **74** with acetic anhydride in the presence of pyridine, affording the intermediate **86** (scheme 6) (304). Then, the latter was converted into the corresponding sulfanyl derivative **87** by reacting with sodium

sulfide. Then, compound **87** was used as starting material for the coupling reaction with 2-bromoethanol affording compound **25**.

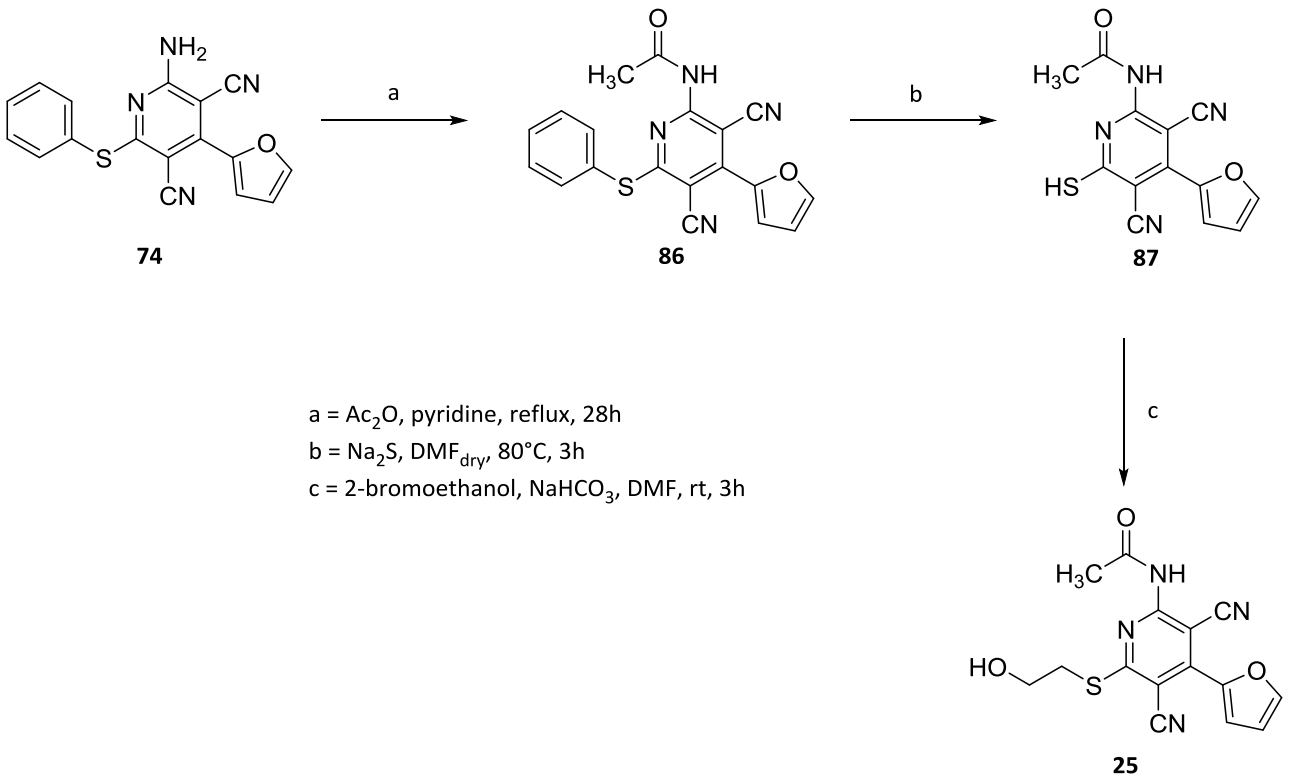

Scheme 6

3.1.2 Chemistry of DCP2B

Concerning the synthesis of the aminopyridine-3,5-dicarbonitrile derivatives targeting the A_{2B} AR, it is pretty similar to the general procedure showed before for the preparation of compound **1-16, B** (scheme 1). The synthesis of compounds **26-34** starts from the one-pot cyclization of the suitable commercial aldehyde to give sulfanylphenyl intermediates **75**, **77**, **88-94** (scheme 7). This reaction has been performed by using diverse cyclization alkaline adjuvant able to work in a phase-transfer system. The synthetic pathway reported in scheme 7 involves the use of sodium sulfide for the achievement of the sulfanyl intermediates (**79, 81, 95-101**) and the coupling reaction with the 2-bromomethylimidazole **102** (scheme 10) in the presence of sodium hydrogencarbonate for obtaining the final compounds **26-34** (scheme 7).

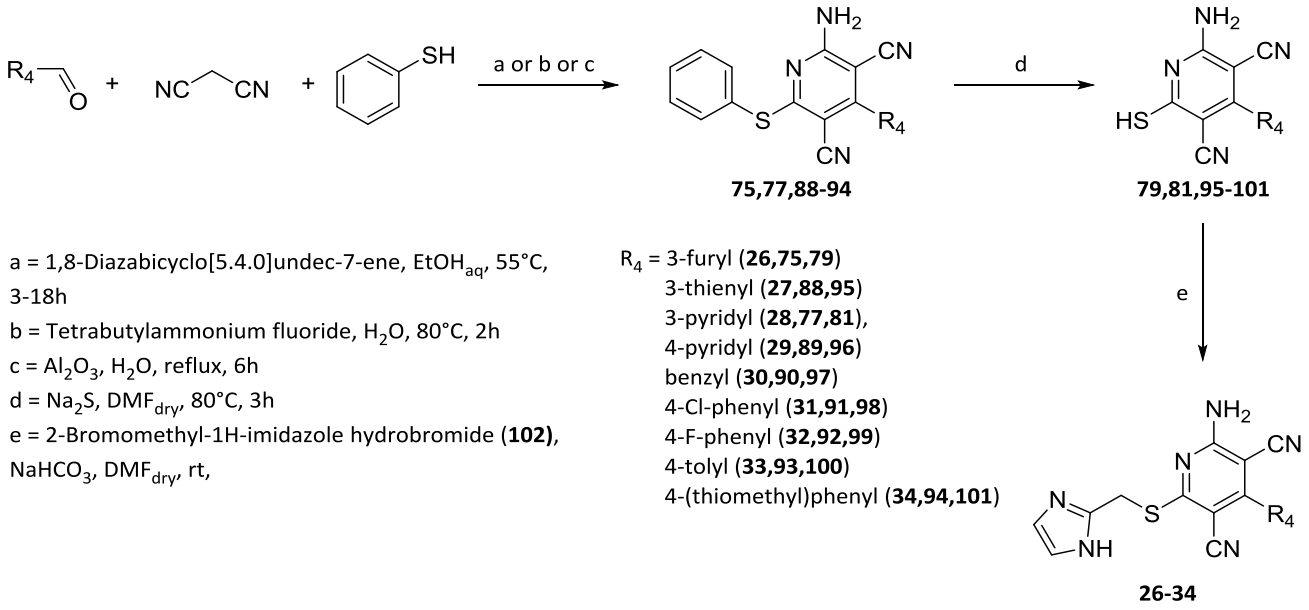

a = 1,8-Diazabicyclo[5.4.0]undec-7-ene, $EtOH_{aq}$, 55°C, 3-18h
b = Tetrabutylammonium fluoride, H_2O, 80°C, 2h
c = Al_2O_3, H_2O, reflux, 6h
d = Na_2S, DMF_{dry}, 80°C, 3h
e = 2-Bromomethyl-1H-imidazole hydrobromide (**102**), $NaHCO_3$, DMF_{dry}, rt,

R_4 = 3-furyl (**26,75,79**)
3-thienyl (**27,88,95**)
3-pyridyl (**28,77,81**),
4-pyridyl (**29,89,96**)
benzyl (**30,90,97**)
4-Cl-phenyl (**31,91,98**)
4-F-phenyl (**32,92,99**)
4-tolyl (**33,93,100**)
4-(thiomethyl)phenyl (**34,94,101**)

Scheme 7

For what may concern the sulfanyl intermediate **104**, the precursor of final compound **35**, a different approach was used: acetaldehyde highlighted a scarce reactivity in the one-pot reaction showed before, so it was necessary to synthesize the intermediate **103** by reaction of trimethylorthobenzoate with malononitrile (305) (Scheme 8). This intermediate allowed an easier cyclization to the sulfanyl compound **104** by direct reaction with thiocyanoacetamide. Treatment of the latter with bromomethyl-2-imidazole hydrobromide **102** (scheme 10) in the presence of sodium hydrogencarbonate afforded the final derivative **35**.

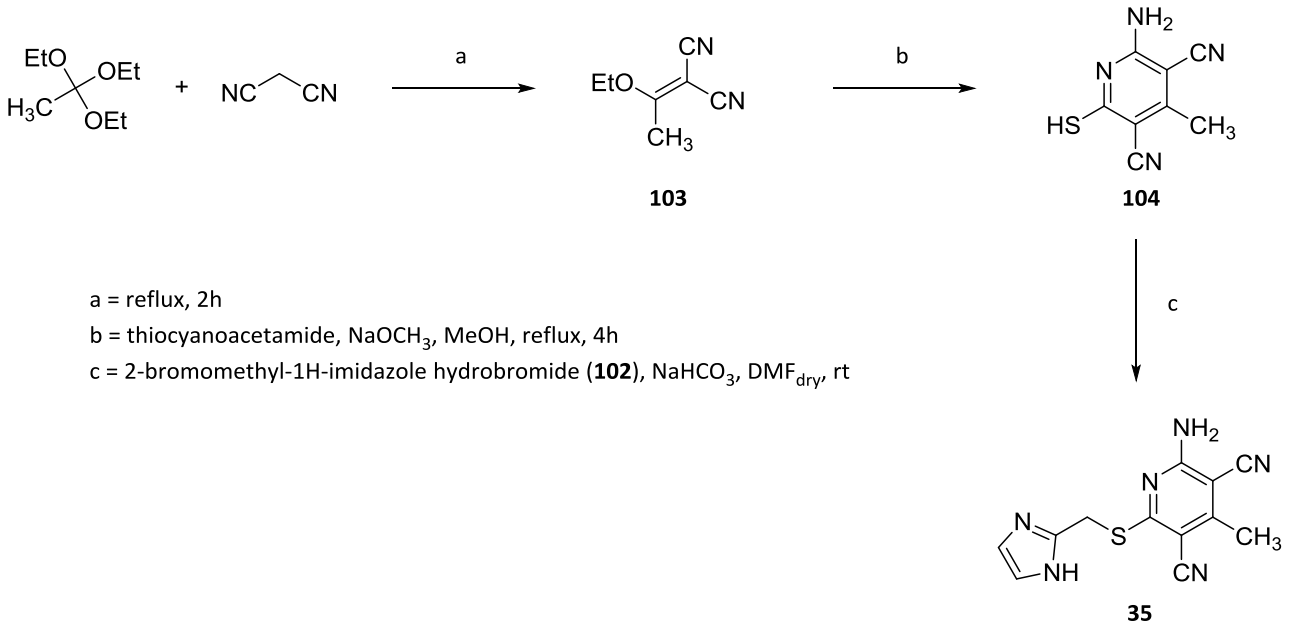

a = reflux, 2h
b = thiocyanoacetamide, $NaOCH_3$, MeOH, reflux, 4h
c = 2-bromomethyl-1H-imidazole hydrobromide (**102**), $NaHCO_3$, DMF_{dry}, rt

Scheme 8

Introduction of an amine function replacing the sulfanyl linker typical of most of the final compounds was performed by using the chloro-intermediate **82** obtained in scheme 3. The latter was used as starting material for coupling with commercial (1H-imidazol-2-yl)methanamine to afford compound **36** (scheme 9).

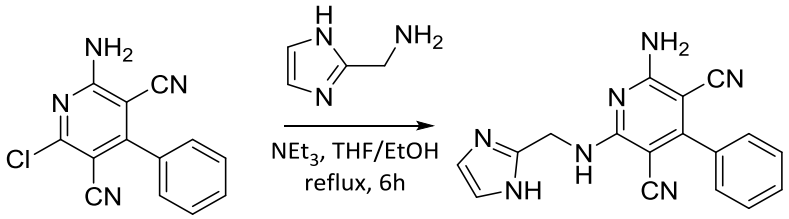

82 **36**

Scheme 9

Due to the unavailability of commercial 2-bromomethyl-1H-imidazole hydrobromide **102**, this product was synthesized (297) (scheme 10) starting from imidazole-2-carboxyaldehyde, which was reduced to the corresponding alcohol **105** using sodium borohydride in absolute ethanol at room temperature for 2h. The latter was transformed into the bromomethyl derivative **102** by treatment with a 33% hydrobromic acid solution in acetic acid at 100°C.

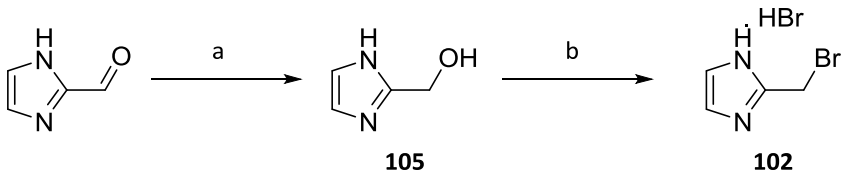

105 **102**

a = sodium borohydride, $EtOH_{abs}$, rt, 2h
b = HBr 33% in acetic acid, 100°C, 4h

Scheme 10

In order to achieve (*para*-O-phenyl)-substituted aldehydes **106-111**, 4-hydroxybenzaldehyde was alkylated at the *para*-OH function with the suitable alkyl halide in refluxing acetone in the presence of potassium carbonate (scheme 11) (306).

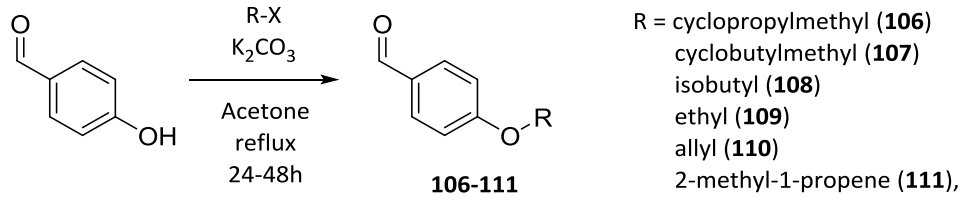

Scheme 11

O-susbtituted aldehydes **106-111** following a one-pot reaction with thiophenol, malononitrile and 1,8-diazabicyclo[5.4.0]undec-7-ene (DBU) in aqueous ethanol (307) afforded the sulfanylphenyl intermediates **112-117** (scheme 12). Initially, compound **112** was synthesized by using Al_2O_3 as base, which was then replaced by DBU, leading to a general procedure with an easier work-up and higher yield. Thus, intermediates **112-117** were transformed into the sulfanyl analogues **118-123** with sodium sulfide in the conditions aforementioned, and then used as nucleophile in the coupling reaction with suitable halides yielding derivatives **37-65**.

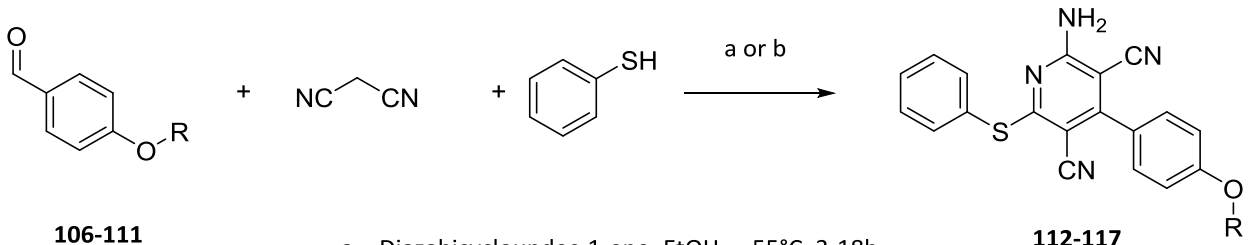

106-111

a = Diazabicycloundec-1-ene, $EtOH_{aq}$, 55°C, 3-18h
b = Al_2O_3, H_2O, reflux, 6h
c = Na_2S, DMF_{dry}, 80°C, 3h
d = R_6CH_2X, $NaHCO_3$, DMF_{dry}, rt

112-117

c

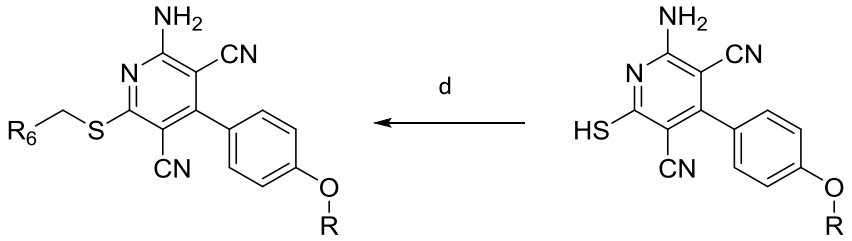

37-65 **118-123**

R = cyclopropylmethyl (**106,112,118, 37-52**)
cyclobutylmethyl (**107,113,119,53,54**)
isobutyl (**108,114,120,55,56**)
ethyl (**109,115,121,57-60**)
allyl (**110,116,122,61-63**)
2-methyl-1-propene (**111,117,123,64,65**)

n°	R	R_6	R_6CH_2X	n°	R	R_6	R_6CH_2X
37	cyclopropylmethyl	imidazol-2-yl	**102**	**52**	cyclopropylmethyl	3-$(CONH_2)C_6H_4$	**c.a.**
38	cyclopropylmethyl	imidazol-5-yl	**c.a.**	**53**	cyclobutylmethyl	imidazol-2-yl	**102**
39	cyclopropylmethyl	4,5-dihydro-1H-imidazol-2-yl	**135**	**54**	cyclobutylmethyl	$CONH_2$	**c.a.**
40	cyclopropylmethyl	benzoimidazol-2yl	**c.a.**	**55**	$CH_2CH(CH_3)_2$	imidazol-2-yl	**102**
41	cyclopropylmethyl	pyrazol-3-yl	**124**	**56**	$CH_2CH(CH_3)_2$	$CONH_2$	**c.a.**
42	cyclopropylmethyl	1,2,4-triazol-1-yl	**c.a.**	**57**	CH_2CH_3	imidazol-2-yl	**102**
43	cyclopropylmethyl	1,2,4-triazol-5-yl	**128**	**58**	CH_2CH_3	$CONH_2$	**c.a.**
44	cyclopropylmethyl	tetrazol-5-yl	**c.a.**	**59**	CH_2CH_3	$CONHCH_3$	**c.a.**
45	cyclopropylmethyl	2-aminothiazol-4-yl	**130**	**60**	CH_2CH_3	pyrazol-3-yl	**124**
46	cyclopropylmethyl	3-pyridyl	**c.a.**	**61**	$CH_2CH=CH_2$	imidazol-2-yl	**102**
47	cyclopropylmethyl	$CONHCH_3$	**c.a.**	**62**	$CH_2CH=CH_2$	$CONH_2$	**c.a.**
48	cyclopropylmethyl	$CONHCH_2OH$	**c.a.**	**63**	$CH_2CH=CH_2$	pyrazol-3-yl	**124**
49	cyclopropylmethyl	CONHOH	**134**	**64**	$CH_2C(CH_3)=CH_2$	imidazol-2-yl	**102**
50	cyclopropylmethyl	$COOCH_3$	**c.a.**	**65**	$CH_2C(CH_3)=CH_2$	$CONH_2$	**c.a.**
51	cyclopropylmethyl	3-$(COOCH_3)C_6H_4$	**c.a.**	**c.a. = commercially available**			

Scheme 12

As previously assumed, some of the halides used to achieve final products are not commercially available, so it has been necessary to synthesize them. The 3-(chloromethyl)-1H-pyrazole **124** was synthesized starting from commercial 3-methylpyrazole, which, in the first step, was oxidized with aqueous potassium permanganate to afford the 3-carboxylic acid **125** (scheme 13). Thus, the latter was transformed into the corresponding ethyl ester **126** using thionyl chloride in absolute ethanol, in a reaction in which was involved the formation of the acyl chloride, immediately reacting with ethanol and yielding compound **126**. This procedure was the preferred one since the direct reduction of the carboxylic acid **125** did not give compound **127** in good yields. In contrast, reduction of **126** with lithium aluminum hydride in anhydrous THF afforded the target **127** in good yields, which was converted into the corresponding chloromethyl derivative **124** by reacting with thionyl chloride in anhydrous dichloromethane (308).

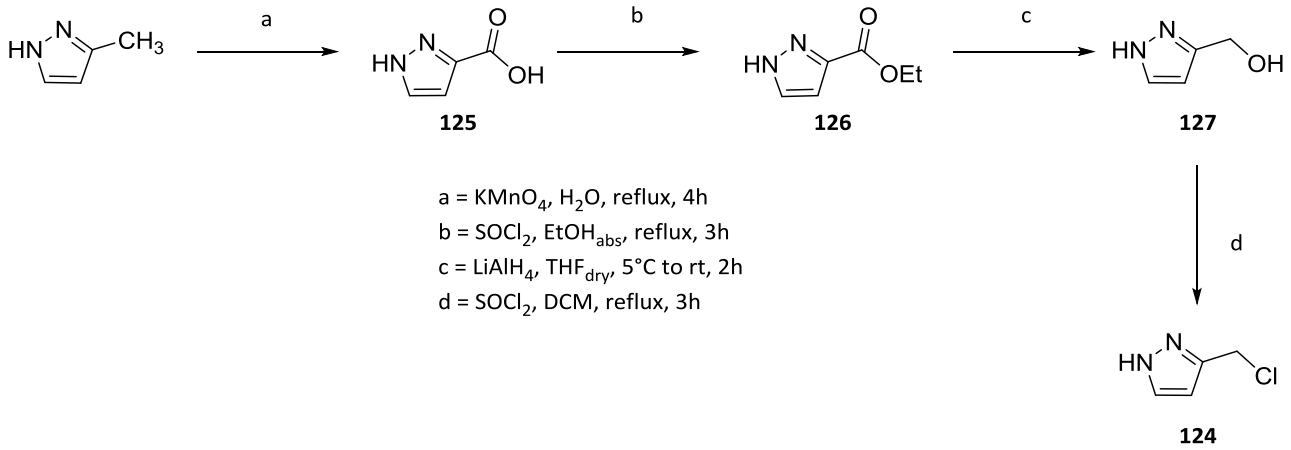

Scheme 13

Moreover, 3-chloromethyl(1H-1,2,4-triazole) hydrochloride **128** was synthesized starting from commercial ethyl 1H-1,2,4-triazole-3-carboxylate, which was previously converted into the corresponding alcohol **129** (scheme 14) using lithium aluminum hydride in anhydrous THF. This intermediate was finally transformed into **128** through a reaction in which thionyl chloride has been used as chlorinating agent (309).

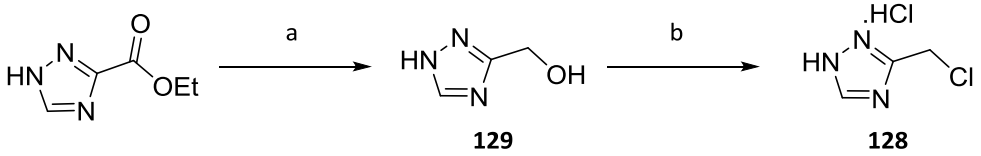

Scheme 14

Furthermore, 4-(chloromethyl)thiazol-2-amine **130** and 4-(chloromethyl)-2-phenylthiazole **131** were synthesized in a similar way, starting from thiourea and thiobenzamide, respectively, by using 1,3-dichloroacetone in dry acetone (scheme 15) (310).

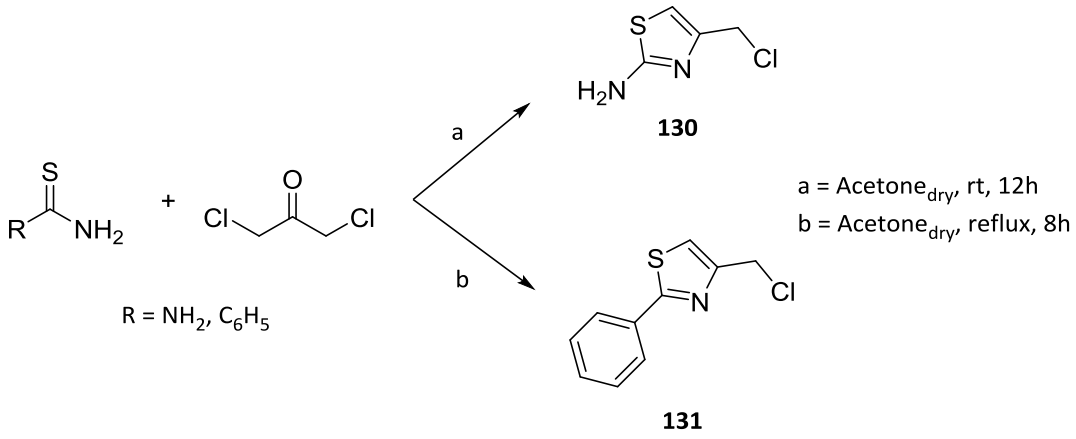

Scheme 15

The 3-(chloromethyl)benzamide (311) **132**, was synthesized starting from commercial 3-(chloromethyl)benzoic acid going through 3-(chloromethyl)benzoyl chloride obtained with oxalyl chloride in DCM using DMF as catalyst (scheme 16). The acyl chloride was not isolated, but it has been immediately used for the next step by reacting with anhydrous ammonia in dioxane to afford the desired compound **132**.

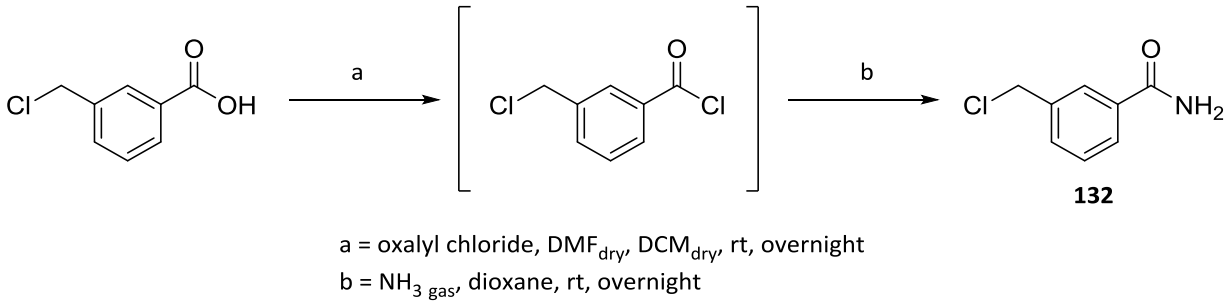

Scheme 16

The synthesis of benzyl 2-chloroacetate **133** (312) starts from commercial chloroacetic acid which was reacted with benzyl alcohol in the presence of p-toluenesulfonic acid (scheme 17). Furthermore, 2-chloro-N-hydroxyacetamide **134** was synthesized (313) from ethyl chloroacetoacetate in a 50% aqueous solution of hydroxylamine.

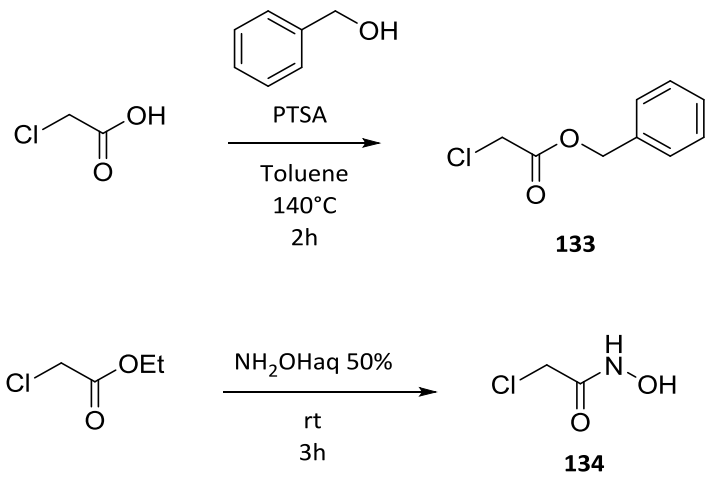

Scheme 17

The 2-(chloromethyl)-4,5-dihydro-1H-imidazole **135** was produced (314) by cyclization of the iminoester hydrochloride **136** which was synthesized (315) (scheme 18) from commercial chloroacetonitrile in a saturated hydrochloric acid solution in absolute ethanol and dry diethyl ether while hydrochloric acid is bubbling. After isolation, the intermediate **136** was cyclized using ethylenediamine in absolute ethanol.

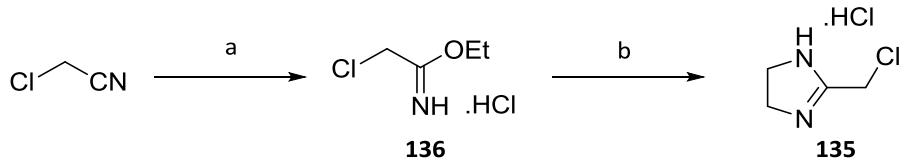

a = HCl_{gas}, $EtOH_{abs}$, $Et_2O_{dry,}$ rt, overnight
b = ethylenediamine, HCl_{gas}, $EtOH_{abs}$, rt, overnight

Scheme 18

In order to obtain compounds **66** and **67** which bear a 4-(*para*-acetamidophenyl) moiety on the aminopyridine-3,5-dicarbonitrile core, it was not possible to achieve intermediate **137** in a one-pot reaction, due to the scarce reactivity of 4-acetamidobenzaldehyde. Thus, the aldehyde was reacted with malononitrile in a straightforward Knoevenagel condensation (scheme 19) (293) in the presence of piperidine as catalyst in ethanol to give intermediate **138** which was isolated to be used in the cyclization reaction involving thiophenol and DBU to yield **137**.

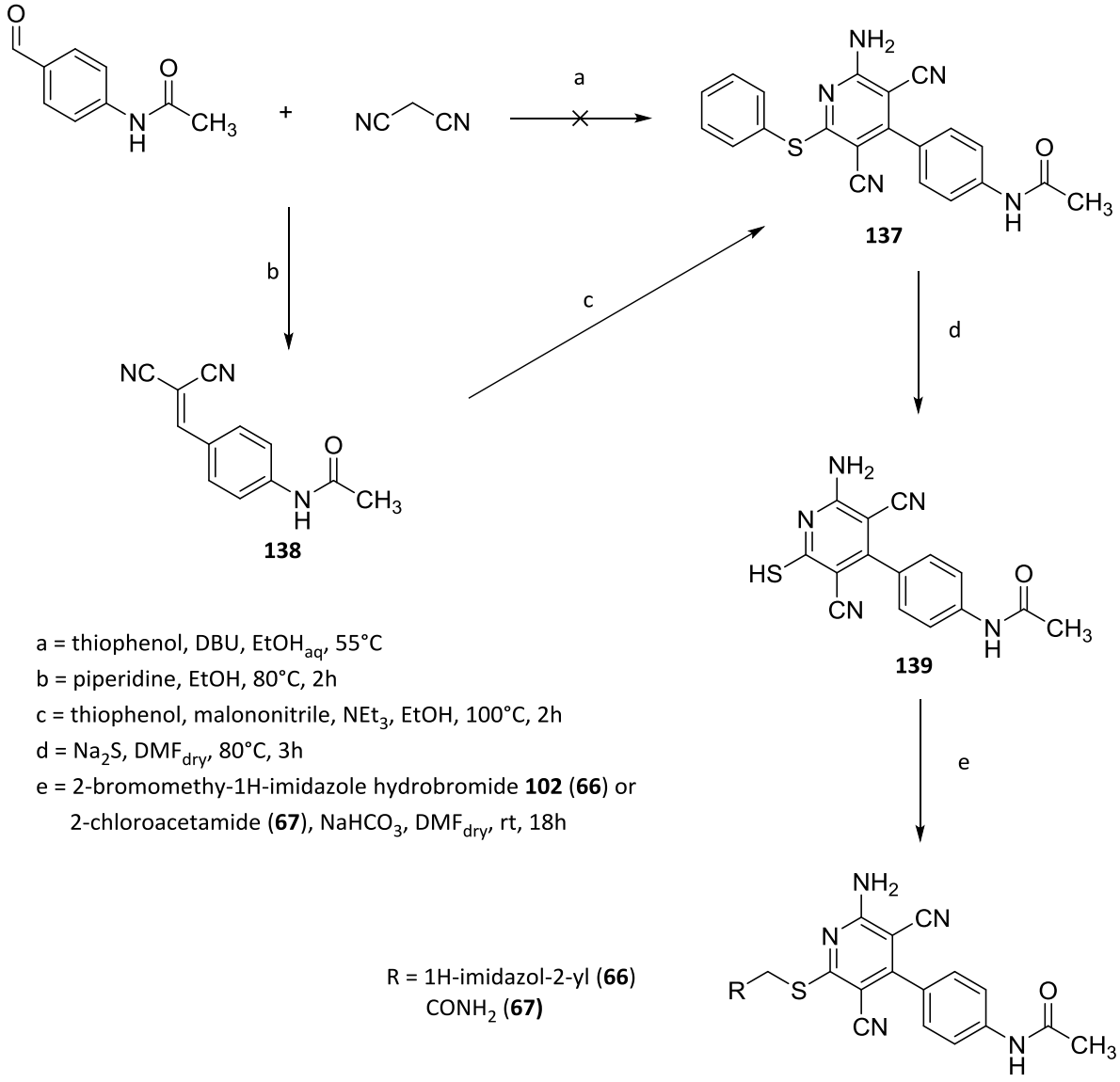

Scheme 19

Then, the sulfanylphenyl derivative **137** was converted into the sulfanyl intermediate **139** using sodium sulfide as previously shown. The latter was used to synthesize the final compounds **66** and **67** by reacting with 2-bromomethyl-1H-imidazole hydrobromide **102** or commercially available 2-chloroacetamide, respectively, in the presence of sodium hydrogencarbonate as base.

In order to shorten the procedure leading to the *para*-oxyphenyl-substituted compounds **37-65**, a further pathway had been evaluated starting from commercial 4-hydroxybenzaldhyde (scheme 20). The latter was reacted with thiophenol, malononitrile and DBU in aqueous ethanol to afford the sulfanylphenyl intermediate **140** that was converted into the corresponding sulfanyl intermediate **141** then coupled with 2-chloroacetamide to yield compound **142**. Here, the O-alkylation with potassium carbonate was expected to produce compound **54**, but a competitive reaction afforded a diverse compound (**69**). In fact, due to the long time reaction and the basicity of the medium, the nitrile group in position 3 of the aminopyridine core

undergoes condensation with the active methylene group on the sulfanylacetamide chain affording the bicyclic compound **69**. This collateral product was characterized through ^{1}H NMR, ^{13}C NMR and IR spectroscopy confirming our hypothesis.

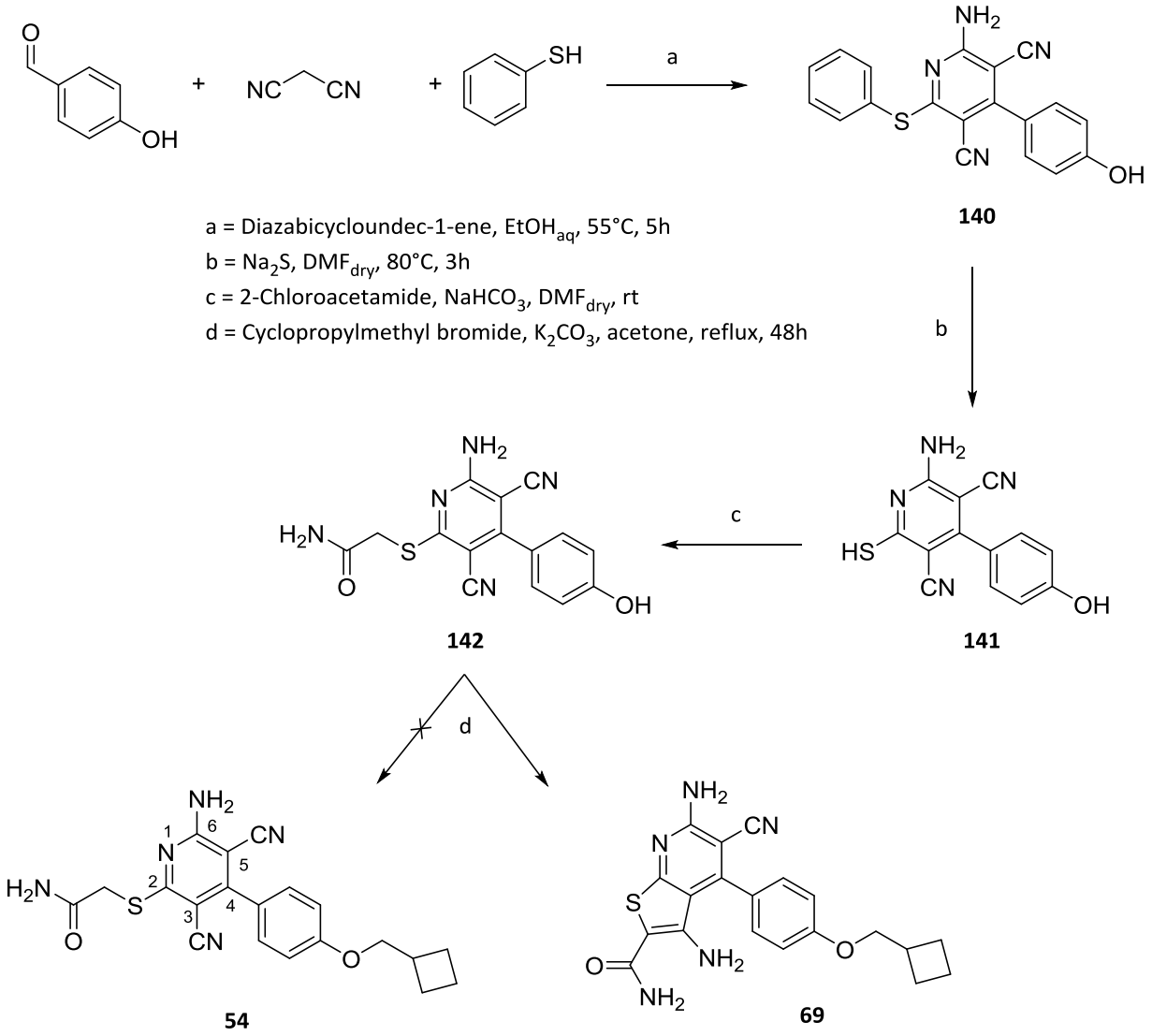

Scheme 20

Consequentially, cyclization of **BAY60-6583** was performed forcing reaction condition (316) which involved potassium hydroxide in absolute ethanol as alkaline reactant to obtain compound **68** (scheme 21).

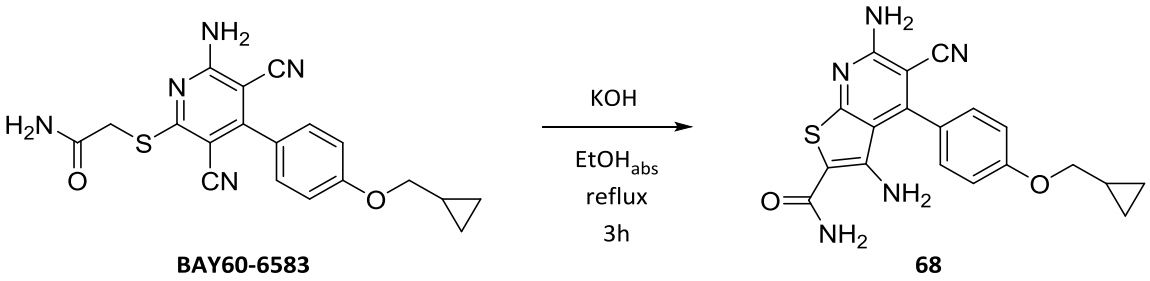

BAY60-6583 **68**

Scheme 21

3.2 Chemistry of 7-amino-2-phenylpyrazolo[1,5-c]pyrimidine-4-carbonitriles

The 7-amino-2-phenylpyrazolo[1,5-c]pyrimidine-4-carbonitrile derivatives **70-73** were prepared following a new and unique synthetic pathway (scheme 22). The synthesis included a one-pot condensation of ethyl cyanoacetate with carbon disulfide in DMF dry, followed by methylation of sulfide groups with methyliodide, to afford intermediate **143**. This latter was cyclized (317) with acetophenone in the presence of potassium hydroxide in dry dimethylsulfoxide (DMSO) yielding the oxo-pyranone **144** in good yields which was used as starting material for the production of the pyrazole **145** by reacting with hydrazine monohydrate in pyridine (318). Furthermore, the pyrazole NH of compound **145** was acylated with a Boc protecting group in order to avoid parasite reactions on the free nitrogen atom. The reaction was performed by using *tert*-butyl anhydride in dry acetonitrile in the presence of triethylamine (TEA), obtaining compound **146**. Condensation of the latter with carbon disulfide using sodium hydride in dry DMSO and following methylation with methyl iodide in a one-pot reaction allowed to obtain intermediate **147**, which was then deprotected by using trifluoroacetic acid in DCM to yield compound **148**. Cyclization of the latter in N-methylpyrrolidin-1-one (NMP) by reacting with a strong excess of cyanamide in the prescence of 4-toluenesulfonic acid afforded compound **149**.

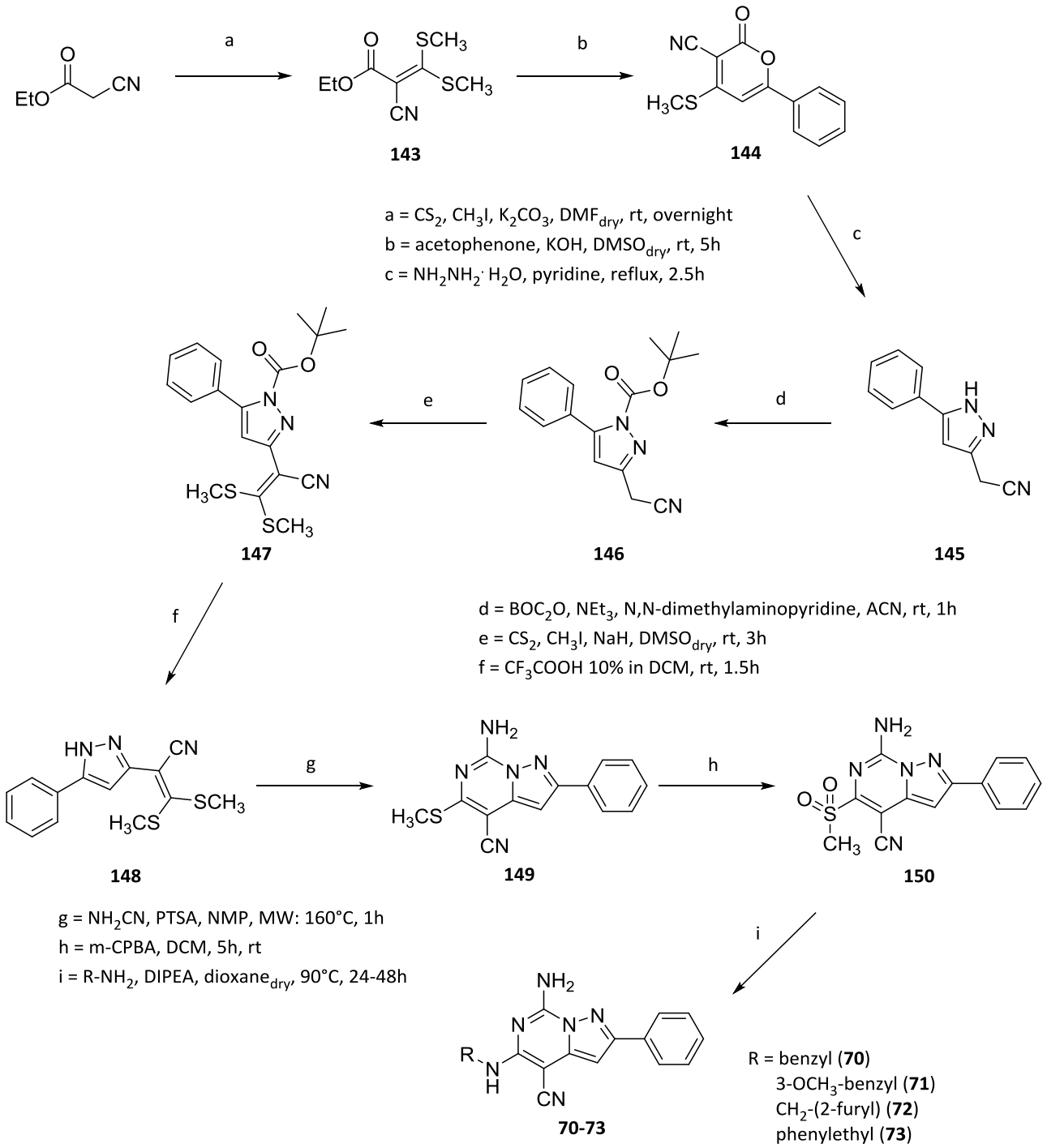

Scheme 9

The reaction was performed in microwave reactor at 160°C for 1h. Consequentially, methylsulfanyl function of compound **149** was oxidize to the methylsulfonyl group with 3-chloroperoxybenzoic acid (m-CPBA) in DCM affording compound **150**. The latter was used as starting material for the reaction with the suitable primary amine in the presence of N,N-diisopropylethylamine (DIPEA) to obtain the desired final compounds **70-73** in high yields.

4. Results and discussions

All the synthesized compounds were evaluated by the group of Prof. Katia Varani at the Medical Science Department – Pharmacology section of the University of Ferrara, for their affinity at human (h) A_1, hA_{2A} and hA_3 AR (expressed as K_i values obtained in binding experiments) displacing the suitable radioligand for each AR subtype ([^{3}H]DPCPX for A_1 AR, [^{3}H]ZM241385 for A_{2A} AR and [^{125}I]AB-MECA for A_3 AR, respectively) stably expressed on chinese hamster ovary (CHO) cells. The potency at the hA_{2B} AR (expressed as EC_{50} values in cAMP functional assay) was assessed in hA_{2B}CHO cells stimulated by 200 nM NECA, at 1µM concentration of the examined compounds. K_i values are means ± SEM of four separate assays each performed in duplicate while EC_{50} values are expressed as means ± SEM of four separate cAMP experiments. Some selected derivatives (**A, C, 1, 2, 4, 5, 9, 14, 15, 26, 36**) were tested to assess their agonistic or antagonistic properities at hA_1 and hA_{2A} ARs. Thus their capability to modulate cAMP production was evaluated on hA_1 and hA_{2A} CHO cells.

4.1 DCP1 series

Based on the preliminary results obtained for compound **A**-**C** (Figure 21), modifications on dicyanopyridine scaffold were performed at position R_6 (Table 5). Firstly, replacement of the methyl carboxylate function of **B** with a nitrile group yielded compound **10** which results equipotent at the hA_1 AR as the leads **A-C**. Aryl homologation on methyl ester function of **B** led to compound **1**, which binds at the hA_{2A} subtype but loses selectivity for the hA_1 AR with respect to the lead **B**. In functional assays **1** shows an inverse agonist profile at the hA_1 AR, while it acts as antagonist at the hA_{2A} AR (Table 6). In order to enlarge information on this kind of residues at position R_6, the methyl ester of **1** was transformed into the carboxamido (**2**) (as aryl homologue of the lead **C**), carboxylic acid (**3**), methyl alcohol (**4**) and nitrile (**5**) analogues which maintain on the whole the same trend of AR affinity with respect to compound **1**. In contrast, compound **2**, **3** and **5** show some affinity for hA_3 AR but in the high nanomolar range thus maintaining a good selectivity. In fact, the carboxylic acid **3** shows more than 100 fold hA_1 selectivity *versus* hA_{2A} and hA_3 receptors, thus higher than the parents **1, 2, 4, 5**. It is important to highlight that compounds **2**, **4** and **5**, such as **1**, act as inverse agonist at hA_1 AR while **2** and **4** behave as hA_{2A} AR antagonists. An interesting result was obtained performing an isosteric replacement of the phenyl ring of compound **1** with a furane moiety obtaining the methyl 5-furan-2-carboxylate derivative **6** which is endowed with good affinity and high selectivity at the hA_1 AR. Meanwhile, modifications at R_4 were performed replacing the 2-furyl moiety of **1** with a 3-furyl (**7**), 2-thienyl (**8**) and 3-pyridyl (**9**) substituent in order to understand if a diverse heterocycle could modulate the affinity and the pharmacological profile of the target compounds. While compound **7** bearing the 3-furyl substituent at R_4

maintains the same trend of affinity of the reference **1**, derivatives **8** and **9** acquire a higher selectivity *versus* the hA_{2A} AR with respect to **1**.

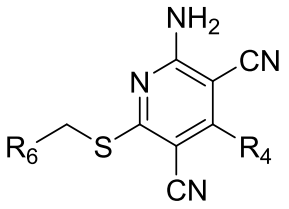

A-C, 1-16

			hA_1 CHO cells	hA_{2A} CHO cells	hA_{2B} cAMP assay	hA_3 CHO cells
n°	R_4	R_6	[^{3}H]DPCPX K_i (nM) or I% at 1μM[a]	[^{3}H]ZM241385 Ki (nM) or I% at 1μM[a]	EC_{50} (nM)[b] (efficacy %)	[^{125}I]ABMECA Ki (nM) or I% at 1μM[a]
A	2-furyl	CH_2OH	57 ± 4 (inverse agonist)	27%	>1000 (7%)	29%
B	2-furyl	$COOCH_3$	108 ± 9	17%	>1000 (4%)	25%
C	2-furyl	$CONH_2$	175 ± 12	21%	>1000 (17%)	177 ± 15
1	2-furyl	3-$(COOCH_3)C_6H_4$	7.22 ± 0.63 (inverse agonist)	68±3 (antagonist)	>1000 (7%)	26%
2	2-furyl	3-$(CONH_2)C_6H_4$	1.32±0.11 (inverse agonist)	67±6 (antagonist)	>1000 (6%)	326±31
3	2-furyl	3-$(COOH)C_6H_4$	4.12±0.38	581±54	>1000 (1%)	611±58
4	2-furyl	3-$(CH_2OH)C_6H_4$	0.98±0.09 (inverse agonist)	31±3 (antagonist)	>1000 (4%)	25%
5	2-furyl	3-$(CN)C_6H_4$	1.02±0.11 (inverse agonist)	93±9	>1000 (7%)	668±64
6	2-furyl	methyl 5-furan-2-carboxylate	82 ± 8	1%	>1000 (7%)	11%
7	3-furyl	3-$(COOCH_3)C_6H_4$	2.11±0.19	96±8	>1000 (7%)	1%
8	2-thienyl	3-$(COOCH_3)C_6H_4$	2.72± 0.21	693 ± 68	982±95 (62%)	15%
9	3-pyridyl	3-$(COOCH_3)C_6H_4$	1.18± 0.11 (inverse agonist)	636±57	>1000 (15%)	8%
10	2-furyl	CN	93 ± 8	887 ± 84	>1000 (1%)	582 ± 56
11	2-furyl	$COOCH_2C_6H_5$	86±7	8%	>1000 (10%)	1%
12	2-furyl	COC_6H_5	23 ± 2	224±21	>1000 (1%)	26%
13	2-furyl	3-pyridyl	1.42±0.15	24±3	>1000 (1%)	948 ± 82
14	2-furyl	2-pyridyl	2.71±0.21 (inverse agonist)	108±9	>1000 (9%)	134±12
15	2-furyl	2-phenylthiazol-4-yl	3.85±0.32 (partial agonist)	523±49	947±92 (29%)	438±41
16	2-furyl	2-aminothiazol-4-yl	1.27 ± 0.11	22 ± 2	>1000 (9%)	193 ± 17

[a]K_i values are means ± SEM of four separate assays each performed in duplicate. Percentage of inhibition (I%) are determined at 1μM concentration of the tested compounds. [b]cAMP experiments in hA_{2B}CHO cells stimulated by 200 nM NECA, at 1μM concentration of the examined compounds. EC_{50} values are expressed as means ± SEM of four separate cAMP experiments.

Table 5

	cAMP assay		
	hA_1 EC_{50} (nM)	$hA_{2A}CHO$ cells EC_{50} (nM)	$hA_{2A}CHO$ cells IC_{50} (nM)
A	128 ± 11	-	-
1	1.43 ± 0.11	< 20%	313 ± 29 (10 µM: 67%)
2	2.84 ± 0.27	< 20%	58 ± 5 (10 µM: 49%)
4	0.98 ± 0.09	< 20%	22 ± 2 (10 µM: 99%)
5	4.82 ± 0.39	-	-
9	6.26 ± 0.58	-	-
14	34 ± 3	-	-
15	4.12 ± 0.37	-	-

Table 6: Functional assays at A_1 and A_{2A} ARs of selected compounds

This data let us to hypothesize that the furan ring is important for the anchoring of these derivatives at the hA_{2A} subtype. Further modifications were performed at R_6 keeping the 2-furyl moiety at position R_4. Thus, compound **11** and **12** were synthesized, spacing the phenyl residue at R_6 from the dicyanopyridine core with respect to compounds **1-6**. While compound **12** maintains the same profile of derivatives **1-5** binding at both hA_1 and hA_{2A} AR, the benzyl ester **11** showed a good affinity for hA_1 AR and high selectivity suggesting the possibility to modulate A_1 selectivity with respect to A_{2A} AR by performing this modification on the sulfanylmethyl function.

Furthermore, in order to evaluate the presence of diverse heteroaryl moieties at position R_6 for the binding at ARs, 3-pyridyl (**13**) and 2-pyridyl (**14**) derivatives were produced which maintain hA_1 and hA_{2A} affinity in the low and in the high nanomolar range, respectively. For compound **14** which behaves as inverse agonist (Table 5 and 6) also the binding at hA_3 subtype increseas. What is noteworthy is that preliminary functional data indicate that compound **13** seems to behave as a weak agonist at the hA_{2A} AR opening the possibility to consider this compound as a lead to design new A_{2A} agonists belonging to this series. Pursuing modifications at position R_6, 2-phenylthiazol-4-yl (**15**) and 2-aminothiazol-4-yl (**16**) derivatives were synthesized. These compounds showed high affinity for hA_1 AR, and compound **15**, acting as a partial agonist, a good selectivity *versus* the other ARs. At this moment, no data are available about the functional profile of the aminotiazole compound **16**, that could have been of help for understanding the potential role of a thiazolyl moiety at R_6 for shifting the profile of these derivatives from inverse agonist to agonist (compare to **15**).

Moreover, replacement of the sulfanyl linker of the lead compound **A** with an amino group (**17**) or an oxygen atom (**20**) results to be detrimental for affinity at hA_1 AR (Table 7), thus confirming the importance of the sulfur atom as linker in this position. While keeping the aminoethanol function of **17**, replacement of the 2-furyl moiety with 2-thienyl (**18**) or phenyl (**19**) substituent enhanced affinity at the A_1 AR with respect to **17**.

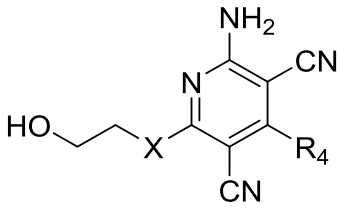

			hA_1 CHO cells	hA_{2A} CHO cells	hA_{2B} cAMP assay	hA_3 CHO cells
n°	R_4	X	[^{3}H]DPCPX K_i(nM) or I% at 1μM	[^{3}H]ZM241385 Ki (nM) or I% at 1μM	EC_{50} (nM) (efficacy %)	[^{125}I]ABMECA Ki (nM) or I% at 1μM
A	2-furyl	S	57 ± 4	27%	>1000 (7%)	29%
17	2-furyl	NH	20%	18%	>1000 (1%)	17%
18	2-thienyl	NH	324 ± 28	33%	>1000 (1%)	29%
19	C_6H_5	NH	943 ± 87	1%	>1000(1%)	1%
20	2-furyl	O	632 ± 53	25%	>1000 (11%)	3%

Table 7

Substitution of the primary amine function with R_2 groups (Table 8) was useful to evaluate the role of this position for the binding at the others ARs. In particular, this information is important to evaluate the mode of binding of these compounds at the A_1 subtype with respect to the adenosine-like ligands. Cycloalkyl groups such as cyclopropyl (**21**) and cyclopentyl (**22**) and also other moieties (compounds **23-25**) have been introduced at R_2 on the basis of advice coming from the SARs on the adenosine-like A_1 AR agonists reported in literature. While compound **21** binds the hA_1 AR as the lead **A**, compound **22** bearing the usual cyclopentyl substituent for selective A_1 ligands was inactive at this subtype. Unexpectedly, also the aryl-substituted compound **23** showed any affinity at the ARs, although some nucleosidic A_1 AR agonists bear this moiety. Nevertheless, this behavior can confirm the diverse binding mode of these non-nucleoside ligands with respect to the nucleoside ones. Compound **24** bearing a NH-benzylamino substituent is endowed with high affinity and good selectivity for the hA_1 AR that are comparable to those of derivative **21**. Probably, an increased length chain of this residue could be useful for the anchoring at the active site of the A_1 AR. Replacement of the amine function of **A** with an acetammido group (compound **25)** enhances hA_3 AR affinity suggesting that an acyl moiety could be useful for shifting the binding of the aminopyridine-3,5-dicarbonitrile derivatives toward the hA_3 AR, as extensively demonstrated for other AR ligands in literature.

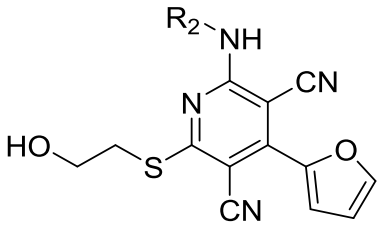

		hA1 CHO cells	hA2A CHO cells	hA2B cAMP assay	hA3 CHO cells
n°	R_2	[^{3}H]DPCPX K_i (nM) or I% at 1μM	[^{3}H]ZM241385 Ki (nM) or I% at 1μM	EC_{50} (nM) (efficacy %)	[^{125}I]ABMECA Ki (nM) or I% at 1μM
A	H	57 ± 4	27%	>1000 (7%)	29%
21	cyclopropyl	89±7	30%	>1000 (4%)	30%
22	cyclopentyl	742 ± 68	8%	>1000 (1%)	780±72
23	4-I-C_6H_5	10%	1%	>1000 (1%)	8%
24	benzyl	65±6	461±42	>1000 (3%)	14%
25	$COCH_3$	243±21	11%	>1000 (3%)	211±18

Table 8

4.2 DCP2B series

All the derivatives designed as A_{2B} AR ligands (Table 9) behave generally as partial agonists (Table 10) with the only exception of derivatives **66, 67** which show a full agonist profile.

Previously reported compound **D** bearing a 2-imidazolyl moiety at position R_6 shows high affinity at all the AR subtypes, and in particular high activity at the hA_{2B} AR behaving as a partial agonist. The trend is similar to that of the analogue **LUF-5845**, reported in literature (296). In order to explore the potentiality of the imidazolyl moiety at position R_6 for activity at A_{2B} AR, the 2-furyl substituent at R_4 of **D** was replaced especially by other heteroaryl and 4-substituted-aryl residues, obtaining a set of compounds showed in Table 9. All these derivatives are endowed with a partial agonist profile at the hA_{2B} AR.

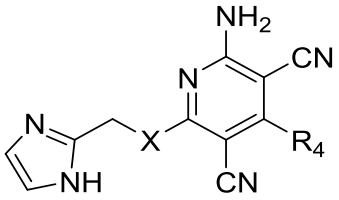

D, 26-37

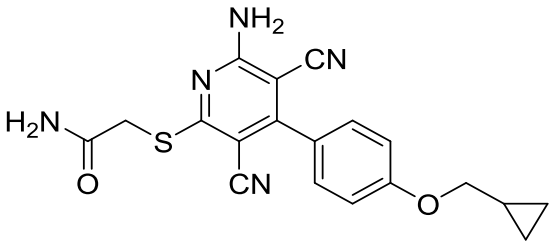

BAY-606583

			hA_1 CHO cells	hA_{2A} CHO cells	hA_{2B} cAMP assay	hA_3 CHO cells
n°	X	R_4	[^{3}H]DPCPX K_i(nM) or I% at 1μM	[^{3}H]ZM241385 Ki (nM) or I% at 1μM	EC_{50} (nM) (efficacy %)	[^{125}I]ABMECA Ki (nM) or I% at 1μM
D	S	2-furyl	12 ± 2	26 ± 2 (partial agonist)	1.7 ± 0.2 (52%)	65 ± 5
26	S	3-furyl	0.77±0.09	37±3 (antagonist)	2.32±0.21 (42%)	274±23
27	S	3-thienyl	1.01±0.09	55±6	3.15±0.29 (47%)	221±20
28	S	3-pyridyl	5.26±0.48	463±38	63±5 (58%)	19%
29	S	4-pyridyl	8.85±0.82	81±7	12.5±1.3 (36%)	26%
30	S	$CH_2C_6H_5$	31%	8%	260±24 (44%)	1%
31	S	4-Cl-C_6H_4	30±4	865±68	109±12 (32%)	850±62
32	S	4-F-C_6H_4	0.78±0.08	139±12	18±2 (76%)	410±38
33	S	4-CH_3-C_6H_4	5.32±0.42	47±4	78±6 (78%)	212±19
34	S	4-SCH_3-C_6H_4	8.32±0.78	227±21	35.7±3.4 (30%)	388±29
35	S	CH_3	74±8	331±32	1%	510±53
36	NH	C_6H_5	140 ± 12	115±10 (antagonist)	1%	19%
37	S	4-($OCH_2C_3H_5$)-C_6H_4	235±24	764±72	9.52±0.91 (70%)	474±45
LUF-5845 (296)	S	4-(OCH_3)-C_6H_4	7	214	9	24
BAY60-6583			31%	2%	31 ± 3	8%

Table 9

	cAMP assay		
	hA_1 EC_{50} (nM)	hA_{2A}CHO cells EC_{50} (nM)	hA_{2A}CHO cells IC_{50} (nM)
D	-	19 ± 2 (39%) Partial Agonists	-
26	0.77 ± 0.09	< 20%	138 ± 12 (10 µM: 64%)
36	-	< 20%	814 ± 72 (10 µM: 93%)

Table 10: Functional assays on A1 and A2A ARs for selected compounds

Substitution at R_4 with different heterocyclic residues such as 3-furyl (**26**), 3-thienyl (**27)**, 3-pyridyl (**28**) and 4-pyridyl (**29**) maintains the activity at the A_{2B} AR, but also scarce selectivity. Various *para*-substituted phenyl groups were also introduced at this position: 4-Cl (**31**), 4-F (**32**), 4-CH_3 (**33**) and 4-SCH_3 (**34**) residues positively influence affinity and activity at A_1 and A_{2B} AR, even if in minor extent for the 4-chloro-substituent, and have different effects on selectivity *versus* the other AR subtypes. However, *para*-substitution with a cyclopropylmethyloxy, which is typical of **BAY60-6583**, makes compound **37** as a very potent and selective hA_{2B} agonist. In fact, **37** results 3-fold more active than **BAY60-6583** at the hA_{2B} AR, and shows also very good selectivity versus the other AR subtypes (25 times *vs* hA_1, 80 times *vs* hA_{2A}, and 50 times *vs* hA_3). Furthermore, it acts as partial agonist. Indeed, substitution at R_4 of a benzyl moiety (**30**) produces a very good selectivity for hA_{2B} but also a decrease of potency is observed. Thus, it remains to be demonstrated whether a compromise between length and dimension of the appended R_4 substituent could exist, in order to target selectively the A_{2B} subtype. Moreover, a methyl group at position R_4 was introduced yielding compound **35** that is totally inactive at the hA_{2B} AR but shows nanomolar affinity for the hA_1 subtype. Replacement of the sulfanyl linker with an amine function (**36**) as performed on **DCP1** series is extremely detrimental for hA_{2B} AR activity, while some affinity for hA_1 and hA_{2A} AR is maintained.

Thus, keeping the 4-cyclopropylmethyloxyphenyl moiety at R_4, the imidazolyl at R_6 was replaced with diverse H-bond donor/acceptor-group containing heterocycles to yield a subset of compounds showed in Table 11. All these derivatives show a partial agonist profile at hA_{2B} AR.

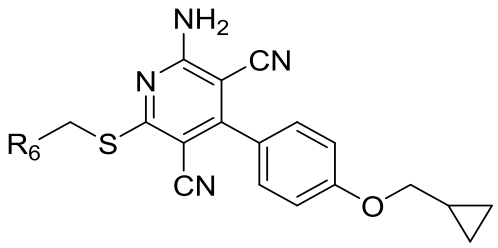

37-52

n°	R_6	hA_1 CHO cells [^{3}H]DPCPX K_i(nM) or I% at 1μM	hA_{2A} CHO cells [^{3}H]ZM241385 Ki (nM) or I% at 1μM	hA_{2B} cAMP assay EC_{50} (nM) (efficacy %)	hA_3 CHO cells [^{125}I]ABMECA Ki (nM) or I% at 1μM
37	imidazol-2-yl	235±24	764±72	9.52±0.91 (70%)	474±45
38	imidazol-5-yl	483 ± 33	14%	139 ± 11 (50%)	6%
39	4,5-dihydro-1H-imidazol-2-yl	1%	7%	7%	1%
40	benzoimidazol-2-yl	21%	6%	12%	1%
41	pyrazol-3-yl	552±54	2%	84±6 (48%)	6%
42	1,2,4-triazol-1-yl	12%	1%	1%	1%
43	1,2,4-triazol-5-yl	338±31	1%	51±4	1%
44	tetrazol-5-yl	3%	1%	25%	1%
45	2-aminothiazol-4-yl	140±12	1%	17%	1%
46	3-pyridyl	67±7	424±37	1%	19%
47	$CONHCH_3$	14%	1%	94±8 (63%)	3%
48	$CONHCH_2OH$	10%	1%	182±14 (57%)	8%
49	CONHOH	536 ± 49	1%	20%	31%
50	$COOCH_3$	23%	1%	1%	1%
51	$3\text{-}(COOCH_3)C_6H_4$	66±5	1%	347±31 (27%)	4%
52	$3\text{-}(CONH_2)C_6H_4$	83±7	25%	12.7±1.1 (69%)	1%
BAY60-6583	$CONH_2$	31%	2%	31 ± 3	8%

Table 11

Firstly, the isomer of compound **37**, which bears an imidazol-5-yl moiety (**38**), was produced. The latter results less active than its isomer at the hA_{2B} AR, but but also at hA_{2A} and hA_3 ARs. Unexpectedly, replacement of the 2-imidazolyl group of **37** with an imidazoline (**39**) was detrimental for hA_{2B} activity. The same is observed for the 2-benzoimidazole moiety (compound **40**). In this case, the inactivity at A_{2B} receptor could be ascribed to the excessive steric hindrance of this moiety at this level. Compound **41**, bearing a 3-pyrazolyl

group shows a good affinity and selectivity at hA_{2B} AR which are comparable with those of the 1,2,4-triazol-5-yl group (**43**). These data, together with those of the 1,2,4-triazol-1-yl compound (**42**), which is totally inactive at all the ARs, suggest how important is the presence at R_6 of H-bond acceptor/donor functions. Compound **42** drastically loses activity at A_{2B} AR due probably to the loss of NH function on the appended triazole moiety useful for a profitable interaction with the binding site. Tetrazolyl-substitution in compound **44** results detrimental for affinity at all ARs, probably due to the excessive acidity of the NH tetrazole moiety. Moreover, confirming data on the **DCP1** series, 2-aminothiazol-4-yl (**45**) and 3-pyridyl (**46**) moieties shift the affinity toward the hA_1 AR, to the detriment of hA_{2B} AR. N-methylacetamido compound **47** and its analogous N-hydroxymethylacetamido **48** result to be highly selective and active at hA_{2B} AR, while hydroxamic acid **49** loses its potency, probably due to the acidity of its R_6 residue, scarcely tolerated by A_{2B} AR. Hence, a methyl carboxylate function results detrimental (compound **50**) for hA_{2B} affinity. Also its aryl homologue **51** has low activity at hA_{2B} AR confirming how both H-bond acceptor and donor functions at this position are essential for receptor-ligand interaction. In fact, 3-benzamido-substituted compound **52** is highly active at hA_{2B} AR while maintains good affinity for hA_1 subtype.

At the end, further substitutions were performed in *para* position of the phenyl moiety at R_4, while keeping few selected substituents (imidazol-2-yl, pyrazol-3-yl, carboxyamido and N-methylcarboxyamido) at position R_6, thus, a subset of compounds were generated whose pharmacological data are expressed in Table 12. It has to be outlined that all the aminodicyanopyridine reported until now behave as partial agonist at the hA_{2B} AR with the only exception of compounds **66** and **67** that show a full agonist profile at this subtype. Preliminary data show that 4-cyclobutylmethyloxy substitution results detrimental for activity at all the ARs (compound **53**), this result being quite unexpected. Furthermore, the 4-isobutyloxy derivatives **55**, **56** show divergent results. In fact, compound **55**, bearing a imidazol-2-yl moiety at R_6 is endowed of modest activity at the hA_{2B} AR, while the carboxamido derivative **56** is completely inactive at this subtype. The 4-ethyloxy substituted compounds **57-60** are endowed from high (**57,58**) to modest (**59,60**) activity at A_{2B} AR but scarce selectivity.

Balanced A_1/A_{2B} AR activity is proper of the 4-allyloxy-substituted compound **61**, which bears the imidazol-2-yl moiety at R_6. However, despite the same 4-allyloxy group on R_4 position, substitution with both carboxyamido (**62**) and pyrazol-3-yl (**63**) moieties resulted detrimental for hA_{2B} AR activity although compound **63** binds with high activity and selectivity the hA_1 AR. Also the 4-methylallyloxy substituent (derivatives **64**) shifts the affinity toward the hA_1 AR. In some case, the replacement of the *para*-cyclopropylmethyloxy-phenyl group at position R_4 typical of the A_{2B} agonist **BAY60-6583** with other *para*-cycloalkyl- or *para*-cycloalkenyl-methyloxyphenyl substituents do not produce a high decrease of hA_{2B} activity but preferentially an increase of affinity at the other ARs, thus reducing the selectivity. Finally, *para*-acetamidophenyl-substituted derivatives **66, 67**, bearing respectively a imidazol-2-yl and a carboxyamido

moiety at R_6, are endowed of high activity at hA_{2B} AR despite a scarce selectivity *versus* the others AR subtypes. However, as already outlined, compounds **66** and **67** are the only two amino-3,5-dicyanopyridines in the whole series having a full agonist profile.

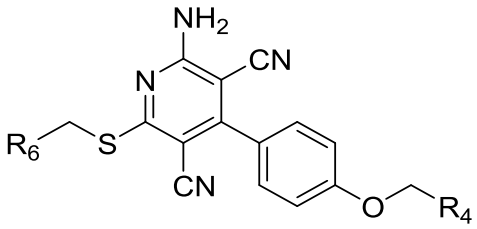

53-67

			hA1 CHO cells	hA2A CHO cells	hA2B cAMP assay	hA3 CHO cells
n°	R_4	R_6	[^{3}H]DPCPX K_i (nM) or (I% at 1μM)	[^{3}H]ZM241385 Ki (nM) or (I% at 1μM)	EC_{50} (nM) (efficacy %)	[^{125}I]ABMECA Ki (nM) or (I% at 1μM)
37	4-($OCH_2C_3H_5$)-C_6H_4	imidazol-2-yl	235±24	764±72	9.52±0.91 (70%)	474±45
53	4-($OCH_2C_4H_7$)-C_6H_4	imidazol-2-yl	25%	4%	12%	574 ± 46
54	4-($OCH_2C_4H_7$)-C_6H_4	$CONH_2$				
55	4-($OCH_2CH(CH_3)_2$)-C_6H_4	imidazol-2-yl	26%	1%	227±21	1%
56	4-($OCH_2CH(CH_3)_2$)-C_6H_4	$CONH_2$	603 ± 52	307 ± 27	1%	9%
57	4-(OCH_2CH_3)-C_6H_4	imidazol-2-yl	8.21±0.73	221±19	11.7±1.2 (62%)	85±6
58	4-(OCH_2CH_3)-C_6H_4	$CONH_2$	345±27	1%	38±3 (66%)	20%
59	4-(OCH_2CH_3)-C_6H_4	$CONHCH_3$	104 ± 8	8%	211 ± 17 (48%)	834 ± 74
60	4-(OCH_2CH_3)-C_6H_4	pyrazol-3-yl	21 ± 2	4%	332 ± 28 (34%)	18%
61	4-($OCH_2CH=CH_2$)-C_6H_4	imidazol-2-yl	16±2	17%	27±3 (56%)	8%
62	4-($OCH_2CH=CH_2$)-C_6H_4	pyrazol-3-yl	44 ±4	8%	7%	13%
63	4-($OCH_2CH=CH_2$)-C_6H_4	$CONH_2$	323 ± 25	18%	11%	444 ± 39
64	4-($OCH_2C(CH_3)=CH_2$)- C_6H_4	imidazol-2-yl	77 ± 6	1%	14%	8%
65	4-($OCH_2C(CH_3)=CH_2$)- C_6H_4	$CONH_2$				
66	$NHCOCH_3$	imidazol-2-yl	83 ± 7	38 ± 3	12 ± 1 (100%)	48 ± 4
67	$NHCOCH_3$	$CONH_2$	17%	572±51	164±12 (92%)	742±67
BAY60-6583			31%	2%	31 ± 3	8%

Table 12

This "result" can be considered as a real breakthrough due to the actually limited number of non-adenosine hA_{2B} AR full agonists reported in literature, as this information can be used to generate in the near future a new series of non-nucleosidic derivatives with this pharmacological profile. However, it has to be clarified the role of the N-acetamido function at *para* position of the 4-phenyl substituent of derivative **66**, **67** in determininig the A_{2B} pharmacological profile of these compounds.

The two bicyclic compounds originated by intramolecular cyclization of both **BAY60-6583** and the analogue **54**, i.e. derivatives **68** and **69,** respectively, bind none of the ARs (Table 13), suggesting that this kind of molecular complication, making the structure more rigid, is detrimental for activity at ARs and in particular at A_{2B} subtype. However, molecular docking at the ARs are on going to obtain some suggestion about the potentiality of this scaffold to be correctly modified and decorated to obtain AR ligands.

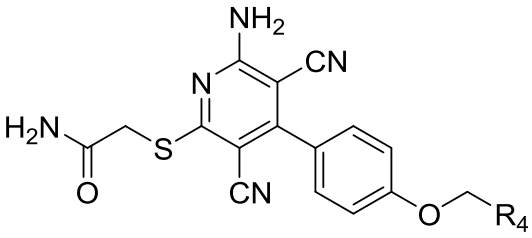

BAY60-6583, 54

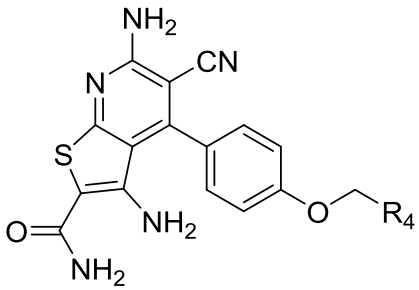

68, 69

		hA1 CHO cells	hA2A CHO cells	hA2B cAMP assay	hA3 CHO cells
n°	R_4	[^{3}H]DPCPX K_i (nM) or I% at 1μM	[^{3}H]ZM241385 Ki (nM) or I% at 1μM	EC_{50} (nM) (efficacy %)	[^{125}I]ABMECA Ki (nM) or I% at 1μM
BAY60-6583	cyclopropyl	31%	2%	31 ± 3	8%
68	cyclopropyl	19%	3%	>1000 (1%)	13%
54	cyclobutyl	25%	4%	>1000 (12%)	574 ± 46
69	cyclobutyl	14%	1%	>1000 (1%)	11%

Table 13

In order to evaluate how a molecular complication of aminopyridine-3,5-dicarbonitriles could modulate the affinity and the pharmacological profile of these derivatives at the ARs, a small set of 7-aminopyrazolo[1,5-c]pyrimidine-4-carbonitriles was synthesized (Table 14). The substituents firstly introduced at position-2

(phenyl group) and -5 (substituted amines) of the scaffold have been selected to make easier the development of a synthetic procedure, new for the most part, that was as much as possible generalizable. Then an investigation in this regard was undertaken and it is still on-going.

The 5-amino substituents are characteristic of hA_{2A} AR antagonists, of which **ZM-241385** (see Table 14) is one of the most popular reported in literature, due to its high affinity and selectivity at this subtype. Evident is the structure similarity of the pyrazolopyrimidine scaffold of **70-73** to that of **ZM-241385** and to those of many other A_{2A} AR antagonists reported in the literature (255).

In fact, as expected, introduction of a phenyl moiety at position 2 of the bicylic scaffold is not the best choice to obtain A_{2A} AR antagonists. Compounds **70-73** preferentially bind the hA_1 AR due to the lack of the 2-furyl moiety, generally mandatory for potent and selective hA_{2A} AR antagonists. Interestingly, compound **71** shows a balanced A_1/A_3 AR affinity.

Despite the small set of synthesized compounds, preliminary information suggest that this new scaffold, suitably decorated, could be a good starting point for the design of new AR ligands.

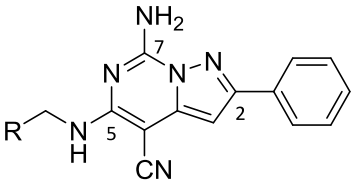

70-73

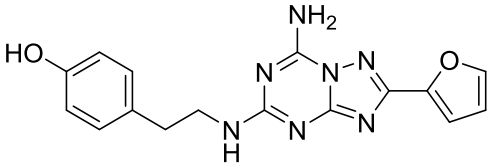

ZM-241385

		hA_1 CHO cells	hA_{2A} CHO cells	hA_{2B} cAMP assay	hA_3 CHO cells
n°	R_5	[^{3}H]DPCPX K_i (nM) or I% at 1μM	[^{3}H]ZM241385 Ki (nM) or I% at 1μM	EC_{50} (nM) (efficacy %)	[^{125}I]ABMECA Ki (nM) or I% at 1μM
70	C_6H_5	193±16	3%	>1000 (1%)	9%
71	3-OCH_3-C_6H_4	116±9	7%	>1000 (1%)	12%
72	2-furyl	64±5	3%	>1000 (2%)	110±11
73	$CH_2C_6H_5$	68±5	1%	>1000 (1%)	1%
ZM-241385 (255)		774	1.6	75*	743

*K_i from binding experiments

Table 14

5. Molecular modeling studies

In order to rationalize the results obtained from pharmacological assays, the synthesized compounds were subjected to a molecular modeling investigation. Docking simulations were performed at both hA_1 and hA_{2B} AR by Prof. Diego Dal Ben at the School of Pharmacy, Medicinal Chemistry Unit of the University of Camerino. Although docking studies are still ongoing some results have emerged. In particular, the newly synthesized amino-3,5-dicyanopyridine derivatives were docked into the binding site of homology models of both hA_1 and hA_{2B} AR built by using the crystal structure of the hA_{2A} receptor as a template.

Molecular modeling studies aimed at analyzing the interaction between AR binding sites and non-nucleoside agonists have been reported in literature (319) (320) (321) (299) (300) (322) (323). While the binding mode of nucleoside agonists has been depicted from experimental results obtained through X-ray crystallography, the interaction between these receptors and agonists based on simplified scaffolds (i.e. pyridine or pyrimidine) has been only simulated by molecular docking approaches. In addition, while for the A_{2A} AR several crystal structures in the activated or inactivated state have been solved and reported, in the case of the A_1 and A_{2B} ARs subtypes the protein architecture has been obtained through homology modeling techniques and then used as target for docking studies.

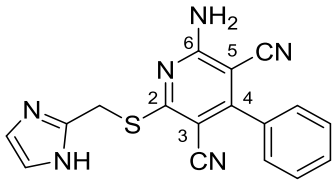

LUF-5833

hA_1 AR K_i = 2.4 nM
hA_{2A} AR K_i = 28 nM
hA_{2B} AR EC_{50} = 19 nM
hA_3 AR K_i = 171 nM

Figure 25

The binding modes obtained in this study for the AR non-nucleoside agonists may be grouped in four families, according to modeling results reported in literature. One of the first non-nucleosidic AR ligand which was evaluated in this study was **LUF-5833** (Figure 25) (323). This compound behaves as an agonist at all the AR subtypes with different degees of efficacies and belongs to the amino-3,5-dicyanopyridine series developed in this thesis. In Figure 26 are shown the four binding modes obtained at the hA_{2A} receptor model for this compound. This set of conformations comprises the potential binding modes suggested not only at the A_{2A} receptor but also at the A_1 and A_{2B} ARs.

In fact, the first binding mode (Figure 26-A) presents the compounds oriented in a way similar to the one previously described for analogue agonists at the ARs (319) (321) (300) (322) (323), where the 5-cyano group

and the 6-amine of the pyridine derivatives giving a polar interaction with the amide function of Asn253$^{6.55}$. The phenyl group in 4-position is located in proximity of residues of TM3,6,7 and the 2-thio substituent points toward the extracellular environment getting close to residues of TM1,2,7. This binding mode was compared with the one of the AR endogenous ligand adenosine, with the nitrogen atom of the 5-cyano group and the 6-amine of pyridines being located in correspondence of the N7 atom and the N^6 amine of adenosine. This binding mode is one of the most populated ones by the A_1 ligands developed in this project, as well as binding mode 3.

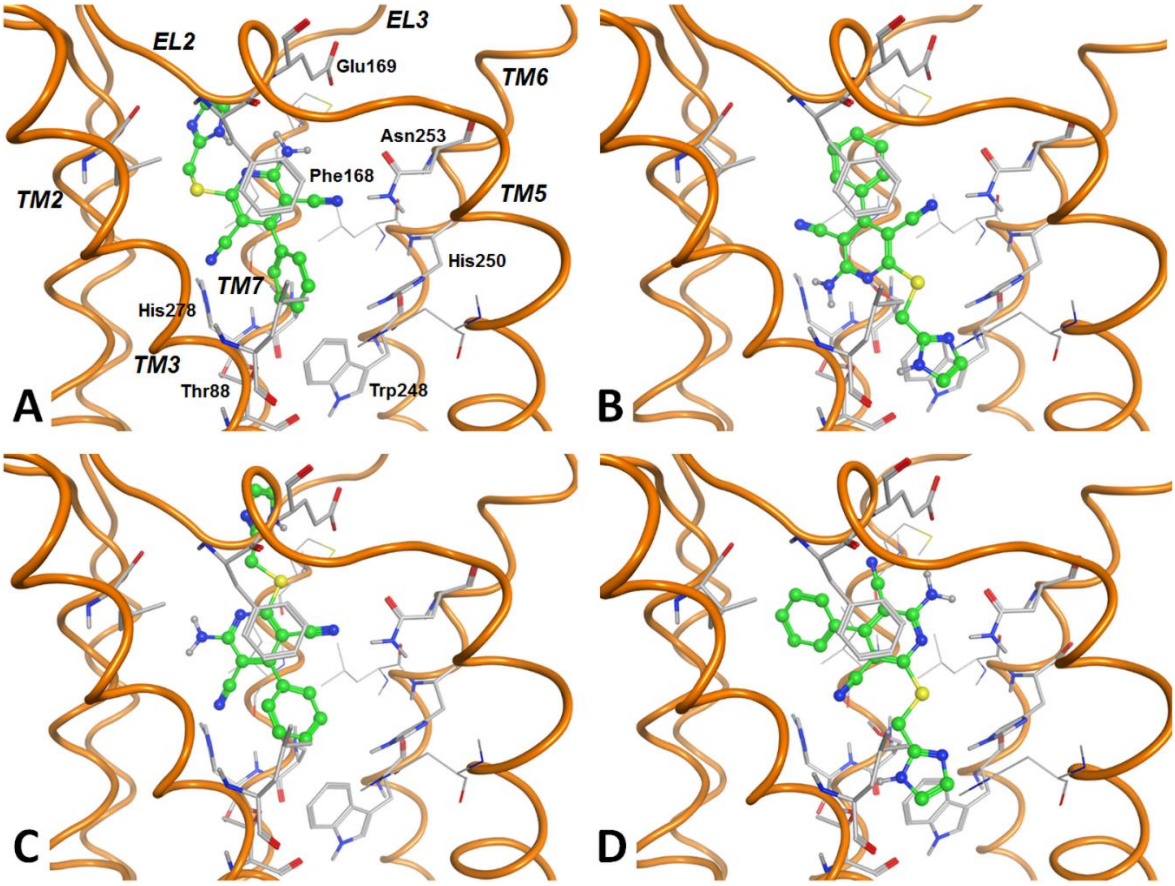

Figure 26: Binding poses of LUF-5833 as example for non-nucleoside AR agonists at A_{2A} AR

The binding mode 2 (Figure 26-B) is a 180° rotated version of binding mode 1 (321) (323). This arrangement makes the exocyclic amine and the proximal cyano group being located close to TM7 residues, while the 3-cyano group gets in proximity of Asn253$^{6.55}$. The 4-phenyl ring gets located at the entrance of the binding cavity, while the sulfanyl substituent is close to TM 3,5,6 residues. The binding mode 3 (Figure 26-C) makes the exocyclic amine and the proximal cyano group being located close to TM7 residues and the 3-cyano group in proximity of Asn253$^{6.55}$. The phenyl group in 4-position is located in proximity of TM 3,6,7 residues while the sulfanyl substituent points toward the extracellular environment. As such as binding mode 1, the number 3 is one of the most populated for the A_1 ligands of this project. The binding mode 4 (Figure 26-D) presents

the N1 atom and the exocyclic amino group giving polar interaction with the Asn253$^{6.55}$ amide function and the 3-cyano group close to TM7 residues. The sulfanyl substituent gets in proximity of TM 3,5,6 residues. In the case of derivatives presenting small and polar groups within this substituent, polar interactions with TM3 and TM6 residues are observable. Even this binding mode was previously described in literature for non-nucleoside agonists of ARs, in particular A_{2B}AR (320) (299) (322).

A classical strategy to improve the A_1 AR affinity for nucleoside compounds has been the introduction of cycloalkyl groups at the N^6 amine function of adenosine derivatives. Comparing the binding mode 1 and 3 at the A_1 AR taking the A_1 selective agonist **15** as template (Figure 27), it may be noticed as the introduction of alkyl or aromatic groups at the exocyclic amine function may be well admitted for binding mode 1 (Figure 27-A) as these substituents would get located at the extracellular environment. The docking of the 6-cyclopentylamino-substituted derivative **22** and of the other analogues **21,23-25** are on going. In fact, the results of binding studies show that the introduction of cycloalkyl groups or aromatic groups at this amine function leads to a decrease of A_1 AR affinity, conversely to what observed for nucleoside derivatives. It may be concluded that the non-nucleoside derivatives follow a different binding strategy than the nucleoside ones. In fact, the binding mode 3 does not provide sufficient free space within the binding cavity to allow the introduction of these substituents at the 6-amine for a matter of steric hindrance, thus suggesting that binding mode 3 could present higher reliability than the binding mode 1, even if further modelling studies and a deepen knowledge in SAR at the aminopyridine-3,5-dicarbonitrile scaffold could be necessary to get a final depiction.

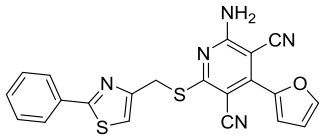

15

hA_1 AR K_i = 3.85 ± 0.32 nM
hA_{2A} AR K_i = 523 ± 49 nM
hA_{2B} AR EC_{50} = 947 ± 92 nM
hA_3 AR K_i = 438±41 nM

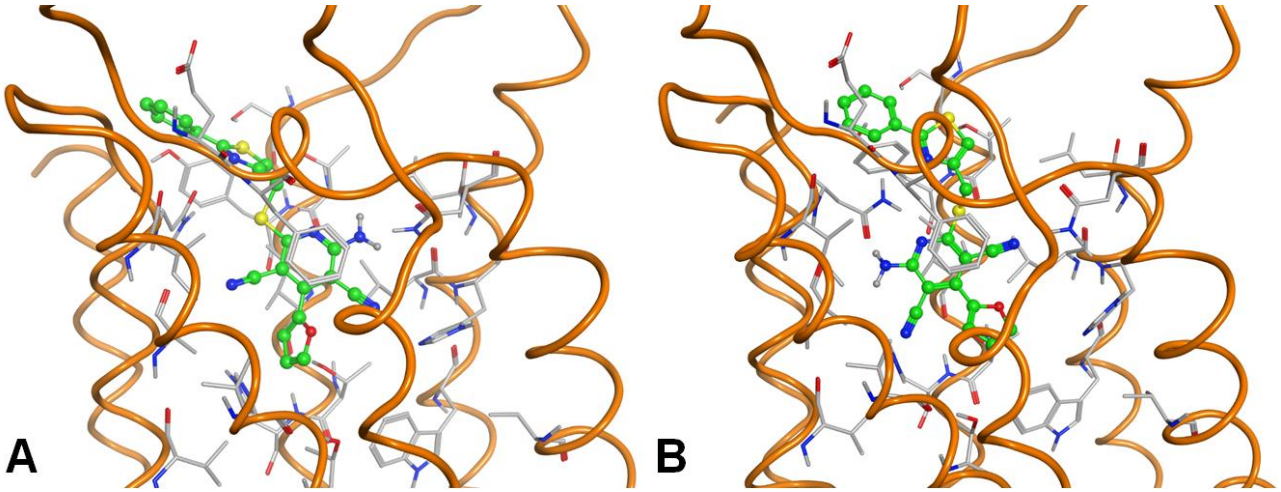

Figure 27: Binding mode 1 (A) and 3 (B) for compound 15 at A_1 AR

Concerning docking at A_{2B} AR, as preliminary step, the study starts from the rebuilding of homology models of the human A_{2B} AR by using as templates the crystal structures of the human A_{2A} AR that is the member of AR family presenting also the highest sequence conservation with the A_{2B} AR. The binding mode of ligands is then simulated by molecular docking tools, followed by energy minimization and post-docking analysis. In this study, it is not possible to depict any correlation between binding scores or interaction energies and activity data, as the potencies of the compounds have been measured as EC_{50} with functional studies and not as K_i affinity with radioligand binding assays. Furthermore, the study provides an interpretation of the interaction features for both series of ligands at the A_{2B} AR but do not consider the interaction with the other AR subtypes. To simulate the binding mode of nucleoside and non-nucleoside agonists at A_{2B} AR and to compare the key ligand-target interaction features of the two structural families of compounds, a molecular docking analysis was performed at homology models of the human A_{2B} AR developed by using two recently published crystal structures of the agonist-bound A_{2A} AR as templates (pdb code: 2YDO; 3.0-Å resolution and pdb code: 3QAK; 2.7-Å resolution, in complex with Ado and UK-432097 (see Figure 5), respectively). The final A_{2B} AR models contain a disulfide bridge given by two cysteine residues belonging to TM3 and extracellular loop (EL) 2 domains (Cys783.25 - where 3.25 indicates the residue position within helix and Cys171, respectively), in agreement with recent mutagenesis studies (324) and as observed in the case of recently reported modelling analyses on this AR subtype (320).

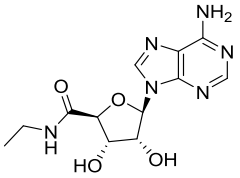

NECA

hA_1 AR K_i = 14 nM
hA_{2A} AR K_i = 20 nM
hA_{2B} AR K_i = 2400 nM
hA_3 AR K_i = 6.2 nM

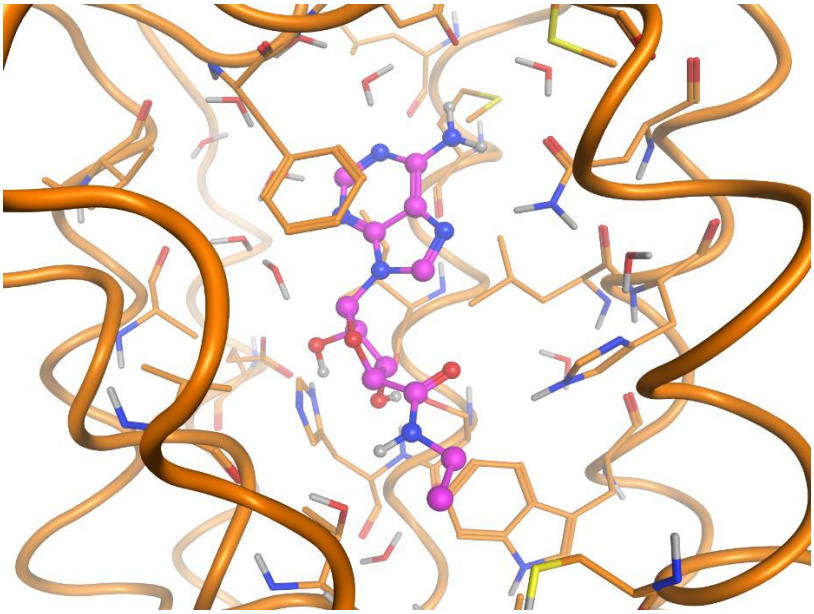

Figure 28: NECA docked in the crystal structure of the A_{2A} AR

The binding sites of the two developed A_{2B} AR models are very similar considering both receptor residues orientation and pocket volumes. Slight differences are still observable, due to diverse arrangements of some residues detectable even at the two A_{2A} AR crystal structures templates. In order to evaluate differences regarding docking at A_{2B} AR between adenosine-like agonist and the aminopyridine-3,5-dicarbonitriles, both **NECA** (Figure 15) and compound **D** were docked. While **NECA** was docked in the crystal structure of the hA_{2A} AR (Figure 28), docking study of compound **D** was performed at hA_{2B} AR homology model (Figure 29).

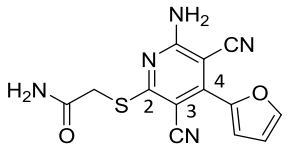

D

hA_1 AR K_i = 12 ± 2 nM
hA_{2A} AR K_i = 26 ± 2 nM
hA_{2B} AR EC_{50} = 1.7 ± 0.2 nM
hA_3 AR K_i = 65 ± 5 nM

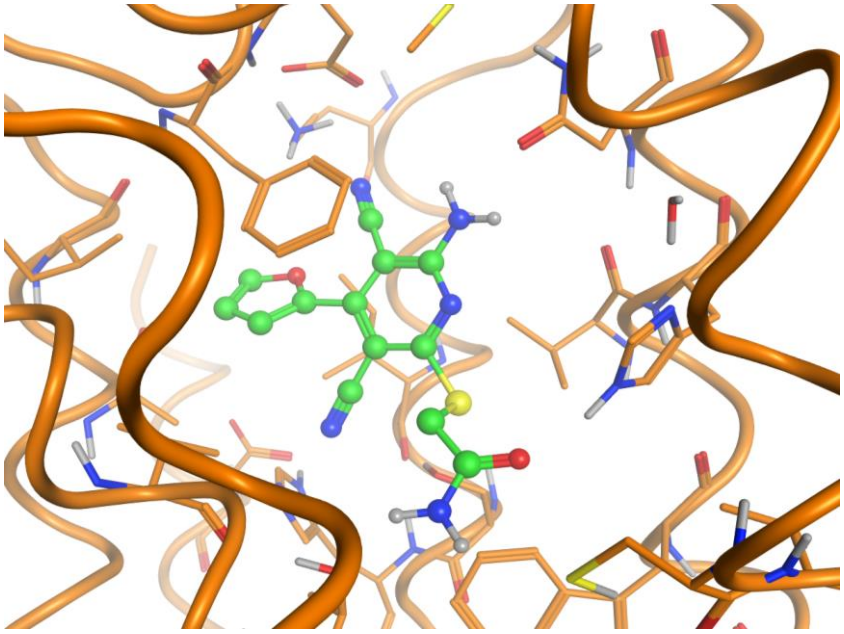

Figure 29: Docking of compound D at A_{2B} AR.

For summarizing, the exocyclic amino group of compound **D** mimics the same function in **NECA**, while the cyano at position-3 of the pyridine scaffold could be essential in keeping the 4-furyl substituents and the 2-sulfanylacetamide function in a non-coplanar conformation. This behavior seems to be mandatory for the agonist profile at the A_{2B} AR of these derivatives.

In fact, considering the non-nucleoside pyridine derivatives, the lowest score and most populated family of docking conformations shows the pyridine ring located in rough correspondence to the adenine scaffold of nucleoside agonists and forming a π-stacking interaction with Phe173 in the EL2 and this conformation seems to be stabilized by the non-coplanarity of the pyridine ring and the substituent at position 2, where H-bond

acceptor and donor group help in reaching a stable conformation. In detail, the interaction of the scaffold with the A_{2B} AR binding site is given as H-bonding between the N1 atom and the exocyclic amino group of pyridines and the amine and carbonyl groups of Asn2546.55 amide function, respectively. This double polar interaction is clearly present only for some derivatives, due to the nature of the 4-substituent that slightly modifies in some cases the orientation of the scaffold. Analogously to the nucleoside agonists, the exocyclic amino group of pyridines gives a H-bond interaction with Glu174 in the case of the 2YDO-based A_{2B} AR model, while in the case of the 3QAK-based model the side chain of the same residue in some cases is not close enough to the ligand amino group and hence not able to provide a clear H-bonding. The sulfanylmethylimidazole group of compound **37** (Figure 30) and the sulfanylacetamide function of compound **D** (Figure 29) at 2-position are inserted between TM3, TM5, and TM6 residues. In the case of compound **37**, the H-bond donor function of imidazole is oriented towards the oxygen atom of Thr893.36, while the acceptor feature points towards the polar hydrogen of His2516.52. The 4'-N-ethyl-carboxyamide function of the nucleoside derivative **NECA** (Figure 28) is in a nearly identical position to the analogue sulfanylacetamide group of compound **D** (Figure 29), suggesting the importance of the presence of a combination of H-bond acceptor and donor features located in this region. The 3-cyano group is inserted in a sub-cavity between Val853.32, Leu863.33, Thr893.36, Ser2797.42, and His2807.43. No clear interaction with binding site is given by this group, even though the presence of some space between this function and the polar groups of Ser2797.42 and His2807.43 could allow the presence of a water molecule providing a sort of "bridge interaction" between ligand and binding site residues, as observed, for example, in the case of a crystal structure of A_{2A} AR in complex with ZM241385 (54). The substituted aromatic group at the 4-position is located in a sub-cavity given by TM1, TM2, TM3, and TM7 residues, in close proximity to Tyr101.35, Ala642.61, Ile672.64, Ser682.65, and Ile2767.39. Further residues in proximity of this group are Val853.32 and Phe173.

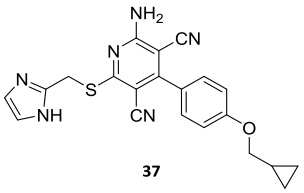

37

hA_1 AR K_i = 235 ± 24 nM
hA_{2A} AR K_i = 764 ± 72 nM
hA_{2B} AR EC_{50} = 9.52 ± 0.91 nM
hA_3 AR K_i = 474 ± 45 nM

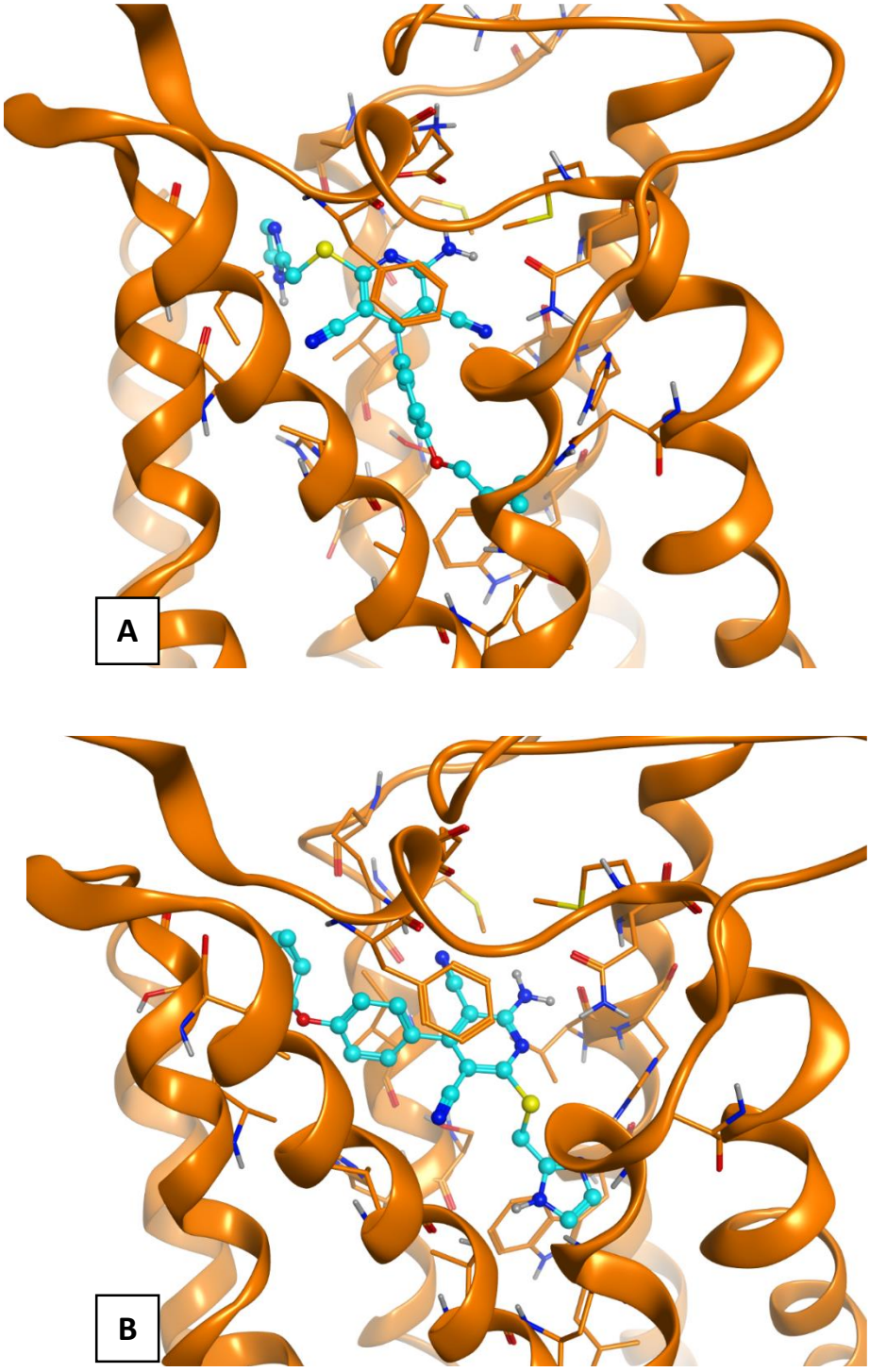

Figure 30: Docking of compound 37 at A_{2B} AR: the first binding mode (A) was observed and reported in literature mainly for a series of A_1 receptor agonists (300)**, while the second (B) was already observed also at the A_{2B} receptor** (299)**.**

The interaction is mainly hydrophobic, and the presence of a hydrophobic group in *para* –position of the phenyl ring (**BAY60-6583**, Figure 31 and compound **37**, Figure 30) suggests the presence of a large hydrophobic feature located within TM1, TM2, and TM7 domains, similar to the e 2-position of nucleosides agonists. This group seems critical in particular for pyridine derivatives. Finally, the 5-cyano group points towards the extracellular environment and is located in proximity to the couple of residues Glu174-Lys269.

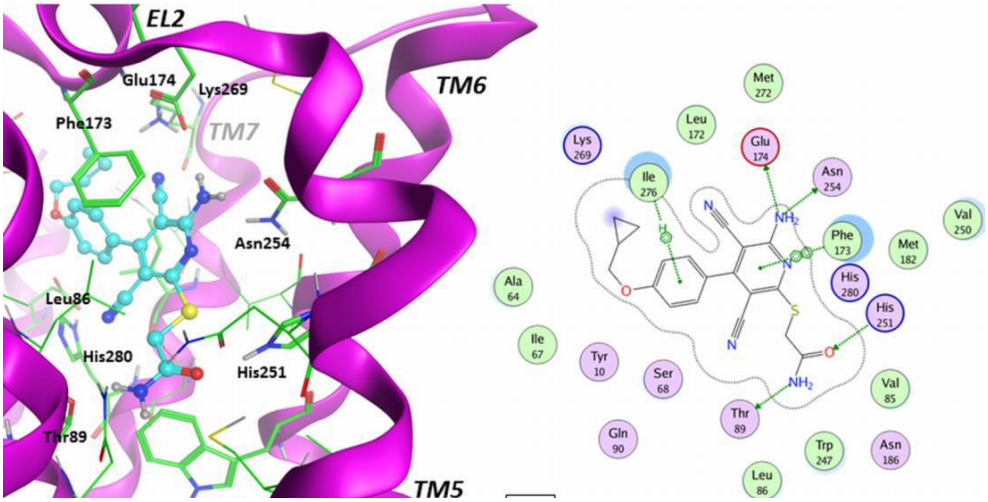

Figure 31: Docking of BAY60-6583 at A_{2B} AR

Concerning in particular docking at A_{2B} AR for compound **37** (Figure 30) receptor interaction is given in particular through Asn254 (TM6) and Phe173 (EL2), even if further contacts with residues belonging to TM2, TM6, and TM7 that probably play a role for receptor activation are observable (300) (299).

6. Evaluation of the antinociceptive effect and stability studies

6.1 Evaluation of the antinociceptive effect

Experimental evidence (325) supports the use of caffeine and of other A_1/A_{2A} antagonists as well A_1 AR agonists in the reduction of hyperalgesia or in antinociception. With this in mind, and to clarify these paradoxical data, the pain reliever effect of compound **1** (dual A_1 inverse agonist/A_{2A} antagonist), derivative **3** (carboxylic acid analogue of **1**, as possible methabolite) and **15**, which behaves as partial A_1 AR agonist (Figure 32), were evaluated in a rat model of chemotherapy-dependent neuropathy induced by oxaliplatin.

Anticancer therapy based on the repeated administration of oxaliplatin is limited by the development of a neuropathic syndrome difficult to treat. Oxaliplatin neurotoxicity is based on complex nervous mechanisms, the comprehension of the role of single neurotransmitters and the knowledge of the signal flow among cells is matter of importance to improve therapeutic chances. Neuropathic pain evolves from the physiological role of nociceptive pain to pathological aspects depending on the complex response of the nervous system to a lesion or disease of its somatosensory component. Electrical, molecular and cellular activity participate in sensitizing nervous circuits of periphery, dorsal horn as well as anterior cingulate gyrus, prefrontal cortex, amygdala, and periaqueductal gray leading to pain-mediating signals (326). The maladaptive plasticity of the central nervous system (CNS) assumes increasing evidence in the pathophysiology of chemotherapy-induced neuropathies (327) (328), a peculiar iatrogenic damage of the nervous tissue that results in therapy dose reduction or discontinuation and negatively influences quality of life on cancer survivors (329). Oxaliplatin is effective in various solid tumors (330) (331). Colorectal cancer is the main target, introduced for the management of the advanced stages oxaliplatin is currently the regimen of choice for the adjuvant treatment of patients with curative resection of node-positive colon cancer (332) (333). The dose-limiting toxicity of this compound is the development of peripheral neuropathy (334) related to the total cumulative dose and to the treatment doseintensity (335). Although acute symptoms typically resolve within a week, cumulative oxaliplatin causes chronic neuropathy in approximately 50% of patients receiving doses higher than 1000 mg/m^2. Signs and symptoms of chronic neuropathy include pain, paresthesia, hypoesthesia, dysesthesia, and changes in proprioception that persist between cycles (336). The pathophysiology of oxaliplatin neurotoxicity involves multiple aspects. Molecular damages to peripheral nerves and dorsal root ganglia (327) result in decreased cellular metabolism and axoplasmatic transport (337). Despite the oxaliplatin limited ability to cross the blood brain barrier (338) (339), the CNS appears strongly involved since oxidative damage (338), peroxisome derangement and intracellular signaling alteration have been shown at spinal and supraspinal

level (327) (339). In the spinal dorsal horn of oxaliplatin-treated mice, Renn and co-workers (328) observed an increased activity of wide dynamic range neurons.

On the other hand, oxaliplatin induces a significant glial cell density increase differently according to cell type, anatomical region and treatment time-points revealing a prominent role of astrocytes (327). In recent years, there have been further significant developments that enhance an understanding of the role of adenosine in nociception. Thus, novel methods useful for taking advantage of A_1 AR antinociceptive effect have been developed (144), and the role of adenosine A_{2A} in nociception has been further elaborated (160). Furthermore, a contribution of endogenous adenosine and AR modulation to the actions of several pharmacological agents, as well as non-pharmacological procedures, used to manage pain has been described. As previously assumed (see Introduction) A_1 AR and A_{2A} AR, as well as A_{2B} AR are fully involved in neuropathic pain modulation.

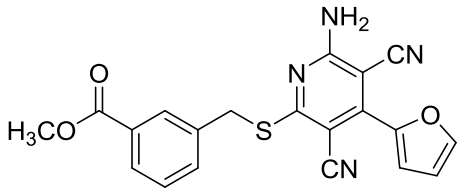

1

hA_1 AR K_i = 7.22 ± 0.63 (inv ago)
hA_{2A} AR K_i = 68 ± 3 (antagonist)
hA_{2B} AR EC_{50} = >1000 (7%)
hA_3 AR K_i = 26%

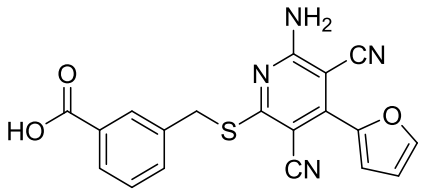

3

hA_1 AR K_i = 4.12 ± 0.38
hA_{2A} AR K_i = 581 ± 54
hA_{2B} AR EC_{50} = >1000 (1%)
hA_3 AR K_i = 611 ± 58

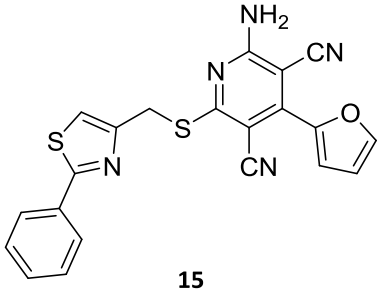

15

hA_1 AR K_i = 3.85 ± 0.32 (partial agonist)
hA_{2A} AR K_i = 523 ± 49
hA_{2B} AR EC_{50} = 947 ± 92 (29%)
hA_3 AR K_i = 438 ± 41

Figure 32: Compound tested in the oxaliplatin-induced allodynia assay

Pro-nociceptive effects mediated by A_{2B} AR activation were discovered only in the last 10 years. And recently, the focus of attention has moved to the antinociceptive effect exerted by A_1 AR agonists at the spinal cord

level thus hypothesizing a therapeutic potential for the treatment of neuropathic pain (258). Also A_{2A} AR seems to be involved in pain response. However, the finding regarding the A_{2A} AR signaling in pain have been controversial, with studies supporting both pro- and anti-nociceptive roles. Moreover, it is still controversial the role in antinociception mediated by one of the most known non selective AR antagonists, caffeine. In fact, with respect to pain, caffeine (100 mg) is an adjuvant analgesic in humans when given in combination with common analgesics (acetylsalicylic acid, acetaminophen/paracetamol, ibuprofen). Furthermore, a few is known about the effect of caffeine (340) in neuropathic pain. Recent reports, assess a role of the potential of caffeine in this disease to its antagonistic properties at A_1 and A_{2A} ARs. The hyperalgesic effect mediated by A_1 AR blockade may be compensated for by an antinociceptive effect of antagonism at A_{2A} subtype. Thus, it is particularly important to deepen the role of the balanced A_1/A_{2A} antagonism of caffeine in nociception.

This oxaliplatin-induced allodynia assay was performed by the group of Prof. Carla Ghelardini at the NEUROFARBA Department – Pharmacology and Toxicology section, of the University of Florence.

		Cold plate (s)			
Treatment	**Before treatment**	**After treatment**			
		15 min	30 min	45 min	60 min
vehicle + vehicle	18.4 ± 0.2	18.6 ± 1.2	19.0 ± 0.4	22.6 ± 0.6	21.4 ± 0.6
oxaliplatin + vehicle	10.9 ± 1.2*	11.7 ± 0.6*	12.0 ± 1.0*	12.5 ± 0.9*	13.4 ± 1.6*
oxaliplatin + **1** (0.03 mg Kg^{-1} p.o.)	11.3 ± 0.3*	12.8 ± 0.6	13.2 ± 0.6	13.0 ± 0.5	14.2 ± 0.6
oxaliplatin + **1** (0.1 mg Kg^{-1} p.o.)	10.3 ± 0.4*	14.5 ± 0.6^	16.8 ± 0.3^^	18.0 ± 0.6^^	14.2 ± 0.3
oxaliplatin + **1** (0.3 mg Kg^{-1} p.o.)	10.3 ± 0.3*	17.0 ± 0.7^^	19.2 ± 0.5^^	17.7 ± 0.6^^	15.0 ± 0.6
oxaliplatin + **3** (0.1 mg Kg^{-1} p.o.)	10.6 ± 0.5*	12.8 ± 1.2	14.0 ± 0.8	11.0 ± 1.1	11.1 ± 0.8
oxaliplatin + **3** (0.3 mg Kg^{-1} p.o.)	11.0 ± 0.4*	14.2 ± 1.5	20.8 ± 1.2^^	14.0 ± 0.6	11.9 ± 0.7
oxaliplatin + **15** (0.3 mg Kg^{-1} p.o.)	11.5 ± 0.5*	12.2 ± 0.5	12.2 ± 1.0	12.7 ± 0.6	12.0 ± 1.2
oxaliplatin + **15** (1.0 mg Kg^{-1} p.o.)	10.6 ± 0.2*	16.6 ± 1.1^	12.0 ± 1.6	12.1 ± 0.5	11.7 ± 0.6

Table 15: Oxaliplatin (2.4 mg kg-1, i.p.) was dissolved in glucose 5% and administered daily for 2 weeks. After 14 days from the first injection of oxaliplatin, P301 (suspended in 1% carboxymethylcellulose) was per os (p.o.) administered. Control animals were treated with vehicles. Pain-related behavior (i.e. lifting and licking of the hind paw) were observed and the time (seconds) of the first sign was recorded. *P<0.01 vs vehicle + vehicle treated animals; ^P<0.05 and ^^P<0.01 vs oxaliplatin + vehicle treated mice. Each value represents the mean of 10 mice

After repeated treatment with oxaliplatin (2.4 mg kg^{-1} daily intraperitoneally for 2 weeks), animals developed a characteristic thermal allodynia to cold stimuli evaluable by the cold plate test (licking latency 10.9 ± 1.2 s in comparison to 18.4 ± 0.2 s of control animals). While the partial agonist **15** showed only a modest effect 30min after treatment (Table 15), a single treatment with **1** *per os* was able to dose-dependently decreased oxaliplatin-induced pain. Starting from 0.1 mg kg^{-1} the compound significantly reduced the cold hypersensitivity for 45 min after administration. The **1** high dose tested (0.3 mg kg^{-1}) was able to fully revert allodynia peaking 30 min after treatment. The behavior of this two compound in this pharmacological assay can be seen as paradoxal: activation of A_1 AR is known to exert an antinociceptive effect in a large variety of pain models in literature while A_1 AR blocking can be associated to pro-nociceptive action. In contrast, the expected pain reliever effect of compound **15**, the A_1 AR partial agonist, was not evidenced in this model. Moreover, the A_1 inverse agonist/A_{2A} antagonist **1** exerts antinociceptive effect that appears to be modulated by A_{2A} AR that could outweigh the pro-nociceptive effect mediated by the A_1 subtype. Also the carboxylic acid **3** (Figure 25) was evaluated in this model in order to clarify if the data on antinociceptive actions of compound **1** could be related to its metabolic hydrolysis to **3**. In this model, **3,** whose pharmacological profile was not yet evaluated, shows to be less active than the corresponding methyl ester **1** in this oxaliplatin-induced allodynia assay at 0.1 mg/Kg p.o. and 0.3 mg/Kg p.o., despite a higher peak of effect at 30 minutes after somministration. These results do not help the understanding of the pathophysiological role of A_1 and A_{2A} ARs in neuropathic pain. Thus, in the future others A_1 AR agonists, dual A_1/A_{2A} AR antagonist or inverse agonist, and A_1 AR inverse agonist already obtained, will be tested in this model. In order to evaluate the potential role of the carboxylic acid **3** as methabolite of the carboxylic ester **1** in the antinociceptive action of this latter, stability studies on human and rat plasma were performed.

6.2 Stability studies

The stability study on compound **1** was performed by the group of Dr. Gianluca Bartolucci at the NEUROFARBA Department – Pharmaceutical Science section, of the University of Florence. The degradation profiles were obtained by using LC-MS/MS analysis monitoring the variation of the analyte **1** concentration, by using **BAY60-6583** as internal standard, at different incubation times. Comparison of results obtained in a phosphate buffer solution (PBS) and plasma permits to distinguish between chemical stability and bioavailability of the analyte. Both Ketoprofene ethyl ester and Enalapril degradation experiments were carried out to check the hydrolytic activity of human or rat plasma batch employed, respectively. In order to summarize all experimental data, the half-life (T1/2) of compound **1** was reported in Table 16.

In the graphs are shown the degradation profiles of **1** in human plasma and PBS (figure 33) and in rat plasma (Figure 34) using Ketoprofen ethyl ester and Enalapril as control enzyme activity of the human and rat plasma, respectively.

The data obtained in this study confirm the stability of **1** during of the whole oxaliplatin-induced neuropathy assay in rats showing a high hydrolyzing time in these conditions.

Compound	Human Plasma T 1/2 (min)	Rat Plasma T 1/2 (min)
KEE	93	-
Enalapril	-	60
1	>240	170

Table 16

Degradation profiles of **1** indicate a similar trend in rat and human plasma, leading to validate the pharmacological model here used.

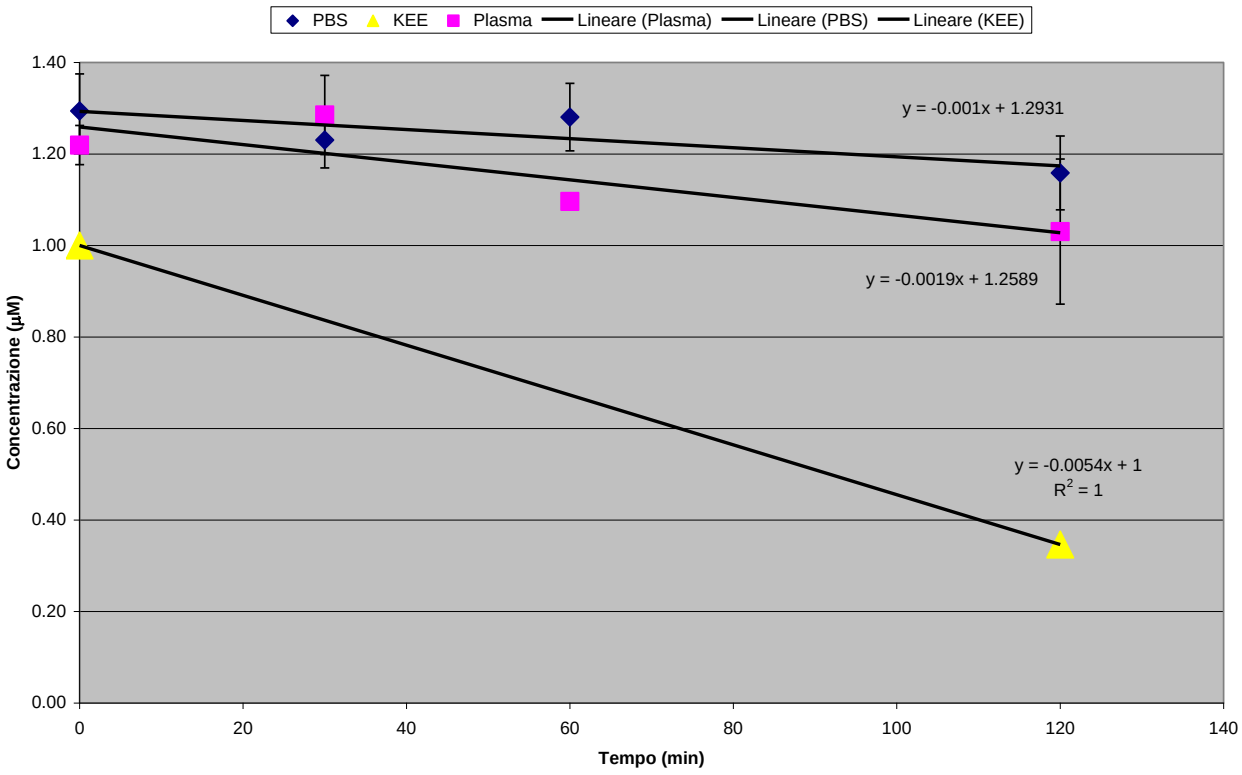

Figure 33

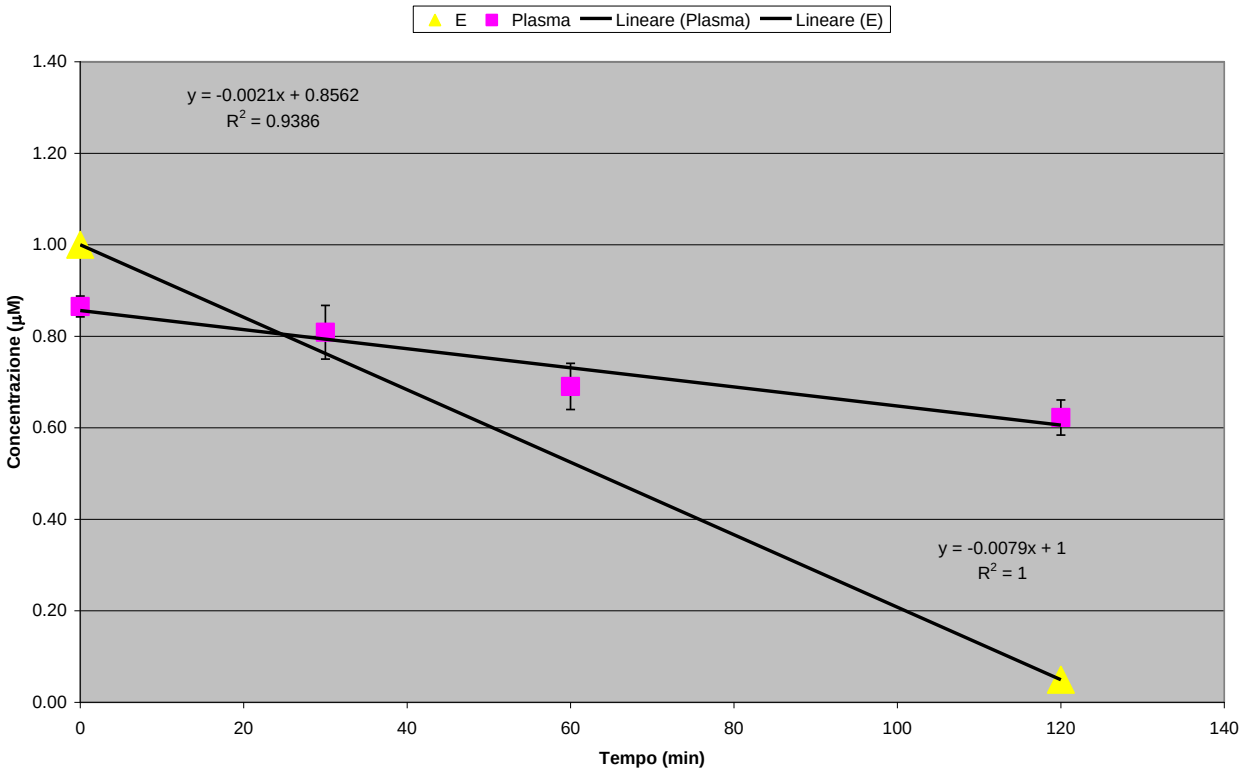
E
Plasma
Lineare (Plasma)
Lineare (E)
y = -0.0021x + 0.8562
R2 = 0.9386
y = -0.0079x + 1
R2 = 1
Concentrazione (µM)
Tempo (min)
1.40
1.20
1.00
0.80
0.60
0.40
0.20
0.00
0
20
40
60
80
100
120
140

Figure 34

7. Studies on oligodendrocytes precursor cells

Current available multiple sclerosis (MS) therapies target immune modulation with some efficacy, however, concomitantly with adverse side effects (341). Oligodendrocytes are the only myelin-producing cells in the CNS (342). Damaged oligodendrocytes no longer generate myelin and remyelination requires generation of new mature oligodendrocytes from the differentiation of oligodendrocyte progenitor cells (OPCs) (Figure 35) (343). These cellular resources are especially active after demyelinating episodes in early phases of MS. Indeed, OPCs actively proliferate, migrate to and repopulate the lesioned areas. Ultimately, efficient remyelination is accomplished when new oligodendrocytes reinvest nude neuronal axons, restoring the normal properties of impulse conduction. As the disease progresses, this fundamental process fails. Multiple causes seem to contribute to such transient decline, including the failure of OPCs to differentiate and enwrap the vulnerable neuronal axons. For example, the observation that OPCs are present in MS lesions but fail to differentiate into mature oligodendrocytes (344) suggests that the remyelination process is blocked at a premyelinating stage in demyelinating lesions. There are no effective remyelination therapies for MS patients. Thus, OPCs are a viable treatment target for MS clinical therapy (345) (346).

Purinergic signaling (exerted by adenosine and ATP) has recently emerged as a most pervasive mechanism for intercellular communication in the nervous system, affecting communication between many types of neurons and all types of glial cells (347). Not only neurons but also glial cells in fact release and respond to purinergic molecules, under both physiological and pathological conditions (348). Concerning oligodendrocytes, it has been demonstrated that purines exert multiple effects including increased motility, proliferation and differentiation of cultured OPCs (349). Among purines, adenosine is a neuromodulator of the CNS. It is known that OPCs express all these receptors, as detected by RT-PCR in cultured OPCs, including A_{2B} AR (350). To date, a functional role has been attributed only to A_1 and A_{2A} AR (349). It has recently clarified the role of A_{2A} AR on oligodendrogenesis, demonstrating that their selective activation decreases outward rectifying, sustained, inward K^+ currents and inhibits in vitro OPC differentiation towards mature, myelinating, oligodendrocytes, without affecting cell division (351). Conversely, adenosine, through the activation of A_1 AR, seems to be a primary activity-dependent signal inhibiting the proliferation and promoting differentiation of premyelinating progenitors into myelinating oligodendrocytes (350) and stimulating OPC migration (352). The functional role of the A_{2B} AR in oligodendrocytes has not yet been clarified because, as already assumed in this thesis, A_{2B} AR is the least studied and still remains the most enigmatic AR subtype. However, there is a growing interest in A_{2B} AR in recent years, as it has been shown to play a role in inflammation and cancer and is even considered a promising new pharmacotherapeutic target (320). Of particular note is that in the brain during different pathological conditions, such cerebral ischemia,

extracellular adenosine is elevated to levels sufficient for A_{2B} AR (349). White matter damage is a clinically important aspect of several central nervous system diseases, including stroke. Cerebral white matter primarily consists of axonal bundles unsheathed with myelin secreted by mature oligodendrocytes, which play an important role in neurotransmission between different areas of gray matter. During the acute phase of stroke, damage to oligodendrocytes leads to white matter dysfunction through the loss of myelin. For effective remyelination to take place, OPCs play critical roles by proliferating and differentiating into mature oligodendrocytes, which help to decrease the burden of axonal injury. Although it was demonstrated that the selective A_{2A} AR antagonism prevented myelin disorganization induced 24 h after occlusion of medial cerebral artery (MCAo) in rat (353), the role of A_{2B} AR both on ischemia-induced neuronal and glial damage was not investigated during cerebral ischemia.

The aim of this study was to clarify the oligodendrogenetic potential of A_{2B} AR, in particular to investigate, in cultured OPCs at different times of maturation (from t0 to t10, Figure 35), whether A_{2B} AR modulates ionic currents and cell proliferation and maturation by using selective A_{2B} AR agonists (commercially available and newly synthetized), alone or in combination with A_{2B} AR selective antagonists. All these experiments were carried out in cultured rat oligodendrocytes by using patch clamp recordings and immunocytochemical analysis (Figure I) and performed by Dr. Anna Maria Pugliese, belonging to the Prof. Felicita Pedata group at the NEUROFARBA Department – Pharmacology and Toxicology section, of the University of Florence.

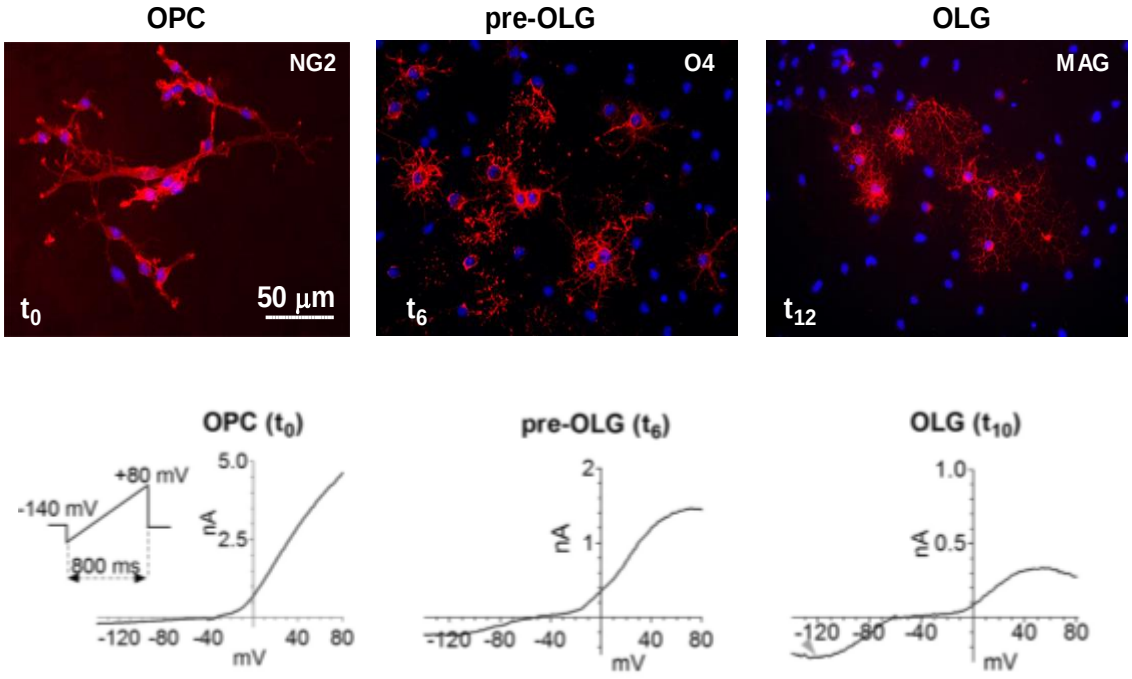

Figure 35: Immunocytochemical analysis of OPCs at different times of maturation and ouward K^+ current variation during maturation

To examine the effects of A_{2B} AR stimulation on the in vitro oligodendrocyte progression towards mature phenotypes, an immunocytochemical labeling of OPC cultures was performed. OPC were allowed to differentiate for different days in differentiation medium (DM) (t6 and t10) in order to characterize the time course of the expression of specific markers of cell differentiation. In parallel experiments, OPC cultures will be differentiated in the presence of different concentrations of the A_{2B} AR agonists **37** and **BAY 60-6583** (Tocris, Italy) (Figure 15) alone or in combination with the A_{2B} AR antagonist **PSB-603** (Figure 16) in order to verify whether A_{2B} AR receptor activation could influence OPC differentiation.

Preliminary experiments demonstrated that selective stimulation of A_{2B} AR in cultured OPCs reduces the amplitude of outward currents, as recorded in patch clamp experiments (Figure 36). The selective stimulation was guaranteed by silenciating A_1, A_{2A} and A_3 ARs in coltures. These currents were abolished when K^+ was replaced by equimolar Cs^+ concentration into the intracellular pipette solution indicating that ramp-evoked outward currents are K^+ currents. Compound **37**, applied at the concentrations of 50 nM, reduces the amplitude of outward currents elicited by a ramp voltage protocol (Figure 36 A and B). Similar effect to that produced by **37** was recorded in the presence of **BAY 60-6583** which was applied at concentrations of 1 and 10 µM. Thus, applying A_{2B} AR antagonist **PSB-603** the effect of both agonists was reverted, confirming the involvement of A_{2B} AR (Figure 37 A and B).

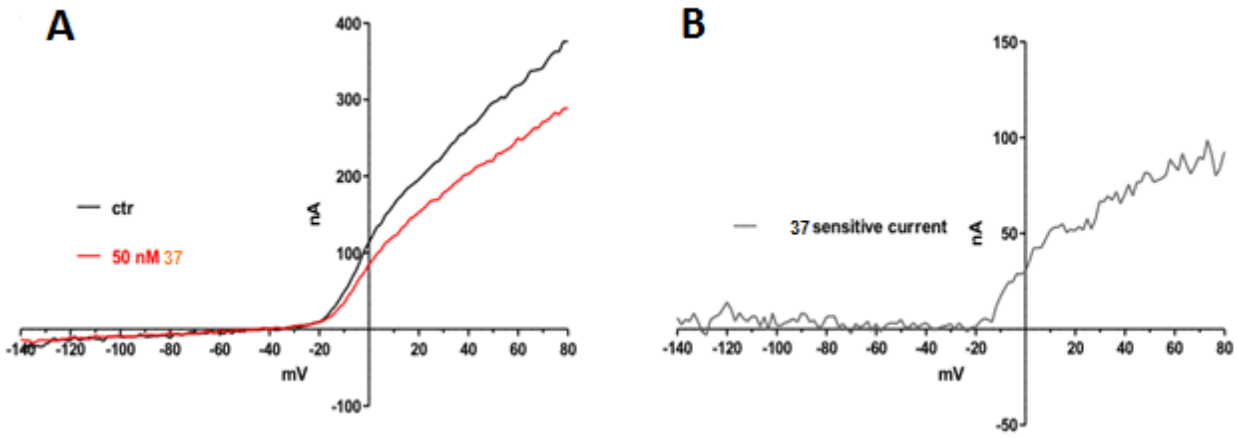

Figure 36: (A) Outward currents elicited by 37 in a ramp voltage protocol; (B) net outward K+ current sensitive to 37

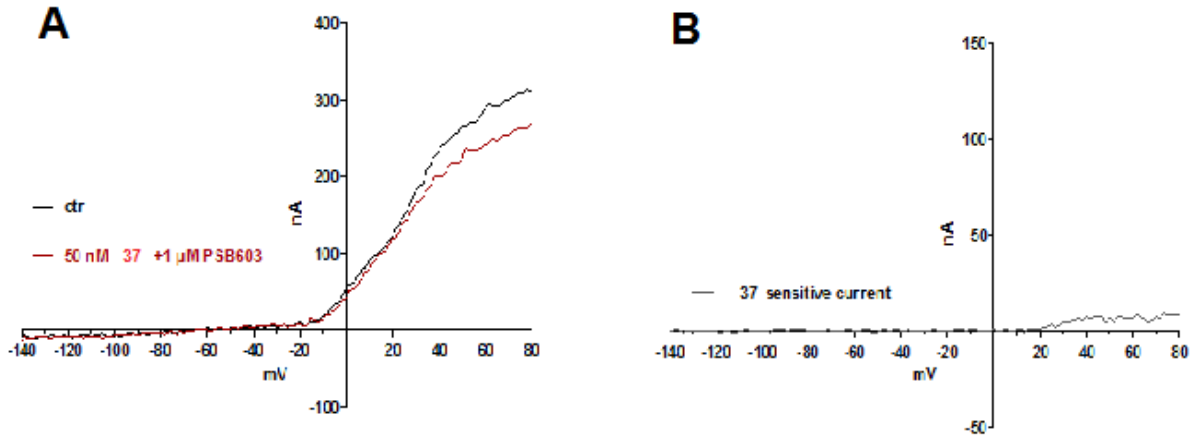

Figure 37: (A) outward currents elicited by 37 in the presence of PSB-603 1µM in a ramp voltage protocol; (B) net outward K^+ current sensitive to 37 in the presence of PSB-603 1µM

Thus, in this assay was demonstrated that A_{2B} AR is involved in OPC maturation. In particular, activation of A_{2B} AR inhibits OPC differentiation in oligodendrocytes by blocking outward K^+ currents, essential for the differentiation process. Furthermore, compound **37** exert its effect at lower concentrations than **BAY60-6583**, the reference agonist reported in literature. Finally, two other compounds acting as full agonist, **66** and **67**, will be tested in this *in vitro* model, despite their scarce selectivity at A_{2B} AR, since in this assay the other AR subtypes will be silenced.

8. Conclusions and perspectives

The research reported in this Ph.D. thesis, though it has to be deepened, furthers our understanding about the ARs. New AR ligands were developed preferentially belonging to the aminopyridine-3,5-dicarbonitrile series whose structure-activity relationships have been till now poorly investigated. In fact, most of the compounds reported in the literature are included in patent documents. In this work, many derivatives were synthesized and biologically evaluated in binding and functional assays in order to assess affinity and selectivity towards a specific AR subtype, but also to evaluate their pharmacological profile. The data obtained confirmed the peculiarity of this series whose derivatives are not only characterized by a wide range of affinities but interestingly endowed with different degree of efficacies at the different ARs.

Based also on molecular modelling studies two set of compounds, named **DCP1** and **DCP2B** were designed preferentially targeting the A_1 and A_{2B} AR, respectively.

- Most of the compounds belonging to the **DCP1** set (compounds **1-25**, Tables 5, 7-8) are endowed with high affinity and good selectivity at the hA_1 AR. Some selected derivatives showed also an inverse agonist profile with the only exception of compound **15** which emerged as partial agonist bearing a peculiar 2-phenylthiazole group at R_6. Thus, further modification at the level of the thiazole moiety will be planned in order to evaluate the importance of this substituent for obtaining hA_1 AR agonists.

  Moreover, when evaluated in an oxaliplatin-induced neuropathic pain model in mice, compound **1** (dual A_1 inverse agonist/A_{2A} antagonist) resulted to revert allodynia at very low doses after oral administration (Table 15). This effect is similar to that exerted by both caffeine and other A_1/A_{2A} antagonists as well as A_1 AR agonists in reverting hyperalgesia and in antinociception.

  Stability studies in mouse and human plasma on **1** (Figure 33, 34) confirmed no significant chemical modification of the compound for the whole duration of the assay. Thus, to clarify this paradoxical data, other molecules belonging to this set, endowed with similar degree of affinities and efficacies with respect to **1,** will be tested in this *in vivo* assay, also to evaluate their potentiality for neuropathic pain treatment.

The results obtained on the **DCP1** set, especially in the *in vivo* assay, suggested that the amino-3,5-dicyanopyridine scaffold could be of interest for obtaining non-nucleoside AR agonists as to prevent two serious problems hampering the development of classical adenosine-like agonists: the low oral bioavailability and the short half-life due to the presence of the typical ribose (or ribose-mimicking) moiety.

- **DCP2B** set is composed of compounds preferentially targeting the hA_{2B} receptor (**26-67**, Tables 9-12). Most of them showed to behave as partial agonist, with the best results concerning activity and selectivity of compound **37**, which is three fold more potent than the reference agonist **BAY60-6583**. This result can be considered a real breakthrough since **BAY60-6583** is absolutely the sole potent and selective hA_{2B} AR agonist reported in literature.

  Moreover, it is noteworthy that derivatives **66** and **67**, showing high activity at the hA_{2B}AR but scarce selectivity, emerged as the only two amino-3,5-dicyanopyridines reported till now which are endowed with a full agonist profile. With this in mind, a study to clarify the structural requirements which are important in determining the A_{2B} pharmacological profile of these compounds is currently on going.

  Thus, identification of new selective hA_{2B} agonists could be of help in deepening the medicinal chemistry and the pharmacology related to this still unknown AR subtype. In fact, compound **37** was used as pharmacological tool in an oligodendrocyte precursor cell (OPC) differentiation assay in order to clarify whether the A_{2B} receptor represents a promising target to modulate endogenous remyelinization process in multiple sclerosis patients. Compound **37** inhibits OPC differentiation into oligodendrocytes at lower concentration than those used for **BAY60-6583** demonstrating the role of A_{2B} AR in this important physiological process (Figure 36, 37).

Moreover, docking studies were performed on selected **DCP1** and **DCP2B** derivatives at A_1 and A_{2B} homology receptor models, respectively, showing the best binding poses for compounds **15** (Figure 27) and **37** (Figure 30) and the most important residues involved in the binding at these two AR subtypes. It seems to clarify the role of R_4 and R_6 substituents, containing atoms or groups able to engage hydrogen-bonding interactions with the receptors, in modulating affinity and efficacy of the amino-3,5-diyanopyridine derivatives.

Moreover, since some affinity was also achieved at the hA_{2A} and hA_3 AR with some of the compounds detailed in this thesis, it may be possible that this heterocycle core could be also manipulated to enhance affinity and selectivity for these subtypes. In fact, neither A_{2A} nor A_3 agonists belonging to the amino-3,5-dicyanopyridine series has been ever designed.

- Preliminary studies on the newly synthesized 7-amino-2-phenylpyrazolo[1,5-c]pyrimidine-4-carbonitrile system, derived from molecular complications of the amino-3,5-dicyanopyridine core, were reported. Biological results on a small set of compounds (**70**-**73**, Table 14), that bind with good affinity the hA_1 AR, indicated that this scaffold suitably decorated could generate new AR ligands. No functional data are currently available, thus preventing any conclusion about the influence of this structural modification on the pharmacological profile of the new compounds. Introduction of suitable substituents on the bicyclic ring in order to modulate affinity and selectivity at the AR subtypes is on going.

9. Experimental section

The microwave-assisted syntheses were performed using an Initiator EXP Microwave Biotage instrument (frequency of irradiation: 2.45 GHz). Silica gel plates (Merck silica gel 60 F254, 250 µm) were used for analytical chromatography; while, preparative silica gel plates (Merck silica gel 60 F254, 2 mm) and silica gel 60 (Merck, 70-230 mesh) were employed for preparative thin layer (TLC) and column chromatography. All melting points were determined on a Gallenkamp melting point apparatus. All final compounds revealed a purity not less than 95%. The IR spectra were recorded with a Perkin-Elmer Spectrum RX I spectrometer or Shimadzu IR-prestige 21 in Nujol mulls and are expressed in cm^{-1}. The ^{1}H NMR spectra were obtained with a Bruker Avance 400 MHz instrument. The chemical shifts are reported in δ (ppm) and are relative to the central peak of the solvent. The following abbreviations are used: s = singlet, d = doublet, t = triplet, m = multiplet, br = broad, and Ar = aromatic protons. The following abbreviation are used for solvents and reactive products: ACN = Acetonitrile, DMF = Dimethylformamide, TEA = Triethylamine, NMP = N-Methyl-2-pyrrolidone, EtOAc = Ethyl acetate, $CHCl_3$ = Chloroform, DCM = Dichloromethane, Et_2O = Diethyl ether, EtOH = Ethanol, HCl = Hydrochloric acid, MeOH = Methanol, D_2O = Deuterium oxide, AcOH = Acetic acid, Py = Pyridine, DIPEA = NN-Diisopropylethylamine, DMSO = Dimethyl sulfoxide, $CDCl_3$ = Deuterated chloroform, THF = Tetrahydrofuran, rt = room temperature, eq = equatorial protons, ax = axial protons, exc D_2O = protons exchanging with deuterium oxide.

General procedure for the synthesis of 74-77, 88-94, 112-117 and 140

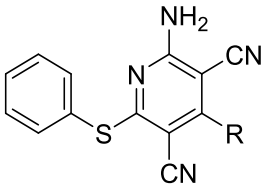

Compound	R	Compound	R
74	2-furyl	**93**	4-CH_3-(C_6H_4)
75	3-furyl	**94**	4-SCH_3-(C_6H_4)
76	2-thienyl	**112**	4-($OCH_2C_3H_5$)-(C_6H_4)
77	3-pyridyl	**113**	4-($OCH_2C_4H_7$)-(C_6H_4)
88	3-thienyl	**114**	4-($OCH_2CH(CH_3)_2$)-(C_6H_4)
89	4-pyridyl	**115**	4-(OCH_2CH_3)-(C_6H_4)
90	$CH_2C_6H_5$	**116**	4-($OCH_2CH=CH_2$)-(C_6H_4)
91	4-Cl-(C_6H_4)	**117**	4-($OCH_2C(CH_3)=CH_2$)- (C_6H_4)
92	4-F-(C_6H_4)	**140**	4-OH-(C_6H_4)

Procedures

Method A: To a stirred solution of the suitable aldehyde (10.00 mmol), 1,8-diazabicycloundec-7-ene (5% mol) and malononitrile (20.00 mmol) in 10% $EtOH_{aq}$ (20ml), thiophenol (10.00 mmol) was added after 20 min. Thus, the reaction mixture was stirred at 55°C for 3 to 18 h. The suspension was then cooled at rt and a solid precipitated which was collected by filtration, washed with Et_2O (5-10 ml) and then dried in oven at 60°C overnight.

Method B: To a solution in water (50 ml) of the suitable aldehyde (10.00 mmol) and malononitrile (20.00 mmol), tetrabutylammonium fluoride (10% mol) is added. After 20 minutes, thiophenol (10.00 mmol) is added and the mixture is allowed to stir at 80°C for 2 hours. After completing of the reaction the mixture is allowed to cool at rt and the water is removed. The residue obtained is dissolved in AcOEt and dried over anhydrous sodium sulfate. The solution is then filtered, the solvent removed under vacuum and the residue obtained is triturated with a mixture Et_2O : EtOH (10:1) and filtered in order to obtain the pure product.

Method C: A suspension of Al_2O_3 (10% p/v) in water (2 ml) was added to a solution of the suitable aldehyde (10.00 mmol) and malononitrile (20.00 mmol) in water (18 ml), and the mixture was allowed to stir at rt for 10 min. After addition of thiophenol (10.00 mmol) the suspension was heated at reflux for 6 h and then cooled at rt. The water was removed under reduced pressure and the residue was triturated with a mixture of Et_2O/EtOH (5:1). The solid obtained was filtered and extracted with hot EtOAc (4 x 100 ml). The dried organic phases (Na_2SO_4) were evaporated in order to obtain the pure compound.

Examples:

2-Amino-4-(furan-2-yl)-6-(phenylthio)pyridine-3,5-dicarbonitrile (74)

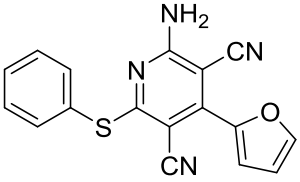

Method B; Yield: 18%; mp: 191-193°C (lit. 178-180°C) (MeOH); ^{1}H NMR (400 MHz, DMSO-d_6): 8.13 (s, 1H, Fur), 7.79 (br s, 2H, NH_2, exc. D_2O), 7.60 (d, 2H, Ar), 7.50 (m, 3H, Ar+Fur), 7.43 (t, 1H, Ar), 6.86 (s, 1H, Fur). IR (cm^{-1}): 3303, 3212, 2215.

2-Amino-4-(furan-3-yl)-6-(phenylthio)pyridine-3,5-dicarbonitrile (75)

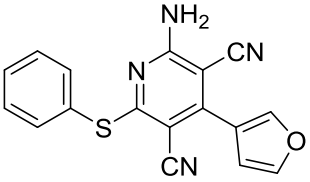

Method B; Yield: 22%; mp: 204-206°C (MeOH); ^{1}H NMR (400 MHz, DMSO-d_6): 8.22-8.29 (m, 1H, Fur), 7.93-7.94 (m, 1H, Fur), 7.81 (br s, 2H, NH2, exc D2O), 7.59- 7.60 (m, 2H, Ar), 7.50-7.51 (m, 3H, Ar), 6.90-6.91 (m, 1H, Fur). IR (cm-1): 3328, 3218, 2220.

2-Amino-6-(phenylthio)-4-(thiophen-2-yl)pyridine-3,5-dicarbonitrile (76)

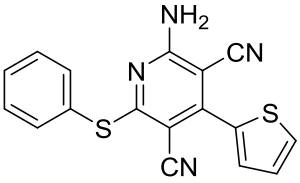

Method B; Yield: 32%; mp: 216-217°C (lit. 208-210°C) (MeOH); ^{1}H NMR (400 MHz, DMSO-d_6): 7.97 (d, 1H, Th, J = 4 Hz), 7.86 (br s, 2H, NH2, exc D2O), 7.58- 7.61 (m, 3H, Ar + Th), 7.50-7.51 (m, 3H, Ar), 7.30 (dd, 1H, Th, J1= 3.7 Hz, J2 = 4.8 Hz); IR (cm-1): 3352, 3216, 2210.

2'-Amino-6'-(phenylthio)-[3,4'-bipyridine]-3',5'-dicarbonitrile (77)

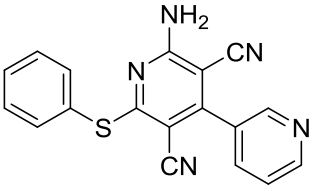

Method C; Yield: 31%; mp: >300°C (EtOH/DMF); ^{1}H NMR (400 MHz, DMSO-d_6): 8.77 (m, 1H, Py), 8.05 (d, 1H Py, J= 8.08 Hz), 7.85 (br s, 2H, NH_2, exc D_2O), 7.60-7.65 (m, 4H, Ar +1H Py), 7.50-7.52 (m, 3H, 2H Ar + 1H Py), IR (cm^{-1}): 3374, 3307, 2212, 2221.

2-Amino-6-(phenylthio)-4-(thiophen-3-yl)pyridine-3,5-dicarbonitrile (88)

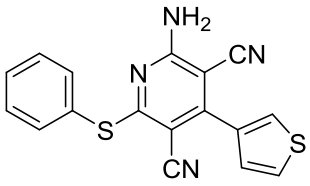

Method B; Yield: 14%; mp: 236-238°C (lit. 235-236°C) (MeOH); ^{1}H NMR (400 MHz, DMSO-d_6): 8.06-8.07 (m, 1H, Th), 7.78-7.80 (m, 3H, NH_2 + Th, 2H exc D_2O), 7.59- 7.61 (m, 2H, Ar), 7.49-7.51 (m, 3H, Ar), 7.40 (d, 1H, Th, J= 4.9 Hz), IR (cm^{-1}): 3333, 3217, 2210.

2-Amino-6-(phenylthio)-[4,4'-bipyridine]-3,5-dicarbonitrile (89)

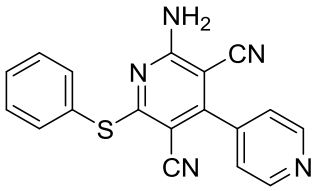

Method C; Yield: 32%; mp: 204-206°C (lit. 208-209°C) (EtOH); ^{1}H NMR (400 MHz, DMSO-d_6): 8.26 (m, 1H, Fur), 7.93 (m, 1H, Fur), 7.81 (br s, 2H, NH_2, exc D_2O), 7.60 (m, 2H, Ar), 6.91 (m, 1H, Fur), 7.51 (m, 3H, Ar); IR (cm^{-1}): 3328, 3218, 2220.

2-Amino-4-benzyl-6-(phenylthio)pyridine-3,5-dicarbonitrile (90)

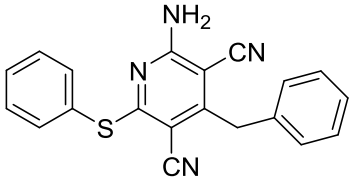

Method C; Yield: 35%; mp: 247-249°C (MeOH); ^{1}H NMR (400 MHz, DMSO-d_6): 7.81 (br s, 2H, NH_2 exc D_2O), 7.58 (m, 2H, Ar), 7.5 (m, 3H, Ar), 7.37 (m, 2H, Ar), 7.28 (m, 3H, Ar), 4.12 (s, 2H, CH_2); IR (cm^{-1}): 3329, 3225, 2198.

2-Amino-4-(4-chlorophenyl)-6-(phenylthio)pyridine-3,5-dicarbonitrile (91) (354)

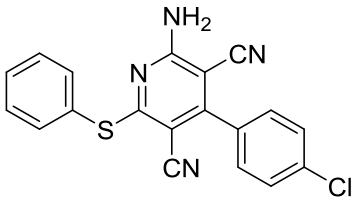

Method C; Yield: 37%; mp: 236-237°C (EtOH); ^{1}H NMR (400 MHz, DMSO-d_6): 7.75 (br s, 2H, NH_2, exc D_2O), 7.49-7.65 (m, 6H, Ar), 7.40-7.44 (m, 3H, Ar)

2-Amino-4-(4-fluorophenyl)-6-(phenylthio)pyridine-3,5-dicarbonitrile (92) (355)

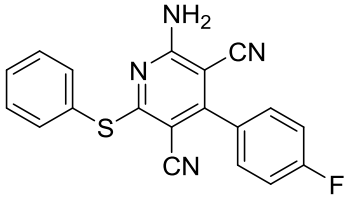

Method C; Yield: 36%; mp: 220-222°C (lit. 221-223°C); ^{1}H NMR (400 MHz, DMSO-d_6): 7.85 (s, 2H, NH_2, exc D_2O), 7.63 (m, 4H, Ar), 7.54 – 7.48 (m, 3H, Ar), 7.44 (t, *J* = 8.8 Hz, 2H, Ar)

2-Amino-6-(phenylthio)-4-(p-tolyl)pyridine-3,5-dicarbonitrile (93) (355)

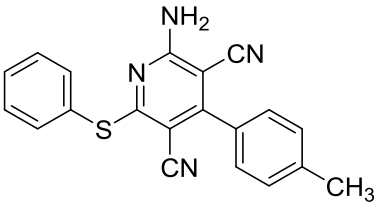

Method C; Yield: 32%; mp: 220-221°C (lit. 208-211°C); ^{1}H NMR (400 MHz, DMSO-d_6): 7.87 (br s, 2H, NH_2, exc D_2O), 7.55-7.65 (m, 3H, Ar), 7.37-7.48 (m, 6H, Ar), 2.41 (s, 3H, CH3)

2-Amino-4-(4-(methylthio)phenyl)-6-(phenylthio)pyridine-3,5-dicarbonitrile (94) (354)

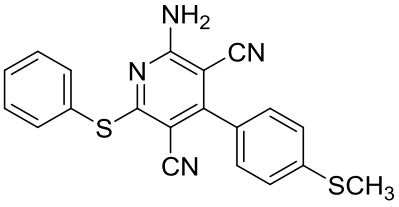

Method C; Yield: 28%; mp: 244-246°C (lit.254-256°C); ^{1}H NMR (400 MHz, DMSO-d_6): 7.81 (br s, 2H, NH_2, exc D_2O), 7.64 – 7.57 (m, 2H, Ar), 7.50 (m, 5H, Ar), 7.43 (m, 2H, Ar), 2.56 (s, 2H)

2-Amino-4-(4-(cyclopropylmethoxy)phenyl)-6-(phenylthio)pyridine-3,5-dicarbonitrile (112)

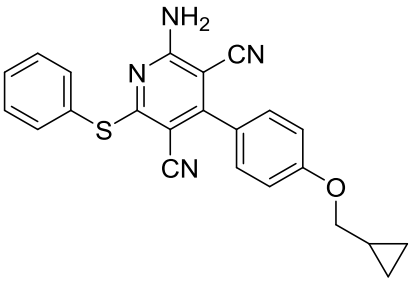

Method A and C; Yield: 33%; mp: 261-263°C (EtOH); ^{1}H NMR (400 MHz, DMSO-d_6): 7.70 (br s, 2H, NH_2 exc D_2O), 7.60-7.62 (m, 2H, Ar), 7.48-7.51 (m, 5H, Ar), 7.10 (d, 2H, Ar, J = 8.1 Hz), 3.92 (d, 2H, CH_2, J = 7.8 Hz), 1.25-1.28 (m, 1H, CH), 0.58-0.62 (m, 2H, 2CH *eq*), 0.36-0.38 (m, 2H, 2CH *ax*); IR (cm^{-1}): 3330, 3220, 2224

2-Amino-4-(4-(cyclobutylmethoxy)phenyl)-6-(phenylthio)pyridine-3,5-dicarbonitrile (113)

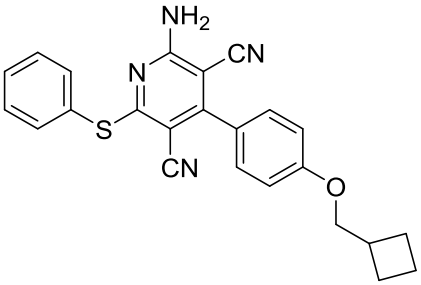

Method A; Yield: 18%; mp: 180-182°C (MeOH); ^{1}H NMR (400 MHz, DMSO-d_6): 7.76 (br s, 2H, NH_2 exc D_2O), 7.61-7.60 (m, 2H, Ar), 7.51-7.49 (m, 3H, Ar), 7.12 (d, 2H, Ar, J = 8.60 Hz), 4.05 (d, 2H, OCH_2, J = 6.5 Hz), 2.77-2.75 (m, 1H, CH), 2.11-2.09 (m, 2H, CH_2), 1.93-1.89 (m, 4H, $2CH_2$); IR (cm^{-1}): 3348, 3280, 2216

2-Amino-4-(4-isobutoxyphenyl)-6-(phenylthio)pyridine-3,5-dicarbonitrile (114)

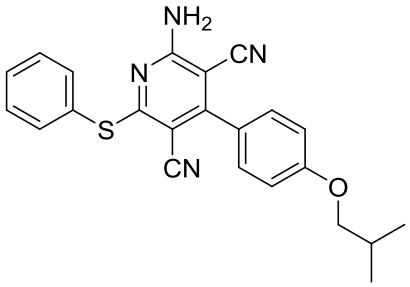

Method A; Yield: 26%; mp: 180-182°C (MeOH); ^{1}H NMR (400 MHz, DMSO-d_6): 7.74 (s, 2H, NH_2, exc D_2O), 7.61-7.59 (m, 2H, Ar), 7.50-7.49 (m, 5H, Ar), 7.11 (d, 2H, Ar, J= 8.76 Hz), 3.84 (d, 2H, OCH_2, J= 6.4 Hz), 2.09-2.02 (m, 1H, CH), 1.02 (s, 3H, CH_3,), 1.00 (s, 3H, CH_3,); IR (cm^{-1}): 3302, 3232, 2214

2-Amino-4-(4-ethoxyphenyl)-6-(phenylthio)pyridine-3,5-dicarbonitrile (115)

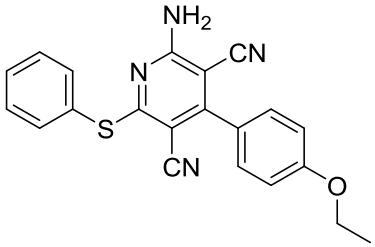

Method A; Yield: 37%; mp: 252-254°C (2-propanol); ^{1}H NMR (400 MHz, DMSO-d_6): 7.6 (s, 2H, NH_2, exc D_2O), 7.62-7.60 (m, 2H, Ar), 7.58-7.48 (m, 5H, Ar), 7.11 (d, 2H, Ar, J= 8.8 Hz), 4.13 (q, 2H, OCH_2, J= 6.8 Hz), 1.37 (t, 3H, CH_3, J= 7.2 Hz); IR (cm^{-1}): 3344, 3215, 2216

4-(4-(Allyloxy)phenyl)-2-amino-6-(phenylthio)pyridine-3,5-dicarbonitrile (116)

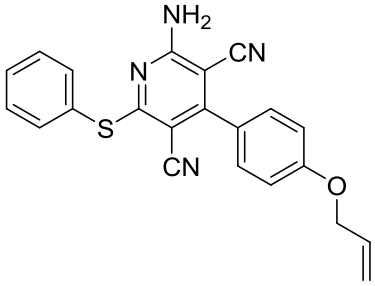

Method A; Yield: 28%; mp: 234-236°C (EtOAc/CHx); ^{1}H NMR (400 MHz, DMSO-d_6): 7.77 (s, 2H, NH_2, exc D_2O), 7.61-7.60 (m, 2H, Ar), 7,59-7.58 (m, 3H, Ar), 7.51 (d, 2H, Ar, J= 8.8 Hz), 7.14 (d, 2H, Ar, J= 8.8), 6.13-6.03 (m, 1H, CH), 5.45 (d, 1H, CH_{allyl}), 5.30 (d, 1H, CH_{allyl}), 4.67 (d, 2H, OCH_2, J= 5.6 Hz); IR (cm^{-1}): 3358, 3215, 2214, 1624

2-Amino-4-(4-((2-methylallyl)oxy)phenyl)-6-(phenylthio)pyridine-3,5-dicarbonitrile (117)

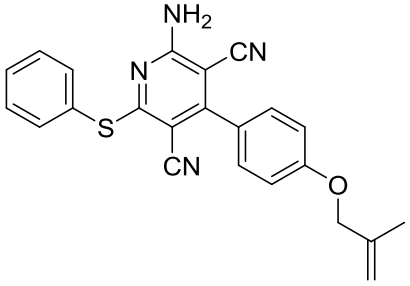

Method A; Yield: 25%; mp: 198-200°C (EtOH); ^{1}H NMR (400 MHz, DMSO-d_6): 7.76 (s, 2H, NH_2, exc D_2O), 7.60-7.61 (m, 2H, Ar), 7.60-7.59 (m, 3H, Ar), 7.55 (d, 2H, Ar, J= 8.4 Hz), 7.14 (d, 2H, Ar, J= 8.4 Hz), 5.11 (d, 1H, CH), 5.00 (d, 1H, CH), 4.58 (s, 2H, CH_2), 1.81 (s, 3H, CH_3); IR (cm^{-1}): 3481, 3369, 2212

2-Amino-4-(4-hydroxyphenyl)-6-(phenylthio)pyridine-3,5-dicarbonitrile (140) (297)

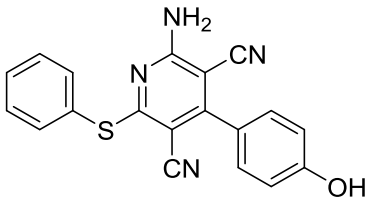

Method A; Yield: 29%; mp: > 300°C (MeOH); ^{1}H NMR (400 MHz, DMSO-d_6): 10.08 (br s, 1H, OH, exc D_2O), 7.72 (br s, 2H, NH_2, exc D_2O), 7.60-7.41 (m, 5H, Ar), 7.40 (d, 2H, Ar, J= 8.4 Hz), 6.92 (d, 2H, Ar, J= 8.4 Hz); IR (cm^{-1}): 3491, 3368, 2216

Synthesis of N-(4-(2,2-dicyanovinyl)phenyl)acetamide (138) (356)

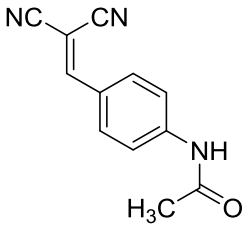

Malononitrile (17.3 mmol) and piperidine (2 gtt) were added to a solution of 4-acetamidobenzaldehyde (17.3 mmol) in EtOH (20 ml). The mixture was heated at 80°C for 2h until reaction completion, then cooled to rt affording an orange solid which was filtered and washed with Et_2O (5 ml) and petroleum ether (2 ml). Yield: 63%; mp: 234-236°C (EtOH); ^{1}H NMR (400 MHz, DMSO-d_6): 10.51 (s, 1H, NH, exc D_2O), 8.37 (s, 1H, CH), 7.94 (d, 2H, Ar, J= 8.4 Hz), 7.80 (d, 2H, Ar, J= 8.8 Hz), 2.11 (s, 3H, CH_3); IR (cm^{-1}): 2224; 1693

Synthesis of N-(4-(2-amino-3,5-dicyano-6-(phenylthio)pyridin-4-yl)phenyl)acetamide (137) (356)

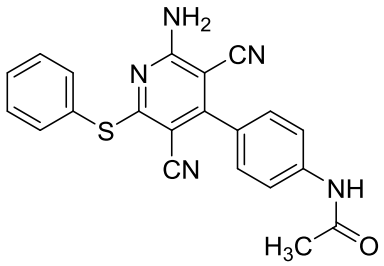

A solution of compound **138** (5.4 mmol), malononitrile (5.4 mmol), thiophenol (5.4 mmol) and TEA (0.54 mmol) in EtOH (30 ml) was heated at 100°C for 2h. Then, cooling at rt afforded a yellow solid which was filtered and washed with Et_2O (5 ml). Yield: 44%; mp: >300°C (EtOH); ^{1}H NMR (400 MHz, DMSO-d_6): 10.24 (s, 1H, NH, exc D_2O), 7.76 (s, 2H, NH_2, exc D_2O), 7.74 (m, 2H, Ar), 7.61-7.60 (m, 5H, Ar,), 7.50 (d, 2H, Ar, J= 8 Hz), 2.10 (s, 3H, CH_3); IR (cm^{-1}): 3481; 3344; 3298; 2212; 1681

General procedure for the synthesis of 78-81, 95-101, 118-123, 139 and 141

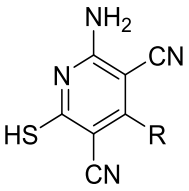

Compound	R	Compound	R
78	2-furyl	**101**	4-SCH_3-(C_6H_4)
79	3-furyl	**118**	4-($OCH_2C_3H_5$)-(C_6H_4)
80	2-thienyl	**119**	4-($OCH_2C_4H_7$)-(C_6H_4)
81	3-pyridyl	**120**	4-($OCH_2CH(CH_3)_2$)-(C_6H_4)
95	3-thienyl	**121**	4-(OCH_2CH_3)-(C_6H_4)
96	4-pyridyl	**122**	4-($OCH_2CH=CH_2$)-(C_6H_4)
97	$CH_2C_6H_5$	**123**	4-($OCH_2C(CH_3)=CH_2$)- (C_6H_4)
98	4-Cl-(C_6H_4)	**139**	4-$NHCOCH_3$
99	4-F-(C_6H_4)	**141**	4-OH-(C_6H_4)
100	4-CH_3-(C_6H_4)		

Procedure:

To a stirred solution of compounds **74-77, 88-94, 112-117, 137** and **140** (10 mmol) in dry DMF (1 ml) maintained at rt and under nitrogen atmosphere, an excess of sodium sulfite (33 mmol) was added. The reaction mixture was then heated at 80°C for 2 h. When the reaction was completed, 1N HCl (25 ml) was added followed by addition of 6N HCl to obtain a huge precipitate which is filtered and washed with water (20 ml) and Et_2O (5 ml).

Examples

2-Amino-4-(furan-2-yl)-6-mercaptopyridine-3,5-dicarbonitrile (78) (357)

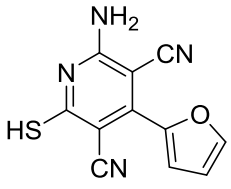

Yield: 96%; mp: 260-261°C (EtOH); ^{1}H NMR (400 MHz, DMSO-d_6): 12.94 (br s, 1H, SH, exc D_2O), 8.12 (d, 1H, Fur, J= 1.4 Hz), 7.85 (br s, 2H, NH_2, exc D_2O), 7.43 (d, 1H, J= 3.6 Hz, Fur), 6.84 (dd, *J* = 3.6, 1.7 Hz, 1H, Fur); IR (cm^{-1}): 3306, 3196, 2214.

2-Amino-4-(furan-3-yl)-6-mercaptopyridine-3,5-dicarbonitrile (79)

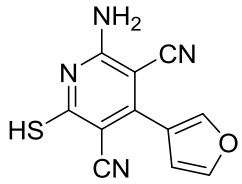

Yield: 92%; mp: 260-262°C (EtOH); ^{1}H NMR (400 MHz, DMSO-d_6): 12.97 (br s, 1H, SH, exc D_2O), 8.25-8.27 (m, 1H, Fur), 8.00 (br s, 2H, NH_2, exc D_2O), 7.90 (t, J= 1.6 Hz, 1H, Fur), 6.84- 6.85 (m, 1H, Fur); IR (cm^{-1}): 3307, 3192, 2216.

2-Amino-6-mercapto-4-(thiophen-2-yl)pyridine-3,5-dicarbonitrile (80) (358)

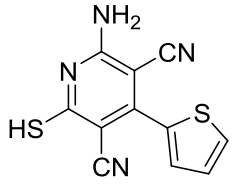

Yield: 90%; mp: 270-272°C (EtOH); ^{1}H NMR (400 MHz, DMSO-d_6): 13.01 (br s, 1H, SH, exc D_2O), 7.80 (br s, 2H, NH_2, exc D_2O), 7.95 (d, J= 5 Hz, 1H, CH *thiophene)*, 7.55 (d, J= 3.6 Hz, 1H, CH *thiophene*), 7.26 (t, J= 4.2 Hz, 1H, CH *thiophene*); IR (cm^{-1}): 3317, 3206, 2216.

2'-Amino-6'-mercapto-[3,4'-bipyridine]-3',5'-dicarbonitrile (81) (359)

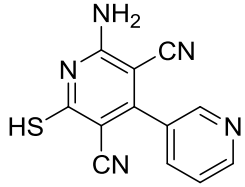

Yield: 86%; mp: >300°C (EtOH/DMF); ^{1}H NMR (400 MHz, DMSO-d_6): 13.20 (br s, 1H, SH, exc D_2O), 8.76-8.79 (m, 2H, Py), 8.27 (br s, 2H, NH_2, exc D_2O), 8.06 (d, J= 7.84 Hz, 1H, Py), 7.66 (t, J = 6.60 Hz, 1H, Py); IR (cm^{-1}): 3319, 3124, 2212.

2-Amino-6-mercapto-4-(thiophen-3-yl)pyridine-3,5-dicarbonitrile (95)

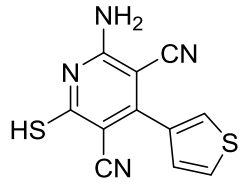

Yield: 89%; mp: 237-239°C (EtOH); ^{1}H NMR (400 MHz, DMSO-d_6): 12.98 (br s, 1H, SH, exc D_2O), 8.03-8.04 (m, 1H, CH *thiophene*), 7.85 (br s, 2H, NH_2, exc D_2O), 7.74-7.76 (m, 1H, CH *thiophene*), 7.34-7.36 (m, 1H, CH *thiophene*); IR (cm^{-1}): 3315, 3204, 2208.

2-Amino-6-mercapto-[4,4'-bipyridine]-3,5-dicarbonitrile (96)

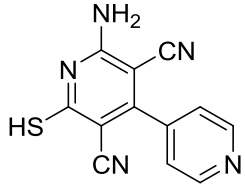

Yield: 89%; mp: >300°C (MeOH); ^{1}H NMR (400 MHz, DMSO-d_6): 13.2 (br s, 1H, SH, exc D_2O), 8.8 (d, J = 1,2 Hz, 2H, Py), 7.56 (d, J = 1,2 Hz, 2H, Py); IR (cm^{-1}): 3310, 3193, 2225.

2-Amino-4-benzyl-6-mercaptopyridine-3,5-dicarbonitrile (97)

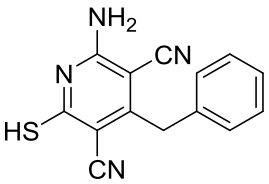

Yield: 80%; mp: 231-233°C (EtOH); ^{1}H NMR (400 MHz, DMSO-d_6): 12.96 (br s, 1H, SH exc D_2O), 7.82 (br s, 2H, NH_2 exc D_2O), 7.36 (m, 2H, Ar), 7.28 (m, 3H, Ar), 4.02 (s, 2H, CH_2); IR (cm^{-1}): 3319, 3280, 2229.

2-Amino-4-(4-chlorophenyl)-6-mercaptopyridine-3,5-dicarbonitrile (98) (354)

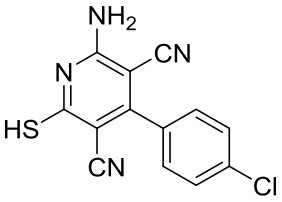

Yield: 80%; mp: 202-204°C (MeOH); ^{1}H NMR (400 MHz, DMSO-d_6): 13.12 (br s, 1H, SH, exc D_2O), 8.01 (br s, 2H, NH_2, exc D_2O), 7.65 (d, J = 8 Hz, 2H, Ar), 7.58 (d, J = 8 Hz, 2H, Ar), IR (cm^{-1}): 3320, 3192, 2220.

2-Amino-4-(4-fluorophenyl)-6-mercaptopyridine-3,5-dicarbonitrile (99) (355)

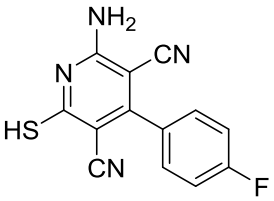

Yield: 86%; mp: 234-236°C (MeOH); ^{1}H NMR (400 MHz, DMSO-d_6): 13.03 (br s, 1H, SH, exc D_2O), 8.01 (br s, 2H, NH_2, exc D_2O), 7.6 (m, 2H, Ar), 7.38 (m, 2H, Ar); IR (cm^{-1}): 3319, 3182, 2224

2-Amino-6-mercapto-4-(p-tolyl)pyridine-3,5-dicarbonitrile (100) (355)

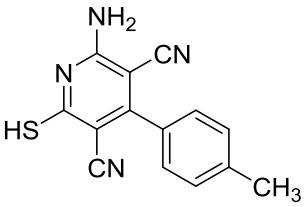

Yield: 83%; mp: 228-230°C (EtOH); ^{1}H NMR (400 MHz, DMSO-d_6): 13.03 (br s, 1H, SH, exc D_2O), 7.97 (br s, 2H, NH_2, exc D_2O), 7.39 (q, 4H, Ar, J = 8.2 Hz), 2.40 (s, 3H, CH_3); IR (cm^{-1}): 3322, 3190, 2215

2-Amino-6-mercapto-4-(4-(methylthio)phenyl)pyridine-3,5-dicarbonitrile (101) (354)

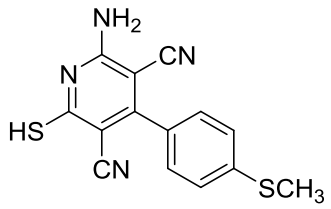

Yield: 82%; mp: 188-190°C (EtOH); ^{1}H NMR (400 MHz, DMSO-d_6): 13.1 (br s, 1H, SH, exc D_2O), 7.45 (d, 2H, Ar, J = 8 Hz), 7.4 (d, 2H, Ar J = 8 Hz), 2.51 (s, 3H, CH_3); IR (cm^{-1}): 3311, 3195, 2222

2-Amino-4-(4-(cyclopropylmethoxy)phenyl)-6-mercaptopyridine-3,5-dicarbonitrile (118) (293)

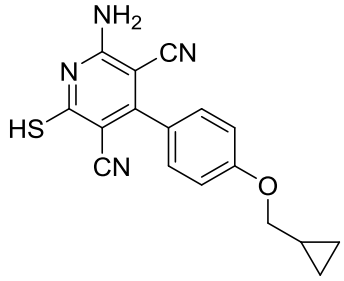

Yield: 80%; mp: 168-170°C (EtOAc); ^{1}H NMR (400 MHz, DMSO-d_6): 12.9 (br s, 1H, SH, exc D_2O), 7.8 (br s, 2H, NH_2, exc D_2O), 7.45 (d, 2H, Ar, J = 8 Hz), 7.08 (d, 2H, Ar, J = 8 Hz), 3.91 (d, 2H, CH_2, J = 7.8 Hz), 1.23-1.27 (m, 1H, CH), 0.57-0.62 (m, 2H, 2CH *eq*), 0.33-0.37 (m, 2H, 2CH *ax*); IR (cm^{-1}): 3309, 3190, 2219

2-Amino-4-(4-(cyclobutylmethoxy)phenyl)-6-mercaptopyridine-3,5-dicarbonitrile (119)

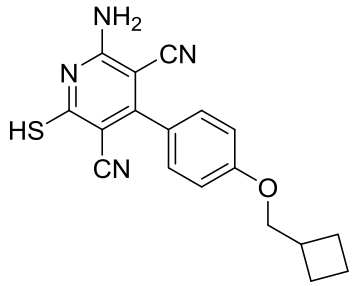

Yield: 84%; mp: 256-259°C (EtOH); ^{1}H NMR (400 MHz, DMSO-d_6): 12.95 (s, 1H, SH, exc D_2O), 7.08 (s, 2H, NH_2, exc D_2O), 7.46 (d, 2H, Ar, J= 8 Hz), 7.09 (d, 2H, Ar, J= 8.4 Hz), 4.04 (d, 2H, OCH_2, J= 6 Hz), 2.87-2.73 (m, 1H, CH), 2.10-1.92 (m, 2H, CH_2), 1.9-1.89 (m, 4H, $2CH_2$); IR (cm^{-1}): 3474, 3335, 2214

2-Amino-4-(4-isobutoxyphenyl)-6-mercaptopyridine-3,5-dicarbonitrile (120)

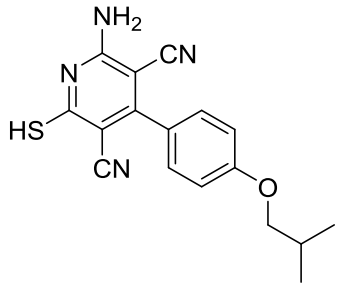

Yield: 86%; ^{1}H NMR (400 MHz, DMSO-d_6): 13.02 (s, 1H, SH, exc D_2O), 7.77 (s, 2H, NH_2, exc D_2O), 7.45 (d, 2H, Ar, J= 8.8 Hz), 7.09 (d, 2H, Ar, J= 8.4 Hz), 3.83 (d, 2H, CH_2, J= 6.4 Hz), 2.06-2.03 (m, 1H, CH), 1.02 (s, 3H, CH_3,), 0.99 (s, 3H, CH_3,)

2-Amino-4-(4-ethoxyphenyl)-6-mercaptopyridine-3,5-dicarbonitrile (121)

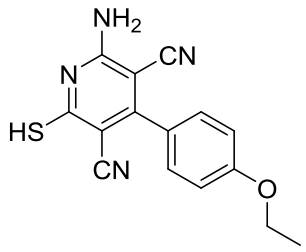

Yield: 76%; mp: 290-292°C (EtOH); ^{1}H NMR (400 MHz, DMSO-d_6): 12.99 (s, 1H, SH, exc D_2O), 8.11 (s, 2H, NH_2, exc D_2O), 7.54 (d, 2H, Ar, J= 8.8 Hz), 7.14 (d, 2H, Ar, J= 8.8 Hz), 4.14 (q, 2H, CH_2, J= 6.8 Hz), 1.38 (t, 3H, CH_3, J= 6.8 Hz); IR (cm^{-1}): 3336, 3117, 2212

4-(4-(Allyloxy)phenyl)-2-amino-6-mercaptopyridine-3,5-dicarbonitrile (122)

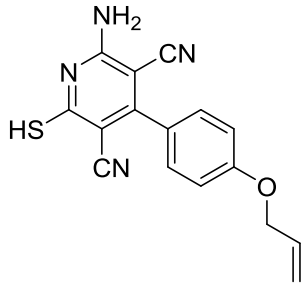

Yield: 84%; mp: 208-211°C (EtOAc); ^{1}H NMR (400 MHz, DMSO-d_6): 12.98 (s, 1H, SH, exc D_2O); 7.90 (s, 2H, NH_2, exc D_2O); 7.47 (d, 2H, Ar, J= 8.6 Hz); 7.12 (d, J= 8.6 Hz, 2H, Ar); 6.11-6.04 (m, 1H, CH *allyl*); 5.47-5.43 (dd, J_{gem}= 1.2 Hz, J_{trans}= 17.2 Hz, 1H, CH), 5.30 (d, J= 10.4 Hz, 1H, CH), 4.66 (d, J= 5.6 Hz, 2H, OCH_2); IR (cm^{-1}): 3476, 3319, 3209, 2212

2-Amino-6-mercapto-4-(4-((2-methylallyl)oxy)phenyl)pyridine-3,5-dicarbonitrile (123)

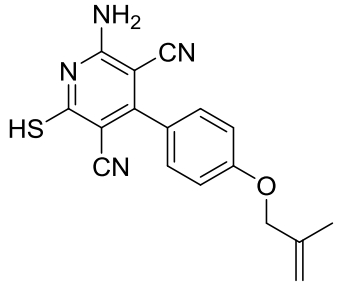

Yield: 72%; (EtOH); ^{1}H NMR (400 MHz, DMSO-d_6): 12.98 (s, 1H, SH, exc D_2O), 8.12-8.10 (s, l, 2H, NH_2, exc D_2O), 7.53 (d, 2H, Ar, J= 7.4 Hz), 7.08 (d, 2H, Ar, J= 8.8), 5.09 (s, 1H, CH), 4.90 (s, 1H, CH), 4.58 (s, 2H, OCH_2), 1.80 (s, 3H, CH_3)

N-(4-(2-amino-3,5-dicyano-6-mercaptopyridin-4-yl)phenyl)acetamide (139) (356)

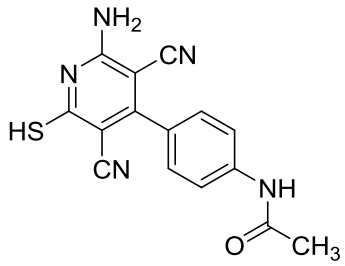

Yield: 40%; mp: 275-277°C (d)(EtOH/EtOAc); ^{1}H NMR (400 MHz, DMSO-d_6): 12.94 (s, 1H, SH, exc D_2O), 10.37 (s, 1H, NH, exc D_2O), 8.19 (s, 2H, NH_2, exc D_2O), 7.73 (d, 2H, Ar, J= 8.0 Hz), 7.44 (d, 2H, Ar, J= 8.0 Hz), 2.08 (s, 3H, CH_3); IR (cm^{-1}): 3317, 3215, 2214, 1539

2-Amino-4-(4-hydroxyphenyl)-6-mercaptopyridine-3,5-dicarbonitrile (141) (297)**:**

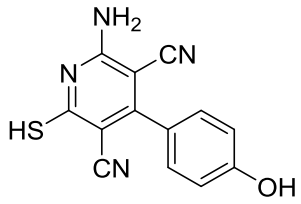

Yield: 69%; mp: >300°C (MeOH); ^{1}H NMR (400 MHz, DMSO-d_6): 12.94 (br s, 1H, SH, exc D_2O), 10.09 (br s, 1H, OH, exc D_2O), 7-96-7.89 (br s, NH_2, exc D_2O), 7.38 (d, 2H, Ar, J= 8.8 Hz), 6.90 (d, 2H, Ar, J= 8.4)

General procedure for the synthesis of p-alkyloxybenzaldehydes (106-111)

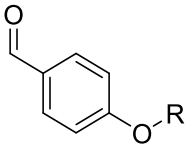

Procedures:

Method A: To a solution of 4-hydroxybenzaldehyde (12.3 mmol) in dried acetone (20 ml), potassium carbonate (18.5 mmol) was added, followed by the suitable alkyl halide (18.5 mmol). The mixture was heated at reflux until starting material disappears (6-48h) monitored by TLC. Then, the mixture was cooled to rt and the insoluble material was filtered and washed with acetone (3 x 20 ml). The resulting filtrates were collected and evaporated under vacuum, affording the desired compounds as viscous oils.

Method B: To a mixture of 4-hydroxybenzaldehyde (8.2 mmol), cyclopropyl methanol (9.02 mmol) and triphenylphosphine (10.66 mmol) in THF dry maintained at 0°C, diethyl azodicarboxylate (DEAD, 10.66 mmol) was carefully added within 10/15 min, keeping temperature under 0°C. The mixture was kept at 0°C for further 10 min, then warmed to rt and stirred for 24h. The reaction mixture was then evaporated carefully until affording a raw semisolid which was purified by silica gel flash chromatography using DCM 9 : MeOH 1 as eluent affording compounds as a viscous oil.

Method C: Potassium carbonate (18.5 mmol), the suitable alkyl halide (18.5 mmol) and potassium iodide (0.123 mmol) were sequentially added to a solution of 4-hydroxybenzaldehyde (12.3 mmol) in DMF dry (15 ml). The mixture was refluxed until reaction completion (TLC monitoring). The mixture was then cooled to rt and water (50 ml) was added. The resulting suspension was extracted with AcOEt (4 x 30 ml) and the organic phases were collected, dried (Na_2SO_4), and the solvent removed under vacuum, affording compounds as a viscous oil.

Examples

4-(Cyclopropylmethoxy)benzaldehyde (106) (360)

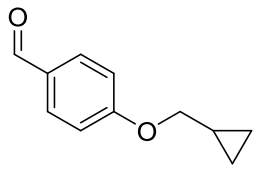

Method A and B; Yield: 77%; ^{1}H NMR (400 MHz, DMSO-d_6): 9.86 (s, 1H, CHO), 7.85 (d, 2H, Ar, J=8.1 Hz), 7.10 (d, 2H, Ar, J=7.7 Hz), 3.93 (d, 2H, CH_2, J=7.8 Hz), 1.22-1.28 (m, 1H, CH), 0.56-0.61 (m, 2H, 2CH *eq*), 0.33-0.36 (m, 2H, CH *ax*)

4-(Cyclobutylmethoxy)benzaldehyde (107) (361)

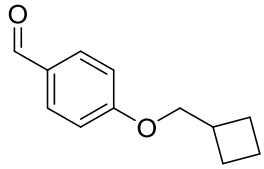

Method A; Yield: 67%; ^{1}H NMR (400 MHz, DMSO-d_6): 9.86 (s, 1H, CHO), 7.85 (d, 2H, Ar, J= 8.8 Hz), 7.11 (d, 2H, Ar, J= 8.4 Hz), 4.06 (d, 2H, OCH_2, J= 6.8 Hz), 2.77-2.71 (m, 1H, CH), 2.08-2.07 (m, 2H, CH_2), 1.90-1.82 (m, 4H, $2CH_2$)

4-Isobutoxybenzaldehyde (108) (362)

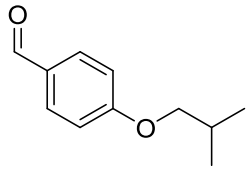

Method C; Yield: 66%; ^{1}H NMR (400 MHz, DMSO-d_6): 9.86 (s, 1H, CHO), 7.85 (d, 2H, Ar, J= 8.8 Hz), 7.10 (d, 2H, Ar, J=8.8 Hz), 3.84 (d, 2H, OCH_2, J= 6.4 Hz), 2.06-1.98 (m, 1H, CH), 1.00 (s, 3H, CH_3,), 0.96 (s, 3H, CH_3,)

4-Ethoxybenzaldehyde (109) (363)

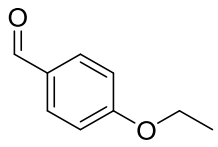

Method A; Yield: 83%; ^{1}H NMR (400 MHz, DMSO-d_6): 9.86 (s, 1H, CHO), 7.85 (d, 2H, Ar, J= 8.4 Hz), 7.10 (d, 2H, Ar, J=8.8 Hz), 4.13 (q, 2H, OCH_2, J= 6.8 Hz), 1.35 (t, 3H, CH_3, J= 7.2 Hz)

4-(Allyloxy)benzaldehyde (110) (364)

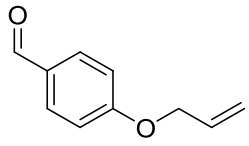

Method A; Yield: 97%; ^{1}H NMR (400 MHz, DMSO-d_6): 9.87 (s, 1H, CHO), 7.87 (d, 2H, Ar, J= 8.6 Hz), 7.15 (d, 2H, Ar, J= 8.7 Hz), 6.10-6.02 (m, 1H, CH_{allyl}), 5.45-5.40 (dd, 1H, CH_2, J_{gem}= 1.6 Hz, J_{cis}=18 Hz), 5.31-5.24 (dd, 1H, CH_2, J_{gem}= 10.4 Hz, J_{trans}= 22 Hz), 4.70 (d, 2H, OCH_2, J= 5.2 Hz)

4-((2-Methylallyl)oxy)benzaldehyde (111) (365)

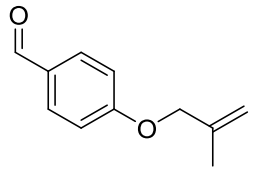

Method A; Yield: 85%; ^{1}H NMR (400 MHz, DMSO-d_6): 9.87 (s, 1H, CHO), 7.86 (d, 2H, Ar, J= 8.4 Hz), 7.13 (d, 2H, Ar, J= 8.4 Hz), 5.09 (d, 1H, CH, J= 0.8 Hz), 4.98 (d, 1H, CH, J= 1.2 Hz), 4.57 (s, 2H, CH_2), 1.77 (s, 3H, CH_3)

Synthesis of 2-(1-ethoxyethylidene)malononitrile (103) (366)

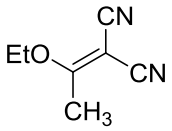

A suspension of malononitrile (0.45 mmol) and triethylorthoacetate (0.5 mmol) was refluxed for 2 h. At reaction completion, the liquid phase was removed by distillation at reduced pressure, affording a solid which was recovered with Et_2O (5 ml), filtered and recrystallized from EtOH. Yield: 82%; mp: 145-147°C (EtOH); ^{1}H NMR (400 MHz, DMSO-d_6): 4.41 (q, 2H, CH_2, *J* = 4 Hz), 2.42 (s, 3H, CH_3), 1.31 (t, 3H, CH_3, *J* = 4 Hz); IR (cm^{-1}): 2245, 2238.

Synthesis of 2-amino-6-mercapto-4-methylpyridine-3,5-dicarbonitrile (104) (367)

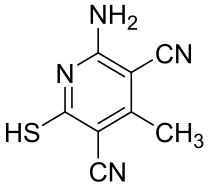

Thiocyanoacetamide (22.3 mmol) was portiowise added to a solution of compound **102** (23.00 mmol) and $NaOCH_3$ (24.79 mmol) in MeOH (25 ml). The reaction mixture was refluxed for 4 h, then, the solvent was removed under vacuum and the resulting yellow solid was recovered with Et_2O and filtered. Yield: 62%; mp: 226-228°C (EtOH); ^{1}H NMR (400 MHz, DMSO-d_6): 12.94 (br s, 1H, SH, exc D_2O), 7.10 (br s, 2H, NH_2, exc D_2O), 2.30 (s, 3H, CH_3); IR (cm^{-1}): 3338, 3253, 2248.

Synthesis of (1H-imidazol-2-yl)methanol (105) (297)

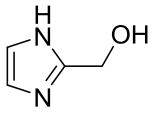

Imidazole-2-carboxyaldehyde (20.8 mmol) was added to a suspension of sodium borohydride (41.6 mmol) in absolute EtOH (30 ml) under nitrogen atmosphere which was then stirred at rt for 2h. After reaction completion, the excess of sodium borohydride was quenched with a 20% aqueous sodium hydroxide solution and the resulting suspension was filtered. The filtrate was extracted with EtOAc (5 x 15 ml) and the collected organic phases were dried (Na_2SO_4), and evaporated under reduced pressure to yield a white solid that was used for the next step without any further purification. Yield: 46%; ^{1}H NMR (400 MHz, DMSO-d_6): 11.89 (s, 1H, NH, exc D_2O), 6.90 (s, 2H, 2CH), (s, 1H, OH, exc D_2O), 4.44 (s, 2H, CH_2).

Synthesis of 2-(bromomethyl)-1H-imidazole hydrobromide (102) (297)

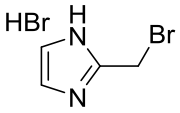

A solution of **104** (3.1 mmol) in 33% HBr in acetic acid (8 ml) was heated at 100°C for 4h. Then, the solvent was removed by distillation at reduced pressure and the red-brown residue was triturated with petroleum ether (10 ml), filtrate and quickly used for the next step without any further purification. Yield: 70%; ^{1}H NMR (400 MHz, DMSO-d_6): 14.00 (s, 1H, NH, exc D_2O), 7.71 (s, 2H, 2CH), 4.84 (s, 2H, CH_2).

Synthesis of 1H-pyrazole-3-carboxylic acid (125) (308)

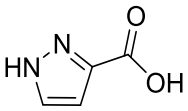

Potassium permanganate (128.7 mmol) was added in small portions to a solution of 3-methyl-1H-pyrazole (58.5 mmol) in water (225 ml), and the mixture was heated at reflux for 4 h. After cooling to rt, the suspension was filtered and the filtrate was concentrated under vacuum to small volume. 6M HCl (80 ml) was added and the mixture was kept cool for 1h to afford a white solid which was collected by filtration and dried at 60°C. Yield: 62%; mp: 193-195°C (Et_2O); ^{1}H NMR (400 MHz, DMSO-d_6): 13.01 (br s, 1H, COOH, exc D_2O), 7.72 (s, 1H, CH), 6.68 (s, 1H, CH).

Synthesis of ethyl 1H-pyrazole-3-carboxylate (126) (368)

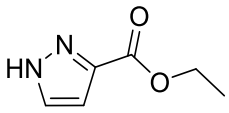

Thionyl chloride (20.6 mmol) was added to a solution of compound **125** (18.7 mmol) in absolute EtOH (20 ml). Then the mixture was refluxed until starting material disappeared (TLC monitoring). The excess of liquid reactant was removed under reduced pressure, and water (25 ml) was added affording a white solid which was collected by filtration and used for the next step without any further purification. Yield: 76%; ^{1}H NMR (400 MHz, DMSO-d_6): 13.48 (s, 1H, NH, exc D_2O), 7.81 (s, 1H, CH), 6.76 (s, 1H, CH), 4.27 (q, *J* = 7.1 Hz, 2H, CH_2), 1.29 (t, *J* = 7.1 Hz, 3H, CH_3).

Synthesis of (1H-pyrazol-3-yl)methanol (127) (308)

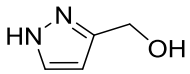

Lithium aluminum hydride (35.7 mmol) was portiowise added to a suspension of compound **126** (17.8 mmol) in anhydrous THF (40 ml), maintained in a ice bath keeping temperature under 5°C. The mixture was allowed to warm at rt, stirred for 2 h and then, while keeping in an ice bath, MeOH (1 ml) was carefully added, followed by a solution of aqueous MeOH (4:1). The resulting solid was filterd and the filtrate was extracted with EtOAc (3 x 25 ml). The collected organic phases were washed with brine (25 ml), dried (Na_2SO_4) and filtered. Evaporation of solvent afforded a yellow oil which was used without any further purification for the next step. Yield: 66%; ^{1}H NMR (400 MHz, DMSO-d_6): 12.58 (s, 1H, NH, exc D_2O), 7.51 (s, 1H, CH), 6.15 (s, 1H, CH), 5.07 (s, 1H, OH, exc D_2O), 4.44 (s, 7H, CH_2).

Synthesis of 3-(chloromethyl)-1H-pyrazole (124) (308)

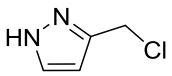

An excess of thionyl chloride (15.1 mmol) was added to a suspension of compound **127** (10.1 mmol) in anhydrous DCM (20 ml), and the mixture was refluxed for 3 h. Then, removal of liquid component under reduced pressure afforded a yellowish solid which is dried in desiccator at rt. Yield: 86%; ^{1}H NMR (400 MHz, DMSO-d_6): 7.66 (s, 1H, CH), 6.32 (s, 1H, CH), 4.72 (s, 2H, CH_2).

Synthesis of (1H-1,2,4-triazol-3-yl)methanol hydrochloride (129) (309)

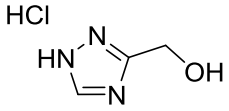

A solution of methyl 1H-1,2,4-triazole-3-carboxylate (7.87 mmol) in anhydrous THF (25 ml) was slowly added to a suspension of lithium aluminum hydride (19.76 mmol) in anhydrous THF (10 ml) and the mixture was refluxed for 12 h. At reaction completion MeOH (1 ml) was carefully added followed by 50 % aqueous MeOH (5 ml) affording a solid that was filtered and washed with MeOH (20 ml). The filtrate was then evaporated and the resulting residue was triturated with absolute EtOH (40 ml) and conc. HCl (1 ml). The mixture was concentrated under vacuum and the resulting semisolid was worked up with a mixture of MeOH and Et_2O (1:1, 10 ml), filtered and dried in desiccator at rt. Yield: 72%; mp: 138-140°C; ^{1}H NMR (400 MHz, DMSO-d_6): 13.85 (br s, 1H, NH, exc D_2O), 8.90 (s, 1H, CH), 5.69 (t, 1H, OH, exc D_2O), 4.70 (s, 2H, CH_2).

Synthesis of 3-(chloromethyl)-1H-1,2,4-triazole (128) (309)

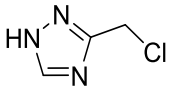

A solution of compound **129** (2.21 mmol) in thionyl chloride (10 ml) was refluxed for 6 h. Then, the excess of chlorinating agent was removed under vacuum affording a residue that was triturated with a mixture Et_2O/EtOH (5:1, 10 ml), filtered and washed with petroleum ether (5 ml). Yield: 40%; mp: 102-104°C; ^{1}H NMR (400 MHz, DMSO-d_6): 14.03 (br s, NH, exc D_2O), 8.54 (s, 1H, CH), 4.77 (s, 2H, CH_2).

Synthesis of 4-(chloromethyl)thiazol-2-amine (130) (310)

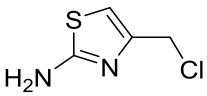

To a solution of 1,3-dichloroacetone (26.8 mmol) in anhydrous acetone (100 ml), thiourea (26.27 mmol) was added in small portions. The mixture was allowed to stir at rt for 12 h. The resulting white solid was filtered, washed with acetone (30 ml) and Et_2O (10 ml), suspended in EtOH (100 ml) and stirred for 3 h at rt. The solid was then removed by filtration and the filtrate was evaporated affording a white solid. Yield: 37%; mp: 117-119°C (Acetone); ^{1}H NMR (400 MHz, DMSO-d_6): 9.13 (br s, 2H, NH_2), 6.96 (s, 1H, CH), 4.67 (s, 2H, CH_2).

Synthesis of 4-(chloromethyl)-2-phenylthiazole (131) (369)

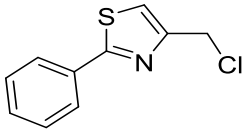

1,3-Dichloroacetone (18.22 mmol) was added to a solution of thiobenzamide (3.64 mmol) in dry acetone (45 ml) and the mixture was refluxed for 8 h. After cooling at rt, the white crystalline precipitated was filtered and washed with fresh acetone (10 ml). The solid obtained was then dissolved in sulfuric acid (1.2 ml) and the resulting solution was stirred for 30 min at rt. Then 20 ml of iced-water was carefully added affording white crystals, that were quickly filtered and stored at 4°C. Yield: 65%; mp: 53-55°C; ^{1}H NMR (400 MHz, $CDCl_3$): 8.05 – 7.89 (m, 2H, Ar), 7.55 – 7.39 (m, 3H, Ar), 7.33 (s, 1H, CH), 4.77 (s, 2H, CH_2).

Synthesis of 3-(chloromethyl)benzamide (132) (311)

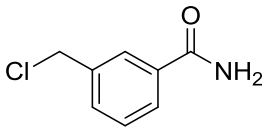

Oxalyl chloride (14.90 mmol) and dry DMF (2 gtt) were added to a solution of 3-(chloromethyl)benzoic acid (6.00 mmol) in anhydrous DCM (30 ml). The reaction mixture was allowed to stir at rt overnight. The solvent was removed under vacuum and the oily residue was immediately dissolved in a saturated ammonia solution in dioxane (100 ml). The reaction mixture was stirred at rt overnight and the resulting white crystals were collected by filtration and washed with Et_2O (2 ml). Yield: 60%; mp: 130-131°C (Et_2O); ^{1}H NMR (400 MHz, DMSO-d_6): 8.0 (br s, 1H, NH, exc D_2O), 7.95 (s, 1H, Ar), 7.83-7.85 (m, 1H, Ar), 7.58-7.60 (m, 1H, Ar), 7.45-749 (m, 1H, Ar), 7.41 (br s, 1H, NH, exc D_2O), 4.81 (s, 2H, CH_2); IR (cm^{-1}): 3350; 3182; 1651.

Synthesis of benzyl 2-chloroacetate (133) (370)

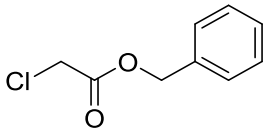

Benzylalcohol (46.24 mmol) and p-toluenesulfonic acid (0.63 mmol) were added to a solution of chloroacetic acid (55.35 mmol) in toluene (25 ml). After heating at 140°C for 2 h, the reaction mixture was cooled to rt and washed with a 5% sodium hydrogencarbonate (2 x 25 ml) and water (25 ml). The collected organic phases were dried (Na_2SO_4) and evaporated affording a yellowish oil that was used without any further purification

for the next step. Yield: 78%; ^{1}H NMR (400 MHz, $CDCl_3$): 7.59 – 7.30 (m, 5H, Ar), 5.25 (s, 2H, OCH_2), 4.12 (s, 2H, CH_2Cl)

Synthesis of 2-chloro-N-hydroxyacetamide (134) (371)

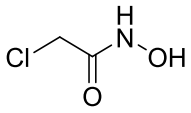

50 % Aqueous solution of hydroxylamine (12.00 mmol) was added to ethyl chloroacetate (12.00 mmol) in a 50 ml round bottomed flask and stirred for 5 minutes at rt. Then, the mixture was cooled at 4°C for 15 min, re-warmed to rt and stirred for 3 h. The precipitate was collected by filtration and used for the next step without any further purification. Yield: 53%; ^{1}H NMR (400 MHz, DMSO): 7.41 (br s, 2H, OH + NH, exc D_2O), 3.94 (s, 2H, CH_2).

Synthesis of ethyl 2-chloroacetimidate hydrochloride (136) (372)

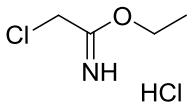

Anhydrous HCl was bubbled for 1 h at 0°C in a solution of chloroacetonitrile (66.22 mmol) in absolute EtOH (5 ml) and Et_2O anhydrous (30 ml), then the reaction mixture was allowed to stir at rt overnight under nitrogen atmosphere. Concentration of the solution under vacuum afforded white crystals that were collected by filtration and used for the following step without any further purification. Yield: 86%; ^{1}H NMR (400 MHz, DMSO): 12.4 (br s, 1H, NH, exc D_2O), 4.38 (s, 2H, CH_2), 4.17 (q, 2H, J = 7.1 Hz, CH_2), 1.22 (t, 3H, J = 7.1 Hz, CH_3).

Synthesis of 2-(chloromethyl)-4,5-dihydro-1H-imidazole (135) (373)

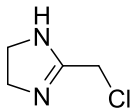

Ethyl 2-chloroacetimidate hydrochloride **136** (9.49 mmol) was added in small portions to a solution of ethylenediamine (14.24 mmol) in absolute EtOH (25 ml) maintained at 0°C. The mixture was stirred at 0°C for 1h, then a solution of anhydrous HCl (82.3 mmol) in absolute EtOH (25 ml) was carefully added in small portions, keeping temperature to 0°C. The mixture was stirred at 0°C for 1 h and then was warmed at rt and

stirred overnight. Concentration at small volume of the mixture afforded a white solid which was filtered and washed with EtOH (5 ml) and Et_2O (5 ml). Yield: 82%; ^{1}H NMR (400 MHz, DMSO): 10.90-10.59 (br s, 2H, NH_2^+, exc D_2O), 4.67 (s, 2H, CH_2), 3.89 (s, 4H, $2CH_2$).

General procedure for the synthesis of final compounds A, 1-16, 26-35, 37-67 and 142

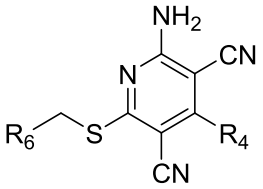

Sodium hydrogencarbonate (2.00 mmol) and the suitable alomethyl-derivative (1.00 mmol) were added to a solution of the mercapto compound **78-81, 95-101, 104, 118-123, 139** and **141** (1.00 mmol) in DMF dry (1 ml). The reaction mixture was stirred at rt until disappearance of the starting material (TLC monitoring). At reaction completion, water was added (25 ml) to precipitate a solid which was collected by filtration and triturated with Et_2O (5 ml). The crude product was then recrystallized or purified by column chromatography or preparative TLC using DCM 9 : MeOH 1, EtOAc 5 : CHx 5 : MeOH 1, CHx 7 : EtOAc 3 or EtOAc 1 : CHx 1 as eluents.

Examples

2-Amino-4-(furan-2-yl)-6-((2-hydroxyethyl)thio)pyridine-3,5-dicarbonitrile (A) (298)

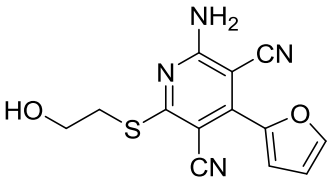

yield: 63%; mp: 171-173°C (EtOAc/CHx); ^{1}H NMR (400 MHz, DMSO-d_6): 8.11-8.12 (m, 1H, Fur), 7.99 (br s, 2H, NH_2, exc D_2O), 7.39 (d, 1H, Fur, J = 3.6 Hz), 6.83 (dd, 1H, Fur, J_1 = 1.72, J_2 = 3.6 Hz), 4.99 (t, 1H, OH, exc D_2O, J = 5.4 Hz), 3.65 (q, 2H, CH_2, J = 12 Hz), 3.33 (t, 2H, CH_2, J = 6.3 Hz); IR (cm^{-1}): 3320, 3219, 2212.

Methyl 3-(((6-amino-3,5-dicyano-4-(furan-2-yl)pyridin-2-yl)thio)methyl)benzoate (1)

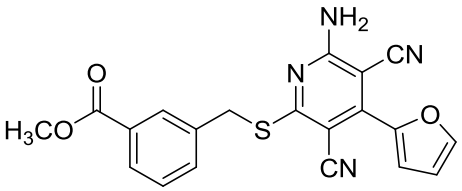

yield: 62%; mp: 208-210°C (MeOH/2-methoxyethanol); ^{1}H NMR (400 MHz, DMSO-d_6): 8.09-8.08 (m, 1H, Fur), 8.00 (sl, 2H, NH_2, exc D_2O), 7.83-7.85 (m, 3H, Ar), 7.47 (t, 1H, Ar, J = 7.72 Hz), 7.38 (d, 1H,

Fur, *J* = 3.64 Hz), 6.83 (dd, 1H, fur, J_1 = 1.72 Hz, J_2 = 3.64 Hz), 4.58 (s, 2H, CH_2), 3.86 (s, 3H, CH_3); IR (cm^{-1}): 2214, 1728.

3-(((6-Amino-3,5-dicyano-4-(furan-2-yl)pyridin-2-yl)thio)methyl)benzamide (2)

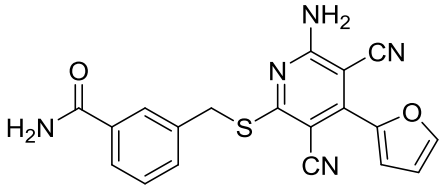

Yield: 43%; mp: 249-251°C (EtOH); ^{1}H NMR (400 MHz, DMSO-d_6): 8.10 (d, *J* = 1.1 Hz, 1H, Fur), 8.07 (br s, 2H, NH_2, exc D_2O) 7.98 (s, 1H, Ar), 7.96 (br s, 1H, NH *amide*, exc D_2O), 7.76 (d, *J* = 7.8 Hz, 1H, Ar), 7.68 (d, *J* = 7.7 Hz, 1H, Ar), 7.49 – 7.29 (m, 3H, Ar, NH *amide*, Fur, *overlapping*, partially exc D_2O), 6.83 (dd, *J* = 3.6, 1.8 Hz, 1H, Fur), 4.53 (s, 2H, CH_2). IR (cm^{-1}): 3424, 3360, 3331, 3213, 2210, 1643

3-(((6-Amino-3,5-dicyano-4-(furan-2-yl)pyridin-2-yl)thio)methyl)benzoic acid (3)

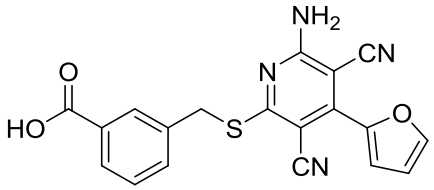

Yield: 35%; mp: 255-257°C (EtOH); ^{1}H NMR (400 MHz, DMSO-d_6): 13.01 (s, 1H, COOH, exc D_2O), 8.10 (d, *J* = 1.0 Hz, 1H, Fur), 8.05 (s, 1H, Ar), 8.13 (br s, 2H, NH_2, exc D_2O), 7.86 – 7.76 (m, 2H, Ar), 7.44 (t, *J* = 7.7 Hz, 1H, Ar), 7.39 (d, *J* = 3.6 Hz, 1H, Fur), 6.83 (dd, *J* = 3.6, 1.7 Hz, 1H, Fur), 4.58 (s, 2H, CH_2). IR (cm^{-1}): 3329, 3327, 2214, 1541

2-Amino-4-(furan-2-yl)-6-((3-(hydroxymethyl)benzyl)thio)pyridine-3,5-dicarbonitrile (4)

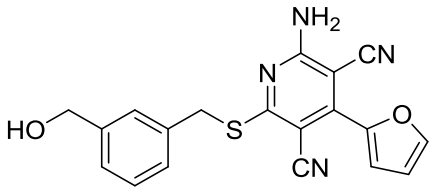

Yield: 43%; mp: 193-195°C (EtOAc); ^{1}H NMR (400 MHz, DMSO-d_6): 8.24 (s, 1H, Fur), 8.10 (br s, 2H, NH_2, exc D_2O), 7.90 (t, *J* = 1.6 Hz, 1H, Fur), 7.42 (s, 1H, Ar), 7.37 (d, *J* = 7.5 Hz, 1H, Ar), 7.27 (t, *J* = 7.5 Hz, 1H, Ar), 7.21 (d, *J* = 7.5 Hz, 1H, Ar), 6.87 (s, 1H, Fur), 5.19 (t, *J* = 5.7 Hz, 1H, OH, exc D_2O), 4.55 – 4.43 (m, 4H, $2CH_2$ partially overlapping). IR (cm^{-1}): 3398, 3314, 3215, 2214

2-Amino-6-((3-cyanobenzyl)thio)-4-(furan-2-yl)pyridine-3,5-dicarbonitrile (5)

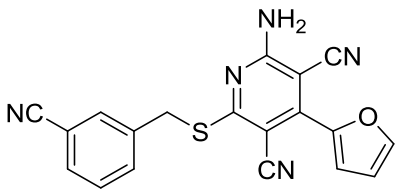

Yield: 68%; mp: 193-195°C (EtOH); ^{1}H NMR (400 MHz, DMSO): 8.23 (s, 1H, Fur), 8.15 (br s, 2H, NH_2, exc D_2O), 8.08 (s, 1H, Fur), 7.90 (dd, *J* = 3.6, 1.8 Hz, 1H, Ar), 7.88 (d, *J* = 8.0 Hz, 1H, Ar), 7.72 (d, *J* = 7.7 Hz, 1H, Ar), 7.53

(t, *J* = 7.8 Hz, 1H, Ar), 6.86 (s, 1H, Fur), 4.50 (s, 2H, CH_2). IR (cm^{-1}): 3410, 3321, 3228, 2227, 2212

Methyl 5-(((6-amino-3,5-dicyano-4-(furan-2-yl)pyridin-2-yl)thio)methyl)furan-2-carboxylate (6)

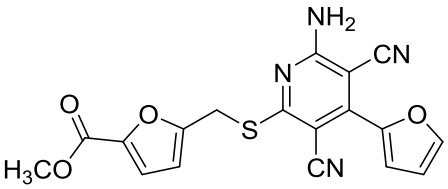

Yield: 64%; mp: 260-262°C (Acetone); ^{1}H NMR (400 MHz, DMSO-d_6): 8.25 (s, 1H, Fur), 7.91 (s, 1H, Fur), 7.25 (d, *J* = 3.5 Hz, 1H, SCH_2Fur), 6.88 (s, 1H, Fur), 6.79 (d, *J* = 3.4 Hz, 1H, SCH_2Fur), 4.62 (s, 2H, CH_2), 3.80 (s, 3H, CH_3). IR (cm^{-1}): 3402, 3334, 3240, 2222, 2210

Methyl 3-(((6-amino-3,5-dicyano-4-(furan-3-yl)pyridin-2-yl)thio)methyl)benzoate (7)

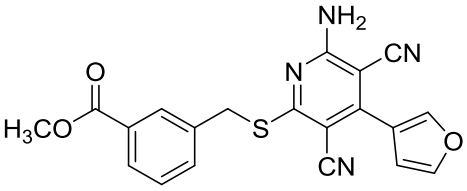

Yield: 61%; mp: 229-231°C (MeOH/2-methoxyethanol); ^{1}H NMR (400 MHz, DMSO-d_6): 8.24 (s, 1H, Fur), 8.09 (s, 1H, Fur), 8.34 – 7.77 (br s, 2H, NH_2, exc D_2O), 7.90 (t, *J* = 1.7 Hz, 1H, Ar), 7.85 (s, 1H, Ar), 7.83 (s, 1H, Ar), 7.47 (t, *J* = 7.7 Hz, 1H, Ar), 6.87 (d, *J* = 1.8 Hz, 1H, Fur), 4.58 (s, 2H, CH_2), 3.86 (s, 3H, CH_3). IR (cm^{-1}): 3373, 3113, 2210, 1527

Methyl 3-(((6-amino-3,5-dicyano-4-(thiophen-2-yl)pyridin-2-yl)thio)methyl)benzoate (8)

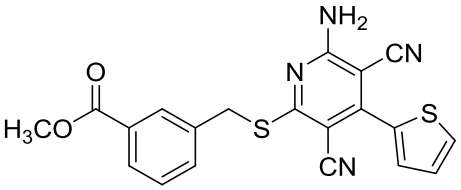

Yield: 76%; mp: 199-201°C (EtOH); ^{1}H NMR (400 MHz, DMSO-d_6): 8.10 (s, 1H, Ar), 7.94 (d, *J* = 5.0 Hz, 1H, CH *thiophene*), 8.55 – 7.72 (m, 2H, NH_2, exc D_2O), 7.86 (s, 1H, Ar), 7.84 (s, 1H, Ar), 7.56 (d, *J* = 2.7 Hz, 1H, CH *thiophene*), 7.47 (t, *J* = 7.7 Hz, 1H, Ar), 7.27 (dd, *J* = 4.9, 3.8 Hz, 1H, CH *thiophene*), 4.59 (s, 2H, CH_2), 3.86 (s, 3H, CH_3). IR (cm^{-1}): 3462, 3329, 3217, 2210, 1547

Methyl 3-(((6'-amino-3',5'-dicyano-[3,4'-bipyridin]-2'-yl)thio)methyl)benzoate (9)

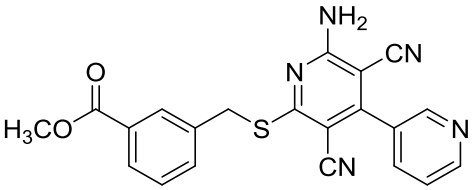

Yield: 21%; mp: 222-224°C (2-methoxyethanol/EtOH); ^{1}H NMR (400 MHz, DMSO-d_6): 8.83 – 8.67 (m, 2H, Ar), 8.23 (br s, 2H, NH_2, exc D_2O), 8.11 (s, 1H, Ar), 8.03 (d, *J* = 7.9 Hz, 1H, Ar), 7.86 (t, *J* = 7.8 Hz, 2H, Ar), 7.61 (dd, *J* = 7.7, 4.9 Hz, 1H, Ar), 7.48 (t, *J* = 7.7 Hz, 1H, Ar), 4.61 (s, 2H, CH_2), 3.86 (s, 3H, CH_3); ^{13}C NMR (100 MHz, DMSO-d_6): 166.44, 159.88, 155.82, 151.73, 149.01, 139.08, 136.86, 134.89, 130.65, 130.36, 129.29, 128.51, 124.01, 115.48, 93.84, 86.77, 52.65, 33.05; IR (cm^{-1}): 3373, 3314, 3152, 2210, 1728

2-Amino-6-((cyanomethyl)thio)-4-(furan-2-yl)pyridine-3,5-dicarbonitrile (10)

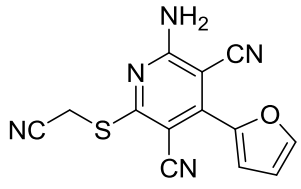

Yield: 43%; mp: 297-299°C (2-methoxyethanol); ^{1}H NMR (400 MHz, DMSO-d_6): 8.16 (br s, 2H, NH_2, exc D_2O), 8.17 – 8.11 (m, 1H, Fur), 7.51 – 7.39 (m, 1H, Fur), 6.86 (dd, *J* = 3.7, 1.8 Hz, 1H, Fur), 4.33 (s, 2H, CH_2). IR (cm^{-1}): 3404, 3319, 3228, 3313, 2257, 2208

Benzyl 2-((6-amino-3,5-dicyano-4-(furan-2-yl)pyridin-2-yl)thio)acetate (11)

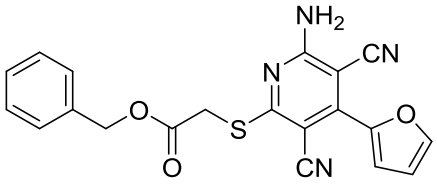

Yield: 30%; mp: 222-224°C (EtOAc/EtOH); ^{1}H NMR (400 MHz, DMSO-d_6): 8.12 (s, 1H, Fur), 7.99 (s, 2H, NH_2, exc D_2O), 7.42 (d, *J* = 3.6 Hz, 1H, Fur), 7.41 – 7.20 (m, 5H, Ar), 6.85 (dd, *J* = 3.6, 1.7 Hz, 1H, Fur), 5.19 (s, 2H, CH_2*Bn*), 4.28 (s, 2H, SCH_2); ^{13}C NMR (100 MHz, DMSO-d_6): 168.41, 166.98, 160.51, 145.44, 144.25, 136.24, 128.85, 128.54, 128.31, 116.99, 116.08, 116.01, 113.35, 89.77, 82.38, 67.10, 32.44; IR (cm^{-1}): 3441, 3314, 3209, 2214, 1732

2-Amino-4-(furan-2-yl)-6-((2-oxo-2-phenylethyl)thio)pyridine-3,5-dicarbonitrile (12)

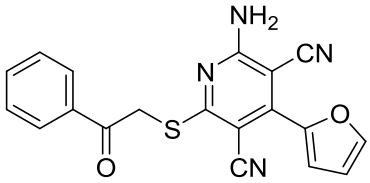

Yield: 47%; mp: 251-253°C (EtOAc); ^{1}H NMR (400 MHz, DMSO-d_6): 8.28 (d, *J* = 5.7 Hz, 1H, Fur), 8.08 (t, *J* = 6.3 Hz, 2H, Ar), 7.94 (br s, 2H, NH_2, exc D_2O), 7.93 (d, *J* = 5.5 Hz, 1H, Fur), 7.71 (dd, *J* = 13.4, 6.6 Hz, 1H, Ar), 7.65 – 7.52 (m, 2H, Ar), 6.91 (d, *J* = 4.8 Hz, 1H, Fur), 5.01 (d, *J* = 5.8 Hz, 2H, CH_2). IR (cm^{-1}): 3485, 3350, 2206, 1618

2-Amino-4-(furan-2-yl)-6-((pyridin-3-ylmethyl)thio)pyridine-3,5-dicarbonitrile (13)

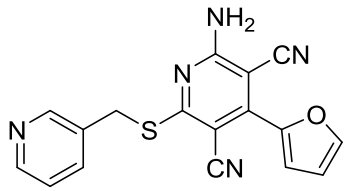

Yield: 80%; mp: 228-230°C (MeOH); ^{1}H NMR (400 MHz, DMSO-d_6): 8.77 (d, *J* = 2.1 Hz, 1H, Fur), 8.45 (dd, *J* = 4.8, 1.5 Hz, 1H, Ar), 8.89 – 7.52 (br s, 2H, NH_2, exc D_2O), 8.10 (d, *J* = 1.7 Hz, 1H, Fur), 7.94 (d, *J* = 7.9 Hz, 1H, Ar), 7.38 (d, *J* = 3.6 Hz, 1H, Ar), 7.34 (dd, *J* = 7.8, 4.8 Hz, 1H, Ar), 6.83 (dd, *J* = 3.6, 1.7 Hz, 1H, Fur), 4.49 (s, 2H, CH_2); IR (cm^{-1}): 3385, 3086, 2206

2-Amino-4-(furan-2-yl)-6-((pyridin-2-ylmethyl)thio)pyridine-3,5-dicarbonitrile (14)

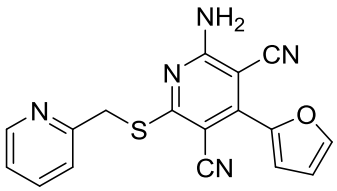

Yield: 44%; mp: 212-214°C (MeOH); ^{1}H NMR (400 MHz, DMSO-d_6): 8.48 (d, *J* = 4.7 Hz, 1H, Ar), 8.11 (br s, 2H, NH_2, exc D_2O), 8.00 (d, *J* = 1.5 Hz, 1H, Fur), 7.75 (td, *J* = 7.7, 1.7 Hz, 1H, Ar), 7.60 (d, *J* = 7.8 Hz, 1H, Ar), 7.37 (d, *J* = 3.6 Hz, 1H, Fur), 7.34 – 7.24 (m, 1H, Ar), 6.80 (dd, *J* = 3.6, 1.7 Hz, 1H, Fur), 4.56 (s, 2H, CH_2); ^{13}C NMR (100 MHz, DMSO-d_6): 167.73, 160.59, 150.03, 145.54, 144.30, 137.29, 124.18, 123.00, 116.85, 116.14, 113.29, 89.68, 82.11, 35.95; IR (cm^{-1}): 3389, 3311, 3148, 2206

2-Amino-4-(furan-2-yl)-6-(((2-phenylthiazol-4-yl)methyl)thio)pyridine-3,5-dicarbonitrile (15)

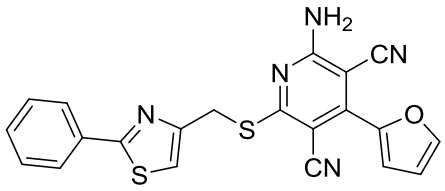

Yield: 75%; mp: 202-204°C (EtOH); ^{1}H NMR (400 MHz, DMSO-d_6): 8.12 (br s, 2H, NH_2, exc D_2O), 8.10 (s, 1H, Fur), 7.93 (dd, *J* = 6.4, 2.7 Hz, 2H, Ar), 7.86 (s, 1H, CH *thiazole*), 7.64 – 7.42 (m, 3H, Ar), 7.39 (d, *J* = 3.6 Hz, 1H, Fur), 6.83 (d, *J* = 1.9 Hz, 1H, Fur), 4.64 (s, 2H, CH_2); IR (cm^{-1}): 3373, 3200, 3178, 3103, 2212

2-Amino-6-(((2-aminothiazol-4-yl)methyl)thio)-4-(furan-2-yl)pyridine-3,5-dicarbonitrile (16)

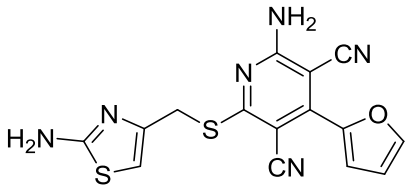

Yield: 79%; mp: 243-245°C (EtOH); ^{1}H NMR (400 MHz, DMSO-d_6): 8.10 (s, 1H, Fur), 8.06 (br s, 2H, NH_2 *Py*, exc D_2O), 7.39 (d, *J* = 3.5 Hz, 1H, Fur), 6.98 (br s, 2H, NH_2 *thiazole,* exc D_2O), 6.84 (s, 1H, CH *thiazole*), 6.62 (s, 1H, Fur), 4.30 (s, 2H, CH_2); IR (cm^{-1}): 3452, 3352, 3317, 3217, 3115, 2218

2-(((1H-Imidazol-2-yl)methyl)thio)-6-amino-4-(furan-3-yl)pyridine-3,5-dicarbonitrile (26)

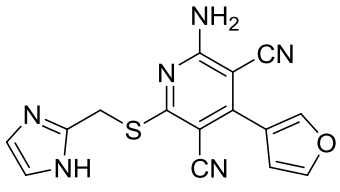

Yield: 53%; mp: 271-273°C dec. (EtOH); ^{1}H NMR (400 MHz, DMSO-d_6): 11.83 (br s,1H, NH *imidazole*, exc D_2O), 8.26 (s, 1H, CH, Fur), 8.02 (br s, 2H, NH_2, exc D_2O), 7.92 (s, 1H, CH, Fur), 7.07 (br s, 1H, CH *imidazole*), 6.88 (s, 1H, CH, Fur), 6.86 (br s, 1H, CH *imidazole*), 4.5 (s, 2H, CH2); IR (cm^{-1}): 3328, 3220, 2211

2-(((1H-Imidazol-2-yl)methyl)thio)-6-amino-4-(thiophen-3-yl)pyridine-3,5-dicarbonitrile (27)

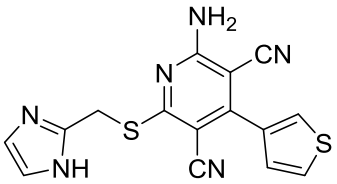

Yield: 73%; 233-235°C (ACN); ^{1}H NMR (400 MHz, DMSO-d_6): 11.83 (br s, 1H, NH *imidazole*, exc D_2O), 8.05 (d, 1H, CH *thiophene*, J = 4 Hz), 8.04 (br s, 2H, NH_2, exc D_2O), 7.78 (t, 1H, CH *thiophene*, J = 4 Hz), 7.39 (d, 1H, CH *thiophene*, J = 4 Hz), 7.07 (br s, 1H, CH *imidazole*), 6.85 (br s, 1H, CH *imidazole*), 4.50 (s, 2H, CH2); ^{13}C NMR (100 MHz, DMSO-d_6): 166.79, 160.36, 153.48, 142.99, 133.83, 129.32, 128.16, 127.92, 115.88, 93.29, 86.01, 27.24; IR (cm^{-1}): 3400,3321,2218

2'-(((1H-Imidazol-2-yl)methyl)thio)-6'-amino-[3,4'-bipyridine]-3',5'-dicarbonitrile (28)

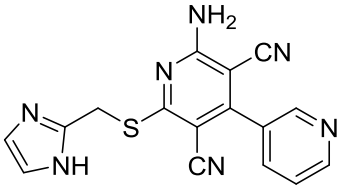

Yield: 64%; mp: 238-240°C (ACN); ^{1}H NMR (400 MHz, DMSO-d_6): 12.18 (br s, 1H, NH *imidazole*, exc D_2O), 8.78 (d, 1H, CH *Py*, J = 4 Hz), 8.75 (s,1H, CH *Py*), 8.25 (br s, 2H, NH_2, exc D_2O), 8.03 (d, 1H, CH *Py*, J = 8 Hz), 7.62 (t, 1H, CH *Py* J = 8 Hz), 7.02 (br s, 2H, CH *imidazole*), 4.54 (s, 2H, CH2); IR (cm^{-1}): 3379, 3308, 2212, 1658

2-(((1H-Imidazol-2-yl)methyl)thio)-6-amino-[4,4'-bipyridine]-3,5-dicarbonitrile (29)

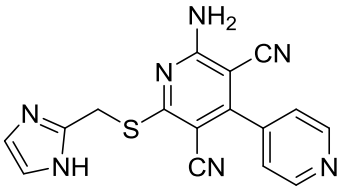

Yield: 64%; mp: > 300°C (EtOH); ^{1}H NMR (400 MHz, DMSO-d_6): 11.87 (br s, 1H, NH *imidazole*, exc D_2O), 8.81 (d, 2H, CH *Py*, J = 8 Hz), 8.2 (br s, 2H, NH_2, exc D_2O), 7. 59 (d, 2H, CH *Py*, J = 8 Hz), 7.09 (s, 1H, CH *imidazole*), 6.86 (s, 1H, CH *imidazole*), 4.52 (s, 2H, CH2); IR (cm-^{1}): 3312, 3175, 2210

2-(((1H-Imidazol-2-yl)methyl)thio)-6-amino-4-benzylpyridine-3,5-dicarbonitrile (30)

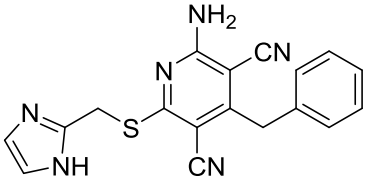

Yield: 70%; mp: 246-248°C dec (EtOH); ^{1}H NMR (400 MHz, DMSO-d_6): 11.82 (br s, 1H, NH *imidazole*, exc D_2O), 8.14 (br s, 2H, NH_2, exc D_2O), 7.34 (d, 2H, Ar, J = 8 Hz), 7.24 (m, 3H, Ar), 6.95 (sl, 2H, CH *imidazole*), 4.47 (s, 2H, SCH2), 4.05 (s, 2H, CH2); ^{13}C NMR (100 MHz, DMSO-d_6): 166.73, 160.33, 159.10, 142.89, 136.61, 129.38, 128.78, 127.64, 115.61, 86.95, 27.15; IR (cm^{-1}): 3431, 3357, 2377

2-(((1H-Imidazol-2-yl)methyl)thio)-6-amino-4-(4-chlorophenyl)pyridine-3,5-dicarbonitrile (31)

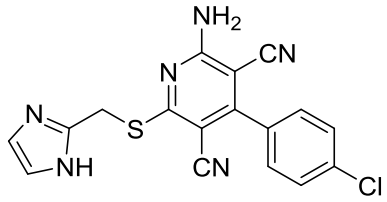

Yield: 42%; mp: 229-231°C dec (EtOH); ^{1}H NMR (400 MHz, DMSO-d_6): 11.87 (br s, 1H, NH *imidazole*, exc D_2O), 8.2 (br s, 2H, NH_2, exc D_2O), 7.65 (d, 2H, Ar, J = 8 Hz), 7.59 (d, 2H, Ar, J = 8 Hz), 7.08 (s, 1H, CH *imidazole*), 6.85 (s, 1H, CH *imidazole*), 4.5 (s, 2H, CH_2); IR (cm^{-1}): 3336, 3244, 2220

2-(((1H-Imidazol-2-yl)methyl)thio)-6-amino-4-(4-fluorophenyl)pyridine-3,5-dicarbonitrile (32)

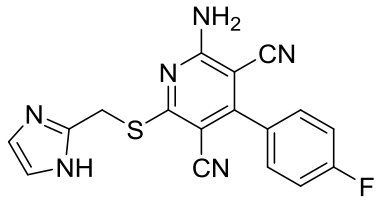

Yield: 80%; mp: 223-225°C dec (EtOAc); ^{1}H NMR (400 MHz, DMSO-d_6): 11.9 (br s, 1H, NH *imidazole*, exc D_2O), 8.2 (br s, 2H, NH_2, exc D_2O), 7.6 (m, 2H, Ar), 7.45 (t, 2H, Ar, J = 8.8 Hz), 7.0 (br s, 2H, CH *imidazole*), 4.5 (s, 2H, CH_2); IR (cm^{-1}): 3314, 3145, 2229

2-(((1H-Imidazol-2-yl)methyl)thio)-6-amino-4-(p-tolyl)pyridine-3,5-dicarbonitrile (33)

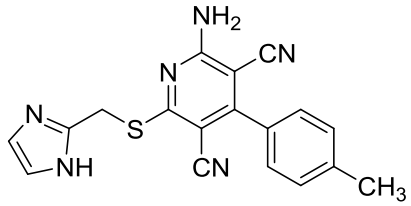

Yield: 67%; mp: 259-261°C dec (EtOH); ^{1}H NMR (400 MHz, DMSO-d_6): 11.85 (br s, 1H, NH *imidazole*, exc D_2O), 8.14 (br s, 2H, NH_2, exc D_2O), 7.4 (d, 2H, Ar, J = 8 Hz), 7.38 (d, 2H, Ar, J = 8 Hz), 7.07 (br s, 1H, CH *imidazole*), 6.86 (sl, 1H, CH *imidazole*), 4.5 (s, 2H, CH_2), 2.39 (s, 3H, CH_3); IR (cm^{-1}): 3318, 3129, 2213

2-(((1H-Imidazol-2-yl)methyl)thio)-6-amino-4-(4-(methylthio)phenyl)pyridine-3,5-dicarbonitrile (34)

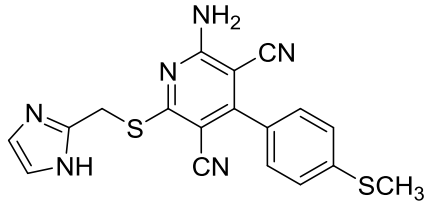

Yield: 95%; mp: 257-259°C (MeOH); ^{1}H NMR (400 MHz, DMSO-d_6): 11.87 (br s, 1H, NH *imidazole*, exc D_2O), 8.12 (br s, 2H, NH_2, exc D_2O), 7.47 (d, 2H, Ar, J = 8 Hz), 7.42 (d, 2H, Ar, J = 8 Hz), 7.08 (s, 1H, CH *imidazole*), 6.85 (s, 1H, CH *imidazole*), 4.5 (s, 2H, CH_2), 2.51 (s, 3H, CH_3); ^{13}C NMR (100 MHz, DMSO-d_6): 166.65, 160.26, 158.33, 143.00, 142.31, 130.19, 129.43, 125.69, 115.81, 93.54, 86.35, 27.23, 14.47; IR (cm^{-1}): 3420, 3390, 2223

2-(((1H-Imidazol-2-yl)methyl)thio)-6-amino-4-methylpyridine-3,5-dicarbonitrile (35)

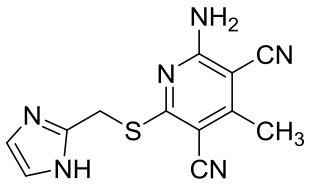

Yield: 66%; mp: 267-269°C (EtOH); ^{1}H NMR (400 MHz, DMSO): 11. 87 (br s, 1H, NH, exc D_2O), 8.12 (br s, 2H, NH_2, exc D_2O), 7.02 (br s, 2H, 2CH *imidazole*), 4.51 (s, 2H, CH_2), 2.43 (s, 3H, CH_3); IR (cm^{-1}): 3455, 3363, 2473

2-(((1H-Imidazol-2-yl)methyl)thio)-6-amino-4-(4-(cyclopropylmethoxy)phenyl)pyridine-3,5-dicarbonitrile (37)

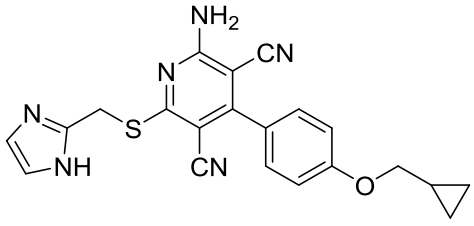

Yield: 63%; mp: 226-228°C (EtOH); ^{1}H NMR (400 MHz, DMSO-d_6): 11.86 (br s, 1H, NH *imidazole*, exc D_2O), 8.15 (br s, 2H, NH_2, exc D_2O), 7.46 (d, 2H, Ar, J = 8.2 Hz), 7.9 (d, 2H, Ar, J = 8 Hz); 7.0 (br s, 2H, CH *imidazole*), 4.5 (s, 2H, CH_2, SCH_2), 3.9 (d, 2H, CH_2, J = 8 Hz), 1.26 (m, 1H, CH *cyclopropyl*), 0.63-0.53 (m, 4H, CH_2 *eq*), 0.46 – 0.23 (m, 2H, CH_2 *ax*); ^{13}C NMR (100 MHz, DMSO-d_6): 166.59, 160.74, 160.32, 158.58, 155.20, 143.02, 130.64, 126.03, 115.96, 115.91, 114.98, 93.64, 86.38, 72.75, 27.21, 10.53, 3.62; IR (cm^{-1}): 3430, 3387, 2229

2-(((1H-Imidazol-5-yl)methyl)thio)-6-amino-4-(4-(cyclopropylmethoxy)phenyl)pyridine-3,5-dicarbonitrile (38)

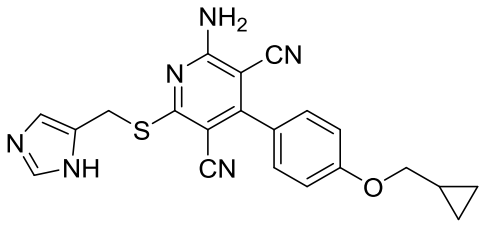

Yield: 32%; mp: 186-188°C (EtOH); ^{1}H NMR (400 MHz, DMSO-d_6): 11.97 (s, 1H, NH *imidazole*, exc D_2O), 8.04 (s, 2H, NH_2, exc D_2O), 7.59 (s, 1H, CH *imidazole*), 7.46 (d, *J* = 8.5 Hz, 2H, Ar), 7.18 (s, 1H, CH *imidazole*), 7.08 (d, *J* = 8.5 Hz, 2H, Ar), 4.40 (s, 2H, SCH_2), 3.90 (d, *J* = 6.9 Hz, 2H, OCH_2), 1.26 (dd, *J* = 15.5, 11.2 Hz, 1H, CH *cyclopropane*), 0.73 – 0.47 (m, 2H, CH *qe*), 0.47 – 0.24 (m, 2H, *ax*); ^{13}C NMR (100 MHz, DMSO-d_6): 167.24, 160.67, 160.17, 158.49, 134.33, 130.63, 126.15, 116.02, 114.94, 93.81, 86.04, 72.72, 10.52, 3.60; IR (cm^{-1}): 3318, 3205, 3080, 2212

2-Amino-4-(4-(cyclopropylmethoxy)phenyl)-6-(((4,5-dihydro-1H-imidazol-2-yl)methyl)thio)pyridine-3,5-dicarbonitrile (39)

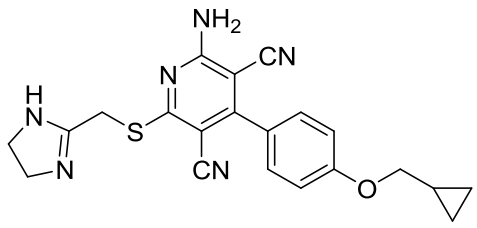

Yield: 37%; mp: 260-262°C (2-propanol/EtOAc); ^{1}H NMR (400 MHz, DMSO-d_6): 7.40 (d, *J* = 8.5 Hz, 2H, Ar), 7.19 (s, 2H, NH_2, exc D_2O), 7.12 (d, *J* = 8.1 Hz, 2H, Ar), 6.44 (s, 1H, NH, exc D_2O), 5.82 (s, 2H, SCH_2), 3.92 (d, *J* = 7.1 Hz, 2H, CH_2), 3.77 (t, *J* = 9.3 Hz, 2H, CH_2 *imidazoline*), 3.23 (t, *J* = 10.4 Hz, 2H, CH_2 *imidazoline*), 1.36 – 1.21 (m, 1H, CH), 0.72 – 0.52 (m, 2H, CH_2 *eq*), 0.50 – 0.29 (m, 2H, CH_2 *ax*)

2-(((1H-Benzo[d]imidazol-2-yl)methyl)thio)-6-amino-4-(4-(cyclopropylmethoxy)phenyl)pyridine-3,5-dicarbonitrile (40)

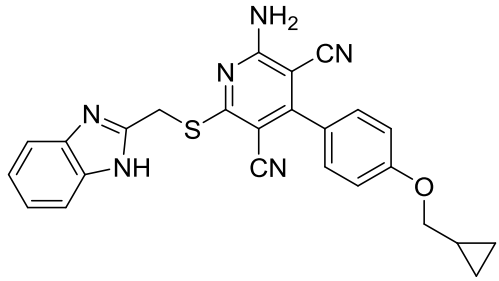

Yield: 64%; mp: >300°C (MeOH); ^{1}H NMR (400 MHz, DMSO-d_6): 12.3 (br s, 1H, NH, exc D_2O), 7.9-8.4 (br s, 2H, NH_2, exc D_2O), 7.57 (d, 1H, J= 7.8, Ar), 7.46-7.48 (m, 3H, Ar), 7.15-7.20 (m, 2H, Ar), 7.09 (d, 2H, J= 8.72, Ar), 4.71 (s, 2H, CH_2), 3.9 (d, 2H, CH_2, J= 7.08), 1.22-1.30 (m, 1H, CH), 0.57-0.62 (m, 2H, 2CH *eq*), 0.33-0.37 (m, 2H, 2CH *ax*); IR (cm^{-1}): 3396; 3331; 2210

2-(((1H-Pyrazol-5-yl)methyl)thio)-6-amino-4-(4-(cyclopropylmethoxy)phenyl)pyridine-3,5-dicarbonitrile (41)

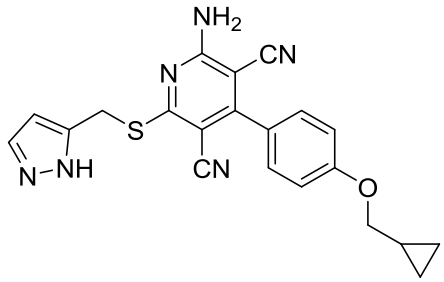

Yield: 37%; mp: 133-136°C (EtOH/CHx); ^{1}H NMR (400 MHz, DMSO-d_6): 12.7 (br s, 1H, NH, exc D_2O), 8.0 (br s, 2H, NH_2, exc D_2O), 7.67 (br s, 1H, CH *pyrazole*), 7.47 (d, 2H, J= 8.28, Ar), 7.09 (d, 2H, J= 8.48, Ar), 6.32 (s, 1H, CH *pyrazole*), 4.49 (s, 2H, CH_2), 3.91 (d, 2H, CH_2, J= 6.88), 1.22-1.26 (m, 1H, CH), 0.58-0.62 (m, 2H, 2CH *eq*), 0.36-0.40 (m, 2H, 2CH *ax*)

2-(((1H-1,2,4-Triazol-1-yl)methyl)thio)-6-amino-4-(4-(cyclopropylmethoxy)phenyl)pyridine-3,5-dicarbonitrile (42)

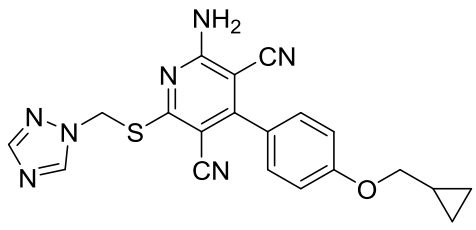

Yield: 40%; mp: 235-237°C (EtOH); ^{1}H NMR (400 MHz, DMSO-d_6): 8.99 (s, 1H), 8.75 – 7.78 (m, 2H, NH_2, exc D_2O), 8.04 (s, 1H, CH *triazole*), 7.47 (d, 2H, Ar, *J* = 8.7 Hz,), 7.08 (d, 2H, Ar, *J* = 8.8 Hz), 6.03 (s, 2H, CH_2), 3.90 (d, 2H, CH_2, *J* = 7.1 Hz), 1.34 – 1.17 (m, 1H, CH *cyclopropyl*), 0.64 – 0.54 (m, 2H, CH_2 *eq*), 0.38-0.32 (m, 2H CH_2 *ax)*; IR (cm^{-1}): 3311, 2212

2-(((1H-1,2,4-Triazol-5-yl)methyl)thio)-6-amino-4-(4-(cyclopropylmethoxy)phenyl)pyridine-3,5-dicarbonitrile (43)

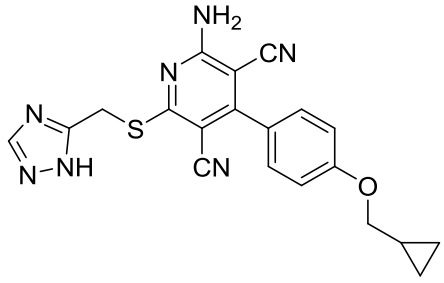

Yield: 72%; mp: 240-242°C (EtOH/Et_2O); ^{1}H NMR (400 MHz, DMSO-d_6): 13.9 (br s, 1H, NH, exc D_2O), 8.3 (br s, 1H, CH *triazole*), 8.1 (sl, 2H, NH_2, exc D_2O), 7.48 (d, 2H, J= 7.80, Ar), 7.09 (d, 2H, J= 8.48, Ar), 4.59 (s, 2H, SCH_2), 3.91 (d, 2H, J= 7.08, OCH_2), 1.23-1.29 (m, 1H, CH), 0.57-0.62 (m, 2H, 2CH *eq*), 0.34-0.37 (m, 2H, 2CH *ax*); IR (cm^{-1}): 3441; 3323; 3207; 2212

2-(((1H-Tetrazol-5-yl)methyl)thio)-6-amino-4-(4-(cyclopropylmethoxy)phenyl)pyridine-3,5-dicarbonitrile (44)

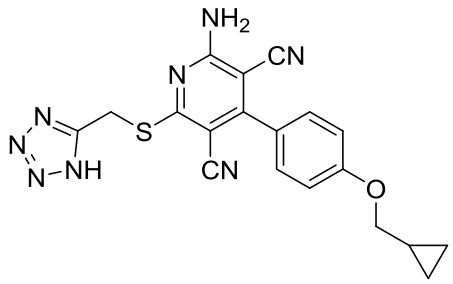

Yield: 64%; mp: 225-227°C (EtOH/Et_2O); ^{1}H NMR (400 MHz, DMSO-d_6): 16.1 (br s, 1H, NH, exc D_2O), 8.0 (br s, 2H, NH_2, exc D_2O), 7.47 (d, 2H, J= 8.64, Ar), 7.09 (d, 2H, J= 8.64, Ar), 4.78 (s, 2H, SCH_2), 3.91 (d, 2H, OCH_2, J= 7.04), 1.24-1.28 (m, 1H, CH), 0.58-0.61 (m, 2H, 2CH *eq*), 0.34-0.37 (m, 2H, 2CH *ax*); IR (cm^{-1}): 3442; 3323; 3224; 2225; 2208

2-Amino-6-(((2-aminothiazol-4-yl)methyl)thio)-4-(4-(cyclopropylmethoxy)phenyl)pyridine-3,5-dicarbonitrile (45)

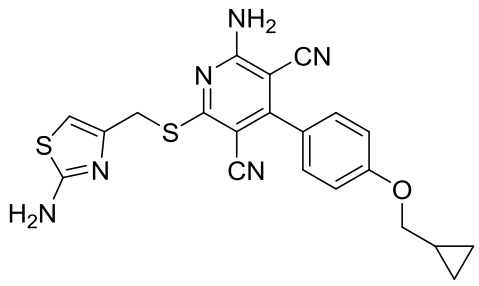

Yield: 87%; mp: 238-240°C (EtOH/Et_2O); ^{1}H NMR (400 MHz, DMSO-d_6): 8.02 (br s, 2H, NH_2, exc D_2O), 7.46 (d, 2H, J= 8.68, Ar), 7.08 (d, 2H, J= 8.72, Ar), 6.98 (br s, 2H, NH_2, exc D_2O), 6.63 (s, 1H, CH *thiazole*), 4.31 (s, 2H, SCH_2), 3.90 (d, 2H, J= 7.04, OCH_2), 1.23-1.29 (m, 1H, CH), 0.57-0.62 (m, 2H, 2CH *eq*), 0.34-0.37 (m, 2H, 2CH *ax*); IR (cm^{-1}): 3423; 3327; 3184-3170; 2216

2-Amino-4-(4-(cyclopropylmethoxy)phenyl)-6-((pyridin-3-ylmethyl)thio)pyridine-3,5-dicarbonitrile (46)

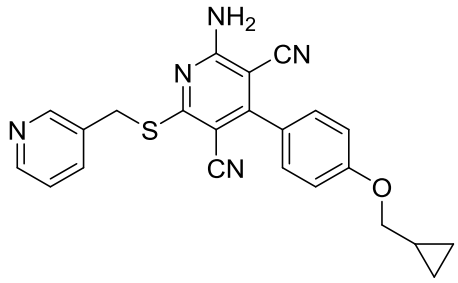

Yield: 80%; 190-192°C (MeOH); ^{1}H NMR (400 MHz, DMSO-d_6): 8.7 (s, 1H, Ar), 8.45 (s, 1H, Ar), 8.11 (br s, 2H, NH_2, exc D_2O), 7.94 (d, 1H, J= 5.68, Ar), 7.42 (d, 2H, J= 6.8 Hz, Ar), 7.35-7.37 (m, 1H, Ar), 7.05 (d, 2H, Ar, J= 6.9 Hz), 4.48 (s, 2H, SCH_2), 3.86 (d, 2H, J= 7.0 Hz, OCH_2), 1.19-1.22 (m, 1H, CH), 0.57-0.59 (m, 2H, 2CH *eq*), 0.30-0.34 (m, 2H, 2CH *ax*); IR (cm^{-1}): 3369; 2212

2-((6-Amino-3,5-dicyano-4-(4-(cyclopropylmethoxy)phenyl)pyridin-2-yl)thio)-N-methylacetamide (47)

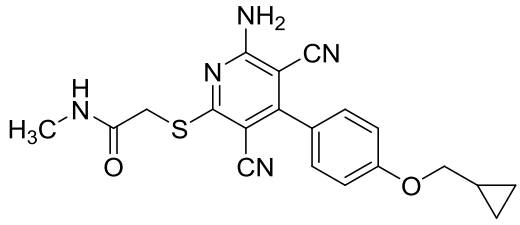

Yield: 71%; mp: 274-276°C (Acetone); ^{1}H NMR (400 MHz, DMSO-d_6): 8.18 – 7.85 (2 br s, 3H, NH_2 + NH, exc D_2O), 7.48 (d, *J* = 8.7 Hz, 2H, Ar), 7.10 (d, *J* = 8.7 Hz, 2H, Ar), 3.89 (s, 2H, SCH_2), 2.62 (d, *J* = 4.5 Hz, 2H, OCH_2), 1.27 (m, 1H, CH), 0.61 (q, *J* = 6.3 Hz, 2H, CH_2 *eq*), 0.36 (q, *J* = 4.5 Hz, 2H, CH_2 *ax*); ^{13}C NMR (100 MHz, DMSO-d_6): 167.78, 166.54, 160.75, 160.16, 158.59, 130.64, 126.03, 115.90, 115.00, 93.69, 86.40, 72.75, 33.72, 26.50, 10.55, 3.60 IR (cm^{-1}): 3390; 3323; 3223; 2208

2-((6-Amino-3,5-dicyano-4-(4-(cyclopropylmethoxy)phenyl)pyridin-2-yl)thio)-N-(hydroxymethyl)-acetamide (48)

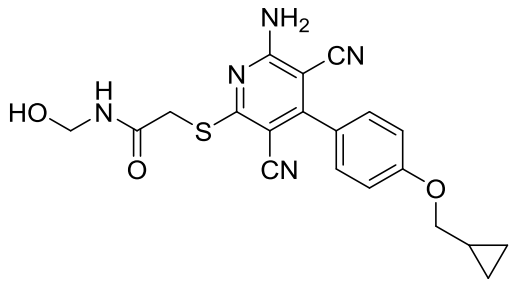

Yield: 79%; mp: 202-204°C (MeOH); ^{1}H NMR (400 MHz, DMSO-d_6): 8.69 (t, 1H, NH, J= 6.28 Hz, exc D_2O); 7.8-8.2 (br s, 2H, NH_2, exc D_2O), 7.46-7.50 (m, 2H, Ar), 7.08-7.12 (m, 2H, Ar), 5.72 (t, 1H, OH, J = 6.42 Hz, exc D_2O), 4.53 (t, 2H, NCH_2O, J= 5.96), 3.90-3.92 (1 d + 1 s, 4H, $2CH_2$ *overlapping*), 1.21-1.31 (m, 1H, CH), 0.58-0.62 (m, 2H, 2CH *eq*), 0.34-0.38 (m, 2H, 2CH *ax*); IR (cm^{-1}): 3394; 3319 bl; 3224; 2208; 1639

2-((6-Amino-3,5-dicyano-4-(4-(cyclopropylmethoxy)phenyl)pyridin-2-yl)thio)-N-hydroxyacetamide (49)

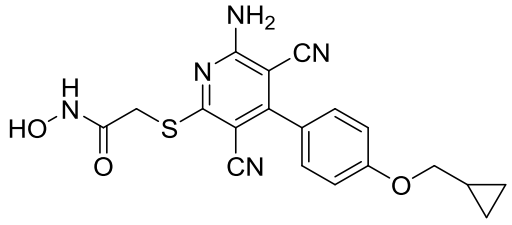

Yield: 60%; mp: 176-178°C (EtOH); ^{1}H NMR (400 MHz, DMSO-d_6): 10.58 (br s, 1H, OH, exc D_2O), 9.06 (br s, 1H, NH, exc D_2O), 8.01 (br s, 2H, NH_2, exc D_2O), 7.48 (d, *J* = 8.6 Hz, 2H, Ar), 7.10 (d, *J* = 8.6 Hz, 2H, Ar), 3.91 (d, *J* = 6.9 Hz, 2H, SCH_2), 3.81 (s, 2H, CH_2), 1.32 – 1.19 (m, 1H, CH), 0.60 (m, 2H, CH_2, *eq*), 0.42 – 0.29 (m, 2H, CH_2 *ax*); IR (cm^{-1}): 3649, 3331, 3223, 2208

Methyl 2-((6-amino-3,5-dicyano-4-(4-(cyclopropylmethoxy)phenyl)pyridin-2-yl)thio)acetate (50)

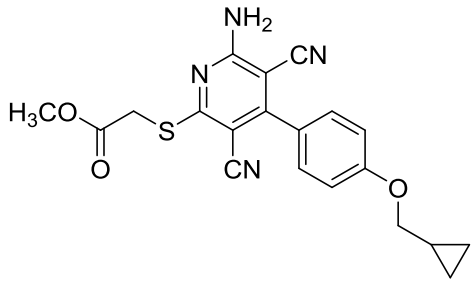

Yield: 41%; mp: 205-207°C (EtOH); ^{1}H NMR (400 MHz, DMSO-d_6): 7.9 (br s, 2H, NH_2, exc D_2O), 7.48 (d, 2H, J= 8.8, Ar), 7.1 (d, 2H, J= 8.84, Ar), 4.20 (s, 2H, SCH_2), 3.91 (d, 2H, J= 7.04, OCH_2), 3.69 (s, 3H, OCH_3), 1.24-1.28 (m, 1H, CH), 0.58-0.62 (m, 2H, 2CH *eq*), 0.35-0.38 (m, 2H, 2CH *ax*); IR (cm^{-1}): 3446; 3342; 3224; 2210; 1739

Methyl 3-(((6-amino-3,5-dicyano-4-(4-(cyclopropylmethoxy)phenyl)pyridin-2-yl)thio)methyl)benzoate (51)

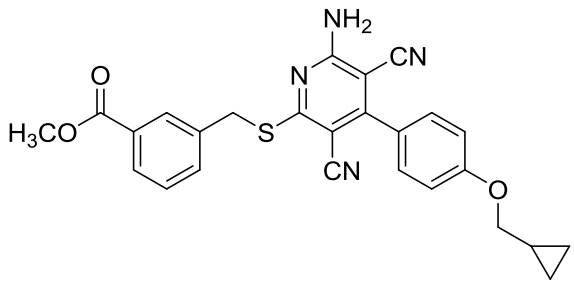

Yield: 58%; mp: 158-160°C (MeOH); ^{1}H NMR (400 MHz, DMSO-d_6): 8.10 (s, 1H, Ar), 7.90-8.35 (br s, 2H, NH_2, exc D_2O), 7.84-7.87 (m, 2H, Ar), 7.44-7.49 (m, 3H, Ar), 7.07 (d, 2H, J= 8.8, Ar), 4.59 (s, 2H, SCH_2), 3.90 (d, 2H, OCH_2 J= 7.04), 3.86 (s, 3H, OCH_3), 1.23-1.27 (m, 1H, CH), 0.58-0.60 (m, 2H, 2CH *eq*), 0.34-0.36 (m, 2H, 2CH *ax*); IR (cm^{-1}): 3396; 3331; 3230; 2210; 1707

3-(((6-Amino-3,5-dicyano-4-(4-(cyclopropylmethoxy)phenyl)pyridin-2-yl)thio)methyl)benzamide (52)

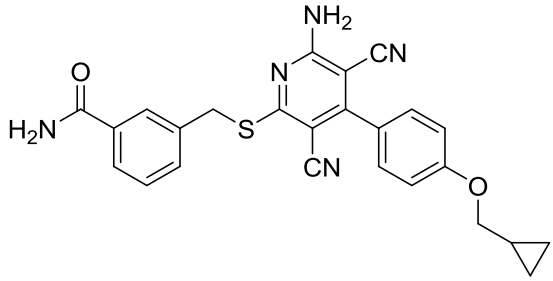

Yield: 47%; mp: 243-245°C (EtOAc/2-methoxyethanol); ^{1}H NMR (400 MHz, DMSO-d_6): 8.05 (br s, 2H, NH_2, exc D_2O), 8.00 (s, 1H, Ar), 7.96 (s, 1H, NH *amide*, exc D_2O), 7.77 (d, 1H, J= 7.80 Hz, Ar), 7.69 (d, 1H, J= 7.73 Hz, Ar), 7.47-7.38 (m, 4H, 2Ar + NH *amide*), 7.07 (d, 2H, J= 8.8, Ar), 4.54 (s, 2H, SCH_2), 3.90 (d, 2H, J= 7.04, OCH_2), 1.22-1.28 (m, 1H, CH), 0.58-0.61 (m, 2H, 2CH *eq*), 0.33-0.37 (m, 2H, 2CH *ax*); IR (cm^{-1}): 3441; 3387; 3356; 3169; 2212; 1635

2-(((1H-Imidazol-2-yl)methyl)thio)-6-amino-4-(4-(cyclobutylmethoxy)phenyl)pyridine-3,5-dicarbonitrile (53)

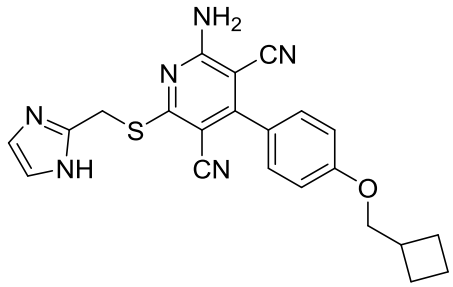

Yield: 20%; 214-216°C (EtOH); ^{1}H NMR (400 MHz, DMSO-d_6): 11.87 (br s, 1H, NH *imidazole*, exc D_2O), 8.10 (br s, 2H, NH_2, exc D_2O), 7.46 (d, 2H, J= 7.76 Hz, Ar), 7.09 (d, 2H, J= 7.76 Hz, Ar), 7.08 (s, 1H, CH *imidazole*), 6.96 (s, 1H, CH *imidazole*), 4.49 (s, 2H, SCH_2), 4.03 (d, 2H, OCH_2, J= 5.96 Hz), 2.7-2.6 (m, 1H, CH *cyclobutyl*), 2.08-2.07 (m, 2H, CH_2 *cyclobutyl*), 1.91-1.88 (m, 4H, $2CH_2$ *cyclobutyl*); IR (cm^{-1}): 3385; 3320; 3217; 2210

2-((6-Amino-3,5-dicyano-4-(4-(cyclobutylmethoxy)phenyl)pyridin-2-yl)thio)acetamide (54)

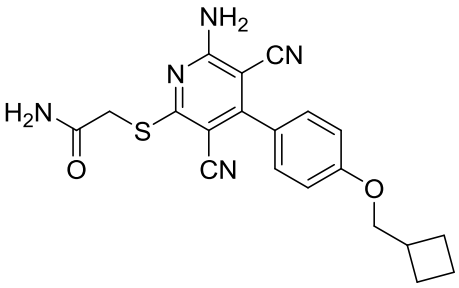

Yield: 21%; mp: 244-246°C (EtOAc/CHx); ^{1}H NMR (400 MHz, DMSO-d_6): 7.99 (br s, NH_2, exc D_2O), 7.50 (br s, 1H, NH_2 *amide*, exc D_2O), 7.49 (d, 2H, J= 8.6 Hz, Ar), 7.26 (s, 1H, NH_2 *amide*, exc D_2O), 7.10 (d, 2H, J= 8.6 Hz, Ar), 4.04 (d, 2H, OCH_2, J= 6.68 Hz), 4.03 (s, 2H, SCH_2), 2.78- 2.67 (m, 1H, CH *cyclobutyl*), 1.99-1.96 (m, 2H, CH), 1-95-1.82 (m, 4H, $2CH_2$ *cyclobutyl*); IR (cm^{-1}): 3664, 3361, 3252, 2214, 1635

2-(((1H-Imidazol-2-yl)methyl)thio)-6-amino-4-(4-isobutoxyphenyl)pyridine-3,5-dicarbonitrile (55)

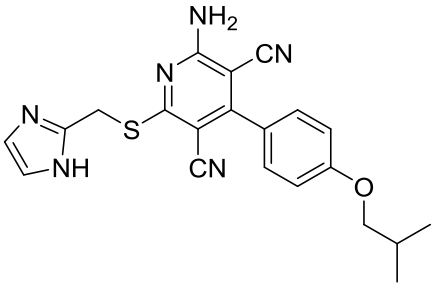

Yield: 31%; mp: 230-232°C (EtOH); ^{1}H NMR (400 MHz, DMSO-d_6): 11.84 (br s, 1H, NH *imidazole*, exc D_2O), 8.14 (s, 2H, NH_2, exc D_2O), 7.47 (d, 2H, J= 8.7 Hz, Ar), 7.10 (d, 2H, J= 8.6 Hz, Ar), 7.08 (s, 1H, CH *imidazole*), 6.85 (s, 1H, CH *imidazole*), 4.50 (s, 2H, SCH_2), 3.84 (d, 2H, OCH_2, J= 6.3 Hz), 2.09-2.02 (m, 1H, CH *isopropyl*), 1.00 (2 d, 6H, 2 CH_3 *isopropyl*, J= 6.7 Hz); IR (cm^{-1}): 3387, 3315, 3215, 2208

2-((6-Amino-3,5-dicyano-4-(4-isobutoxyphenyl)pyridin-2-yl)thio)acetamide (56)

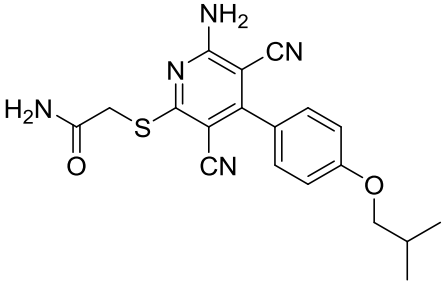

yield: 21%; mp: 233-235°C (EtOH); ^{1}H NMR (400 MHz, DMSO-d_6): 7.99 (br s, 2H, NH_2, exc D_2O), 7.49 (s, 1H, NH_2 *amide*, exc D_2O), 7.48 (d, 2H, J= 8.4 Hz, Ar), 7.25 (s, NH_2 *amide*, exc D_2O), 7.11 (d, 2H, J= 8.8 Hz, Ar), 3.88 (s, 2H, SCH_2), 3.84 (d, 2H, OCH_2, J= 6.4 Hz), 2.08-2.02 (m, 1H, CH *isopropyl*), 1.00 (d, 6H, J= 6.8 Hz, $2CH_3$ *isopropyl*); IR (cm^{-1}): 3537; 3375; 3196; 2208; 1639

2-(((1H-Imidazol-2-yl)methyl)thio)-6-amino-4-(4-ethoxyphenyl)pyridine-3,5-dicarbonitrile (57)

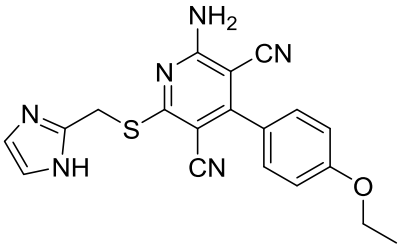

Yield: 41%; mp: 242-244°C (EtOH); ^{1}H NMR (400 MHz, DMSO-d_6): 11.84 (br s, 1H, NH *imidazole*, exc D_2O), 8.12 (s, 2H, NH_2, exc D_2O), 7.47 (d, 2H, J= 8.6 Hz, Ar), 7.09 (d, 2H, J= 8.7 Hz, Ar), 7.08 (s, 1H, CH *imidazole*), 6.85 (s, 1H, CH *imidazole*), 4.49 (s, 2H, SCH_2), 4.2 (q, 2H, J= 6.8 Hz, OCH_2), 1.36 (t, 3H, J= 6.8 Hz, CH_3); ^{13}C NMR (100 MHz, DMSO-d_6): 166.60,

160.65, 160.32, 158.56, 143.01, 130.67, 126.06, 115.94, 115.89, 114.94, 93.66, 86.40, 63.83, 27.23, 15.06; IR (cm^{-1}): 3506, 3398, 3159, 2212

2-((6-Amino-3,5-dicyano-4-(4-ethoxyphenyl)pyridin-2-yl)thio)acetamide (58)

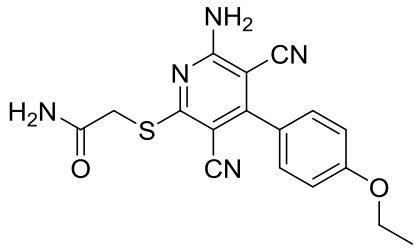

Yield: 35%; mp: 235-237°C (EtOH); ^{1}H NMR (400 MHz, DMSO-d_6): 7.98 (br s, 2H, NH_2, exc D_2O), 7.50 (s, 1H, NH_2 *amide*, exc D_2O), 7.48 (d, 2H, J= 8.8 Hz, Ar), 7.23 (s, 1H, NH_2 *amide*, exc D_2O), 7.10 (d, 2H, J= 8.8 Hz, Ar), 4.12 (q, 2H, OCH_2, J= 7.2 Hz), 3.88 (s, 2H, SCH_2), 1.36 (t, 3H, J= 7.2 Hz, CH_3); IR (cm^{-1}): 3396, 3180, 2210, 1637

2-((6-Amino-3,5-dicyano-4-(4-ethoxyphenyl)pyridin-2-yl)thio)-N-methylacetamide (59)

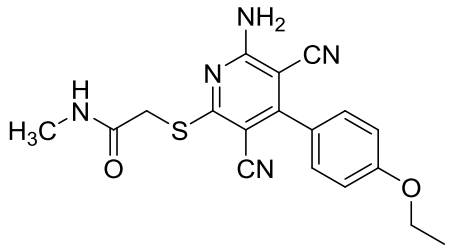

Yield: 32%; mp: 262-264°C (EtOH); ^{1}H NMR (400 MHz, DMSO-d_6): 7.96 (br s, 1H, NH, exc D_2O), 7.95 (br s, 2H, NH_2, exc D_2O), 7.48 (d, 2H, J= 8.5 Hz, Ar), 7.09 (d, 2H, J= 8.4 Hz, Ar), 4.12 (q, 2H, J= 7.2 Hz, OCH_2), 3.88 (s, 2H, CH_2), 1.36 (t, 3H, J= 6.8 Hz, CH_3); ^{13}C NMR (100 MHz, DMSO): 167.78, 166.54, 160.15, 158.57, 130.67, 126.05, 115.93, 114.94, 63.83, 33.71, 26.56, 15.07; IR (cm^{-1}): 3394, 3223, 2210, 1637

2-(((1H-Pyrazol-5-yl)methyl)thio)-6-amino-4-(4-ethoxyphenyl)pyridine-3,5-dicarbonitrile (60)

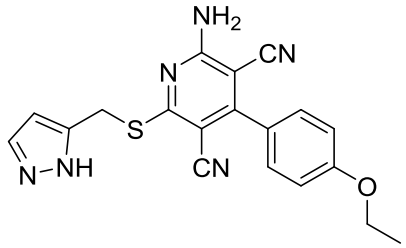

Yield: 29%; mp: 195-197°C (EtOH); ^{1}H NMR (400 MHz, DMSO-d_6): 12.72 (br s, 1H, NH *pyrazole*, exc D_2O), 8.05 (s, 2H, NH_2, exc D_2O), 7.65 (s, 1H, CH *pyrazole*), 7.47 (d, 2H, J= 8.3 Hz, Ar), 7.09 (d, 2H, J= 8.4 Hz, Ar), 6.31 (s, 1H, CH *pyrazole*), 4.48 (s, 2H, SCH_2), 4.11 (q, 2H, J= 6.8 Hz, OCH_2), 1.36 (t, 3H, J= 6.8 Hz, CH_3); IR (cm^{-1}): 3456, 3319, 3215, 2218

2-(((1H-Imidazol-2-yl)methyl)thio)-4-(4-(allyloxy)phenyl)-6-aminopyridine-3,5-dicarbonitrile (61)

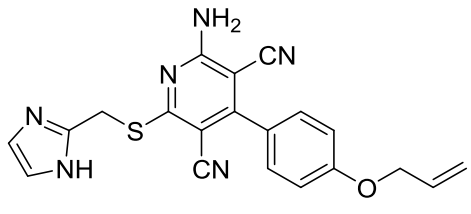

Yield: 21%; mp: 216-218°C (EtOH/EtOAc); ^{1}H NMR (400 MHz, DMSO-d_6): 11.86 (s, 1H, NH *imidazole*, exc D_2O), 8.09 (s, 2H, NH_2, exc D_2O), 7.48 (d, 2H, J= 8.5 Hz, Ar), 7.12 (d, 2H, J= 8.6 Hz, Ar),

7.07 (s,1H, CH *imidazole*), 6.85 (s, 1H, CH *imidazole*), 6.11-6.04 (m, 1H *vinyl*, CH), 5.40 (d, 1H, CH *vinyl*), 5.30 (d, 1H, CH *vinyl*), 4.62 (d, 2H, J= 5.2 Hz, OCH_2), 4.48 (s, 2H, SCH_2)

2-((4-(4-(Allyloxy)phenyl)-6-amino-3,5-dicyanopyridin-2-yl)thio)acetamide (62)

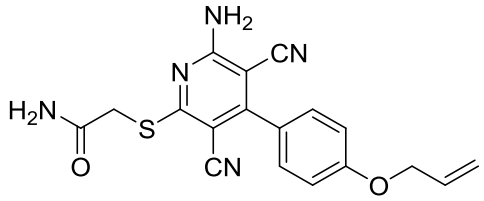

Yield: 67%; mp: 204-206°C (EtOH); ^{1}H NMR (400 MHz, DMSO-d_6): 8.00 (s, 2H, NH_2, exc D_2O), 7.50 (d, *J* = 8.6 Hz, 3H, Ar + NH *amide*, partially exc D_2O), 7.26 (s, 1H, NH *amide*, exc D_2O), 7.14 (d, *J* = 8.7 Hz, 2H, Ar), 6.08 (ddd, *J* = 22.4, 10.5, 5.3 Hz, 1H, CH *allyl*), 5.45 (d, *J* = 17.3 Hz, 1H, CH_2 *allyl*), 5.30 (d, *J* = 10.5 Hz, 1H, CH_2 *allyl*), 4.67 (d, *J* = 5.1 Hz, 2H, OCH_2), 3.89 (s, 2H, SCH_2); IR (cm^{-1}): 3325, 3215, 3184, 2212

2-(((1H-Pyrazol-5-yl)methyl)thio)-4-(4-(allyloxy)phenyl)-6-aminopyridine-3,5-dicarbonitrile (63)

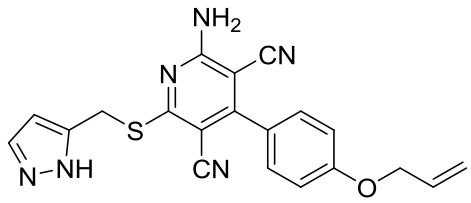

Yield: 65%; mp: 129-131°C (EtOH); ^{1}H NMR (400 MHz, DMSO-d_6): 12.75 (s, 1H, NH *pyrazole*, exc D_2O), 8.06 (s, 2H, NH_2, exc D_2O), 7.59 (s, 1H, CH *pyrazole*), 7.49 (d, *J* = 8.7 Hz, 2H, Ar), 7.13 (d, *J* = 8.7 Hz, 2H, Ar), 6.32 (s, 1H, CH *pyrazole*), 6.18 – 5.95 (m, 1H, CH *allyl*), 5.45 (d, *J* = 17.3 Hz, 1H, CH_2 *allyl*), 5.30 (d, *J* = 10.4 Hz, 1H, CH_2 *allyl*), 4.67 (d, *J* = 5.2 Hz, 2H, OCH_2), 4.49 (s, 2H, SCH_2); ^{13}C NMR (100 MHz, DMSO): 160.25, 160.23, 158.49, 133.86, 130.67, 128.81, 126.41, 125.65, 118.35, 115.95, 115.18, 111.08, 109.95, 105.12, 93.71, 86.31, 68.84; IR (cm^{-1}): 3335, 3179, 2210

2-(((1H-Imidazol-2-yl)methyl)thio)-6-amino-4-(4-((2-methylallyl)oxy)phenyl)pyridine-3,5-dicarbonitrile (64)

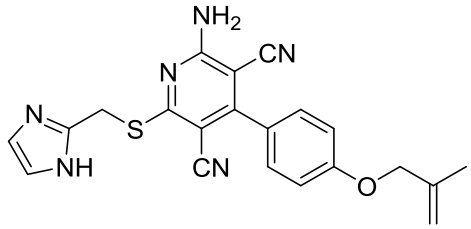

Yield: 36%; mp: 224-226 (EtOH/EtOAc); ^{1}H NMR (400 MHz, DMSO-d_6): 11.85 (br s, 1H *imidazole*, exc D_2O), 8.08 (s, 2H, NH_2, exc D_2O), 7.48 (d, 2H, J= 8.4 Hz, Ar), 7.12 (d, 2H, J= 8.4 Hz, Ar), 7.07 (s, 1H, CH *imidazole*), 6.85 (s, 1H, CH *imidazole*), 5.09 (s, 1H, CH_2 *propene*), 4.99 (d, 1H, CH_2 *propene*), 4.56 (s, 2H, SCH_2), 4.49 (s, 2H, OCH_2), 1.79 (s, 3H, CH_3); ^{13}C NMR (100 MHz, DMSO-d_6): 167.19, 161.03, 160.95, 159.11, 143.71, 141.67, 131.75, 131.28, 126.93, 116.58, 115.93, 115.80, 113.79, 94.22, 87.00, 72.14, 27.75, 20.32; IR (cm^{-1}): 3404, 3377, 3336, 2210

2-((6-Amino-3,5-dicyano-4-(4-((2-methylallyl)oxy)phenyl)pyridin-2-yl)thio)acetamide (65)

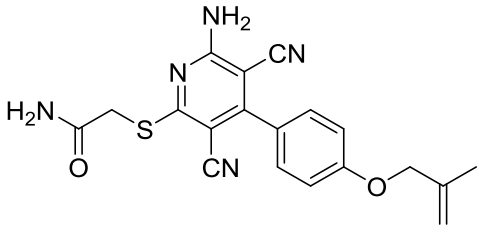

Yield: 27%; mp: 224-226°C (EtOH); ^{1}H NMR (400 MHz, DMSO-d_6): 7.99 (s, NH_2, exc D_2O), 7.51 (s, 1H, NH_2 *amide*, exc D_2O), 7.50 (d, 2H, J= 8.6 Hz, Ar), 7.25 (s, 1H, NH_2 *amide*, exc D_2O), 7.13 (d, 2H, J= 8.6 Hz, Ar), 5.10 (s, 1H, CH_2 *propene*), 4.99 (s, 1H, CH_2 *propene*), 4.57 (s, 2H, OCH_2), 3.88 (s, 2H, SCH_2), 1.08 (s, 3H, CH_3); IR (cm^{-1}): 3481, 3334, 3234, 2212, 1681

N-(4-(2-(((1H-Imidazol-2-yl)methyl)thio)-6-amino-3,5-dicyanopyridin-4-yl)phenyl)acetamide (66) (295)

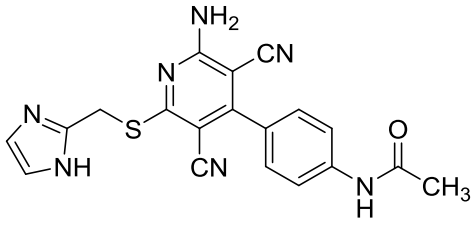

Yield: 61%; mp: 266-268°C (EtOH/CHx); ^{1}H NMR (400 MHz, DMSO-d_6): 11.84 (br s, 1H, NH *imidazole*, exc D_2O), 10.22 (s, 1H, NH *amide*, exc D_2O), 8.11 (s, NH_2, exc D_2O), 7.73 (d, 2H, J= 8.3 Hz, Ar), 7.46 (d, 2H, J= 8.4 Hz, Ar), 7.05 (s, 1H, CH *imidazole*), 6.86 (s, 1H, CH *imidazole*), 4.49 (s, 2H, CH_2), 2.09 (s, 3H, CH_3); IR (cm^{-1}): 3387, 3211, 2214, 1683

2-((4-(4-Acetamidophenyl)-6-amino-3,5-dicyanopyridin-2-yl)thio)acetamide (67)

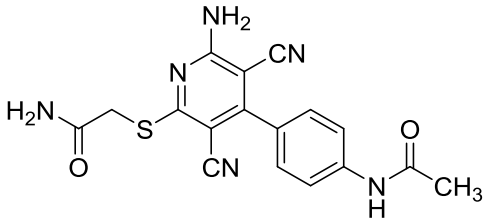

Yield: 19%; 279-281°C (MeOH); ^{1}H NMR (400 MHz, DMSO-d_6): 10.21 (br s, 1H, $NHCOCH_3$, exc D_2O), 8.00 (s, 2H, NH_2, exc D_2O), 7.74 (d, 2H, J= 7.6 Hz, Ar), 7.48 (d, 2H, J= 8.4 Hz, Ar), 7.47 (s, 1H, NH_2 *amide*, exc D_2O), 7.24 (s, 1H, NH_2 *amide*, exc D_2O), 3.88 (s, 2H, CH_2), 2.09 (s, 3H, CH_3); ^{13}C NMR (100 MHz, DMSO-d_6): 169.38, 169.27, 166.67, 160.10, 158.52, 141.70, 129.72, 128.44, 119.12, 115.82, 93.65, 86.29, 33.78, 24.57; IR (cm^{-1}): 3419, 3367, 2208, 1647

2-((6-Amino-3,5-dicyano-4-(4-hydroxyphenyl)pyridin-2-yl)thio)acetamide (142)

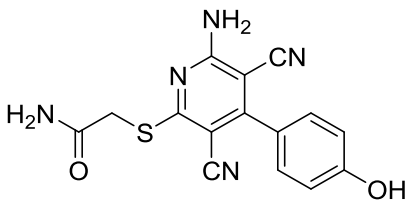

Yield: 24%; (EtOH); ^{1}H NMR (400 MHz, DMSO-d_6): 10.08 (br s, 1H, OH, exc D_2O), 7.97 (br s, 2H, NH_2, exc D_2O), 7.50 (br s, 1H, NH_2 *amide*, exc D_2O), 7.38 (d, 2H, Ar, J= 8.4 Hz), 7.24 (s, 1H, NH_2 *amide*, exc D_2O), 6.92 (d, 2H, Ar, J= 8.4 Hz), 3.88 (s, 2H, CH_2); IR (cm^{-1}): 3331, 3176, 2214, 1658

Synthesis of 2-chloro-4-(furan-2-yl)-6-((2-hydroxyethyl)thio)pyridine-3,5-dicarbonitrile (85)

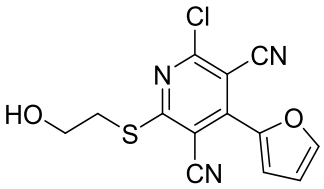

Isoamylnitrite (9.05 mmol) was added to a suspension of equimolar amount of copper (II) chloride in ACN dry (5 ml) under nitrogen atmosphere and the reaction mixture was stirred 20 min at rt. Then, **A** (1.51 mmol) was added and the reaction was allowed to proceed for a weekend. 1N HCl was then added and the resulting mixture was extracted with DCM (4 x 25 ml). The collected organic phases were washed with brine (2 x 20ml) and dried (NA_2SO_4). The solvent was removed under vacuum and the yellow residue triturated with Et_2O, filtered and recrystallized by EtOH. Yield: 67 %; mp: 197-199°C (EtOH); ^{1}H NMR (400 MHz, DMSO-d_6): 8.27 (s, 1H,Fur), 7.66 (d, *J* = 3.6 Hz, 1H, Fur), 6.95 (d, *J* = 3.6 Hz, 1H, Fur), 3.70 (t, *J* = 6.3 Hz, 2H, CH_2), 3.41(t, *J* = 6.3 Hz, 2H, CH_2); IR (cm^{-1}): 2230

General procedure for the synthesis of compounds (21-24)

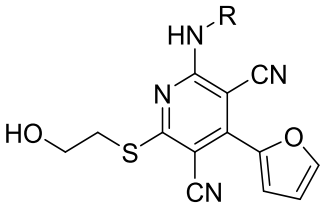

Procedure

An ecess of the suitable primary amine (2.00 mmol) was added to a solution of **85** (1.00 mmol) in DMF dry (0.5 ml) and the mixture was stirred at rt for 5-16 h. At reaction completion, water (40 ml) was added in order to afford a solid which was filtered and washed with Et_2O (5 ml).

Examples

2-(Cyclopropylamino)-4-(furan-2-yl)-6-((2-hydroxyethyl)thio)pyridine-3,5-dicarbonitrile (21)

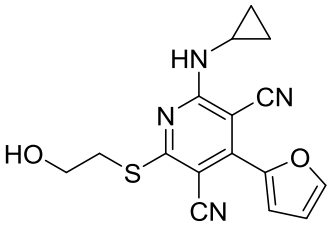

Yield: 91%; mp: 214-216°C (MeOH); ^{1}H NMR (400 MHz, DMSO-d_6): 8.29 (br s, 1H, NH, exc D_2O), 8.10 (s, 1H, Fur), 7.37 (d, *J* = 3.4 Hz, 1H, Fur), 6.84 (s, 1H, Fur), 5.01 (t, *J* = 5.4 Hz, 1H, OH, exc D_2O), 3.70 (dd, *J* = 12.1, 6.2 Hz, 2H, O-CH_2), 3.38

(t, *J* = 6.5 Hz, 2H, CH_2), 2.97 – 2.84 (m, 1H, CH *cyclopropyl*), 0.80 (m, 2H, CH *eq*), 0.75 – 0.61 (m, 2H, CH *ax*); IR (cm^{-1}): 3491, 3302, 2210

2-(Cyclopentylamino)-4-(furan-2-yl)-6-((2-hydroxyethyl)thio)pyridine-3,5-dicarbonitrile (22)

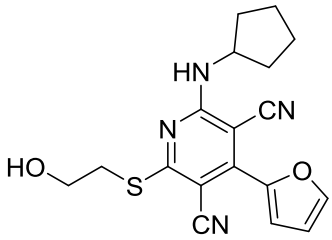

Yield: 89%; mp: 185-187°C (MeOH); ^{1}H NMR (400 MHz, DMSO-d_6): 8.10 (s, 1H, Fur), 7.83 (d, *J* = 6.8 Hz, 1H, NH, exc D_2O), 7.36 (d, *J* = 3.5 Hz, 1H, Fur), 6.82 (s, 1H, Fur), 5.03 (t, *J* = 5.3 Hz, 1H, OH, exc D_2O), 4.60 – 4.37 (m, 1H, CH *cyclopentyl*), 3.67 (dd, *J* = 12.1, 6.2 Hz, 2H, OCH_2), 3.31 (t, *J* = 6.2 Hz, 2H, SCH_2) 1.96 (dd, *J* = 10.6, 6.4 Hz, 2H, CH_2 *cyclopentyl*), 1.82 – 1.46 (m, 6H, $3CH_2$ *cyclopentyl*); ^{13}C NMR (100 MHz, DMSO-d_6): 168.59, 157.83, 145.56, 144.17, 116.73, 116.31, 116.07, 113.23, 89.74, 83.21, 59.98, 53.70, 33.33, 32.26, 24.29; IR (cm^{-1}): 3466, 3348, 2210

4-(Furan-2-yl)-2-((2-hydroxyethyl)thio)-6-((4-iodophenyl)amino)pyridine-3,5-dicarbonitrile (23)

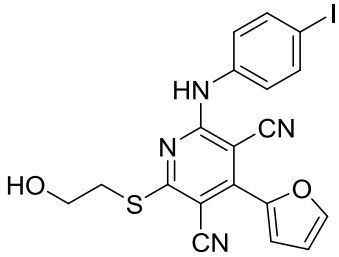

Yield: 99%; mp: 218-220°C (Acetone); ^{1}H NMR (400 MHz, DMSO-d_6): 9.93 (br s, 1H, NH, exc D_2O), 8.15 (s, 1H, Fur), 7.72 (d, *J* = 8.5 Hz, 2H, Ar), 7.45 (d, *J* = 3.5 Hz, 1H, Fur), 7.38 (d, *J* = 8.6 Hz, 2H, Ar), 6.96 – 6.78 (m, 1H, Fur), 4.96 (t, *J* = 5.8 Hz, 1H, OH, exc D_2O), 3.58 – 3.46 (m, 2H, OCH_2), 3.16 (t, *J* = 6.1 Hz, 2H, SCH_2); ^{13}C NMR (100 MHz, DMSO-d_6): 178.96, 168.75, 156.80, 145.36, 144.60, 138.22, 137.53, 126.43, 117.20, 115.92, 115.83, 113.36, 92.69, 89.73, 59.82, 33.60 ; IR (cm^{-1}): 3394, 3296, 2216

2-(Benzylamino)-4-(furan-2-yl)-6-((2-hydroxyethyl)thio)pyridine-3,5-dicarbonitrile (24)

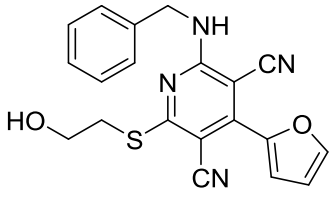

Yield: 86%; mp: 171-173°C (MeOH); ^{1}H NMR (400 MHz, DMSO-d_6): 8.80 (s, 1H, NH, exc D_2O), 8.11 (s, 1H, Fur), 7.40 (d, *J* = 3.5 Hz, 1H, Fur), 7.38 – 7.29 (m, 4H, Ar), 7.25 (s, 1H, Ar), 6.85 (s, 1H, Fur), 4.98 (t, *J* = 5.4 Hz, 1H, OH, exc D_2O), 4.70 (d, *J* = 5.4 Hz, 2H, $NHCH_2$), 3.48 (dd, *J* = 11.6, 5.9 Hz, 2H, OCH_2), 3.16 (t, *J* = 6.1 Hz, 2H, SCH_2); ^{13}C NMR (100 MHz, DMSO-d_6): 168.81, 158.22, 145.51, 144.02, 139.43, 128.80, 127.35, 116.83, 116.22, 116.08, 113.29, 90.03, 83.13, 59.74, 45.18, 33.42; IR (cm^{-1}): 3344, 2208

Synthesis of N-(3,5-dicyano-4-(furan-2-yl)-6-(phenylthio)pyridin-2-yl)acetamide (86)

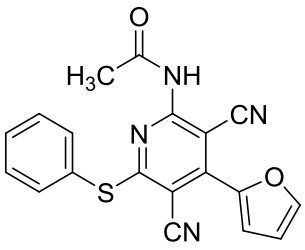

A solution of compound **74** (0.94 mmol) and dry pyridine (0.23 mmol) in acetic anhydride (21.16 mmol, 2 ml) was refluxed for 28h. After removal of the solvent under vacuum, a brown solid was obtained which was recovered with Et_2O and purified by silica gel column chromatography, eluting system CHX /EtOAc 7:3. Yield: 41%; mp: 213-215°C (EtOH); ^{1}H NMR (400 MHz, DMSO-d_6): 10.82 (s, 1H, NH, exc D_2O), 8.23 (d, *J* = 1.2 Hz, 1H, Fur), 7.69 – 7.62 (m, 2H, Ar), 7.54 (m, *J* = 15.1, 4.6 Hz, 3H, Ar), 6.92 (dd, *J* = 3.7, 1.8 Hz, 1H, Fur), 1.92 (s, 3H, CH_3); IR (cm^{-1}): 3358, 3147, 2216, 1705

Synthesis of N-(3,5-dicyano-4-(furan-2-yl)-6-mercaptopyridin-2-yl)acetamide (87)

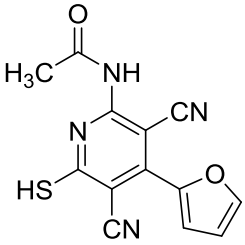

Sodium sulfide (1.19 mmol) was added to a solution of compound **86** (0.36 mmol) in dry DMF (0.5 ml), and the reaction mixture was heated at 80°C for 3h. Then, 0.1N HCl (25 ml) was added followed by addition of 6N HCl up to that a huge precipitate is formed. The solid was collected by filtration, washed with water (20 ml) and Et_2O (5 ml), and used for the next reaction without any further purification. Yield: 98%; ^{1}H NMR (400 MHz, DMSO-d_6): 12.99 (s, 1H, SH, exc D_2O), 8.19 (s, 1H, Fur), 7.50 (d, *J* = 3.4 Hz, 1H, Fur), 6.89 (s, 1H, Fur), 2.23 (s, 3H, CH_3)

Synthesis of N-(3,5-dicyano-4-(furan-2-yl)-6-((2-hydroxyethyl)thio)pyridin-2-yl)acetamide (25)

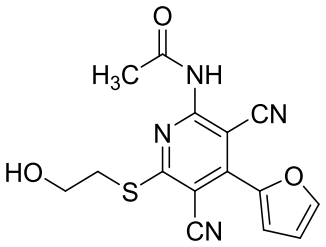

Sodium hydrogencarbonate (0.53 mmol) and 2-bromoethanol (0.39 mmol) were sequentially added to a stirred solution of compound **87** (0.35 mmol) in dry DMF (1 ml). The reaction mixture was kept at rt for 3h and then water was added affording a light brown solid which was filtered and washed with water (10 ml) and Et_2O (5 ml). The crude product was purified by preparative TLC using EtOAc as eluting system and then recrystallized. Yield: 20%; mp: 164-166°C (MeOH); ^{1}H NMR (400 MHz, DMSO-d_6): 11.13 (s, 1H, NH, exc D_2O), 8.21 (s, 1H, Fur), 7.53 (d, *J* = 3.6 Hz, 1H, Fur), 6.90 (dd, *J* = 3.6, 1.7 Hz, 1H, Fur), 5.07 (s, 1H, OH, exc D_2O), 3.70 (t, *J* = 6.2 Hz, 2H, OCH_2), 3.42 (t, *J* = 6.2 Hz, 2H, SCH_2), 2.21 (s, 3H, CH_3); ^{13}C NMR (100 MHz, DMSO-d_6): 169.37, 168.55, 155.12, 144.96, 144.30, 118.22, 115.22, 115.09, 113.76, 113.27, 98.59, 94.79, 59.69, 33.87, 24.06; IR (cm^{-1}): 3321, 2218, 1718

Synthesis of 3,6-diamino-5-cyano-4-(4-(cyclopropylmethoxy)phenyl)thieno[2,3-b]pyridine-2-carboxamide (68)

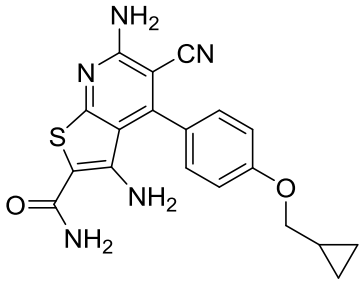

A solution of **BAY-606583** (0.71 mmol) and potassium hydroxide (1.42 mmol) in absolute EtOH (10 ml) was refluxed for 3h. After completion of the reaction, iced-water (30 ml) was added and the mixture was neutralized with 5N HCl, then the green solid was filtered and washed with water (10 ml) and Et_2O (5 ml). Yield: 85%; mp: 260-262°C (1,4-Dioxane); ^{1}H NMR (400 MHz, DMSO-d_6): 7.42 (d, 2H, J= 8 Hz, Ar); 7.28 (br s, 2H, NH_2, exc D_2O); 7.12 (d, 2H, J= 8.4 Hz, Ar); 6.97 (br s, 2H, NH_2, exc D_2O); 5.70 (s, 2H, NH_2 *amide*, exc D_2O); 3.91 (d, 2H, J= 6.8 Hz, OCH_2); 1.28-1.27 (m, 1H, CH), 0.66-0.51 (m, 2H, CH_2 *eq*), 0.44-0.27 (m, 2H, CH_2 *ax*); ^{13}C NMR (100 MHz, DMSO-d_6): 167.23, 163.83, 160.08, 158.93, 152.75, 146.75, 130.05, 125.74, 116.43, 115.29, 114.78, 93.36, 90.93, 72.71, 10.56; IR (cm^{-1}): 3466, 3452, 3346, 3315, 3136, 2214, 1629.

Synthesis of 3,6-diamino-5-cyano-4-(4-(cyclobutylmethoxy)phenyl)thieno[2,3-b]pyridine-2-carboxamide (69)

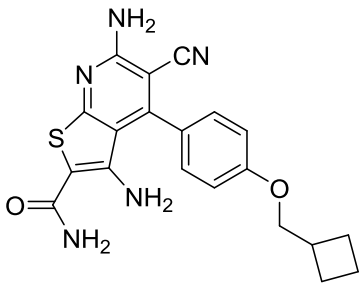

Equimolar amount of potassium carbonate and the suitable alkyl halide (4.61 mmol) were sequentially added to a solution of compound **142** (3.07 mmol) in dry acetone (20 ml). The mixture was heated at reflux for 98h. Then, the mixture was cooled to rt, filtered and the insoluble material was extracted with acetone (3 x 20 ml). The collected organic phases were evaporated under vacuum affording a solid which was recovered with water (40ml) and the mixture was extracted with DCM (4 x 25 ml), washed with brine (2 x 25 ml) and dried (Na_2SO_4). The solid obtained after removal of the solvent was purified by preparative TLC, eluting system EtOAc/CHX 6:4. Yield: 18%; mp: 260-262°C (Dioxane); ^{1}H NMR (400 MHz, $CDCl_3$): 7.37 (d, 2H, J= 8.4 Hz, Ar); 7.10 (d, 2H, J= 8.4 Hz, Ar); 5.90 (s, 2H, NH_2 *amide*, exc D_2O); 5.49 (s, 2H, NH_2, exc D_2O); 5.22 (s, 2H, NH_2, exc D_2O); 4.03 (d, 2H, J= 6.4 Hz, OCH_2); 2.88-2.82 (m, 1H, CH); 2.20-2.17 (m, 2H, CH_2); 2.05-1.90 (m, 4H, $2CH_2$); ^{13}C NMR (100 MHz, DMSO-d_6): 167.26, 163.82, 160.25, 158.92, 152.78, 146.78, 130.03, 125.72, 116,41, 115.31, 114.75, 93.31, 90.91, 72.02, 34.39, 18.56; IR (cm^{-1}): 3462, 3323, 3216, 3190, 2220, 1639

Synthesis of 2-amino-4-(furan-2-yl)-6-methoxypyridine-3,5-dicarbonitrile (83) (374)

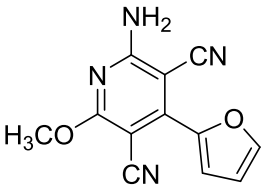

A solution of sodium methoxide (30.45 mmol) in MeOH (20 ml) was rapidly added to a solution of 2-furaldehyde (20.82 mmol), malononitrile (20.82 mmol) and tetrabutylammonium fluoride (2.08 mmol) in MeOH (10 ml) at rt. Then, further malononitrile (20.82 mmol) was added and the mixture was allowed to reflux for 3h. After completion, the reaction mixture was filtered over celite pad and the filtrate evaporated under vacuum. The crude residue was purified by silica gel column chromatography using DCM as eluent. Yield: 7%; mp: 205-207°C (EtOH); ^{1}H NMR (400 MHz, DMSO-d_6): 8.09 (s, 1H, Fur), 8.05 (br s, 2H, NH_2, exc D_2O), 7.38 (s, 1H, Fur), 6.83 (s, 1H, Fur), 3.97 (s, 3H, CH_3); IR (cm^{-1}): 3406, 3345, 3244, 2222

Synthesis of 2-amino-4-(furan-2-yl)-6-hydroxypyridine-3,5-dicarbonitrile (84)

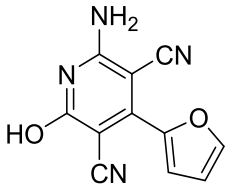

Compound **83** (1.41 mmol) was suspended in a mixture of glacial acetic acid (4 ml) and concentrated HCl (1 ml) and heated at 100°C for 2 h. Then, the reaction mixture was cooled at rt affording a precipitate which was collected by filtration, washed with water (20 ml) and Et_2O (5 ml) and dried in oven at 60°C. Yield: 81%; mp: 186-188°C (EtOH); ^{1}H NMR (400 MHz, DMSO-d_6): 11.85 (br s, 1H, OH, exc D_2O), 8.08 (d, *J* = 1.1 Hz, 1H, Fur), 7.72 (br s, 2H, NH_2, exc D_2O), 7.36 (d, *J* = 3.6 Hz, 1H, Fur), 6.82 (dd, *J* = 3.6, 1.7 Hz, 1H, Fur); IR (cm^{-1}): 3319, 3199, 2226, 2212

Synthesis of 2-amino-4-(furan-2-yl)-6-(2-hydroxyethoxy)pyridine-3,5-dicarbonitrile (20)

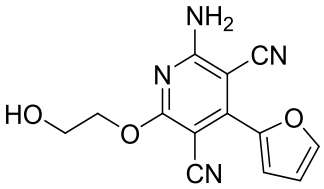

A sealed tube containing a mixture of compound **84** (0.53 mmol), 2-bromoethanol (0.58 mmol) and sodium hydrogencarbonate (0.79 mmol) in dry DMF (1 ml) was irradiated at 80°C in a microwave reactor for 3 h. After completion, water (30 ml) was added and the mixture was extracted with DCM (3 x 25 ml). The collected organic layers were washed with brine (2 x 20 ml), dried (Na_2SO_4) and evaporated under reduced pressure to yield a pale green solid that was purified by preparative TLC using DCM/MeOH 9:1 as eluent. Yield: 56%; mp: 207-209°C (EtOH); ^{1}H NMR (400 MHz, DMSO-d_6): 8.09 (s, 1H, Fur), 8.03 (br s, 2H, NH_2, exc D_2O), 7.38 (d, *J* = 3.5 Hz, 1H, Fur), 6.93 – 6.69 (m, 2H, Fur), 4.91 (t, *J* = 5.3 Hz, 1H, OH, exc D_2O), 4.54 – 4.17 (m, 2H, OCH_2), 3.73 (dd, *J* = 10.0, 5.2 Hz, 2H, CH_2OH); ^{13}C NMR (100 MHz, DMSO-d_6): 166.70, 162.20, 146.50, 145.86, 116.47, 116.36, 115.79, 113.19, 79.48, 69.52, 64.57, 59.40

Synthesis of 2-amino-6-chloro-4-phenylpyridine-3,5-dicarbonitrile (82) (301)

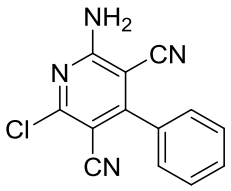

Malononitrile (15.13 mmol) was added in small portions to a solution of trimethylorthobenzoate (7.53 mmol) in dry pyridine (0.6 ml). The mixture was heated at 100°C for 6 h and then cooled in ice bath. Concentrated HCl (2.7 ml) was carefully added and the mixture was heated again at 100°C for 2h. After cooling to rt, the resulting precipitate was collected by filtration, suspended in a saturated aqueous solution of sodium hydrogencarbonate, re-filtered and finally washed with water (10 ml). Yield: 61%; mp: >300°C (MeOH); ^{1}H NMR (400 MHz, DMSO-d_6): 7.57-7.61 (m, 5H, Ar), 8.27 (br s ,1H, NH_2, exc D_2O), 8.68 (br s, 1H, NH_2, exc D_2O); IR (cm^{-1}): 3356, 3179, 2225, 1660, 1564

General procedure for synthesis of 6-amino substituted compounds 19,36

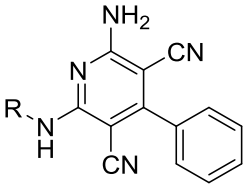

Procedure

Equimolar amount of the suitable primary amine and triethylamine (2.00 mmol) were added to a solution of compound **82** (1.00 mmol) in a mixture THF/EtOH (2:1, 10.5 ml) and the reaction was refluxed for 1.5-6 h. Then, water (20 ml) was added affording a precipitate which was collected by filtration and washed with Et_2O (5 ml).

Examples

2-Amino-6-((2-hydroxyethyl)amino)-4-phenylpyridine-3,5-dicarbonitrile (19)

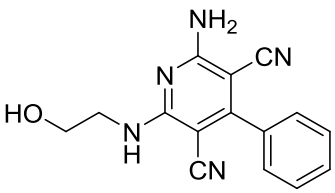

Yield: 22%; mp: 230-231°C (EtOH); ^{1}H NMR (400 MHz, DMSO-d_6): 7.55-7.53 (m, 3H, Ar), 7.47-7.45 (m, 2H, Ar), 7.37 (br s, 2H, NH_2, exc D_2O), 7.20 (t, *J* = 5.1 Hz, 1H, NH, exc D_2O), 4.74 (t, *J* = 5.2 Hz, 1H, OH, exc D_2O), 3.54 (q, *J* = 10.8 Hz, 2H, $NHCH_2$), 3.47 (t, *J* = 5.8 Hz, 2H, OCH_2); IR (cm^{-1}): 3472, 3345, 3223, 2204.

2-(((1H-Imidazol-2-yl)methyl)amino)-6-amino-4-phenylpyridine-3,5-dicarbonitrile (36)

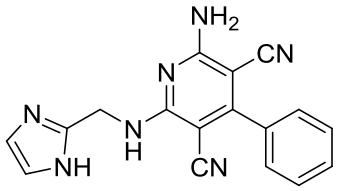

Yield: 57%; mp: 208-210°C (EtOH); ^{1}H NMR (400 MHz, DMSO-d_6): 11.64 (br s, 1H, NH *imidazole*, exc D_2O), 8.38 (br s, 2H, NH_2, exc D_2O), 7.88 (t, *J* = 5.5 Hz, 1H, NH, exc D_2O), 7.61-7.45 (m, 5H, Ar), 7.04 (s, 1H, CH *imidazole*), 6.83 (s, 1H, CH *imidazole*), 4.56 (d, *J* = 5.5 Hz, 2H, CH_2); IR (cm^{-1}): 3360, 3322, 3186, 2207.

Synthesis of 2-amino-4-(furan-2-yl)-6-((2-hydroxyethyl)amino)pyridine-3,5-dicarbonitrile (17)

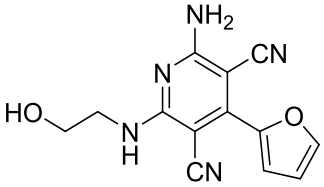

A solution of compound **74** (0.47 mmol) and 2-aminoethanol (1.88 mmol) in DMF (2 ml) was heated at 100°C for 4h. After cooling at rt, water (10 ml) was added and the resulting precipitate was filtered and washed with water (10 ml) and Et_2O (5 ml). Yield: 92%; mp: 230-232°C (EtOH); ^{1}H NMR (400 MHz, DMSO-d_6): 8.03 (d, *J* = 0.96 Hz, 1H, Fur), 7.33 (br s, 2H, NH_2, exc D_2O), 7.24 (d, *J* = 0.56 Hz, 1H, Fur), 7.19 (t, *J* = 5.36 Hz, 1H, NH, exc D_2O), 6.78 (dd, *J* = 3.5, 1.7 Hz, 1H, Fur), 4.76 (t, 1H, OH, exc D_2O), 3.54 (q, *J* = 11 Hz, 2H, $NHCH_2$), 3.47 (q, *J* = 11 Hz, 2H, OCH_2); IR (cm^{-1}): 3334, 2204.

Synthesis of 2-amino-6-((2-hydroxyethyl)amino)-4-(thiophen-2-yl)pyridine-3,5-dicarbonitrile (18)

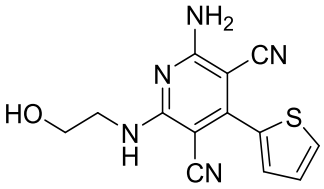

A solution of compound **76** (0.60 mmol) and 2-aminoethanol (2.40 mmol) in DMF (2 ml) was heated at 100°C for 2h. After cooling at rt, water (10 ml) was added and the resulting precipitate was filtered, washed with water (10 ml) and Et_2O (5 ml) and recrystallized from EtOH. Yield: 88%; 220-222°C (EtOH); ^{1}H NMR (400 MHz, DMSO-d_6): 7.87 (d, *J* = 4.7 Hz, 1H, CH *thiophene*), 7.47 (d, *J* = 1.6 Hz, 1H, CH *thiophene*), 7.42 (br s, 2H, NH_2, exc D_2O), 7.26-7.22 (m, 2H, NH + CH *thiophene*, partially exc D_2O), 4.74 (t, *J* = 5.1 Hz, 1H, OH, exc D_2O), 3.54 (q, *J* = 10.9 Hz, 2H, $NHCH_2$), 3.48 (q, *J* = 10.9, 2H, OCH_2); IR (cm^{-1}): 3491, 3451, 3338, 2202.

Synthesis of ethyl 2-cyano-3,3-bis(methylthio)acrylate (143) (375)

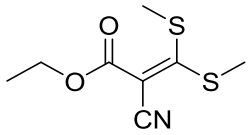

Potassium carbonate (100 mmol) was added to a solution of ethyl cyanoacetate (100 mmol) in DMF dry (95 ml) and the mixture was allowed to stir at rt for 3h under nitrogen atmosphere. Then, carbon disulfide (300 mmol) was slowly dropped in the reaction mixture and the suspension stirred again for 2h before adding methyl iodide (200 mmol) and stirring at rt overnight. Then, addition of water (400 ml) while strong stirring yielded a solid that was collected by filtration and dried in desiccator. Yield: 88%; ^{1}H NMR (400 MHz, DMSO-d_6): 4.21 (q, *J* = 7.1 Hz, 2H CH_2), 2.73 (s, 3H, SCH_3), 2.62 (s, 3H, SCH_3), 1.25 (t, *J* = 7.1 Hz, 3H CH_3); IR (cm^{-1}): 3262, 2207, 1697

Synthesis of 4-(methylthio)-2-oxo-6-phenyl-2H-pyran-3-carbonitrile (144) (317)

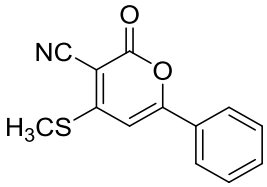

Compound **143** (4.87 mmol) and acetophenone (6.33 mmol) were sequentially added to a suspension of potassium hydroxide (5.84 mmol) in DMSO dry (20 ml). The reaction mixture was allowed to stir at rt for 5h. When the reaction was completed, iced water (70 ml) was added and the mixture was stirred for 2h to afford a yellow solid that was collected by filtration, washed with water (100 ml) and dried in oven at 60°C overnight. Yield: 56%; ^{1}H NMR (400 MHz, DMSO-d_6): 8.06 (d, *J* = 7.3 Hz, 2H, Ar), 7.74 – 7.49 (m, 3H, Ar), 7.26 (s, 1H, Ar), 2.85 (s, 3H, SCH_3).

Synthesis of 2-(5-phenyl-1H-pyrazol-3-yl)acetonitrile (145) (376)

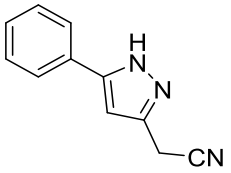

A solution of compound **144** (1.43 mmol) and hydrazine monohydrate (2.16 mmol) in pyridine (25 ml) was heated at reflux for 2.5h. The solvent was then removed under vacuum and the residue was recovered with $CHCl_3$ (50 ml). The organic phase was washed with water (2 x 25 ml), dried (Na_2SO_4) and the solvent evaporated under reduced pressure. The brown residue was triturated with petroleum ether (5 ml) and EtOH (1 drop) and recovered by filtration. Yield: 71%; ^{1}H NMR (400 MHz, DMSO-d_6): 13.31 (br s, 1H, exc D_2O, NH), 7.74 (d, *J* = 7.5 Hz, 2H, Ar), 7.46 (t, *J* = 7.3 Hz, 2H, Ar), 7.41 – 7.32 (m, 1H, Ar), 6.68 (s, 1H, CH *pyrazole*), 4.00 (s, 2H, CH_2). IR (cm^{-1}): 3135, 3113, 2250.

Synthesis of tert-butyl 3-(cyanomethyl)-5-phenyl-1H-pyrazole-1-carboxylate (146)

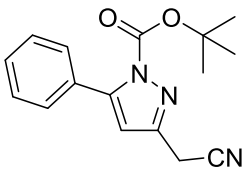

Dry TEA (5.97 mmol), dimethylaminopyridine (0.35 mmol) and BOC-anhydride (2.63 mmol) were added to a stirred solution of compound **145** (1.76 mmol) in dry ACN at 0°C. After reagent addition, the mixture was allowed to warm to rt and stirred for 1h. Then, brine (10 ml) was added and the mixture extracted with EtOAc (3 x 5 ml). The collected organic phases were dried (Na_2SO_4) and the solvent removed under vacuum, leading to a red residue which was triturated with Et_2O and filtered to yield a light brown solid, used for the next step without any further purification. Yield: 86%; ^{1}H NMR (400 MHz, DMSO-d_6): 7.90 (d, *J* = 7.0 Hz, 2H, Ar), 7.53 – 7.37 (m, 3H, Ar), 7.08 (s, 1H, CH *pyrazole*), 4.39 (s, 2H, CH_2), 1.63 (s, 9H, CH_3 *t-Bu*).

Synthesis of tert-butyl 3-(1-cyano-2,2-bis(methylthio)vinyl)-5-phenyl-1H-pyrazole-1-carboxylate (147)

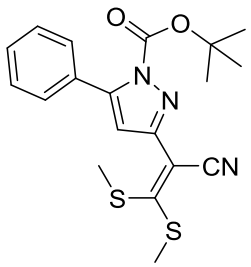

Compound **146** (3.52 mmol) was dissolved in dry DMSO (20 ml) at 0°C and carbon disulfide (7.94 mmol), methyl iodide (14.12 mmol) were added and followed by the portion wise addition of sodium hydride (7.06 mmol, 60% in mineral oil) while keeping the temperature under 10°C. After 30min at 5°C, the mixture was warmed to rt and stirred for 3h. Then, the mixture was transferred into a 250 ml round bottomed flask and a saturated solution of ammonium chloride (20 ml) was added, followed by addition of cold water (150 ml). The mixture was stirred until an orange gluey solid is formed, then the aqueous layer was removed by decantation. The residue was suspended in 2-propanol and after few minutes of stirring an off-white solid precipitated which was collected by filtration. Yield: 61%; ^{1}H NMR (400 MHz, DMSO-d_6): 7.91 (d, *J* = 6.9 Hz, 2H, Ar), 7.55-7.37 (m, 3H, Ar), 7.31 (s, 1H, CH *pyrazole*), 2.65 (s, 3H, SCH_3), 2.39 (s, 3H, SCH_3), 1.60 (s, 9H, CH_3 *t-Bu*).

Synthesis of 3,3-bis(methylthio)-2-(5-phenyl-1H-pyrazol-3-yl)acrylonitrile (148)

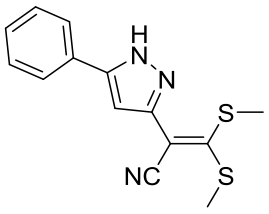

Compound **147** (0.77 mmol) was allowed to stir in of a 10% solution of trifluoroacetic acid in DCM dry (25 ml) for 1,5h. Then, the solvents were removed under reduced pressure affording a brown solid that was triturated with a saturated solution of sodium bicarbonate (25 ml), collected by filtration and dried in oven at 60°C. Yield: 93%; ^{1}H NMR (400 MHz, DMSO-d_6): 13.70 (br s, 1H, NH), 7.79 (d, *J* = 7.5 Hz, 2H, Ar), 7.47 (t, *J* = 7.5 Hz, 2H, Ar), 7.38 (t, *J* = 7.4 Hz, 1H, Ar), 7.04 (s, 1H, CH *pyrazole*), 2.59 (s, 3H, SCH_3), 2.50 (s, 3H, overlapping with DMSO-d_6, SCH_3).

Synthesis of 7-amino-5-(methylthio)-2-phenylpyrazolo[1,5-c]pyrimidine-4-carbonitrile (149)

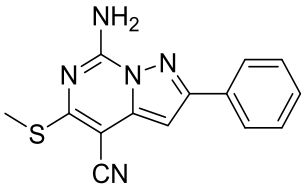

A solution of compound **148** (2.78 mmol), cyanamide (8.35 mmol) and paratoluensulfonic acid (2.78 mmol) in NMP (3 ml) was irradiated with microwave at 160°C for 1h (4 x 15 min cycle). At the end of each irradiation cycle, cyanamide (8.35 mmol) was added. The reaction mixture was diluted with water (200 ml) and stirred for 5h to afford a solid that was collected by filtration and extracted with acetone (50 ml). The solvent was evaporated under reduced pressure affording a yellow solid that was recovered with petroleum ether (10 ml). Yield: 89%; mp: 104-106°C (MeOH); ^{1}H NMR (400 MHz, DMSO-d_6): 8.95 (br s, 1H, NH_2, exc D_2O), 8.52 (br s, 1H, NH_2, exc D_2O), 8.10 (d, *J* = 6.9 Hz, 2H, Ar), 7.48 (m, 3H, Ar), 6.96 (s, 1H, CH *pyrazole*), 2.63 (s, 3H, SCH_3). IR (cm^{-1}): 3319, 2204.

Synthesis of 7-amino-5-(methylsulfonyl)-2-phenylpyrazolo[1,5-c]pyrimidine-4-carbonitrile (150)

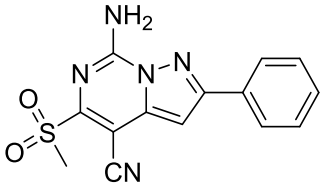

3-Chloroperoxybenzoic acid (4.53 mmol) was added to a solution of compound **149** (1.81 mmol) in DCM dry (40 ml) at 0°C. The mixture was allowed to stir at 0 – 5°C for 2h and then at rt for further 5h. The solvent was then removed under vacuum at rt and a 5% sodium bicarbonate solution (25 ml) was added to the residue. The mixture was stirred for 20 min and the resulting solid was filtered and washed with water (20 ml) and petroleum ether (10 ml) affording a brown powder which was dried in oven at 60°C. Yield: 86%; (MeOH); ^{1}H NMR (400 MHz, DMSO-d_6): 9.35 (br s, 1H, NH_2, exc D_2O), 8.90 (br s, 1H, NH_2, exc D_2O), 8.18 (dd, *J* = 11.3, 4.4 Hz, 2H, Ar), 7.61 – 7.41 (m, 4H, Ar + *pyrazole*), 3.36 (s, 3H, SO_2CH_3).

General procedure for the synthesis of compound (70-73)

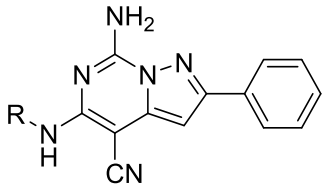

Procedure

A solution of compound **150** (1.00 mmol), the suitable primary amine (7.1 mmol) and N,N-diisopropylethylamine (4.1 mmol) in anhydrous dioxane (10 ml) was heated at 90°C for 24-48 h. After completion, the reaction mixture was allowed to cool at rt and water (40 ml) was added. Extraction was performed with EtOAc (3 x 20 ml) and the collected organic phases were washed with brine (2 x 20 ml), dried (Na_2SO_4), and evaporated under vacuum to yield the final compounds which were purified by silica gel column chromatography or by recrystallization.

Examples

7-Amino-5-(benzylamino)-2-phenylpyrazolo[1,5-c]pyrimidine-4-carbonitrile (70)

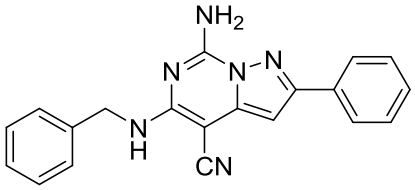

Yield: 84%; mp:245-247°C (EtOH); ^{1}H NMR (400 MHz, DMSO-d_6): 8.43 (br s, 1H, NH_2, exc D_2O), 8.02 (dt, *J* = 3.3, 1.9 Hz, 2H, Ar), 7.98 (br s, 1H, NH_2, exc D_2O), 7.79 (t, *J* = 6.1 Hz, 1H, NH, exc D_2O), 7.51 – 7.39 (m, 3H, Ar), 7.39 – 7.28 (m, 4H, Ar), 7.28 – 7.18 (m, 1H, Ar), 6.55 (s, 1H, CH), 4.63 (d, *J* = 6.1 Hz, 2H, CH_2); ^{13}C NMR (100 MHz, DMSO-d_6): 157.90, 155.73, 148.69, 144.17, 140.68, 132.47, 129.61, 129.15, 128.66, 127.80, 127.10, 126.93, 118.03, 90.60, 60.25, 44.42; IR (cm^{-1}): 3222, 3136, 2251

7-Amino-5-((3-methoxybenzyl)amino)-2-phenylpyrazolo[1,5-c]pyrimidine-4-carbonitrile (71)

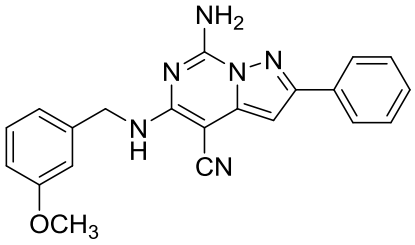

Yield: 79%; mp: 198-200°C (MeOH); ^{1}H NMR (400 MHz, DMSO-d_6): 8.43 (br s, 1H, NH_2, exc D_2O), 8.07 – 7.99 (m, 2H, Ar), 7.96 (br s, 1H, NH_2, exc D_2O), 7.75 (t, *J* = 6.2 Hz, 1H, NH, exc D_2O), 7.53 – 7.37 (m, 3H, Ar), 7.29 – 7.19 (m, 1H, Ar), 6.94 (d, *J* = 7.4 Hz, 2H, Ar), 6.80 (dd, *J* = 9.1, 1.6 Hz, 1H, Ar), 6.55 (s, 1H, CH), 4.59 (d, *J* = 6.1 Hz, 2H, CH_2), 3.74 (s, 3H, CH_3); ^{13}C NMR (100 MHz, DMSO-d_6): 159.68, 157.86, 155.73, 148.66, 144.14, 142.31, 132.46, 129.76, 129.60, 129.16, 126.93, 119.96, 118.02, 113.59, 112.44, 90.62, 55.40, 44.37; IR (cm^{-1}): 3203, 3100, 2251

7-Amino-5-((furan-2-ylmethyl)amino)-2-phenylpyrazolo[1,5-c]pyrimidine-4-carbonitrile (72)

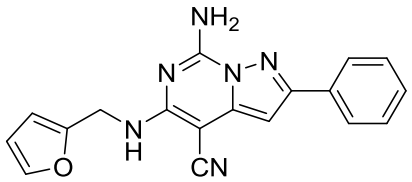

Column chromatography eluent CHx 1 : EtOAc 1; Yield: 55%; mp: 206-208°C (EtOAc); ^{1}H NMR (400 MHz, DMSO-d_6): 8.49 (br s, 1H, NH_2, exc D_2O), 8.19 – 7.86 (m, 3H, Ar + NH_2, partially exc D_2O), 7.67 (t, *J* = 5.9 Hz, 1H, NH, exc D_2O), 7.57 (d, *J* = 0.9 Hz, 1H, Fur), 7.52 – 7.36 (m, 3H, Ar), 6.56 (s, 1H, CH), 6.40 (dd, *J* = 3.1, 1.8 Hz, 1H, Fur), 6.32 (d, *J* = 3.0 Hz, 1H, Fur), 4.59 (d, *J* = 5.8 Hz, 2H, CH_2); ^{13}C NMR (100 MHz, DMSO-d_6): 157.64, 155.73, 153.45, 148.63, 144.05, 132.43, 129.61, 129.15, 126.92, 117.84, 110.91, 107.46, 90.14, 38.09; IR (cm^{-1}): 3304, 3188, 3150, 2199

7-Amino-5-(phenethylamino)-2-phenylpyrazolo[1,5-c]pyrimidine-4-carbonitrile (73)

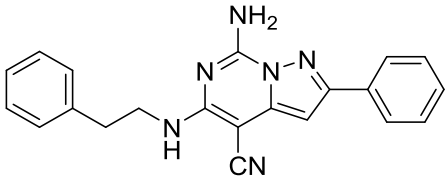

Yield: 60%; mp: 232-234°C (MeOH); ^{1}H NMR (400 MHz, DMSO-d_6): 8.43 (br s, 1H, NH_2, exc D_2O), 8.02 (d, *J* = 7.6 Hz, 2H, Ar), 7.97 (br s, 1H, NH_2, exc D_2O), 7.45 (dt, *J* = 21.6, 7.1 Hz, 3H, Ar), 7.37 – 7.15 (m, 6H, Ar + NH, partially exc D_2O), 6.53 (s, 1H, CH), 3.61 (dd, *J* = 14.6, 6.2 Hz, 2H, N-CH_2), 2.95 – 2.82 (m, 2H, CH_2-Ph); ^{13}C NMR (100 MHz, DMSO-d_6): 157.88, 155.65, 148.68, 144.21, 139.97, 132.50, 129.57, 129.24, 129.13, 128.75, 126.90, 126.52, 118.09, 90.27, 43.20, 36.05; IR (cm^{-1}): 3333, 3157, 2193

10. Visiting period at Università Bonn

During my Ph.D. course I spent six months at Università Bonn, Pharmazeutische Chemie I department in the group of Professor Christa E. Müller under the supervision of Dr. Thanigaimalai Pillayiar. For many years, the group of Professor Müller has been specialized on the study of GPCRs and in particular on purinergic signaling. Recently, one of the most important aim of the group has been the deorphanization of the so called orphan receptors. In particular, the completion of the human genome sequencing project has identified approximately 720 genes that belong to the GPCR superfamily. Approximately half of these genes are thought to encode sensory receptors. Of the remaining 360 receptors, the natural ligand has been identified for approximately 210 receptors, leaving 150 so-called orphan GPCRs with no known ligand or function (377). The identification of ligands active at orphan GPCRs has been achieved through the development of a number of experimental approaches, including the screening of putative small molecule and peptide ligands, reverse pharmacology, and the use of bioinformatics to predict candidate ligands (378). Following expression, candidate ligands are screened against the receptor to identify molecules capable of specific regulation of that receptor. Such ligands can include tissue extracts, expressed or purified proteins or small peptides, natural and synthetic small molecules, and lipids. Once a candidate ligand is identified, further studies are performed to confirm that the activity of the ligand is specific to the receptor. In recent years, small-molecule, peptide, protein, and lipid ligands have been identi- fied for many orphan GPCRs. However, approximately 160 orphan GPCRs remain for which there is no known ligand. Efforts continue to identify ligands for these receptors, however, it is now necessary to investigate alternative strategies. Such studies may involve the identification of new ligands using bioinformatics to predict likely peptide or protein ligands. It may be that the remaining orphan GPCRs are atypical in that they do not signal through heterotrimeric G-proteins. If this is the case, then the assays used to date, which all rely upon G-protein activation of a signal transduction cascade, cannot be used for these receptors. In support of this hypothesis, there is an emerging literature describing G-protein-independent signaling by GPCRs. The identification of ligands at such receptors depends on the development of new assays. It is also possible that not all of these receptors will have ligands; receptors have been identified that act as trafficking factors, are believed to act as ligand sinks, and exhibit constitutive signaling in the absence of ligand. The challenge in the coming years is to identify the biological function of the remaining orphan GPCRs.

MrgX-4 is an orphan G-protein coupled receptor (GPCR) that belongs to a family called MAS-related genes (Mgrs) (379). This GPCRs family takes its name from the first receptor discovered, MAS1 oncogene that is activated by binding angiotensin (1-7): it mediates a range of effect mostly opposed to the activation of angiotensin-II activated angiotensin receptor. MrgX-4 belongs to a class of receptors (MrgX1-7) which seems

to be selectively expressed in the small-diameter sensory neurons of dorsal root ganglia: this is one of the nowadays known evidences that lead to expect a promising involvement in neuropathic pain for this class of GPCRs. Besides, this family has not been found in rodents, making a deepening of the physiopatholgical role more complicated. MrgX receptors were cloned from rhesus monkey and functionally characterized alongside their human orthologues. Most of the human and rhesus MrgX receptors displayed high constitutive activity in a cellular proliferation assay. Proliferative responses mediated by human or rhesus MrgX-1, or rhesus MrgX-2 were partially blocked by pertussis toxin (PTX). Proliferative responses mediated by rhesus MrgX-3 and both human and rhesus MrgX-4 were PTX insensitive. These results indicate that human and rhesus MrgX-1 and MrgX-2 receptors activate both G_q- and G_i-regulated pathways, while MrgX-3 and MrgX-4 receptors primarily stimulate G_q-regulated pathways (379). The aim of my work was synthesizing agonist at MrgX-4 through a synthetic pathway partially shown in figure I. Neither complete synthesis (scheme 23), nor the twelve synthesized compounds and related pharmacological data can be showed in this thesis, in order to safeguard a future patent application or future pubblications.

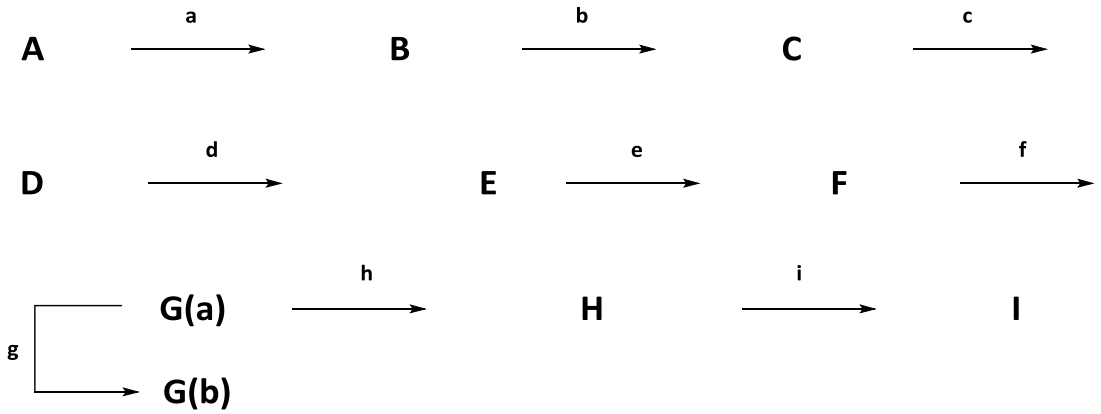

(a) HMDS, $(NH_4)_2SO_4$, reflux, 60-70 °C, I_2, alkylbromide , 120 °C, 2 h, $NaHCO_3$, 70-75%; (b) Aq. AcOH, HNO_2, 60-65 °C, 68-75%; (c) Aq-NH_3 (15% or 25%), $Na_2S_2O_3$, 70 °C, 50-70 %; (d) R-COOH, ethyldicarbodiimide HCl, Methanol, 24 h, rt, 70-85%; (e) 3-iodopropyl acetate, K_2CO_3, DMF, rt, 24 h, 60-70%; (f) P_2O_5, DMF, 100 °C, 10-30 min, 70-80%; (g) CH_3I, K_2CO_3, DMF, rt, 24 h, 80-90%; (h) KOH/methanol/H_2O, 90-100% ; (i) $PO(OMe)_3/POCl_3$, rt, 30 min, H_2O, 60-80%.

Scheme 23

References

1. **Fredholm B. B., et al.** International union of pharmacology. XXV. Nomenclature and classification of adenosine receptors. *Pharmacol. Rev.* 2001, Vol. 53, pp. 527–552.

2. **Fredholm B.B., et al.** Fredholm BB, et al. International Union of Basic and Clinical Pharmacology. LXXXI. Nomenclature and classification of adenosine receptors — an update. *Pharmacol. Rev.* 2011, Vol. 63, pp. 1-34.

3. **Eltzschig H.K., et al.** Purinergic signaling during inflammation. *N. Engl. J. Med.* 2012, Vol. 367, pp. 2322–2333.

4. **Eltzschig H.K.** Adenosine: an old drug newly discovered. *Anesthesiology.* 2009, Vol. 111, pp. 904–915.

5. **Grenz A., et al.** Equilibrative nucleoside transporter 1 (ENT1) regulates postischemic blood flow during acute kidney injury in mice. *J. Clin. Invest.* 2012, Vol. 122, pp. 693–710.

6. **Sun D., et al.** Mediation of tubuloglomerular feedback by adenosine: evidence from mice lacking adenosine 1 receptors. *Proc. Natl. Acad. Sci.* 2001, Vol. 98, pp. 9983–9988.

7. **Rosenberger P., et al.** Hypoxia-inducible factor-dependent induction of netrin-1 dampens inflammation caused by hypoxia. *Nature Immunol.* 2009, Vol. 10, pp. 195–202.

8. **Huang Z.L., et al.** Adenosine A2A, but not A1, receptors mediate the arousal effect of caffeine. *Nature Neurosci.* 2005, Vol. 8, pp. 858–859.

9. **Lazarus M., et al.** Arousal effect of caffeine depends on adenosine A2A receptors in the shell of the nucleus accumbens. *J. Neurosci. Off. J. Soc. Neurosci.* 2011, Vol. 31, pp. 10067-10075.

10. **Liu X.L., et al.** Genetic inactivation of the adenosine A2A receptor attenuates pathologic but not developmental angiogenesis in the mouse retina. *Invest. Ophthalmol. Vis. Sci.* 2010, Vol. 51, pp. 6625–6632.

11. **Haskò G., et al.** Adenosine receptors: therapeutic aspects for inflammatory and immune diseases. *Nat. Rev. Drug Discov.* 2008, Vol. 7, pp. 759-770.

12. **Eltzschig H.K., et al.** Hypoxia and inflammation. *N. Engl. J. Med.* 2011, Vol. 364, pp. 656–665.

13. —. Ischemia and reperfusion — from mechanism to translation. *Nature Med.* 2011, Vol. 17, pp. 1391–1401.

14. **Fredholm B.B.** Adenosine, an endogenous distress signal, modulates tissue damage and repair. *Cell Death Differ.* 2007, Vol. 14, pp. 1315–1323.

15. **Delacretaz E.** Clinical practice. Supraventricular tachycardia. *N. Engl. J. Med.* 2006, Vol. 354, pp. 1039–1051.

16. **Jacobson K.A., et al.** Adenosine receptors as therapeutic targets. *Nat Rev Drug Discov.* 2006, Vol. 5, pp. 247-264.

17. **Fredholm B., et al.** Actions of adeosine at its receptors in the CNS: insights from knckouts and drugs. *Annu. Rev. Pharmacol. Toxicol.* 2005, Vol. 45, pp. 385–412.

18. **Massie B.M., et al.** Rolofylline, an adenosine A1-receptor antagonist, in acute heart failure. *N. Engl. J. Med.* 2010, Vol. 363, pp. 1419-1428.

19. **Teerlink J.R., et al.** The safety of an adenosine A1-receptor antagonist, rolofylline, in patients with acute heart failure and renal impairment: findings from PROTECT. *Drug Saf.* 2012, Vol. 35, pp. 233-244.

20. **Müller C. E., et al.** Medicinal chemistry of adenosine, P2Y and P2X receptors. *Neuropharmacology.* 2016, Vol. 104, pp. 31-49.

21. **Sun Y., et al.** Schematic presentation of the role of A2BAR invarious human diseases. *Frontiers in Chemistry.* 2016, Vol. 4, 37.

22. **Ballesteros J.A., et al.** Integrated methods for the construction of three-dimensional models and computational probing of structure-function relations in G protein coupled receptors. *Meth. Neurosci.* 1995, Vol. 25, pp. 366-428.

23. **Fredriksson, R., et al.** The G-protein-coupled receptors in the human genome form five main families. Phylogenetic analysis, paralogon groups, and fingerprints. *Mol. Pharmacol.* 2003, Vol. 63 (6), pp. 1256-1272.

24. **Howard A.D., et al.** Orphan G-protein-coupled receptors and natural ligand discovery. *Trends Pharmacol. Sci.* 2001, Vol. 22 (3), pp. 132-140.

25. **Ji T.H., et al.** G protein-coupled receptors. I. Diversity of receptor-ligand interactions. *J. Biol. Chem.* 1998, Vol. 273 (28), pp. 17299-17302.

26. **Pin J.P., et al.** Evolution, structure, and activation mechanism of family 3/C G-protein coupled receptors. *Pharmacol. Ther.* 2003, Vol. 98 (3), pp. 325-354.

27. **Knoflach F., et al.** Positive allosteric modulators of metabotropic glutamate 1 receptor: characterization, mechanism of action, and binding site. *Proc. Natl. Acad. Sci. USA.* 2001, Vol. 98 (23), pp. 13402-13407.

28. **Carroll F.Y., et al.** BAY36-7620: a potent non-competitive mGlu1 receptor antagonist with inverse agonist activity. *Mol. Pharmacol.* 2001, Vol. 59 (5), pp. 965-973.

29. **Pagano A., et al.** The non-competitive antagonists 2-methyl-6-(phenylethynyl)pyridine and 7-hydroxyiminocyclopropan[b]chromen-1a-carboxylic acid ethyl ester interact with overlapping binding pockets in the transmembrane region of group I metabotropic glutamate receptors. *J. Biol. Chem.* 2000, Vol. 275 (43), pp. 33750-33758.

30. **Pin G.P., et al.** The activation mechanism of class-C G-protein coupled receptors. *Biol. Cell.* 2004, Vol. 69 (5), pp. 335-342.

31. **Kunishima N., et al.** Structural basis of glutamate recognition by a dimeric metabotropic glutamate receptor. *Nature.* 2000, Vol. 407 (6807), pp. 971-977.

32. **Tsuchiya D., et al.** Structural views of the ligand-binding cores of a metabotropic glutamate receptor complexed with an antagonist and both glutamate and Gd3+. *Proc. Natl. Acad. Sci. USA.* 2002, Vol. 99(5), pp. 2660–2665.

33. **Angers S., et al.** Dimerization: an emerging concept for G protein-coupled receptor ontogeny and function. *Annu. Rev. Pharmacol. Toxicol.* 2002, Vol. 42, pp. 409–435.

34. **Mesnier D., et al.** Cooperative conformational changes in a G-protein-coupled receptor dimer, the leukotriene B(4) receptor BLT1. *J. Biol. Chem.* 2004, Vol. 279 (48), pp. 49664–49670.

35. **Burnstock G.** Purinergic Nerves. *Pharmacol. Rev.* 1972, Vol. 24, pp. 509-581.

36. **Westfall D. P., et al.** Direct Evidence against a Role of ATP as the Nonadrenergic, Noncholinergic Inhibitory Neurotransmitter in Guinea Pig Tenia Coli. *Proc. Natl. Acad. Sci. U.S.A.* 1982, Vol. 79, pp. 7041-7045.

37. **Abbracchio M. P., et al.** Puringergic signaling in the nervous system: an overview. *Trends Neurosci.* 2009, Vol. 32, pp. 19-29.

38. **Pankratov Y., et al.** Quantal release of ATP in mouse cortex. *J. Gen. Physiol.* 2007, Vol. 129, pp. 257–265.

39. **Bowser D.N., et al.** Vesicular ATP is the predominant cause of intercellular calcium waves in astrocytes. *J. Gen. Physiol.* 2007, Vol. 129, pp. 485–491.

40. **Zhang Z., et al.** Regulated ATP release from astrocytes through lysosome exocytosis. *Nat. Cell Biol.* 2007, Vol. 9, pp. 945–953.

41. **Vasiliou V., et al.** Human ATP-Binding Cassette (ABC) transporter family. *Hum. Genomics.* 2009, Vol. 3, pp. 281–290.

42. **Scemes E., et al.** Connexin and pannexin mediated cell-cell communication. *Neuron Glia Biol.* 2007, Vol. 3, pp. 199–208.

43. **Okada S.F., et al.** Voltage-Dependent Anion Channel-1 (VDAC-1) contributes to ATP release and cell volume regulation in murine cells. *J. Gen. Physiol.* 2004, Vol. 124, pp. 513–526.

44. **Schwarz N., et al.** Activation of the P2X7 ion channel by soluble and covalently bound ligands. *Purinergic Signal.* 2009, Vol. 5, pp. 139–149.

45. **Lazarowski E.R., et al.** Vesicular and conductive mechanisms of nucleotide release. *Purinergic Signal.* 2012, Vol. 8, pp. 359–373.

46. **Jacobson K.A.** Structure-based approaches to ligands for G-protein-coupled adenosine and P2Y receptors, from small molecules to nanoconjugates. *J. Med. Chem.* 2013, Vol. 56, pp. 3749-3767.

47. **Dale N., et al.** Release of adenosine and ATP during ischemia and epilepsy. *Curr. Neuropharmacol.* 2009, Vol. 7, pp. 160–179.

48. **Sitkovsky M. V.** T regulatory cells: hypoxia-adenosinergic suppression and re-direction of the immune response. *Trends Immunol.* 2009, Vol. 30, pp. 102–108.

49. **Klotz K. N.** Adenosine Receptors and Their Ligands. *Naunyn. Schmiedebergs Arch. Pharmacol.* 2000, Vol. 362, pp. 382–391.

50. **Van Calker D., et al.** Adenosine regulates, via two different types ofreceptors, the accumulation of cyclic AMP in cultured brain cells. , 33,. *J. Neurochem.* 1979, Vol. 33, pp. 999-1005.

51. **Londos C., et al.** Subclasses of external adenosine receptors. *Biochem.* 1979, Vol. 77, pp. 2551-2554.

52. **Daly J.W., et al.** Subclasses of adenosine receptors in the central nervous system: interaction with caffeine and related methylxanthines. *Cell. Mol. Neurobiol.* 1983, Vol. 3, pp. 69-80.

53. **Zhou Q.Y., et al.** Molecular cloning and characterization of an adenosine receptor: the A3 adenosine receptor. *Proc. Natl. Acad. Sci. USA.* 1992, Vol. 89, pp. 7432-7436.

54. **Jaakola V.P., et al.** The 2.6 Å crystal structure of a human A2A adenosine receptor bound to an antagonist. *Science.* 2008, Vol. 322, pp. 1211–1217.

55. **Kim J., et al.** Site-directed mutagenesis identifies residues involved in ligand recognition in the human A2A adenosine receptor. *J. Biol. Chem.* 1995, Vol. 270, pp. 13987–13997.

56. **Doré A. S., et al.** Structure of the adenosine A2A receptor in complex with ZM241385 and the xanthines XAC and caffeine. *Structure.* 2011, Vol. 19, pp. 1283-1293.

57. **Xu F., et al.** Structure of an agonist-bound human A2A adenosine receptor. *Science.* 2011, Vol. 332, pp. 322–327.

58. **Ciruela F., et al.** Immunological identification of A1 adenosine receptors in brain cortex. *J. Neurosci. Res.* 1995, Vol. 42, pp. 818–828.

59. **Yoshioka K., et al.** Hetero-oligomerization of adenosine A1 receptors with P2Y1 receptors in rat brains. *FEBS Lett.* 2002, Vol. 531, pp. 299–303.

60. **Briddon S.J., et al.** Plasma membrane diffusion of G protein-coupled receptor oligomers. *Biochim. Biophys. Acta.* 2008, Vol. 1783, pp. 2262-2268.

61. **Vidi P.A., et al.** Fluorescent and bioluminescent protein-fragment complementation assays in the study of G protein-coupled receptor oligomerization and signaling. *Mol. Pharmacol.* 2009, Vol. 75, pp. 733–739.

62. **Lynge J., et al.** Adenosine A2B receptors modulate cAMP levels and induce CREB but not ERK1/2 and p38 phosphorylation in rat skeletal muscle cells. *Biochem. Biophys. Res. Commun.* 2003, Vol. 307, pp. 180–187.

63. **Canals M, et al.** Adenosine A2A-dopamine D2 receptor-receptor heteromerization: qualitative and quantitative assessment by fluorescence and bioluminescence energy transfer. *J. Biol. Chem.* 2003, Vol. 278, pp. 46741–46749.

64. **Fuxe K., et al.** Adenosine A2A and dopamine D2 heteromeric receptor complexes and their function. *J. Mol. Neurosci. MN.* 2005, Vol. 26, pp. 209–220.

65. **Smith N. J., et al.** Allostery at G protein-coupled receptor homo- and heteromers: uncharted pharmacological landscapes. *Pharmacol. Rev.* 2010, Vol. 62, pp. 701–725.

66. **Krupnick J.G., et al.** The role of receptor kinases and arrestins in G protein-coupled receptor regulation. *Annu. Rev. Pharmacol. Toxicol.* 1998, Vol. 38, pp. 289–319.

67. **Bunemann M., et al.** G-protein coupled receptor kinases as modulators of G-protein signalling. *J. Physiol.* 1999, Vol. 517, pp. 5–23.

68. **Goodman O.B., et al.** Beta-arrestin acts as a clathrin adaptor in endocytosis of the beta2-adrenergic receptor. *Nature.* 1996, Vol. 383, pp. 447–450.

69. **Tsao P., et al.** Downregulation of G protein-coupled receptors. *Curr. Opin. Neurobiol.* 2000, Vol. 10, pp. 365-369.

70. **Klaasse E.C., et al.** Internalization and desensitization of adenosine receptors. *Purinergic Signal.* 2008, Vol. 4, pp. 21–37.

71. **Parsons W.J., et al.** Heterologous desensitization of the inhibitory A1 adenosine receptor-adenylate cyclase system in rat adipocytes. Regulation of both Ns and Ni. *J. Biol. Chem.* 1987, Vol. 262, pp. 841–847.

72. **Green A.** Adenosine receptor down-regulation and insulin resistance following prolonged incubation of adipocytes with an A1 adenosine receptor agonist. *J. Biol. Chem.* 1987, Vol. 262, pp. 15702–15707.

73. **Longabaugh J.P., et al.** Modification of the rat adipocyte A1 adenosine receptor-adenylate cyclase system during chronic exposure to an A1 adenosine receptor agonist: Alterations in the quantity of GS alpha and Gi alpha are not associated with changes in their mRNAs. *Mol. Pharmacol.* 1989, Vol. 36, pp. 681–688.

74. **Jajoo S., et al.** Role of beta-arrestin1/ERK MAP kinase pathway in regulating adenosine A1 receptor desensitization and recovery. *Am. J. Physiol. Cell Physiol.* 2010, Vol. 298, pp. C56–C65.

75. **Pereira M.R., et al.** Modulation of A1 adenosine receptor expression by cell aggregation and long-term activation of A2a receptors in cultures of avian retinal cells: Involvement of the cyclic AMP/PKA pathway. *J. Neurochem.* 2010, Vol. 113, pp. 661-673.

76. **Brito R., et al.** Expression of A1 adenosine receptors in the developing avian retina: In vivo modulation by A(2A) receptors and endogenous adenosine. *J. Neurochem.* 2012, Vol. 123, pp. 239–249.

77. **Palmer T.M., et al.** Desensitization of the canine A2a adenosine receptor: delineation of multiple processes. *Mol. Pharmacol.* 1994, Vol. 45, pp. 1082–1094.

78. —. Identification of an A2a adenosine receptor domain specifically responsible for mediating short-term desensitization. *Biochemistry.* 1997, Vol. 36, pp. 832–838.

79. **Matharu A.L., et al.** Rapid agonist-induced desensitization and internalization of the A(2B) adenosine receptor is mediated by a serine residue close to the COOH terminus. *J. Biol. Chem.* 2001, Vol. 276, pp. 30199–30207.

80. **Mundell S.J., et al.** A dominant negative mutant of the G protein-coupled receptor kinase 2 selectively attenuates adenosine A2 receptor desensitization. *Mol. Pharmacol.* 1997, Vol. 51, pp. 991-998.

81. —. Characterization of G protein-coupled receptor regulation in antisense mRNA-expressing cells with reduced arrestin levels. *Biochemistry.* 1999, Vol. 38, pp. 8723-8732.

82. **Claing A., et al.** Multiple endocytic pathways of G protein-coupled receptors delineated by GIT1 sensitivity. *Proc. Natl. Acad. Sci. USA.* 2000, Vol. 97, pp. 1119-1124.

83. **Peters D.M., et al.** Agonist-induced desensitization of A2B adenosine receptors. *Biochem. Pharmacol.* 1998, Vol. 55, pp. 873-882.

84. **Trincavelli M.L., et al.** Regulation of A2B adenosine receptor functioning by tumour necrosis factor a in human astroglial cells. *J. Neurochem.* 2004, Vol. 91, pp. 1180-1190.

85. **Moriyama K., et al.** Adenosine A2A receptor is involved in cell surface expression of A2B receptor. *J. Biol. Chem.* 2010, Vol. 285, pp. 39271–39288.

86. **Ferguson G., et al.** Subtype-specific kinetics of inhibitory adenosine receptor internalization are determined by sensitivity to phosphorylation by G protein-coupled receptor kinases. *Mol. Pharmacol.* 2000, Vol. 57, pp. 546-552.

87. **Palmer T.M., et al.** Agonist-dependent phosphorylation and desensitization of the rat A3 adenosine receptor. Evidence for a G-protein-coupled receptor kinase-mediated mechanism. *J. Biol. Chem.* 1995, Vol. 270, pp. 29607-29613.

88. —. Identification of threonine residues controlling the agonist-dependent phosphorylation and desensitization of the rat A(3) adenosine receptor. *Mol. Pharmacol.* 2000, Vol. 57, pp. 539-545.

89. **Trincavelli M.L., et al.** A3 adenosine receptors in human astrocytoma cells: Agonist-mediated desensitization, internalization, and down-regulation. *Mol. Pharmacol.* 2002, Vol. 62, pp. 1373-1384.

90. —. Involvement of mitogen protein kinase cascade in agonist-mediated human A(3) adenosine receptor regulation. *Biochim. Biophys. Acta.* 2002, Vol. 1591, pp. 55-62.

91. **Fredholm B. B., et al.** Actions of adenosine at its receptors in the CNS: insights from knockouts and drugs. *Annu. Rev. Pharmacol. Toxicol.* 2005, Vol. 45, pp. 385-412.

92. **Trincavelli M. L., et al.** Adenosine receptors: what we know and what we are learning. *Curr. Top. Med. Chem.* 2010, Vol. 10, pp. 860-877.

93. **Faulhaber-Walter R., et al.** Lack of A1 adenosine receptors augments diabetic hyperfiltration and glomerular injury. *J. Am. Soc. Nephrol. JASN.* 2008, Vol. 19, pp. 722-730.

94. **Schwarzschild M. A., et al.** Targeting adenosine A2A receptors in Parkinson's disease. *Trends Neurosci.* 2006, Vol. 29, pp. 647-654.

95. **Wei C.J., et al.** Selective inactivation of adenosine A2A receptors in striatal neurons enhances working memory and reversal learning. *Learn. Mem.* 2011, Vol. 18, pp. 459-474.

96. **Zlomuzica A., et al.** Superior working memory and behavioural habituation but diminished psychomotor coordination in mice lacking the ecto-5'-nucleotidase (CD73) gene. *Purinergic Signal.* 2013, Vol. 9, pp. 175-182.

97. **Ledent C., et al.** Aggressiveness, hypoalgesia and high blood pressure in mice lacking the adenosine A2a receptor. *Nature.* 1997, Vol. 388, pp. 674-678.

98. **Chen J.F., et al.** A2A adenosine receptor deficiency attenuates brain injury induced by transient focal ischemia in mice. *J. Neurosci.* 1999, Vol. 19, pp. 9192-9200.

99. **Ohta A., et al.** Role of G-protein-coupled adenosine receptors in downregulation of inflammation and protection from tissue damage. *Nature.* 2001, Vol. 414, pp. 916-920.

100. **Chen J.F., et al.** Adenosine A2A receptors and brain injury: broad spectrum of neuroprotection, multifaceted actions and “fine tuning” modulation. *Prog. Neurobiol.* 2007, Vol. 83, pp. 310-331.

101. **Qiu M.H., et al.** The role of nucleus accumbens core/shell in sleep-wake regulation and their involvement in modafinil-induced arousal. *PLoS ONE.* 2012, Vol. 7 e45471.

102. **Eckle T., et al.** Adora2b-elicited Per2 stabilization promotes a HIF-dependent metabolic switch crucial for myocardial adaptation to ischemia. *Nat. Med.* 2012, Vol. 18, pp. 774-782.

103. **Yang D., et al.** The A2B adenosine receptor protects against inflammation and excessive vascular adhesion. *J. Clin. Invest.* 2006, Vol. 116, pp. 1913-1923.

104. **Eckle T., et al.** A2B adenosine receptor dampens hypoxia-induced vascular leak. *Blood.* 2008, Vol. 111, pp. 2024-2035.

105. **Koscso B., et al.** Stimulation of A2B adenosine receptors protects against trauma-hemorrhagic shock-induced lung injury. *Purinergic Signal.* 2013, Vol. 9, pp. 427-432.

106. **Grenz A., et al.** Adora2b adenosine receptor signaling protects during acute kidney injury via inhibition of neutrophil-dependent TNF-alfa release. *J. Immunol. Baltim. Md 1950.* 2012, Vol. 189, pp. 4566-4573.

107. **Eckle T., et al.** A2B adenosine receptor signaling attenuates acute lung injury by enhancing alveolar fluid clearance in mice. *J. Clin. Invest.* 2008, Vol. 118, pp. 3301-3315.

108. **Carroll S.H., et al.** A2B adenosine receptor promotes mesenchymal stem cell differentiation to osteoblasts and bone formation in vivo. *J. Biol. Chem.* 2012, Vol. 287, pp. 15718–15727.

109. **Koupenova M., et al.** A2b adenosine receptor regulates hyperlipidemia and atherosclerosis. *Circulation.* 2012, Vol. 125, pp. 354-363.

110. **Cekic C., et al.** Adenosine A2B receptor blockade slows growth of bladder and breast tumors. *J. Immunol.* 2012, Vol. 188, pp. 198-205.

111. **Yang J., et al.** Adenosine A3 receptors regulate heart rate, motor activity and body temperature. *Acta Physiol. Oxf. Engl.* 2010, Vol. 199, pp. 221–230.

112. **Cerniway R.J., et al.** Targeted deletion of A(3) adenosine receptors improves tolerance to ischemia-reperfusion injury in mouse myocardium. *Am. J. Physiol.* 2001, Vol. 281, pp. H1751–H1758.

113. **Harrison G.J., et al.** Effects of A(3) adenosine receptor activation and gene knock-out in ischemic-reperfused mouse heart. *Cardiovasc. Res.* 2002, Vol. 53, pp. 147-155.

114. **Zhao Z., et al.** A role for A3 adenosine receptor in determining tissue levels of cAMP and blood pressure: studies in knock-out mice. *Biochem. Biophys. Acta.* 2000, Vol. 1500, pp. 280-290.

115. **Lee H.T., et al.** A3 adenosine receptor knockout mice are protected against ischemia- and myoglobinuria-induced renal failure. *Am J Physiol Renal Physiol.* 2003, Vol. 284, pp. F267-F273.

116. **Avila M.Y., et al.** Knockout of A3 adenosine receptors reduces mouse intraocular pressure. *Invest Ophthalmol. Vis. Sci.* 2002, Vol. 43, pp. 3021-3026.

117. **Linden J.** Regulation of leukocyte function by adenosine receptors. *Adv. Pharmacol. San Diego Calif.* 2011, Vol. 61, pp. 95-114.

118. **Boison D.** Adenosine dysfunction in epilepsy. . *Glia 2012, 60, 1234–1243.*

119. **Ahmad A., et al.** Adenosine A2A receptor is a unique angiogenic target of HIF-2α in pulmonary endothelial cells. *Proc. Natl. Acad. Sci.* 2009, Vol. 106, pp. 10684–10689.

120. **Kong T., et al.** HIF-dependent induction of adenosine A2B receptor in hypoxia. *FASEB J. Off. Publ. Fed. Am. Soc. Exp. Biol.* 2006, Vol. 20, pp. 2242-2250.

121. **Eltzschig H. K., et al.** Central role of sp1-regulated CD39 in hypoxia/ischemia protection. *Blood.* 2009, Vol. 113, pp. 224-232.

122. **Hart M.L., et al.** Hypoxia-inducible factor-1α–dependent protection from intestinal ischemia/reperfusion injury involves ecto-5′-nucleotidase (CD73) and the A2B adenosine receptor. *J. Immunol.* 2011, Vol. 186, pp. 4367–4374.

123. **Csoka B., et al.** A2B adenosine receptors protect against sepsis-induced mortality by dampening excessive inflammation. *J. Immunol. Baltim. Md. 1950.* 2010, Vol. 185, pp. 542-550.

124. **Lappas C. M., et al.** Adenosine A2A receptor activation limits graft-versus-host disease after allogenic hematopoietic stem cell transplantation. *J. Leukoc. Biol.* 2010, Vol. 87, pp. 345-354.

125. **Lau C. L., et al.** The role of adenosine A2A receptor signaling in bronchiolitis obliterans. *Ann. Thorac. Surg.* 2009, Vol. 88, pp. 1071-1078.

126. **Li L., et al.** Dendritic cells tolerized with adenosine A2AR agonist attenuate acute kidney njury. *J. Clin. Invest.* 2012, Vol. 122, pp. 3931-3942.

127. **Castillo C.A., et al.** Modulation of adenosine A1 and A2A receptors in C6 glioma cells during hypoxia: nvolvement of endogenous adenosine. *J. Neurochem.* 2008, Vol. 105, pp. 2315-2329.

128. **Dai S.S., et al.** Local glutamate level dictates adenosine A2A receptor regulation of neuroinflammation and traumatic brain injury. *J. Neurosci.* 2010, Vol. 30, pp. 5802-5810.

129. **Popoli P., et al.** Blockade of striatal adenosine A2A receptor reduces, through a presynaptic mechanism, quinolinic acid-induced excitotoxicity: possible relevance to neuroprotective interventions in neurodegenerative diseases of the striatum. *J. Neurosci.* 2002, Vol. 22, pp. 1967-1975.

130. **Chen J.F., et al.** Neuroprotection by caffeine and A(2A) adenosine receptor inactivation in a model of parkinson's disease. *J. Neurosci. Off. J. Soc. Neurosci.* 2001, Vol. 21 RC143.

131. **Canas P.M., et al.** Adenosine A2A receptor blockade prevents synaptotoxicity and memory dysfunction caused by beta-amyloid peptides via p38 mitogen-activated protein kinase pathway. *J. Neurosci.* 2009, Vol. 29, pp. 14741–14751.

132. **Blum D., et al.** A dual role of adenosine A2A receptors in 3-nitropropionic acid-induced striatal lesions: implications for the neuroprotective potential of A2A antagonists. *J. Neurosci.* 2003, Vol. 23, pp. 5361-5369.

133. **Chou S.Y., et al.** CGS21680 attenuates symptoms of Huntington's disease in a transgenic mouse model. *J. Neurochem.* 2005, Vol. 93, pp. 310-320.

134. **Deaglio S., et al.** Adenosine generation catalyzed by CD39 and CD73 expressed on regulatory T-cells mediates immune suppression. *J. Exp. Med.* 2007, Vol. 204, pp. 1257-1265.

135. **Chen J.F, et al.** Adenosine receptors as drug targets — what are the challenges? *Nat. Rev. Drug. Discov.* 2013, Vol. 12, pp. 265-286.

136. **Vallon V., et al.** Adenosine and kidney function. *Physiol. Rev.* 2006, Vol. 86, pp. 901-940.

137. **Cotter G, et al.** The PROTECT pilot study: a randomized, placebo-controlled, dose-finding study of the adenosine A1 receptor antagonist rolofylline in patients with acute heart failure and renal impairment. *J. Card. Fail.* 2008, Vol. 14, pp. 631-640.

138. **Voors A.A., et al.** Effects of the adenosine A1 receptor antagonist rolofylline on renal function in patients with acute heart failure and renal dysfunction: results from PROTECT (placebo- controlled randomized study of the selective adenosine A1 receptor antagonist rolofyll. *J. Am. Coll. Cardiol.* 2011, Vol. 57, pp. 1899-1907.

139. **Green S.J., et al.** Partial adenosine A1 receptor agonism: a potential new therapeutic strategy for heart failure. *Heart Fail. Rev.* 2016, Vol. 21, pp. 95-102.

140. **Zablocki J. A., et al.** Partial A1 adenosine receptor agonists from a molecular perspective and their potential use as chronic ventricular rate control agents during atrial fibrillation (AF). *Curr. Top. Med. Chem.* 2004, Vol. 4, pp. 839-854.

141. **Fraser H., et al.** N-[3-(R)-tetrahydrofuranyl]-6-aminopurine riboside, an A1 adenosine receptor agonist, antagonizes catecholamine-induced lipolysis without cardiovascular effects in awake rats. *J. Pharmacol. Exp. Ther.* 2003, Vol. 305, pp. 225-231.

142. **Bayes M., et al.** Gateways to clinical trials. *Methods Find. Exp. Clin. Pharmacol.* 2003, Vol. 25, pp. 831-855.

143. **Tendera M., et al.** The new oral adenosine A1 receptor agonist capadenoson in male patients with stable angina. *Clin. Res. Cardiol.* 2012, Vol. 101, pp. 585-591.

144. **Sawynok J., et al.** Adenosine receptor activation and nociception. *Eur. J. Pharmacol.* 1998, Vol. 347, pp. 1-11.

145. **Schubert P., et al.** Modulation of nerve and glial function by adenosine: role in the development of ischemic damage. *Int. J. Biochem.* 1994, Vol. 26, pp. 1227–1236.

146. **Li X., et al.** Adenosine reduces glutamate release in rat spinal synaptosomes. *Anesthesiology.* 2005, Vol. 103, pp. 1060–1065.

147. **Horiuchi H., et al.** Adenosine A1 receptor agonists reduce hyperalgesia after spinal cord injury in rats. *Spinal Cord.* 2010, Vol. 48, pp. 685–690.

148. **Imlach L., et al.** A positive allosteric modulator of the adenosine A1 receptor selectively inhibits primary afferent synaptic transmission in a neuropathic pain model. *Mol. Pharmacol.* 2015, Vol. 88, pp. 460–468.

149. **Rappold P.M., et al.** Astrocytes and therapeutics for Parkinson's disease. *Neurother. J. Am. Soc. Exp. Neurother.* 2010, Vol. 7, pp. 413-423.

150. **de Lera Ruiz M., et al.** Adenosine A2A receptor as a drug discovery target. *J Med Chem.* 2014, Vol. 57, pp. 3623-3650.

151. **Naganawa M., et al.** Formation of binding potential maps of adenosine A1 and A2A receptors using independent component analysis without arterial blood sampling. *J. Cereb. Blood Flow Metab.* 2005, Vol. 25, p. S606.

152. **Richardson P.J., et al.** Adenosine A2A receptor antagonists as new agents for the treatment of Parkinson's disease. *Trends Pharmacol. Sci.* 1997, Vol. 18, pp. 338-344.

153. **Chen J.F., et al.** The adenosine A2A receptor as an attractive target for Parkinson's disease treatment. *Drug News Perspect.* 2003, Vol. 16, pp. 597-604.

154. **Jenner P., et al.** Adenosine, adenosine A2A antagonists, and Parkinson's disease. *Parkinsonism Relat. Disord.* 2009, Vol. 15, pp. 406-413.

155. **Hauser R.A., et al.** Preladenant in patients with Parkinson's disease and motor fluctuations: a phase 2, double-blind, randomised trial. *Lancet Neurol.* 2011, Vol. 10, pp. 221-229.

156. **Guttman M.** Efficacy of istradefylline in Parkinson's diease patients treated with levodopa with motor response complications: results of the KW-6002 US-018 study. *Mov. Disord.* 2006, Vol. 21 (Suppl. 15), p. 585.

157. **Meissner W.G., et al.** Priorities in Parkinson's disease research. *Nature Rev. Drug Discov.* 2011, Vol. 10, pp. 377-393.

158. **Shaikh G., et al.** Signaling pathways involving adenosine A2A and A2B receptors in wound healing and fibrosis. *Purinergic Signalling.* 2016, Vol. 12, pp. 191-197.

159. **Wallace K. L., et al.** Adenosine A2A receptors induced on iNKT and NK cells reduce pulmonary inflammation and injury in mice with sickle cell disease. *Blood.* 2010, Vol. 116, pp. 5010–5020.

160. **Hussey M. J., et al.** Reduced response to the formalin test and lowered spinal NMDA glutamate receptor binding in adenosine A2A receptor knockout mice. *Pain.* 2007, Vol. 129, pp. 287–294.

161. **Borghi V., et al.** Formalin-induced pain and mu-opioid receptor density in brain and spinal cord are modulated by A1 and A2a adenosine agonists in mice. *Brain Res.* 2002, Vol. 956, pp. 339–348.

162. **van der Hoeven D., et al.** A role for the low-affinity A2B adenosine receptor in regulating superoxide generation by murine neutrophils. *J. Pharmacol. Exp. Ther.* 2011, Vol. 338, pp. 1004–1012.

163. **Csoka B., et al.** Adenosine promotes alternative macrophage activation via A2A and A2B receptors. *FASEB J.* 2012, Vol. 26, pp. 376-386.

164. **Ryzhov S., et al.** Effect of A2B adenosine receptor gene ablation on adenosine-dependent regulation of proinflammatory cytokines. *J. Pharmacol. Exp. Ther.* 2008, Vol. 324, pp. 694-700.

165. **Ma D.F., et al.** Hypoxia-inducible adenosine A2B receptor modulates proliferation of colon carcinoma cells. *Hum. Pathol.* 2010, Vol. 41, pp. 1550–1557.

166. **Wei Q., et al.** A2B adenosine receptor blockade inhibits growth of prostate cancer cells. *Purinergic Signal.* 2013, Vol. 9, pp. 271-280.

167. **Vecchio E. A., et al.** Ligand-independent adenosine A2B receptor constitutive activity as a promoter of prostate cancer cell proliferation. *J. Pharmacol. Exp. Ther.* 2016, Vol. 357, pp. 36-44.

168. **Kasama H., et al.** Adenosine A2B receptor promotes progression of human oral cancer. *BMC Cancer.* 2015, Vol. 15, p. 563.

169. **Stagg J., et al.** Anti-CD73 antibody therapy inhibits breast tumor growth and metastasis. *Proc. Natl. Acad. Sci. U.S.A.* 2010, Vol. 107, pp. 1547-1552.

170. **Desmet C. J., et al.** Identification of a pharmacologically tractable Fra-1/ADORA2B axis promoting breast cancer metastasis. *Proc. Natl. Acad. Sci. U.S.A.* 2013, Vol. 110, pp. 5139–5144.

171. **Ntantie E., et al.** An adenosine-mediated signaling pathway suppresses prenylation of the GTPase Rap1B and promotes cell scattering. *Sci. Signal.* 2013, Vol. 6, p. ra39.

172. **Ryzhov S., et al.** Host A(2B) adenosine receptors promote carcinoma growth. *Neoplasia.* 2008, Vol. 10, pp. 987-995.

173. **Feoktistov I., et al.** Differential expression of adenosine receptors in human endothelial cells: role of A2B receptors in angiogenic factor regulation. *Circ. Res.* 2002, Vol. 90, pp. 531-538.

174. —. Mast cell-mediated stimulation of angiogenesis: cooperative interaction between A2B and A3 adenosine receptors. *Circ. Res.* 2003, Vol. 92, pp. 485-492.

175. **Merighi S., et al.** A(2B) and A(3) adenosine receptors modulate vascular endothelial growth factor and interleukin - 8 expression in human melanoma cells treated with etoposide and doxorubicin. *Neoplasia.* 2009, Vol. 11, pp. 1064-1073.

176. **Novitskiy S. V., et al.** Adenosine receptors in regulation of dendritic cell differentiation and function. *Blood.* 2008, Vol. 112, pp. 1822-1831.

177. **Yang M., et al.** HIF-dependent induction of adenosine receptor A2B skews human dendritic cells to a Th2-stimulating phenotype under hypoxia. *Immunol. Cell Biol.* 2010, Vol. 88, pp. 165-171.

178. **Mendis S., et al.** Global atlas on cardiovascular disease prevention and control. *World Health Organization in collaboration with the World Heart Federation and the World Stroke Organization.* pp. 3-18.

179. **Weber C., et al.** Atherosclerosis: current pathogenesis and therapeutic options. *Nature Med. 17:1410–1422.* 2011, Vol. 17, pp. 1410–1422.

180. **Gessi S., et al.** Adenosine modulates HIF-1{alpha}, VEGF, IL-8, and foam cell formation in a human model of hypoxic foam cells. *Arterioscler. Thromb. Vasc. Biol.* 2010, Vol. 30, pp. 90–97.

181. **Xi J., et al.** Adenosine A2A and A2B receptors work in concert to induce a strong protection against reperfusion injury in rat hearts. *J. Mol. Cell. Cardiol.* 2009, Vol. 47, pp. 684–690.

182. **Murry C. E., et al.** Preconditioning with ischemia: a delay of lethal cell injury in ischemic myocardium. *Circulation.* 1986, Vol. 74, pp. 1124–1136.

183. **Eckle T., et al.** Hypoxia-inducible factor-1 is central to cardioprotection: a new paradigm for ischemic preconditioning. *Circulation.* 2008, Vol. 118, pp. 166-175.

184. —. Cardioprotection by ecto-5'-nucleotidase (CD73) and A2B adenosine receptors. *Circulation.* 2007, Vol. 115, pp. 1581-1590.

185. **Koeppen M., et al.** Adora2b signaling on bone marrow derived cells dampens myocardial ischemia-reperfusion injury. *Anesthesiology.* 2012, Vol. 116, pp. 1245–1257.

186. **Maas J. E., et al.** Evidence that the acute phase of ischemic preconditioning does not require signaling by the A2B adenosine receptor. *J. Mol. Cell. Cardiol.* 2010, Vol. 49, pp. 886–893.

187. **Kornowski R., et al.** In-stent restenosis: contributions of inflammatory responses and arterial injury to neointimal hyperplasia. *J. Am. Coll. Cardiol.* 1998, Vol. 31, pp. 224–230.

188. **Yang D., et al.** The A2b adenosine receptor protects against vascular injury. *Proc. Natl. Acad. Sci. USA.* 2008, Vol. 105, pp. 792-796.

189. **Bot I., et al.** Adenosine A(2)B receptor agonism inhibits neointimal lesion development after arterial injury in apolipoprotein E-deficient mice. *Arterioscler. Thromb. Vasc. Biol.* 2012, Vol. 32, pp. 2197–2205.

190. **Wynne B. N., et al.** Vascular smooth muscle cell signaling mechanisms for contraction to angiotensin II and endothelin-1. *J. Am. Soc. Hypertens.* 2009, Vol. 3, pp. 84–95.

191. **Balwierczak J. L., et al.** Comparative effects of a selective adenosine A2 receptor agonist, CGS 21680, I and nitroprusside in vascular smooth muscle. *Eur. J. Pharmacol.* 1991, Vol. 196, pp. 117–123.

192. **Zhang W., et al.** Elevated ecto-5'-nucleotidase-mediated increased renal adenosine signaling via A2B adenosine receptor contributes to chronic hypertension. *Circ. Res.* 2013, Vol. 112, pp. 1466-1478.

193. **Valladares D., et al.** Adenosine A(2B) receptor mediates an increase on VEGF-A production in rat kidney glomeruli. *Biochem. Biophys. Res. Commun.* 2008, Vol. 366, pp. 180-185.

194. **Patel L., et al.** The effects of adenosine A2B receptor inhibition on VEGF and nitric oxide axis-mediated renal function in diabetic nephropathy. *Ren. Fail.* 2014, Vol. 36, pp. 916-924.

195. **Tak E., et al.** CD73-dependent generation of adenosine and endothelial Adora2b signaling attenuate diabetic nephropathy. *J. Am. Soc. Nephrol.* 2014, Vol. 25, pp. 547-563.

196. **Eisenstein A., et al.** The many faces of the A2B adenosine receptor in cardiovascular and metabolic diseases. *J. Cell. Physiol.* 2015, Vol. 230, pp. 2891–2897.

197. **Dai Y., et al.** A2B adenosine receptor-mediated induction of IL-6 promotes CKD. *J. Am. Soc. Nephrol.* 2011, Vol. 22, pp. 890-901.

198. **Grenz A., et al.** The reno-vascular A2B adenosine receptor protects the kidney from ischemia. *PLoS Med.* 2008, Vol. 5, p. e137.

199. —. Adora2b adenosine receptor signaling protects during acute kidney injury via inhibition of neutrophil-dependent TNF-alpha release. *J. Immunol.* 2012, Vol. 189, pp. 4566–4573.

200. —. Equilibrative nucleoside transporter 1 (ENT1) regulates post ischemic blood flow during acute kidney injury in mice. *J. Clin. Invest.* 2012, Vol. 122, pp. 693–710.

201. **Rusing D., et al.** The impact of adenosine and A(2B) receptors on glucose homoeostasis. *J. Pharm. Pharmacol.* 2006, Vol. 58, pp. 1639–1645.

202. **Johnston-Cox H., et al.** The A2B adenosine receptor modulates glucose homeostasis and obesity. *PLoS ONE.* 2012, Vol. 7, p. e40584.

203. —. The macrophage A2B adenosine receptor regulates tissue insulin sensitivity. *PLoS ONE.* 2014, Vol. 9, p. e98775.

204. **Merighi S., et al.** Adenosine receptors and diabetes: focus on the A(2B) adenosine receptor subtype. *Pharmacol. Res.* 2015, Vol. 99, pp. 229–236.

205. **Wen J., et al.** A2B Adenosine receptor agonist improves erectile function in diabetic rats. *Tohoku J. Exp. Med.* 2015, Vol. 237, pp. 141–148.

206. **Nemeth Z. H., et al.** Adenosine receptor activation ameliorates type 1 diabetes. *FASEB J.* 2007, Vol. 21, pp. 2379–2388.

207. **Figler R.A., et al.** Links between insulin resistance, adenosine A2B receptors, and inflammatory markers in mice and humans. *Diabetes.* 2011, Vol. 60, pp. 669–679.

208. **Csoka B., et al.** A2B adenosine receptors prevent insulin resistance by inhibiting adipose tissue inflammation via maintaining alternative macrophage activation. *Diabetes.* 2014, Vol. 63, pp. 850-866.

209. **Hu X., et al.** Sustained elevated adenosine via ADORA2B promotes chronic pain through neuro-immune interaction. *Cell Reports.* 2016, Vol. 16, pp. 106–119.

210. **Basbaum A. I., et al.** Cellular and molecular mechanisms of pain. *Cell.* 2009, Vol. 139, pp. 267–284.

211. **McMahon S. B., et al.** Crosstalk between the nociceptive and immune systems in host defence and disease. *Nat. Rev. Neurosci.* 2015, Vol. 16, pp. 389–402.

212. **Chiu I. M., et al.** Neurogenic inflammation and the peripheral nervous system in host defense and immunopathology. *Nat. Neurosci.* 2012, Vol. 15, pp. 1063–1067.

213. **Larochelle A., et al.** Bone marrow-derived macrophages and the CNS: an update on the use of experimental chimeric mouse models and bone marrow transplantation in neurological disorders. *Biochim. Biophys. Acta.* 2016, Vol. 1862, pp. 310–322.

214. **Salvatore C.A., et al.** Disruption of the A(3) adenosine receptor gene in mice and its effect on stimulated inflammatory cells. *J. Biol. Chem.* 2000, Vol. 275, pp. 4429–4434.

215. **Tilley S.L., et al.** Identification of A3 receptor- and mast cell-dependent and -independent components of adenosine-mediated airway responsiveness in mice. *J. Immunol.* 2003, Vol. 171, pp. 331–337.

216. **Zhong H., et al.** Activation of murine lung mast cells by the adenosine A3 receptor. *J. Immunol.* 2003, Vol. 171, pp. 338–345.

217. **Hua X., et al.** Adenosine induces airway hyperresponsiveness through activation of A3 receptors on mast cells. *J. Allergy Clin. Immunol.* 2008, Vol. 122, pp. 107–113.

218. **Morschl E., et al.** A3 adenosine receptor signaling influences pulmonary inflammation and fibrosis. *Am. J. Respir. Cell. Mol. Biol.* 2008, Vol. 39, pp. 697–705.

219. **Burnstock G., et al.** Purinergic signaling in the airways. *Pharmacol. Rev.* 2012, Vol. 64, pp. 834–868.

220. **Reeves J. J., et al.** Studies on the effects of adenosine A3 receptor stimulation on human eosinophils isolated from non-asthmatic or asthmatic donors. *Inflamm. Res.* 2000, Vol. 49, pp. 666–672.

221. **Spicuzza L., et al.** Adenosine in the airways: implications and applications. *Eur. J. Pharmacol.* 2006, Vol. 533, pp. 77–88.

222. **Young H. V., et al.** A3 adenosine receptor signaling contributes to airway inflammation and mucus production in adenosine deaminase-deficient mice. *J. Immunol.* 2004, Vol. 173, pp. 1380-1389.

223. **Varani K., et al.** Alteration of adenosine receptors in patients with chronic obstructive pulmonary disease. *Am. J. Respir. Crit. Care Med.* 2006, Vol. 173, pp. 398-406.

224. **Matot I., et al.** A3 adenosine receptors and mitogen-activated protein kinases in lung injury f ollowing in vivo reperfusion. *Crit. Care.* 2006, Vol. 10, p. R65.

225. **da Rocha Lapa F., et al.** Anti-inflammatory effects of inosine in allergic lung inflammation in mice: evidence for the participation of adenosine A2A and A3 receptors. *Purinergic Signal.* 2013, Vol. 9, pp. 325-336.

226. **Gazoni L. M., et al.** Activation of A1, A2A, or A3 adenosine receptors attenuates lung ischemia reperfusion injury. *J. Thorac. Cardiovasc. Surg.* 2010, Vol. 140, pp. 440-446.

227. **Mulloy D. P., et al.** Adenosine A3 receptor activation attenuates lung ischemia-reperfusion injury. *Ann. Thorac. Surg.* 2013, Vol. 95, pp. 1762-1767.

228. **Ochaion A., et al.** The anti-inflammatory target A(3) adenosine receptor is over-expressed in rheumatoid arthritis, psoriasis and Crohn's disease. *Cell. Immunol.* 2009, Vol. 258, pp. 115–122.

229. **Varani K., et al.** Normalization of A2A and A3 adenosine receptor up-regulation in rheumatoid arthritis patients by treatment with anti-tumor necrosis factor alpha but not methotrexate. *Arthritis Rheum.* 2009, Vol. 60, pp. 2880-2891.

230. —. A2A and A3 adenosine receptor expression in rheumatoid arthritis: upregulation, inverse correlation with disease activity score and suppression of inflammatory cytokine and metalloproteinase release. *Arthritis Res. Ther.* 2011, Vol. 13, p. R197.

231. **Bar-Yehuda S., et al.** The anti-inflammatory effect of A3 adenosine receptor agonists: a novel targeted therapy for rheumatoid arthritis. *Expert Opin. Investig. Drugs.* 2007, Vol. 16, pp. 1601-1613.

232. **Forrest C. M., et al.** Modulation of cytokine release by purine receptors in patients with rheumatoid arthritis. *Clin. Exp. Rheumatol.* 2005, Vol. 23, pp. 89-92.

233. **Silverman M. H., et al.** Clinical evidence for utilization of the A3 adenosine receptor as a target to treat rheumatoid arthritis: data from a phase II clinical trial. *J. Rheumatol.* 2008, Vol. 35, pp. 41-48.

234. **Rath-Wolfson L., et al.** IB-MECA, an A3 adenosine receptor agonist prevents bone resorption in rats with adjuvant induced arthritis. *Clin. Exp. Rheumatol.* 2006, Vol. 24, pp. 400–406.

235. **Bar-Yehuda S., et al.** Induction of an antiinflammatory effect and prevention of cartilage damage in rat knee osteoarthritis by CF101 treatment. *Arthritis Rheum.* 2009, Vol. 60, pp. 3061–3071.

236. **Ochaion A., et al.** The A3 adenosine receptor agonist CF502 inhibits the PI3K, PKB/Akt and NF-kappaB signaling pathway in synoviocytes from rheumatoid arthritis patients and in adjuvant-induced arthritis rats. *Biochem. Pharmacol.* 2008, Vol. 76, pp. 482–494.

237. **van Troostenburg A. M., et al.** Tolerability, pharmacokinetics and concentration-dependent hemodynamic effects of oral CF101, an A3 adenosine receptor agonist, in healthy young men. *Int. J. Clin. Pharmacol. Ther.* 2004, Vol. 42, pp. 534–542.

238. **Zhang W., et al.** OARSI recommendations for the management of hip and knee osteoarthritis, Part II: OARSI evidence-based, expert consensus guidelines. *Osteoarthritis Cartilage.* 2008, Vol. 16, pp. 137–162.

239. **Fotheringham J. A., et al.** Activation of adenosine receptors inhibits tumor necrosis factor-alpha release by decreasing TNF-alpha mRNA stability and p38 activity. *Eur. J. Pharmacol.* 2004, Vol. 497, pp. 87–95.

240. **Varani K., et al.** Expression and functional role of adenosine receptors in regulating inflammatory responses in human synoviocytes. *Br. J. Pharmacol.* 2010, Vol. 160, pp. 101-115.

241. **Fishman P., et al.** Pharmacological and therapeutic effects of A3 adenosine receptor agonists. *Drug Discov. Today.* 2012, Vol. 17, pp. 359-366.

242. **Fini M., et al.** Functional tissue engineering in articular cartilage repair: is there a role for electromagnetic biophysical stimulation? *Tissue Eng. Part B Rev.* 2013, Vol. 19, pp. 353–367.

243. **Yang H., et al.** The cross-species A3 adenosine-receptor antagonist MRS 1292 inhibits adenosine-triggered human nonpigmented ciliary epithelial cell fluid release and reduces mouse intraocular pressure. *Curr. Eye Res.* 2005, Vol. 30, pp. 747–754.

244. **Wang Z., et al.** Nucleoside-derived antagonists to A3 adenosine receptors lower mouse intraocular pressure and act across species. *Exp. Eye Res.* 2010, Vol. 90, pp. 146–154.

245. **González-Fernández E., et al.** A3 Adenosine receptors mediate oligodendrocyte death and ischemic damage to optic nerve. *Glia.* 2014, Vol. 62, pp. 199–216.

246. **Avni I., et al.** Treatment of dry eye syndrome with orally administered CF101: data from a phase 2 clinical trial. *Ophthalmology.* 2010, Vol. 117, pp. 1287-1293.

247. **Fishman P., et al.** Targeting the A3 adenosine receptor for glaucoma treatment (review). *Mol. Med. Rep.* 2013, Vol. 7, pp. 1723–1725.

248. **Bar-Yehuda S., et al.** Inhibition of experimental autoimmune uveitis by the A3 adenosine receptor agonist CF101. *Int. J. Mol. Med.* 2011, Vol. 28, pp. 727-731.

249. **Sawynok J., et al.** Adenosine A3 receptor activation produces nociceptive behaviour and edema by release of histamine and 5-hydroxytryptamine. *Eur. J. Pharmacol.* 1997, Vol. 333, pp. 1–7.

250. **Paoletta S., et al.** Rational design of sulfonated A3 adenosine receptor-selective nucleosides as pharmacological tools to study chronic neuropathic pain. *J. Med. Chem.* 2013, Vol. 56, pp. 5949–5963.

251. **Chen Z., et al.** Controlling murine and rat chronic pain through A3 adenosine receptor activation. *FASEB J.* 2012, Vol. 26, pp. 1855–1865.

252. **Varani K., et al.** The stimulation of A(3) adenosine receptors reduces bone-residing breast cancer in a rat preclinical model. *Eur. J. Cancer.* 2013, Vol. 49, pp. 482–491.

253. **Janes K., et al.** A3 adenosine receptor agonist prevents the development of paclitaxel-induced neuropathic pain by modulating spinal glial-restricted redox-dependent signaling pathways. *Pain.* 2014, Vol. 155, pp. 2560-2567.

254. —. Spinal neuroimmmune activation is independent of T-cell infiltration and attenuated by A3 adenosine receptor agonists in a model of oxaliplatin-induced peripheral neuropathy. *Brain Behav. Immun.* 2015, Vol. 44, pp. 91-99.

255. **Müller C.E., et al.** Recent developments in adenosine receptor ligands and their potential as novel drugs. *Biochem. Biophys. Acta - Biomembr.* 2011, Vol. 1808, pp. 1290-1308.

256. **Goldman N., et al.** Adenosine A1 receptors mediate local anti-nociceptive effects of acupuncture. *Nat. Neurosci.* 2010, Vol. 13, pp. 883-888.

257. **Elzein E., et al.** A1 adenosine receptor agonists and their potential therapeutic applications. *Exp. Opin. Investig. Drugs.* 2008, Vol. 17, pp. 1901-1910.

258. **Luongo L., et al.** 5'-Chloro-5'-deoxy-(±)-ENBA, a potent and selective adenosine A1 receptor agonist, alleviates neuropathic pain in mice through functional glial and microglial changes without affecting Motor or cardiovascular functions. *Molecules.* 2012, Vol. 17, pp. 13712-13726.

259. **Franchetti P., et al.** N6-cycloalkyl- and N6-bicycloalkyl-C5' (C2')-modified adenosine derivatives as high-affinity and selective agonists at the human A1 adenosine receptor with antinociceptive effects in mice. *J. Med. Chem.* 2009, Vol. 52, pp. 2393-2406.

260. **Ochoa-Cortes F., et al.** Potential for developing purinergic drugs for gastrointestinal diseases. *Inflamm. Bowel Dis.* 2014, Vol. 20, pp. 1259-1287.

261. **Korboukh I., et al.** Orally active adenosine A1 receptor agonists with antinociceptive effects in mice. *J. Med. Chem.* 2012, Vol. 55, pp. 6467-6477.

262. **Schaddelee M. P., et al.** Pharmacokinetic/pharmacodynamics modelling of the anti-hyperalgesic and anti-nociceptive effect of adenosine A1 receptor partial agonists in neuropathic pain. *Eur. J. Pharmacol.* 2005, Vol. 514, pp. 131-140.

263. **Tosh D. K., et al.** Structural sweet spot for A1 adenosine receptor activation by truncated (N)-methanocarba nucleosides: receptor docking and potent anticonvulsant activity. *J. Med. Chem.* 2012, Vol. 55, pp. 8075-8090.

264. **Serchov T., et al.** Increased signaling via adenosine A1 receptors, sleep Deprivation, Imipramine, and Ketamine inhibit Depressive-like Behavior via Induction of Homer1a. *Neuron.* 2015, Vol. 87, pp. 549-562.

265. **Okuro M., et al.** Effects of paraxanthine and caffeine on sleep, locomotor activity, and body temperature in orexin/ataxin-3 transgenic narcoleptic mice. *Sleep.* 2010, Vol. 33, pp. 930-942.

266. **Loram L. C., et al.** Enduring reversal of neuropathic pain by a single intrathecal injection of adenosine 2A receptor agonists: a novel therapy for neuropathic pain. *J. Neurosci.* 2009, Vol. 29, pp. 14015-14025.

267. **Lebon G., et al.** Molecular determinants of CGS21680 binding to the human adenosine A2A receptor. *Mol. Pharmacol.* 2015, Vol. 87, pp. 907-915.

268. **Ferrè S., et al.** G protein-coupled receptor oligomerization revisited: functional and pharmacological perspectives. *Pharmacol. Rev.* 2014, Vol. 66, pp. 413-434.

269. **Bonaventura J., et al.** Allosteric interactions between agonists and antagonists within the adenosine A2A receptor-dopamine D2 receptor heterotetramer. *Proc. Natl. Acad. Sci. U. S. A.* 2015, Vol. 112.

270. **Navarro G., et al.** Purinergic signaling in Parkinson's disease. *Relevance Treat. Neuropharmacol.* 2015, Vol. 104, pp. 161-168.

271. **Liu W., et al.** Structural basis for allosteric regulation of GPCRs by sodium ions. *Science.* 2012, Vol. 337, pp. 232-236.

272. **Leone R. D., et al.** A2aR antagonists: Next generation checkpoint blockade for cancer immunotherapy. *Comput. Struct. Biotechnol. J.* 2015, Vol. 13, pp. 265-272.

273. **Gao Z. G., et al.** 2-Substituted adenosine derivatives: affinity and efficacy at four subtypes of human adenosine receptors. *Biochem. Pharmacol.* 2004, Vol. 68, pp. 1985-1993.

274. **Baraldi P. G., et al.** Synthesis and biological evaluation of novel 1-deoxy-1-[6-[((hetero)arylcarbonyl)hydrazino]-9H-purin-9-yl]-N-ethyl-β-D-ribofuranuronamide derivatives as useful templates for the development of A2B adenosine receptor agonists. *J. Med. Chem.* 2007, Vol. 50, pp. 374-380.

275. **Albrecht B., et al.** A2B receptor activation mimics postconditioning in a rabbit infarct model. *Circulation.* 2006, Vol. 114, pp. II-14-II-15.

276. **Alnouri M. W., et al.** Selectivity is species-dependent: characterization of standard agonists and antagonists at human, rat, and mouse adenosine receptors. *Purinergic Signal.* 2015, Vol. 11, pp. 389-407.

277. **Hinz S., et al.** BAY 60-6583 acts as a partial agonist at adenosine A2B receptors. *J. Pharmacol. Exp. Ther.* 2014, Vol. 349, pp. 427-436.

278. **Ortore A., et al.** A2B receptor ligands: past, present and future trends. *Curr. Top. Med. Chem.* 2010, Vol. 10, pp. 923–940.

279. **Cheung A. W.-H., et al.** 4-Substituted-7-N-alkyl-N-acetyl 2-aminobenzothiazole amides: druglike and non-xanthine based A2B adenosine receptor antagonists. *Bioorg. Med. Chem. Lett.* 2010, Vol. 20, pp. 4140–4146.

280. **Eastwood P., et al.** Discovery of N-(5,6-diarylpyridin-2-yl)amide derivatives as potent and selective A2B adenosine receptor antagonists. *Bioorg. Med. Chem. Lett.* 2010, Vol. 20, pp. 1697–1700.

281. **Klotz K. N., et al.** [3H]HEMADO- a novel tritiated agonist selective for the human adenosine A3 receptor. *Eur. J. Pharmacol.* 2007, Vol. 556, pp. 14-18.

282. **Little J. W., et al.** Endogenous adenosine A3 receptor activation selectively alleviates persistent pain states. *Brain.* 2015, Vol. 138, pp. 28-35.

283. **Tosh D. K., et al.** Structure-guided design of A3 adenosine receptor selective nucleosides: combination of 2-arylethynyl and bicyclo[3.1.0]hexane substitutions. *J. Med. Chem.* 2012, Vol. 55, pp. 4847-4860.

284. —. In vivo phenotypic screening for treating chronic neuropathic pain: modification of C2-arylethynyl group of conformationally constrained A3 adenosine receptor agonists. *J. Med. Chem.* 2014, Vol. 57, pp. 9901-9914.

285. —. Efficient, large-scale synthesis and preclinical studies of MRS5698, a highly selective a3 adenosine receptor agonist that protects against chronic neuropathic pain. *Purinerg. Signal.* 2015, Vol. 11, pp. 371-387.

286. **Auchampach J. A., et al.** Synthesis and pharmacological characterization of [125I]MRS5127, a high affinity, selective agonist radioligand for the A3 adenosine receptor. *Biochem. Pharmacol.* 2010, Vol. 79, pp. 967–973.

287. **Jeong L. S., et al.** Structure activity relationships of truncated D- and L-4'-thioadenosine derivatives as species-independent A3 adenosine receptor antagonists. *J. Med. Chem.* 2008, Vol. 51, pp. 6609–6613.

288. **Lenzi O., t al.** 2-Phenylpyrazolo[4,3-d]pyrimidin-7-one as a new scaffold to obtain potent and selective human A3 adenosine receptor antagonists: new insights into the receptor-antagonist recognition. *J. Med. Chem.* 2009, Vol. 52, pp. 7640–7652.

289. **Squarcialupi L., et al.** 2-Arylpyrazolo[4,3-d]pyrimidin-7-amino derivatives as new potent and selective human A3 adenosine receptor antagonists. Molecular modeling studies and pharmacological evaluation. *J. Med. Chem.* 2013, Vol. 56, pp. 2256–2269.

290. **Colotta V., et al.** Novel potent and highly selective human A(3) adenosine receptor antagonists belonging to the 4-amido-2-arylpyrazolo[3,4-C]quinoline series: molecular docking analysis and pharmacological studies. *Bioorg. Med. Chem.* 2009, Vol. 17, pp. 401–410.

291. **Catarzi D., et al.** Pyrazolo[1,5-C]quinazoline derivatives and their simplified analogues as adenosine receptor Antagonists: synthesis, structure-affinity relationships and molecular modeling studies. *Bioorg. Med. Chem.* 2013, Vol. 21, pp. 283–294.

292. **Squarcialupi L., et al.** 7-Amino-2-phenylpyrazolo[4,3-d]pyrimidine derivatives: structural investigations at the 5-position to target human A_1 and A(2A) adenosine receptors. Molecular modeling and pharmacological studies. *Eur. J. Med. Chem.* 2014, Vol. 84, pp. 614-627.

293. **Rosentreter U., et al.** *Substituted 2-thio-3,5-dicyano-4-aryl-6-aminopyridines and the use thereof. WO2001/025210* 2001.

294. —. *Substituted 2-thio-3,5-dicyano-4-phenyl-6-aminopyridines and their use as adenosine receptor-selective ligands. WO2003/03008384* 2003.

295. —. *Substituted 2-thio-3,5-dicyano-4-phenyl-6-aminopyridines and their use as adenosine receptor-selective ligands. US2004/0176417* 2004.

296. **Beukers M. W., et al.** Structure-affinity relationships of adenosine A2B receptor ligands. *Med. Res. Rev.* 2006, Vol. 26, pp. 667-698.

297. **Beukers M.W., et al.** New, non-adenosine, high-potency agonists for the human adenosine A2B receptor with an improved selectivity profile compared to the reference agonist N-ethylcarboxamidoadenosine. *J. Med. Chem.* 2004, Vol. 47, pp. 3707-3709.

298. **Maglieri M.** 2-Amminopiridine-3,5-dicarbonitrili quali nuovi agonisti del recettore A2B dell'adenosina. 2013.

299. **Dal Ben D., et al.** Simulation and comparative analysis of binding modes of nucleoside and non-nucleoside agonists at the A2B adenosine receptor. *In Silico Pharmacol.* 2013, Vol. 1, 24.

300. **Louvel J., et al.** Structure-kinetics relationships of Capadenoson derivatives as adenosine A 1 receptor agonists. *Eur. J. Med. Chem.* 2015, Vol. 101, pp. 681-691.

301. **Murray T., et al.** Synthesis of heterocyclic compounds containing three contiguous hydrogen bonding sites in all possible arrangements. *Tetrahedron.* 1995, Vol. 51, pp. 635-648.

302. **Harada H., et al.** *Medicine comprising dicyanopyridine derivative. US20030232860 (A1)*

303. **Rosentreter U., et al.** *Substituierte 2-thio-3,5-dicyano-4-aryl-6-aminopyridine und ihre verwendung als adenosinrezeptor-selektive liganden. WO2002070485 (A1)* 2002.

304. **Dyachenko V. D., et al.** 3-Amino-3-thioxopropanamide in the synthesis of functionally substituted nicotinamides. *Russian Journal of Organic Chemistry.* 2003, Vol. 39, pp. 1174–1179.

305. **Ferlin M. G., et al.** Synthesis of 1,4-dihydro-2-methyl-4-oxo-nicotinic acid: Ochiai's route failed. *Tetrahedron.* 2006, Vol. 62, pp. 6222 - 6227.

306. **Krahn T., et al.** *USE OF SUBSTITUTED 2-THIO-3,5-DICYANO-4-PHENYL-6-AMINOPYRIDINES FOR THE TREATMENT OF REPERFUSION INJURY AND REPERFUSION DAMAGE. WO2006099958 (A1)* 2006.

307. **Hao D., et al.** Synthesis of 2-amino-4-phenyl-6-(phenylsulfanyl)-3,5-dicyanopyridines by tandem reaction. *Res. Chem. Intermed.* 2014, Vol. 40, pp. 587-594.

308. **Shen T. Y., et al.** *Certain lower-alkyl sulfinylmethyl pyridines. US3438992* 1969.

309. **Schneider F., et al.** *Hoppe-Seyler's Zeitschrift fuer Physiologische Chemie.* 1962, Vol. 327, pp. 74-85.

310. **Gonzales Cabrera D., et al.** Novel orally active antimalarial thiazoles. *J. Med. Chem.* 2011, Vol. 54, pp. 7713-7719.

311. **Watson C. Y., et al.** Synthesis of 3-substituted benzamides and 5-substituted isoquinolin-1(2H)-ones and preliminary evaluation as inhibitors of poly(ADP-ribose)polymerase (PARP). *Bioorg. Med. Chem.* 1998, Vol. 6, pp. 721-734.

312. **Bezwada R. S., et al.** *FUNCTIONALIZED BIODEGRADABLE TRICLOSAN MONOMERS AND OLIGOMERS FOR CONTROLLED RELEASE. US2009105352 (A1)*

313. **Ngo H., et al.** Synthesis and characterization of allosteric probes of substrate channeling in the tryptophan synthase bienzyme complex. *Biochemistry.* 2007, Vol. 46, pp. 7713–7727.

314. **Kyprianidou P., et al.** The synthesis of several tritiated non-nucleoside, HIV-1 reverse transcriptase inhibitors. *Polyhedron.* 2009, Vol. 28, pp. 3171-3176.

315. **Hamill T. G., et al.** The synthesis of several tritiated non-nucleoside, HIV-1 reverse transcriptase inhibitors. *J. Labelled Cpd. Radiopharm.* 1998, Vol. 41, pp. 319-327.

316. **Gad-Elkareem M. A. M., et al.** Reactions with 3,6-diaminothieno[2,3-b]-pyridines: synthesis and characterization of several new fused pyridine heterocycles. *Heteroatom Chemistry.* 2007, Vol. 18, pp. 405-413.

317. **Mitsuyama M., et al.** Synthesis and fluorescence of 2H-pyrone derivatives for organic light-emitting diodes (OLED). *Journal of Heterocyclic Chemistry.* 2007, Vol. 44, pp. 115-132.

318. **Maurya H. K., et al.** A carbanion induced synthesis of highly congested pyrazole and imidazole containing heterocycles. *Tetrahedron Lett.* 2014, Vol. 55, pp. 1715-1719.

319. **Lane J. R., et al.** A novel nonribose agonist, LUF5834, engages residues that are distinct from those of adenosine-like ligands to activate the adenosine A2A receptor. *Mol. Pharmacol.* 2012, Vol. 81, pp. 475-487.

320. **Thimm D., et al.** Ligand-specific binding and activation of the human adenosine A(2B) receptor. *Biochemistry.* 2013, Vol. 52, pp. 726-740.

321. **Li J., et al.** Ligand-dependent activation and deactivation of the human adenosine A2A receptor. *J. Am. Chem. Soc.* 2013, Vol. 135, pp. 8749-8759.

322. **Rodriguez D., et al.** Molecular docking screening using agonist-bound GPCR structures: probing the A2A adenosine receptor. *J. Chem. Inf. Model.* 2015, Vol. 55, pp. 550-563.

323. **Dal Ben D., et al.** Simulation and comparative analysis of different binding modes of non-nucleoside agonists at the A2A adenosine receptor. *Mol. Inform.* 2016, Vol. 35, pp. 403-413.

324. **Schiedel A. C., et al.** The four cysteine residues in the second extracellular loop of the human adenosine A2B receptor: role in ligand binding and receptor function. *Biochem. Pharmacol.* 2011, Vol. 82, pp. 389–399.

325. **Riviera-Oliver M., et al.** Using caffeine and other adenosine receptor antagonists and agonists as therapeutic tools against neurodegenerative diseases: a review. *Life Sci.* 2014, Vol. 101, pp. 1-9.

326. **von Hehn C. A., et al.** Deconstructing the neuropathic pain phenotype to reveal neural mechanisms. *Neuron.* 2012, Vol. 73, pp. 638-652.

327. **Di Cesare Mannelli L., et al.** Morphologic features and glial activation in rat oxaliplatin dependent neuropathic pain. *J. Pain.* 2013, Vol. 14, pp. 1585-1600.

328. **Renn C. L., et al.** Multimodal assessment of painful peripheral neuropathy induced by chronic oxaliplatin-based chemotherapy in mice. *Mol. Pain.* 2011, Vol. 7, p. 29.

329. **Hershman D. L., et al.** Prevention and management of chemotherapy-induced peripheral neuropathy in survivors of adult cancers: American society of clinical oncology clinical practice guideline. *J. Clin. Oncol.* 2014, Vol. 32, pp. 1941-1967.

330. **Fu S., et al.** Clinical application of oxaliplatin in epithelial ovarian cancer. *Int. J. Gynecol. Cancer.* 2006, Vol. 16, pp. 1717-1732.

331. **Martin M., et al.** Platinum compounds in the treatment of advanced breast cancer. *Clin. Breast Cancer.* 2001, Vol. 2.

332. **Andrè T., et al.** Multicenter International study of Oxaliplatin/5-Fluorouracil/Leucovorin in the adjuvant treatment of Colon Cancer (MOSAIC) investigators. Oxaliplatin, fluorouracil, and leucovorin as adjuvant treatment for colon cancer. *N. Engl. J. Med.* 2004, Vol. 350, pp. 2343-2351.

333. **Ducreux M., et al.** Capecitabine plus oxaliplatin (XELOX) versus 5-fluorouracil/leucovorin plus oxaliplatin (FOLFOX-6) as first-line treatment for metastatic colorectal cancer. *Int. J. Cancer.* 2011, Vol. 128, pp. 682-690.

334. **Wolf S., et al.** Chemotherapy induced peripheral neuropathy: prevention and treatment strategies. *Eur. J. Cancer.* 2008, Vol. 44, pp. 1507-1515.

335. **Argyriou A. A., et al.** Chemotherapy-induced peripheral neurotoxicity (CIPN): an update. *Crit. Rev. Oncol. Hematol.* 2012, Vol. 82, pp. 51-77.

336. **Kiernan M. C., et al.** The pain with platinum: oxaliplatin and neuropathy. *Eur. J. Cancer.* 2007, Vol. 43, pp. 2631-2633.

337. **Ta L. E., et al.** Neurotoxicity of oxaliplatin and cisplatin for dorsal root ganglion neurons correlates with platinum-DNA binding. *Neurotoxicology.* 2006, Vol. 27, pp. 992-1002.

338. **DI Cesare Mannelli L., et al.** Oxaliplatin-induced oxidative stress in nervous system-derived cellular models: could it correlate with in vivo neuropathy? *Free Radic. Biol. Med.* 2013, Vol. 61, pp. 143-150.

339. **Zanardelli M., et al.** Oxaliplatin neurotoxicity involves peroxisome alterations. PPARgamma agonism as preventive pharmacological approach. *PLoS One.* 2014, Vol. 9, p. e102758.

340. **Wu W.-P., et al.** Effect of acute and chronic administration of caffeine on pain-like behaviors in rats with partial sciatic nerve injury. *Neuroscience Lett.* 2006, Vol. 402, pp. 164-166.

341. **English C., et al.** New FDA-approved disease-modifying therapies for multiple sclerosis. *Clin Ther.* 2015, Vol. 37, pp. 691-715.

342. **Franklin R. J., et al.** Remyelination in the CNS: from biology to therapy. *Nat Rev Neurosci.* 2008, Vol. 9, pp. 839-855.

343. **Simon C., et al.** Progenitors in the adult cerebral cortex: cell cycle properties and regulation by physiological stimuli and injury. *Glia.* 2011, Vol. 59, pp. 869-881.

344. **Chang A., et al.** NG2-positive oligodendrocyte progenitor cells in adult human brain and multiple sclerosis lesions. *J Neurosci.* 2000, Vol. 20, pp. 6404-6412.

345. **Kremer D., et al.** The complex world of oligodendroglial differentiation inhibitors. *Ann Neurol.* 2011, Vol. 69, pp. 602-618.

346. **Kipp M., et al.** Pathology of multiple sclerosis. *CNS Neurol Disord Drug Targets.* 2012, Vol. 11, pp. 506-517.

347. **Fields R. D., et al.** Purinergic signalling in neuron-glia interactions. *Nat Rev Neurosci.* 2006, Vol. 7, pp. 423-436.

348. **Pedata F., et al.** Purinergic signalling in brain ischemia. *Neuropharmacology.* 2016, Vol. 104, pp. 105-130.

349. **Coppi E., et al.** Role of adenosine in oligodendrocyte precursor maturation. *Front Cell Neurosci.* 2015, Vol. 9, p. 155.

350. **Stevens B., et al.** Adenosine: a neuron-glial transmitter promoting myelination in the CNS in response to action potentials. *Neuron.* 2002, Vol. 36, pp. 855-868.

351. **Coppi E., et al.** Adenosine A_2A receptors inhibit delayed rectifier potassium currents and cell differentiation in primary purified oligodendrocyte cultures. *Neuropharmacology.* 2013, Vol. 73, pp. 301-310.

352. **Othman T., et al.** Oligodendrocytes express functional A1 adenosine receptors that stimulate cellular migration. *Glia.* 2003, Vol. 44, pp. 166-172.

353. **Melani A., et al.** Selective adenosine A2a receptor antagonism reduces JNK activation in oligodendrocytes after cerebral ischaemia. *Brain.* 2009, Vol. 132, pp. 1480-1495.

354. **Ranu B. C., et al.** An improved procedure for the three-component synthesis of highly substituted pyridines using ionic liquid. *J. Org. Chem.* 2007, Vol. 72, pp. 3152-3154.

355. **Chang L. C. W., et al.** A series of ligands displaying a remarkable agonistic-antagonistic profile at the adenosine A1 receptor. *J. Med. Chem.* 2005, Vol. 48, pp. 2045-2053.

356. **Rosentreter U., et al.** *SUBSTITUTED 2-THIO-3,5-DICYANO-4-ARYL-6-AMINOPYRIDINES AND THE USE THEREOF. WO0125210 (A2)* 2001.

357. **Dyachenko A. D., et al.** A new route to partially hydrogenated thiazolo[3,2-a]pyridine. *Chem. Het. Comp.* 2004, Vol. 40, pp. 650-659.

358. **Hironori H., et al.** *MEDICINE COMPRISING DICYANOPYRIDINE DERIVATIVE. EP1302463 (A1)* 2003.

359. **Nell P., et al.** *SUBSTITUTED AZABICYCLIC COMPOUNDS AND THE USE THEREOF. US2011/3845 (A1)* 2011.

360. **Pevarello P., et al.** Synthesis and anticonvulsant activity of a new class of 2-[(arylalkyl)amino]alkanamide derivatives. *J. Med. Chem.* 1998, Vol. 41, pp. 579-590.

361. **Fan Y. H., et al.** Structure-activity requirements for the antiproliferative effect of troglitazone derivatives mediated by depletion of intracellular calcium. *Bioorg. Med. Chem.* 2004, Vol. 14, pp. 2547-2550.

362. **Ashton M. J., et al.** Heterocyclic analogues of chlorcyclizine with potent hypolipidemic activity. *J. Med. Chem.* 1984, Vol. 27, pp. 1245-1253.

363. **Gibbons L. K., et al.** *N-(sulfonyloxy) benzimidoyl halides as bactericidal or fungicidal agents. US3983246 (A)* 1976.

364. **Woods J. G., et al.** *Meta-bridged styryloxy resins. US4640849 (A)* 1987.

365. **Vollrath R., et al.** *DE2108932 (A1)* 1972.

366. **Taylor E. C., et al.** The synthesis of 4-aminoisoxazolo[5,4-d]pyrimidines. *J. Org. Chem.* 1964, Vol. 29, pp. 2116–2120.

367. **Diaa A. I., et al.** Design, synthesis and biological study of novel pyrido[2,3-d]pyrimidine as anti-proliferative CDK2 inhibitors. *Eur. J. Med. Chem.* 2011, Vol. 46, pp. 5825-5832.

368. **Schweiger M., et al.** *ATGListatin and pharmaceutical composition comprising the same. US9206115 B2* 2015.

369. **Silberg A., et al.** Beiträge zum Studium der Thiazole, I. Über die Herstellung und die Eigenschaften von 2-Aryl-4-halogenmethyl-thiazolen. *Eur. J. Inorg. Chem.* 1961, Vol. 94, pp. 2887–2894.

370. **Euranto E. K., et al.** Chlorination of benzyl esters of aliphatic acids. *Acta Chem. Scand. 1947 - 1999.* 1970, Vol. 24, pp. 50-54.

371. **Schroth W., et al.** 2-Acylmethyl-1, 3, 4-dioxazole durch Ketovinylierung von Hydroxamsäuren. *Zeitschrift für Chemie.* 1978, Vol. 18, pp. 57-58.

372. **Wang Y., et al.** A click chemistry mediated in vivo activity probe for dimethylarginine dimethylaminohydrolase. *J. Am. Chem. Soc.* 2009, Vol. 131, pp. 15096–15097.

373. **Scholz D., et al.** Aryloxyacetamidines and 2-(aryloxymethyl)-imidazolines. *J. Am. Chem. Soc.* 1947, Vol. 69, pp. 1688-1690.

374. **Castedo Q. R., et al.** Synthesis and pharmacological activity of some nitrofuraldehyde cyanopyridine derivatives. *Eur. J. Med. Chem.* 1984, Vol. 19, pp. 555-557.

375. **Peseke K., et al.** Synthesen mit 1,3-dithietanen—V: Reaktionen der 2,4-bis-(alkoxycarbonyl-cyan-methylen)-1,3-dithietane mit o-phenylendiaminen. *Tetrahedron.* 1976, Vol. 32, pp. 483-485.

376. **Parmar V. S., et al.** Synthesis of E- and Z-pyrazolylacrylonitriles and their evaluation as novel antioxidants. *Bioorg. Med. Chem.* 1999, Vol. 7, pp. 1425-1436.

377. **Wise A., et al.** The identification of ligands at orphan G-protein coupled receptors. *Annu. Rev. Pharmacol. Toxicol.* 2004, Vol. 44, pp. 43–66.

378. **Howard A.D., et al.** Orphan G-protein-coupled receptors and natural ligand discovery. *Trends in Pharmacol. Sci.* 2001, Vol. 22, pp. 132-140.

379. **Zhang L., et al.** Cloning and expression of MRG receptors in macaque, mouse and human. *Brain Res. Mol. Brain Res.* 2005, Vol. 133, pp. 187-197.

380. **Borrmann T., et al.** 1-Alkyl-8-(piperazine-1-sulfonyl)phenylxanthines: development and characterization of adenosine A2B receptor antagonists and a new radioligand with subnanomolar affinity and subtype specificity. *J. Med. Chem.* 2009, Vol. 52, pp. 3994-4006.